An Integrated Multi-Isotope and Element Distribution Study of the Irish Biosphere

Submitted for the degree of Doctor of Philosophy

2017

Saskia E. Ryan



Trinity College Dublin
Coláiste na Tríonóide, Baile Átha Cliath
The University of Dublin

Declaration

I declare that this thesis has not been submitted as an exercise for a degree at this or any other university and it is entirely my own work.

I agree to deposit this thesis in the University's open access institutional repository or allow the library to do so on my behalf, subject to Irish Copyright Legislation and Trinity College Library conditions of use and acknowledgement.

Saskia E. Ryan

An Integrated Multi-Isotope and Element Distribution Study of the Irish Biosphere

Saskia E. Ryan

Abstract

Geochemical variation in major and trace element concentrations and multiple isotope systems ($^{87}Sr/^{86}Sr$, $\delta^{18}O$, $\delta^{2}H$, $\delta^{13}C$, $\delta^{15}N$) are explored within the Irish biosphere. This is done through the analysis of an array of environmental sample media, including vegetation, tree cores, soils, streamwaters and archaeological human remains. This integrated and comprehensive approach informs on spatial and temporal geochemical changes in the biosphere and demonstrates how local and regional characteristic values can be used as a proxy for element provenance and geographical discrimination.

$^{87}Sr/^{86}Sr$ are employed by a wide range of science-based disciplines including geology, environmental science, archaeology and forensic science for multiple applications including geochronology, element cycling, geochemical fingerprinting and tracing the mobility of pre-historic humans and animals. For archaeological provenance studies, there are a number of potential limitations associated with the use of $^{87}Sr/^{86}Sr$ as a tracer, including possible contributions from multiple geochemical reservoirs, a lack of environmental reference baseline data and a general gap in understanding how different geochemical proxies may complement $^{87}Sr/^{86}Sr$ data. These challenges are examined by this research using case studies from selected sites in Ireland.

This thesis has revealed the following new insights: (1) The $^{87}Sr/^{86}Sr$ of vegetation progressively diverges from a marine $^{87}Sr/^{86}Sr$ value with increasing distance from the coast along coastal transects. (2) Geochemical topsoil datasets (including Na, Ca and Mg cation concentrations) further demonstrate a high marine element-contribution along the western coastal perimeter of Ireland and in areas covered by blanket peat. (3) Surface waters exhibit clear binary mixing between atmospheric and minerogenic end-members. (4) Tree core records illustrate a small but marked change in $^{87}Sr/^{86}Sr$ values in the mid-20th century, taken to reflect the introduction and intensive use of modern fertiliers. (5) Statistically, soil-parent materials derived from both bedrock and Quaternary sediments can control the $^{87}Sr/^{86}Sr$ distribution within the environment. (6) Rare earth elements (REE) in the plant-soil-streamwater interface demonstrate complex fractionations between media. (7) Isotope biosphere variations in Ireland can be successfully applied to answer questions relating to past human subsistence and mobility.

The implications of this research are that local biologically-available $^{87}Sr/^{86}Sr$ ranges should not be inferred from geological proxies in areas proximal to the coast and regions subject to high levels of precipitation or from intensively farmed land. It is also shown that the ability to use isotopic variation to study past human provenance is greatly improved by using combined isotope systems ($^{87}Sr/^{86}Sr$, $\delta^{18}O$, $\delta^{2}H$, $\delta^{13}C$, $\delta^{15}N$).

Acknowledgements

The past four years of research have been formative, challenging and enjoyable. I have been fortunate to meet many talented, intelligent people along this journey whom I would like to thank sincerely for their help, inspiration and friendship:

First, I am indebted to my supervisor, Dr. Quentin G. Crowley for advice, encouragement and belief in my capabilities throughout all stages of this project. For further research expertise and guidance: Prof. Noreen Tuross and my confirmation panel members, Prof. Balz Kamber and Dr. Catherine Rose.

For technical training and support:
Dr. Cora McKenna and Dr. Michael Babechuk (Trinity College Dulbin (TCD) Geochemistry), Prof. Jane Evans and Ms. Carlyn Stewart (NERC Isotope Geoscience Facility, Keyworth), Dr. Mark Kavanagh (Centre for the Environment, TCD), Dr. Mags Duncan, Mr. Francis Hendron, Mr. Neil Kearny, Ms. Maura Morgan and Mr. Noel McGinley (Department of Geology, TCD). Dr. Patrick Veale (Department of Engineering, TCD), Prof. Sasha Turchyn and Dr. Andrea Erheart (University of Cambridge), Dr. David Brown (Queen's University, Belfast (QUB)) and Prof. Stephen Daly (Department of Geology, University College Dublin (UCD)). I thank Dr. Linda Reynard (Harvard University) with whom I had the pleasure of sharing an office. She taught me a great deal about the measurement of stable isotopes through formal instruction and casual conversations. I especially thank Mr. Michael Murphy (Chief Technical Officer, Department of Geology, UCD) whose expertise in analytical geochemistry was indispensable and his enthusiasm encouraged my undergraduate-self to pursue a research career.

For samples:
Dr. Andy Halpin and Dr. Nessa O'Connor (National Museum of Ireland), Dr. Kate Knights (Geological Survey of Ireland (GSI)), Dr. Matthew Seaver (UCD, Archaeology). I am especially grateful to the National Museum of Ireland for their trust in me with precious archaeological samples. They have shown that they believe

in the importance of this science despite its sometimes-invasive nature on finite material and my own competence to treat these specimens with due respect and care.

I am grateful to the following organisations for providing funding and access to equipment for the research included in this thesis: Trinity Postgraduate Research Studentship, TCD Geochemistry Laboratory, The National Centre for Irish Isotope Geochemistry UCD, the Centre for the Environment TCD, the Mourne Cooley Gullion GeoBursary, Trinity Travel Bursary, NIGL Keyworth Nottingham. The Department of Earth Sciences at the University of Cambridge, Belfast Dendrochronology Laboratory (QUB), Vrije Universiteit Brussel and the Geological Survey of Ireland (Geoscience Fulbright scholarship and GSI Shortcall).

The GSI Geoscience Fulbright Award offered me the opportunity of a lifetime. I will continually aim to be an ambassador of the Fulbright values of mutual understanding and shared learning. The Biogeochemistry Laboratory at Harvard University was an exceptional Fulbright host laboratory and I am indebted to Prof. Noreen Tuross for giving me access to everything I needed to complete and surpass my research goals and facilitated many other fruitful opportunities during my time at Harvard and beyond.

For fun and welcome distractions: All my fellow postgrads in the Geology Department. A special thanks to Clare, who has accompanied me on my Trinity journey from undergraduate to doctorate, being a most supportive friend throughout. HX48 was a sanctuary from all things work-related, made so by my close friends and housemates, Shauna and Clive. My Bostonian housemate, Jessica, who made the transition to American life such a pleasure. Dr. Christophe Snoeck (VUB), Ms. Niamh Daly (UCC), Ms. Elise Alonsi and Ms. Eileen Deegan, for showing me the value of collaborative studies.

My sister, Vita, for words of wisdom, friendship and reminding me of the many ties between the arts and sciences.

Nicolas, for unwavering support, patience and encouragement to seek out opportunities, even when they meant spending long periods away from each other.

My greatest thanks go to my parents, Michael and Valerie. I have learned from their example the value of continual learning and hard work. They have offered guidance, critiqued my writing and supported me throughout the past four years and my entire education. I thank my Dad for his orienteering expertise, advice and wonderful company on fieldwork. Discovering many of the most remote, natural parts of Ireland on our adventures are some of the fondest memories I have of my Ph.D.

Table of Contents

Chapter 1: Introduction 1

1 Aims and Scope of the Thesis 1

2 Structure and Layout 5

3 Author Contributions 5

References 7

Chapter 2: Marine and Anthropogenic-derived Strontium in the Terrestrial Environment: Implications for Biosphere Mapping 11

Abstract 11

1 Introduction 13

1.1 Influence of atmospheric-derived Sr 14

1.2 Cation ratios 18

1.3 Atmospheric and geogenic Sr systematics in mineral waters 19

1.4 Time-resolved changes in Sr recorded by trees 20

2 Materials and Methods 21

2.1 Sample Collection and Preparation 21

2.2 Sample Digestion 22

2.3 Separation of Strontium 23

2.4 Quadrupole ICP-MS (TCD) 24

2.5 Thermal Ionisation Mass Spectrometry (TIMS) 24

2.6 Equations 25

3 Results and Discussion 27

3.1 Sr variability of coastal transect samples 27

3.2 Marine influence on coastal transects 33

3.3 Bioavailability of strontium in soils 38

3.4 Molar cation ratios in topsoils 39

3.5 Geogenic and atmospheric mixing of Sr in the hydrological system 42
3.6 Implications for biosphere mapping 47
3.7 $^{87}Sr/^{86}Sr$ variability in the biosphere through time 48
4 Conclusion 54
Acknowledgements 56
References 57
5 Supplementary Tables 73

Chapter 3: $^{87}Sr/^{86}Sr$ and trace element mapping of geosphere-hydrosphere-biosphere interactions: A case study in Ireland 77
Abstract 77
1 Introduction 79
1.1 Estimating element bioavailability in soil 80
1.2 REE translocation to plants 82
1.3 REE in the hydrological system 83
1.4 Study site 84
2 Materials and Methods 86
2.1 Sampling strategy 86
2.2 Sample preparation and digestions 87
2.3 Quadrupole ICP-MS determination of trace elements 88
2.4 TIMS 90
2.5 MC-ICP-MS 90
2.6 Statistical analysis 90
2.7 Biological Absorption Coefficient (BAC) 91
3 Results 92
3.1 Sr isotopic and concentration data 92
3.2 Statistical assessment of spatial $^{87}Sr/^{86}Sr$ variation 97

3.3 REE: 101
3.3.1 Soil leachates 104
3.3.2 Vegetation 105
3.3.3 Dissolved load in streamwater 105
4 Discussion: 106
4.1 Sr isotope and concentration data 106
4.2 Suitability of sample media used for bioavailable Sr mapping 108
4.3 Relationship between bedrock/Quaternary geology and biosphere 109
4.4 Archaeological implications 112
4.5 REE in the biosphere 114
4.5.1 Translocation of REE from soil to biomass 115
4.5.2 Dissolved load in streamwater 121
5 Conclusion 125
Acknowledgments 126
References 127

Chapter 4: Early Medieval Reliance on the Land and the Local: An Integrated Multi-Isotope Study ($^{87}Sr/^{86}Sr$, $\delta^{18}O$, $\delta^{2}H$, $\delta^{13}C$, $\delta^{15}N$) of Diet and Migration 147
Abstract 147
1 Introduction 148
1.1 Aims and Rationale: 148
1.2 Early medieval Farming Practices in Ireland 149
1.3 Combined Isotope Analyses of Human Remains 151
1.3.1 Reconstructing Paleo-diet 151
1.3.2 Reconstructing Mobility 152
1.4 Geology of Co. Meath 156

2 Archaeological Sites 158
2.1 Johnstown 158
2.2 Raystown 158
2.3 Collierstown 159
2.4 Excavation Details 159
3 Materials and Methods 160
3.1 Rationale for Sampled Tissues 160
3.2 Bone and Teeth Sample Preparation 161
3.3 Carbon and Nitrogen Isotopes 162
3.4 Oxygen and Hydrogen Isotopes 163
3.5 Strontium Isotopes 164
3.6 Statistical Methods 164
4 Results and Discussion 166
4.1 Difference in Diet Spatially and Temporally 166
4.2 Migration 173
4.2.1 $^{87}Sr/^{86}Sr$ 173
4.2.2 $\delta^{18}O$ 178
4.2.3 $\delta^{2}H$ 182
5 Conclusion: 186
Acknowledgements 187
References 188
6 Supplementary Tables 208

Chapter 5: Synthesis 219
References 225

Chapter 1: Introduction

1 Aims and Scope of the Thesis

This thesis has three central aims: (i) Defining the influence of marine and anthropogenic Sr contribution on the Sr budget of the biosphere (ii) Characterising $^{87}Sr/^{86}Sr$ and rare earth element (REE) distribution in the biosphere of County (Co.) Meath, accounting for both local bedrock and surficial geology types, and (iii) Geochemical fingerprinting of three early medieval archaeological populations in Co. Meath.

(i) *Defining the influence of marine and anthropogenic Sr contribution on the Sr budget of the biosphere*.

$^{87}Sr/^{86}Sr$ vary across environments based on the age and mineral composition of bedrock geology/soil, as well as other inputs such as marine, anthropogenic and Quaternary sediment contributions (Price et al., 2002; Bentley, 2006; Evans et al., 2010; Voerkelius et al., 2010; Maurer et al., 2012; Slovak and Paytan, 2012; Frei and Frei, 2013; Gosz and Moore, 1989; Graustein and Armstrong, 1983; Capo et al., 1998). A geographical region can have characteristic $^{87}Sr/^{86}Sr$ values that are transferred into the teeth and bones of individuals sourcing their food and water locally, acting as an archive of these local values (Montgomery, 2010; Bentley, 2006; Sillen and Kavanagh, 1982). One can compare the values of mineralised human tissue to environmental baseline data for investigating mobility. However, whilst $^{87}Sr/^{86}Sr$ biosphere values vary spatially in a somewhat predictable way, the exact inputs of Sr from non-geogenic sources and the extent to which they effect local and regional $^{87}Sr/^{86}Sr$ variations are not fully understood.

Biosphere maps have previously been used to estimate spatial variations in $^{87}Sr/^{86}Sr$ (e.g. Bataille et al., 2014; Bentley and Knipper, 2005; Evans et al., 2010; Frei and Price, 2011) but represent only an approximation of bioavailable $^{87}Sr/^{86}Sr$ values, without factoring in other sources/end-members of Sr, although these are acknowledged. In the context of Ireland, an island on the western-most extremity of Europe, $^{87}Sr/^{86}Sr$ predictions based on bedrock are likely to be inaccurate in certain

environments due to marine, atmospheric and anthropogenic-fertiliser inputs. Whether these factors measurably influence the $^{87}Sr/^{86}Sr$ composition of the Irish biosphere is examined here. This is done at:

1. a local scale by measuring $^{87}Sr/^{86}Sr$ ratios of (a) plants taken along coastal transects, (b) river water with a constrained catchment bedrock $^{87}Sr/^{86}Sr$ composition and (c) tree cores to provide a time-resolved record of changes in chemical composition over the last 100 years.
2. at a regional scale examining soil geochemistry, using seawater-characteristic Na concentrations as a reference, to determine if the marine chemical fingerprint can be traced in topsoils (A-horizon).

In addition to $^{87}Sr/^{86}Sr$ compositions, element concentrations are useful for tracing element sources by constraining possible endmember inputs. Tellus and Tellus Border are regional mapping projects which have gathered geo-environmental data for extensive regions of Ireland. The Tellus dataset is integrated with the data produced in this thesis to comprehensively address element-sourcing from marine and anthropogenic reservoirs.

(ii) Characterising $^{87}Sr/^{86}Sr$ and REE distribution in the biosphere of Co. Meath, accounting for both local bedrock and surficial geology types.

$^{87}Sr/^{86}Sr$ values and REE concentrations are employed to study geosphere-hydrosphere-biosphere interactions in the contemporary environment and to spatially define geochemical variations between soil, plants and streamwaters. Given that surficial sediments lie at the geosphere-biosphere interface, it follows that they have the potential to impede the transfer of the local geogenic $^{87}Sr/^{86}Sr$ value into the biosphere. Much of the bedrock geology of Ireland is covered by glacial sediments with some parts of the country covered with more than 30 m of glacial deposits (Fay et al., 2007). Differences between the spatial distribution of $^{87}Sr/^{86}Sr$ in plants are statistically examined using one-way ANOVA in the context of underlying bedrock and Quaternary sediment to determine if the latter has an appreciable influence on the biosphere $^{87}Sr/^{86}Sr$ range of Co. Meath.

Archaeological provenance studies in Ireland are currently limited by a lack of constrained baseline $^{87}Sr/^{86}Sr$ data. For $^{87}Sr/^{86}Sr$ based studies to successfully trace element cycling or migratory patterns, it is imperative to have good quality reference material with which to compare archaeological data. Systematic geochemical sampling, using a variety of media, is undertaken to better understand the complexity of $^{87}Sr/^{87}Sr$ distribution in the biosphere and the extent to which this geographic variation can be resolved using these different sample types. This is done with a specific view to determining the bioavailable composition, i.e. the fraction of Sr in soil that is available for uptake by plants, and the composition of the plants themselves, which in turn act as a source of bio-available Sr for their consumers. The baseline bioavailable $^{87}Sr/^{86}Sr$ values derived here can be used in complementary archaeological studies with the aim of distinguishing peoples originating from distal locations versus local human populations that lived in the region of the burial sites. This dataset also contributes to the present archive of bioavailable $^{87}Sr/^{86}Sr$ for the entire island of Ireland.

From an environmental process standpoint, $^{87}Sr/^{86}Sr$ variation can be used to examine element transfer within the biosphere. Rare earth elements (REE) and $^{87}Sr/^{86}Sr$ are independent tracers that can be employed together to define geochemical reservoirs and investigate geosphere-biosphere-hydrosphere interactions. Like $^{87}Sr/^{86}Sr$, REE can be used to correlate solute sources in natural waters to a specific lithology owing to their characteristic terrestrial, atmospheric and marine source signatures (Goldstein and Jacobsen, 1988; Palmer and Edmond, 1992; Sholkovitz, 1995; Aubert et al., 2001; Lawrence et al., 2006), but unlike $^{87}Sr/^{86}Sr$ isotopes, which are not significantly fractionated in rivers, REE can fractionate (Bau, 1999). The ionic radii of most trivalent REE are similar to that of Ca^{2+}, whilst the bigger Eu^{2+} has a similar radius to Sr^{2+} and thus, REE can substitute for these elements and thus, occur in rocks which contain Ca and Sr (Aide and Aide, 2012). In terms of REE's physical characteristics, they show very diverse behaviours which make them a useful additional tool for examining element distribution and cycling within the soil-plant-surface water ecosystem. Although not a primary focus of this study, REE and their behaviour in different media highlights complex fractionation owing to the environmental processes associated with element mobility and transfer between reservoirs.

(iii) *Geochemical fingerprinting of three early medieval archaeological populations in Co. Meath.*

Sr is a non-essential nutrient but readily substitutes for calcium (Ca), not only in geological materials, but also in plant and animal tissues. Strontium undergoes a cycling process in the biosphere whereby it is initially released from bedrock by weathering, then carried though the soil and enters the food chain by transfer into vegetation, animals and humans (Ericson, 1985). $^{87}Sr/^{86}Sr$ preserved in plants and animals are controlled by the bioavailable Sr during nutrient uptake. $^{87}Sr/^{86}Sr$ values, which can be characteristic of a region, are transferred through the biosphere without significant fractionation (Blum et al., 2000; Graustein, 1989). As a result, humans/animals consuming plants and drinking water from an isotopically constrained region can be linked to the source rock by the $^{87}Sr/^{86}Sr$ value in their tissue, sometimes enabling the reconstruction of an organism's origin (Bentley, 2006; Montgomery, 2010; Slovak and Paytan, 2012; Sillen and Kavanagh, 1982).

The geographic region of this research, Co. Meath, is an important archaeological area where centuries of excavation and study have produced a vast resource of ancient human and animal remains. Selected samples from this archive are contrasted to biosphere mapping values which act as a reference database of local $^{87}Sr/^{86}Sr$ ranges with a view to deciphering potential mobility in three early medieval Irish communities within a 30 km radius. The strength of this study lies in the combined use of multiple isotope systems ($^{87}Sr/^{86}Sr$, $\delta^{18}O$, $\delta^{2}H$, $\delta^{13}C$, $\delta^{15}N$), which improves the confidence at which the determination of non-locals can be made. Ranges in $\delta^{18}O$ and $\delta^{2}H$ values of bone collagen are used with $^{87}Sr/^{86}Sr$ to geochemically discriminate between potential areas of origin of the people whose skeletal remains are analysed here. In addition, $\delta^{15}N$ and $\delta^{13}C$ shed light on the relative importance of terrestrial and marine sources of foodstuffs. This information, supplied by multi-isotope data, broadens our view of the cultural dynamics of society during this period when used in combination with existing archaeological and artefactual evidence. Using several lines of evidence in this manner allows for comprehensive interpretations.

2 Structure and Layout

The structure of the thesis is based around the three central aims detailed above. Chapters Two, Three and Four, address aims (i), (ii) and (iii) respectively. The abstract and conclusion of each of these core chapters are self-contained, whilst the over-arching conclusions of these studies are synthesised in Chapter Five. The wider implications of the research findings to the study and use of element and isotope biosphere values for geographic discrimination are also discussed.

3 Author Contributions

The three core chapters (Two, Three and Four) of this thesis have been prepared as manuscripts for publication in selected academic journals. Several co-authors contributed to these bodies of work and details of their contribution are expanded on below. In each case, all co-authors edited the respective manuscripts. Dr. Quentin G. Crowley advised on all sections of the thesis and contributed through guidance, discussion and editing. Being first author, I wrote each of these manuscripts in their entirety.

Chapter 2: Marine-derived Strontium in the Terrestrial Environment: Implications for Biosphere Mapping
Authors: Ryan, S.E., Crowley, Q.G., Snoeck, C. and Deegan, E.
Contributions: S.E.R. conducted the fieldwork/sample collection and carried out the vast majority of isotopic analysis. E.D. permitted the inclusion of some unpublished data that were the subject of her M.Sc. thesis, supervised by Q.G.C. - C.S provided analytical assistance for samples analysed for $^{87}Sr/^{86}Sr$ composition at Vrije Universiteit Brussel. Financial support for the project was provide by Q.G.C. through a Geological Survey of Ireland shortcall grant.

Chapter 3: High Spatial Resolution Geochemical Mapping of Surface Processes: A Case Study in Ireland
Status: Submitted for publication in Applied Geochemistry.
Authors: Ryan, S.E., Snoeck, C., Crowley, Q.G. and Babechuk, M.G.

Contributions: S.E.R. designed the experiment, conducted the fieldwork/sample collection and prepared, carried out the vast majority of the isotope analyses and measured the element concentrations of the samples. Q.G.C. contributed through guidance, discussion and editing. M.G.B. provided analytical support for Q-ICP-MS measurements and carried out the data reduction of the resulting trace element dataset. C.S. permitted the inclusion of some unpublished data and provided analytical assistance for samples analysed for $^{87}Sr/^{86}Sr$ composition at VUB.

Chapter 4: Early Medieval Reliance on the Land and the Local: An integrated multi-isotope study ($^{87}Sr/^{86}Sr$, $\delta^{18}O$, $\delta^{2}H$, $\delta^{13}C$, $\delta^{15}N$) of diet and migration.

Authors: Ryan, S.E., Reynard, L.M., Crowley, Q.G., Snoeck, C. and Tuross, N.

Contributions: S.E.R. designed the experiment, obtained archaeological material and associated licenses, carried out sample preparation for both stable isotope measurements of bone collagen and tooth enamel sampling for $^{87}Sr/^{86}Sr$. L.M.R provided analytical support with stable isotope analyses. C.S. carried out ICP-MS $^{87}Sr/^{86}Sr$ analysis at VUB. Q.G.C. and N.T. supervised the project. N.T. provided financial support for all analyses. S.E.R. was supported by a Geological Survey of Ireland sponsored Fulbright scholarship for research at Harvard University.

References

Aide, M.T., and Aide, C., 2012, Rare Earth Elements: Their Importance in Understanding Soil Genesis: ISRN Soil Science, v. 2012, p. 1–11.

Aubert, D., Stille, P., and Probst, A., 2001, REE fractionation during granite weathering and removal by waters and suspended loads: Sr and Nd isotopic evidence: Geochimica et Cosmochimica Acta, v. 65, p. 387–406.

Bataille, C.P., Brennan, S.R., Hartmann, J., Moosdorf, N., Wooller, M.J., and Bowen, G.J., 2014, A geostatistical framework for predicting variations in strontium concentrations and isotope ratios in Alaskan rivers: Chemical Geology, v. 389, p. 1–15.

Bau, M., 1999, Scavenging of dissolved yttrium and rare earths by precipitating iron oxyhydroxide: Experimental evidence for Ce oxidation, Y-Ho fractionation, and lanthanide tetrad effect: Geochimica et Cosmochimica Acta, v. 63, p. 67–77.

Bentley, R.A., 2006, Strontium Isotopes from the Earth to the Archaeological Skeleton: A Review: Journal of Archaeological Method and Theory, v. 13, p. 135–187.

Bentley, R.A., and Knipper, C., 2005, Geographical patterns in biologically available strontium, carbon and oxygen isotope signatures in prehistoric SW Germany: Archaeometry, v. 47, p. 629–644.

Blum, J.D., Taliaferro, E.H., Weisse, M.T., and Holmes, R.T., 2000, Changes in Sr/Ca, Ba/Ca and $^{87}Sr/^{86}Sr$ ratios between trophic levels in two forest ecosystems in the northeastern U.S.A.: Biogeochemistry, v. 49, p. 87–101.

Capo, R.C., Stewart, B.W., and Chadwick, O.A., 1998, Strontium isotopes as tracers of ecosystem processes: Theory and Methods: Geoderma, v. 82, p. 197–225.

Ericson, J.E., 1985, Strontium isotope characterization in the study of prehistoric human ecology: Journal of Human Evolution, v. 14, p. 503–514.

Evans, J.A., Montgomery, J., Wildman, G., and Boulton, N., 2010, Spatial variations in biosphere $^{87}Sr/^{86}Sr$ in Britain: Journal of the Geological Society, London, v. 167, p. 1–4.

Fay, D., Kramers, G., and Zhang, C., 2007, Soil Geochemical Atlas of Ireland: Teagasc and Environmental Protection Agency Ireland, 1-120 pp.

Frei, R., and Frei, K.M., 2013, The geographic distribution of Sr isotopes from surface waters and soil extracts over the island of Bornholm (Denmark) – A base for provenance studies in archaeology and agriculture: Applied Geochemistry, v. 38, p. 147–160.

Frei, K.M., and Price, T.D., 2012, Strontium isotopes and human mobility in prehistoric Denmark: Archaeological and Anthropological Sciences, v. 4, p. 103–114.

Goldstein, S.J., and Jacobsen, S.B., 1988, Rare earth elements in river waters: Earth and Planetary Science Letters, v. 89, p. 35–47.

Gosz, J.R., and Moore, D.I., 1989, Strontium isotope studies of atmospheric inputs to forested in New Mexico watersheds: Biogeochemistry, v. 8, p. 115–134.

Graustein, W.C., 1989, $^{87}Sr/^{86}Sr$ ratios measure the sources and flow of strontium in terrestrial ecosystems: Stable isotopes in ecological research, p. 491–512.

Graustein, W.C., and Armstrong, R., 1983, The use of $^{87}Sr/^{86}Sr$ ratios to measure atmospheric transport into forested watersheds: Science, v. 219, p. 289–292.

Lawrence, M.G., Greig, A., Collerson, K.D., and Kamber, B.S., 2006, Rare earth element and yttrium variability in South East Queensland waterways: Aquatic Geochemistry, v. 12, p. 39–72.

Maurer, A.-F., Galer, S.J.G., Knipper, C., Beierlein, L., Nunn, E. V, Peters, D., Tütken, T., Alt, K.W., and Schöne, B.R., 2012, Bioavailable $^{87}Sr/^{86}Sr$ in different environmental samples-effects of anthropogenic contamination and implications for isoscapes in past migration studies.: The Science of the Total Environment, v. 433, p. 216–29.

Montgomery, J., 2010, Passports from the past: Investigating human dispersals using strontium isotope analysis of tooth enamel.: Annals of human biology, v. 37, p. 325–46.

Palmer, M.R., and Edmond, J.M., 1992, Controls over the strontium isotope composition of river water: Geochimica et Cosmochimica Acta, v. 56, p. 2099–2111.

Price, T.D., Burton, J.H., and Bentley, R.A., 2002, The characterization of biologically available strontium isotope ratios for the study of prehistoric migration: Archaeometry, v. 1, p. 117–135.

Sholkovitz, E.R., 1995, The aquatic chemistry of rare earth elements in rivers and estuaries: Aquatic Geochemistry, v. 1, p. 1–34.

Sillen, A., and Kavanagh, M., 1982, Strontium and paleodietary research: A review: American Journal of Physical Anthropology, v. 25, p. 67–90.

Slovak, N.M., and Paytan, A., 2012, Applications of Sr isotopes in archaeology, in M. Baskaran (Ed.), Handbook of Environmental Isotope Geochemistry: Springer Berlin Heidelberg, p. 743-768.

Voerkelius, S., Lorenz, G.D., Rummel, S., Quétel, C.R., Heiss, G., Baxter, M., Brach-Papa, C., Deters-Itzelsberger, P., Hoelzl, S., Hoogewerff, J., Ponzevera, E., Van Bocxstaele, M., and Ueckermann, H., 2010, Strontium isotopic signatures of natural mineral waters, the reference to a simple geological map and its potential for authentication of food: Food Chemistry, v. 118, p. 933–940.

Chapter 2: Marine and Anthropogenic-derived Strontium in the Terrestrial Environment: Implications for Biosphere Mapping

Co-authors: Quentin G. Crowley, Eileen Deegan and Christophe Snoeck

Abstract

Spatial variations in strontium isotopes, expressed as $^{87}Sr/^{86}Sr$, are translated from bedrock through the biosphere without significant fractionation from environmental or biological processes. Consequently, $^{87}Sr/^{86}Sr$ may be used as a geochemical tracer for multiple applications including characterising animal and archaeological human population dynamics and/or migration patterns. This practice requires careful characterisation of environmental values, from soils, plants and surface waters and necessitates an understanding of how $^{87}Sr/^{86}Sr$ is affected by variable bedrock compositions, differential weathering processes, mineral soil formation, as well as possible atmospheric/marine and anthropogenic inputs. Here, geochemical mapping and analyses of $^{87}Sr/^{86}Sr$ values from vegetation, bulk soils, water-soluble soil extracts and surface water is used to investigate and quantify the extent of marine-derived Sr in the terrestrial biosphere. Samples were collected across a broad area of Ireland from both coastal and inland regions, encompassing a wide variation in bedrock lithologies and at varying distances from the coastline. The $^{87}Sr/^{86}Sr$ signature of vegetation from coastal sites was found to be strongly affected by marine inputs with plants growing within 1 km from the coastline having on average 84% (n = 5, SD = 3%) of their Sr budget originating from marine sources and this fraction decreases inland.

Topsoil samples from regions along the western coastline and regions of blanket peat coverage are enriched in Sr, Na and Ca cations, which indicates a considerable marine geochemical contribution to those coastal environments. Strontium isotope, major and trace element data of surface water from the River Main catchment, located in County (Co.) Antrim, Ireland are presented. $^{87}Sr/^{86}Sr$ and Sr concentrations reflect water-rock interaction between run-off that has interacted with local basalt bedrock and atmospherically-derived Sr. These data plot systematically along a

$^{87}Sr/^{86}Sr$ vs. 1/Sr binary mixing line, clearly demonstrating mixing between these distinctive geochemical reservoirs. Correlations between river water $^{87}Sr/^{86}Sr$ composition with major and trace elements, including Ca, Na, Al and Y/Ho, are calculated and discussed.

Tree cores were taken from beech trees, *Fagus sylvatica L.,* spanning 100 years of age and their geochemical archives are explored in order to examine changes in element availability and sources over time, including $^{87}Sr/^{86}Sr$ composition. There is a progressively decreasing concentration trend observed in the cores for several elements including strontium and calcium. The variation imposed by intensified use of modern fertilisers was observed with a small but notable offset in $^{87}Sr/^{86}Sr$ values pre- and post-1956. Thus, these time-resolved data provide a better context of past element behaviour in this setting.

Atmospheric and anthropogenic derived-Sr contributions to surface water, plants and soils, as demonstrated in this study, highlight that studies employing $^{87}Sr/^{86}Sr$ biosphere data for the purposes of provenancing must account for non-geosphere cation sources. $^{87}Sr/^{86}Sr$ biosphere maps inferred from bedrock compositions are of limited use in most coastal areas, peat bogs or regions subject to high precipitation, or where anthropogenic inputs to the Sr budget are a possibility.

1 Introduction

The Rb-Sr decay system and Sr isotopes have been used extensively as a geological dating tool and for magmatic tracing, however, Sr isotopes have become more recently valued as an effective agency for provenance studies and tracing environmental processes. Natural variations in $^{87}Sr/^{86}Sr$ ratios from different reservoirs make it possible to trace certain processes operating within the biosphere-geosphere interface (Capo et al., 1998). However, to use Sr as a tracer, reference data are required for the geographical locations under study. Notably, within Europe country-scale isoscapes have been produced for Britain (Evans et al., 2010), Denmark (Frei and Frei, 2011, 2013) and France (Willmes et al., 2014). The Aegean has also been mapped (Nafplioti, 2011) and mineral waters have been analysed from all across Europe (Voerkelius et al., 2010; Montgomery et al., 2006). To date, only a very limited number of studies have assessed $^{87}Sr/^{86}Sr$ variation in the Irish biosphere through the use of plants, natural water and/or soils (Knudson et al., 2012; Voerkelius et al., 2010; Snoeck et al., 2016; Cahill Wilson and Standish, 2016; Kador et al., 2014; Sheridan et al., 2013; Wallace et al., 2010), with some studies using British biosphere values for baseline estimates (Montgomery et al., 2014).

Sr undergoes a cycling process in the biosphere whereby it is initially released from bedrock by weathering and then transferred through the soil, vegetation and ingested by animals and humans (Bataille and Bowen, 2012; Laffoon et al., 2012; Bentley, 2006; Montgomery, 2010). $^{87}Sr/^{86}Sr$ vary with Rb/Sr ratios and the age of the material (Faure and Powell, 1972) and as natural/biological processes do not significantly fractionate Sr isotopes, the $^{87}Sr/^{86}Sr$ ratio of a geographic area can strongly reflect that of the underlying geology as $^{87}Sr/^{86}Sr$ signatures are transferred from the bedrock to overlying soils (Graustein, 1989). However there can be other important controls on the $^{87}Sr/^{86}Sr$ ratios of overlying soils and vegetation, which can result in biosphere averaging (Blum et al., 1993; Capo et al., 1998; Miller et al., 1993). The measured differences in $^{87}Sr/^{86}Sr$ ratios are the result of mixing of Sr from different sources with different isotopic compositions (Faure and Powell, 1972). Non-local sources of Sr, such as sea-spray, rainfall and fertilisers, can produce a skewed value from the otherwise bedrock-predicted biologically-available Sr. Biosphere samples may become homogenised or reflect more the $^{87}Sr/^{86}Sr$ signature of a particular reservoir

of Sr. Therefore, rather than looking at the $^{87}Sr/^{86}Sr$ signatures in biosphere samples as a direct translation from bedrock, it is more appropriate to examine them in terms of a mixing system with inputs and outputs from different reservoirs (Bentley, 2006). $^{87}Sr/^{86}Sr$ from geological material and models based on bedrock age (West et al., 2009; Beard and Johnson, 2000) have been used as a reference for potential variation. However, whilst such a method can be useful at large scales and in environments that are not subject to Sr enrichment from seawater, $^{87}Sr/^{86}Sr$ values inferred from geological maps may not be appropriate for provenance-orientation studies and their interpretation of archaeological data in island or coastal environments.

Here, the following question is addressed:
Is the Sr composition of the Irish biosphere measurably influenced by the input of sea salts via the atmosphere and if so, how far inland can this effect be observed? This is done at:

1. a local-scale by measuring $^{87}Sr/^{86}Sr$ ratios of (a) plants taken along coastal transects, (b) a local river with a constrained catchment bedrock $^{87}Sr/^{86}Sr$ composition and (c) tree cores to provide a time-resolved record of changes in chemical composition over the last 100 years.
2. at a regional-scale examining soil geochemistry, using seawater-characteristic Na concentrations as a reference, to determine if the marine chemical fingerprint can be traced in topsoils (A-horizon).

1.1 Influence of atmospheric-derived Sr

In coastal areas, both sea spray and rainfall have $^{87}Sr/^{86}Sr$ indistinguishable or very close to that of present-day seawater with a value of 0.7092 (Hess et al., 1986; McArthur et al 2001). This value is intermediate between oceanic basalts (0.703–0.706) and continental rocks (0.710–0.740) (Clarke and Fritz, 1997). The influence of marine-derived Sr on terrestrial ecosystems, particularly in coastal regions subject to direct sea salt deposition, is an important consideration when characterising human and animal $^{87}Sr/^{86}Sr$ signatures because biosphere components can incorporate Sr that reflects this distinct marine/atmospheric contribution (Bentley et al., 2003; Whipkey

et al., 2000; Grupe et al., 2011). The cycling of elements such as strontium and calcium is of interest due to the extensive use of Sr as a tracer of soil-plant-atmosphere processes and of calcium, as an essential plant nutrient. Whilst these elements are predominantly supplied by weathering of parent bedrock to the soil, atmospheric/marine-derived inputs of these cations can dominate in certain environments such as the Hawaiian Islands (Kennedy et al., 1998; Vitousek et al., 1999; Whipkey et al., 2000). Marine aerosol is generated by the formation and bursting of bubbles in the open sea (Woodcock, 1953). While large particles are deposited rapidly on the ocean, smaller particles are carried onshore but the amount of sea salt deposited in an interior location decreases rapidly as it moves away from the coast (Guelle et al., 2001). Large quantities of marine aerosols can be deposited in the terrestrial biosphere by onshore winds, which are predominantly coming from the Atlantic on the west coast of Ireland. These aerosols are then deposited and mixed into the soil profile by precipitation and runoff.

Although rainwater and seawater generally have a very close isotopic composition, the concentration of Sr is significantly less with ocean water concentrations being about 100 times that of rainwater (Bentley, 2006). Based on $^{87}Sr/^{86}Sr$ values alone, it is difficult to separate sea-spray and rainfall into distinguishable endmembers as both components are derived from seawater and therefore will have the same isotopic ratio as seawater itself (0.70918). As rainwater tends to have low Sr concentrations relative to plants and soil water, the effect of rainfall on the terrestrial biosphere is more strongly noticed in regions of consistent high precipitation, such as the western coast of Ireland and parts of Britain (Evans et al., 2009, 2010) or coastal areas subject to sea-spray/sea-splash (Whipkey et al., 2000; Montgomery et al., 2006; Vitousek et al., 1999; Evans and Bullman, 2009; Frei and Frei, 2013). As Ireland has such a large stretch of coastline relative to landmass, two of the main factors to be taken into account when examining the Sr contributions to the biosphere are rainwater and sea-spray. As seen from the Mean Annual Rainfall map (Fig. 1), the western areas receive high levels of rainfall (>1600 mm/annum) compared to other parts of the country, suggesting that these are regions that are likely to be influenced by marine processes.

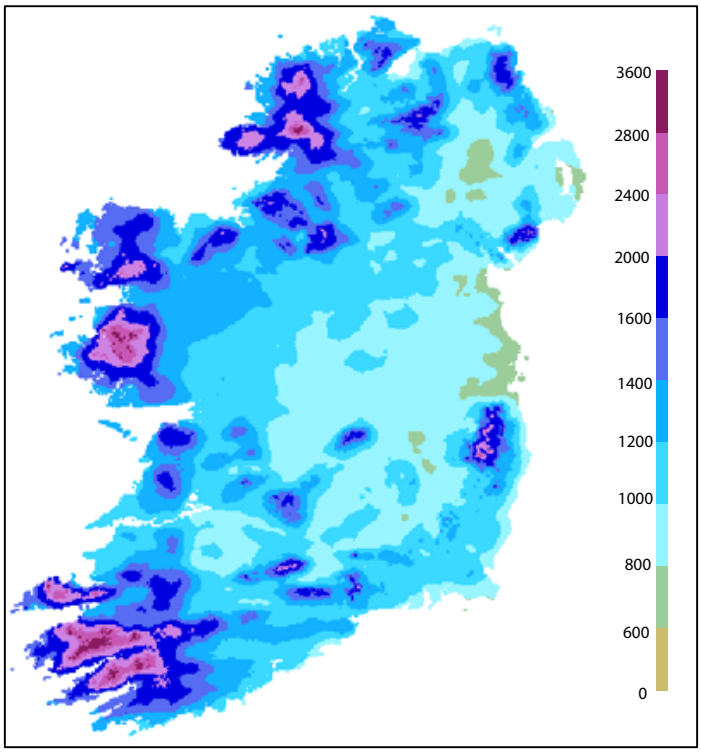


Figure 1. Mean Annual Rainfall (mm) 1981-2010. Reproduced with permission from Met Éireann.

Here, Sr isotopic and geochemical data from temperate coastal sites in Ireland are presented and discussed. The marine contribution of Sr from representative coastal settings in Ireland to both plants and soils are quantified by using $^{87}Sr/^{86}Sr$ values and the cation content of topsoils collected from the national database, Tellus. The main objective is to identify areas where there is significant atmospheric/direct sea-spray contributions of strontium to the terrestrial coastal biosphere. Ireland provides an ideal study site in that it has an extensive coastline on the western-most extremity of Europe.

The distance over which marine Sr is transported inland is estimated to range 100-150 km (English et al., 2001, Reimann 2000). Based on measurements from fresh snow across a 450 km long transect across the Scandinavian Peninsula, seawater was found to contribute about 90%, with a $^{87}Sr/^{86}Sr$ ratio of 0.7098, in close proximity to the Atlantic coast, whilst marine contribution diminished to 10-30% at 300 km inland (Andersson et al., 1990). In Ireland, stable sulphur isotope ratios ($^{34}S/^{32}S$) were used as a tracer of marine input and the inland extent of a coastal signal (Zazzo et al., 2011) where the relative proportion of marine S in wool keratin was found to be negatively correlated with distance to the west coast; Almost all sulphur contained in west coast

wool is of marine origin, with relatively high ^{34}S values remaining >100km inland. In a study by Aherne and Farrell, (2002) it was found that there was a decline in the proportion of sea-salt sulphate contained in precipitation, from 70% in the west to <15% in the east of Ireland. These studies illustrate that the marine contribution of S is significant and emphasise the need to quantify this potential influence on other elements in the biosphere, including Sr.

Numerous studies have demonstrated atmospheric derived Sr as a potentially important, even dominant, source in soil-plant systems (Capo et al., 1998; Miller et al., 1993; Åberg et al., 1989; Gosz and Moore, 1989; Graustein and Armstrong, 1983; Chadwick et al., 1999; Kennedy et al., 1998; Vitousek et al., 1999; Whipkey et al., 2000; Laffoon et al., 2012; Shaw et al., 2009; Probst et al., 2000; Hodell et al., 2004; Warham, 2012; Montgomery et al., 2007). In the Hawaiian Islands, atmospheric inputs were found to supply >85% of the Sr budget in the soil with a change from weathering to atmospheric sources of Sr with increasing substrate age (Kennedy et al., 1998;Whipkey et al., 2000). In a temperate forest environment, Kennedy et al., (2002) noted that atmospheric Sr dominated the cations taken up by trees (90%). In natural soil profiles at a coastal site in South Australia, the $^{87}Sr/^{86}Sr$ of soil labile cations were >90% sourced from marine solutes in rainfall (Green et al., 2004). In Scandinavia, seawater was found to contribute about 90% of the Sr to snow in close proximity to the coast, but only contributes about 10-30% 300 km further inland (Andersson et al., 1990).

In environments that are more comparable to Ireland such as the Outer Hebrides, in NW Scotland, seawater Sr dominates with biosphere $^{87}Sr/^{86}Sr$ below 0.7105, despite the island being underlain by radiogenic granites and gneisses ($^{87}Sr/^{86}Sr$ ~0.715), (Montgomery et al., 2003). Evans et al., (2010) emphasise the capacity of precipitation to alter $^{87}Sr/^{86}Sr$ in marine settings and suggest that rainwater acts to dampen $^{87}Sr/^{86}Sr$ relative to the bedrock contribution. The above studies demonstrate that atmospheric deposition can supply a significant proportion of the nutrient cations in certain terrestrial ecosystems.

1.2 Cation ratios

Tellus (covering the North of Ireland) and Tellus Border (extending to the border counties) are geochemical surveying projects carried out by the Geological Survey of Northern Ireland and the Geological Survey of Ireland respectively. The Tellus database is ideal for use as part of this project as it extends over a large geographic area of Ireland (approximately 26,100 km^2) with high topsoil sample density (one sample per 2 km^2 for Tellus and one sample per 4 km^2 for Tellus Border). Integrating such extensive datasets provides a robust comparative dataset for use in combination with transect samples analysed for their Sr isotope composition. Topsoil geochemistry generally reflects that of the parent bedrock but here, it is examined if a marine chemical source is a significant contributor in coastal sites.

Na, Ca and Sr cation concentrations and molar cation ratios can be used to assess differences in relative element content geographically in soil. For island regions, such as Ireland, the main source of base cation particles, especially sodium and magnesium, is the aerosol produced from the sea surface (sea salt aerosol (SSA)) (Werner et al., 2011). The highest values of total SSA emission are noted for regions with the highest wind speed, especially over the North Atlantic Ocean. Using the Fine Resolution Atmospheric Multi-pollutant Exchange Model (FRAME), a gradient in concentration is observed from the coastal regions towards low concentrations over land in the UK (Werner et al., 2011). Observed coastal-terrestrial gradients in Sr and Na in moss from Oslo were attributed to the steady input of marine aerosols near the coast (Reimann et al., 2006).

Sodium is a standard reference element for comparison with other ions for determining seawater influence in the atmosphere and in precipitation (Berner and Berner, 1987). Na, Sr and Ca have conservative concentration profiles in the oceans (Millero and Sohn, 1992) with some systematic variations with depth and at coastal fresh water-marine mixing areas (de Villiers and Nelson, 1999). In highly weathered soils, replenishment of certain cations sourced from the parent material may not compensate for the rate at which they are lost through weathering and leaching of the soil profile (Likens et al., 1996) and thus, the degree of weathering of the soils is an important factor in the availability of cations. In heavily weathered rainforest soils,

the predominant input of cations was found to be atmospheric, while arid to semi-arid soils and very young soils are dominated by parent material weathering (Whipkey et al., 2000), hence the degree of weathering is a key factor in atmospheric cation availability. Examining the chemistry of the quasi-total (aqua-regia digested) topsoil, with a focus on marine fingerprinting elements informs on the sources and availability of Sr in soils.

Mapping the 'raw' or 'absolute' element data as point data is useful as it facilitates the detection of local deviations from the dominant process in an area (Reimann, 2005). Such maps can be informative but an issue arises from the compositional nature of the dataset i.e. geochemical components form a multivariate system which should generally be analysed as a whole, not component-wise (McKinley et al., 2016). These authors investigated the limitations imposed by the compositional nature of geochemical data on the presentation and interpretation of such values. The limitations are caused by the constant sum (closure) effect (Chayes, 1960) whereby if one component increases (due to the addition of a pollutant or a diluent) the mass of all other components remains unaffected, and their apparent proportions (concentrations) must decrease (Tolosana-Delgado and van den Boogaart, 2013). Patterns, trends or anomalies could misleadingly be an artefact of the constant sum constraint. To account for the relative nature of geochemical data, element (log)-ratios are used in addition to individual element concentrations, since (log)-ratios are not confined by unit or any other fixed sum constraint of components (McKinley et al., 2016).

1.3 Atmospheric and geogenic Sr systematics in mineral waters

One of the limitations of using Sr isotopes for provenance, both in terms of geochemical tracing in environmental samples and in human/animal migration studies, is the lack of constrained information about the relative contribution of Sr from various sources. Mass balance equations and isotope mixing models (Bataille et al., 2014; Montgomery et al., 2007) can be used to quantify the proportion of Sr in a mixture of different end-members and can therefore aid with elucidating the weighted sources of Sr to the biosphere. The sources of Sr controlling the $^{87}Sr/^{86}Sr$ composition of surface water are constrained by the relationships between the Sr isotopic composition and concentration ratios (Négrel et al., 2001, 2004; Roy et al., 1999;

Hogan et al., 2000; Shand et al., 2009). In doing so, the mixing of Sr between different reservoirs in the biosphere can be modelled, allowing one to discriminate between the inputs from various sources using.

As Ireland is subject to high rainfall levels, biosphere $^{87}Sr/^{86}Sr$ in many environments will have two dominant end-members: atmospheric and weathering inputs. The relative input from these distinct reservoirs to the hydrological system is examined in this study. Several Sr isotope studies of rivers and lakes have produced information on the sources of Sr and the mixing of waters of various origins with different $^{87}Sr/^{86}Sr$ and Sr contents (e.g. Négrel et al., 2000; Négrel and Roy, 1998; Négrel, 2006; Négrel and Deschamps, 1996; Semhi et al., 2000, 2009; Bain and Bacon, 1994; Ojiambo et al., 2003; Bain et al., 1998) and here the mixing relationship is used to infer the degree to which marine-Sr influences a local river system in Co. Antrim.

1.4 Time-resolved changes in Sr recorded by trees

Tree cores can be used as time-resolved records of environmental change given that the annual growth patterns serve as incremental archives of past chemical changes. Trace element concentrations measured from tree cores have been used extensively to reconstruct past pollution (e.g. Barnes et al., 1976; Beramendi-Orosco et al., 2013; Padilla and Anderson, 2002; Cui et al., 2013; Miller et al., 2014; Rich et al., 2012; García-Suárez et al., 2009; Yu et al., 2007; Baes and Mclaughlin, 1984) Such monitoring of past element sourcing is based on the assumption that measured compositions of tree rings reflect the element availability for uptake by the tree (Hagemeyer, 1993; Stille et al., 2012). $^{87}Sr/^{86}Sr$ values recorded by tree rings have been used to examine changes in the prominent element reservoir sources over time (Drouet et al., 2005; Åberg et al., 1990; Poszwa et al., 2003) and similarly, in this study, $^{87}Sr/^{86}Sr$ values from two tree cores from Co. Antrim are examined to test if patterns of past atmospheric rainfall deposition are recorded. By measuring $^{87}Sr/^{86}Sr$ in a core from a tree growing on modern agricultural soils and the other from an undisturbed woodland it is also possible to assess the degree to which anthropogenic inputs of Sr have changed the local biosphere $^{87}Sr/^{86}Sr$ values over time.

2 Materials and Methods

A geological map of Ireland (Geological Survey of Ireland, 2016) was initially used for the identification of possible sample sites on the basis of variations in underlying bedrock and surficial geology. Both soil and vegetation samples were collected from localities in NW, NE, E and SE Ireland and co-ordinates were recorded using a hand-held GPS. Sample localities encompass a wide range of geological strata and vary in distance from the coast (see Fig. 2).

2.1 Sample Collection and Preparation

The sampling methods followed in this study were adapted from those outlined by the Geochemical Baseline Survey of the Environment (GBASE), British Geological Survey (BGS) (Johnson et al., 2005; Smyth, 2007, Smyth & Johnson). Disturbed/agricultural land was avoided. Soil samples were taken from a depth of 5-20cm. All samples were air dried and subsequently dried in an oven at 120°C for 24 hours. The vegetation collected consisted of twiggy deciduous material that was broken into approximately 0.5cm pieces and milled in a planetary mill (with zirconium oxide grind bowls and balls). Additionally, tree cores were taken from two beech trees, *Fagus sylvatica L.*, both on the same bedrock, the Upper Basalt Formation in Co. Antrim. One tree was selected from an agricultural site and the other was growing in an undisturbed woodland. Trees were within ~600 m of each other, which ensured that the trees were receiving similar atmospheric and bedrock Sr input. Two cores were taken from the north and south side of each tree using a 5.15 mm diameter increment borer to characterise natural heterogeneity within each tree and between trees. The fine rooting depths of beech trees are shallow (Schmid, 2002), and soil cover was relatively thin with some roots growing directly on rock. Cores were stored in paper straws before being prepared for analysis.

Streamwater was collected from the active portions of small first- and second-order catchment locations that integrate material from an area of no more than a few square kilometres. The ‘clean hands, dirty hands’ sampling procedure (U.S. EPA, 1996) was adopted. Water samples were collected in acid-cleaned polypropylene bottles filtered

immediately by 0.45 μm pore size Millipore HDPE membranes, acidified with ultrapure HNO_3 (to 1% v/v) and stored refrigerated (~4°C) until analysis.

Soil can be deemed to consist of two major phases: the unleachable detritus and the leachable pool (Sholkovitz et al., 1994). To separate these two major phases and hence characterise the bioavailable Sr that can be desorbed by natural solutions in the soil (soil-exchangeable cations) leaching experiments using ultra-pure H_2O were performed on selected soil samples and bulk soil was analysed to assess the whole pool of cations (mineral fraction).

The soil samples were sieved to 2mm and milled as for the vegetation samples and combusted at 600°C for 2 hours. For leaching the soils, a 1g aliquot of the untreated bulk soil was shaken with 10ml of deionised H_2O and allowed to leach at room temperature for 24 hours. A single extraction method using a simple deionised water leach is recommended by (Ettler et al., 2007) for mobilisation of soil cations as it is efficient for an estimate of the easily-exchangeable soil fraction.

2.2 Sample Digestion

Fieldwork and subsequent sample analyses were split over two years and carried out in multiple laboratories (University College Dublin, Vrije Universiteit Brussel, NERC British Geological Survey, Queen's University Belfast Dendrochronology Laboratory and University of Cambridge). Digestion of plant samples at Vrije Universiteit Brussel differed slightly, following the method outlined in Snoeck et al., (2016) and $^{87}Sr/^{86}Sr$ were analysed on a Multi-Collector Inductively-Coupled-Plasma Mass-Spectrometry (MC-ICP-MS) following the procedure detailed in (Snoeck et al., 2015). Samples analysed at NERC, BGS, followed a modified procedure outlined in the supplementary material in Evans et al., (2010), with $^{87}Sr/^{86}Sr$ measured on a Thermo Scientific Triton Thermal Ionisation Mass Spectrometer (TIMS). All details outlined below relate to the analyses carried out at University College Dublin (UCD) and University of Cambridge.

Bulk soil samples were digested in 5ml 48% HF and 1ml 15M HNO_3 for approximately 18 hours. Samples were digested in acid-cleaned Savillex Teflon beakers in Parr bombs at 150°C for 48 hours and dried down. They were then converted to nitrate to break down any insoluble fluorides by the addition of three 1ml aliquots of 15M HNO_3, drying on the hotplate after each addition. To subsequently convert the sample to chloride, 1ml of 6M HCl was added. On dryness, 10ml 6M HCl was added and left for approximately 18 hours after which they were dried. Samples were converted to nitrate by adding 1ml 8M HNO_3, three times and dissolving the residue in 2ml of 1M HNO_3. Vegetation samples followed the same procedure, except HF was not used and an extra 4ml 1M HNO_3 was added at the end of the digestion. The samples were then taken up in 1M HNO_3 and centrifuged.

15 mL of sample was evaporated in PMP beakers to which 1 mL of concentrated HNO_3 was subsequently added and left to react for approximately 12 hours in order to attack organics and convert to nitrate for loading on the column. The concentrated HNO_3 was then evaporated and the sample was redissolved in 2 mL of 2 mol/L HNO_3

Soil samples used to evaluate cation composition were collected during the Tellus and Tellus Border Surveys and were prepared using a slightly modified methodology from that outlined above: Topsoils from a depth of 5-20 cm were collected, dried, sieved to 2 mm and homogenised. A 1g sub-sample of the Tellus soils was digested in aqua regia, followed by trace element analysis by ICP-OES and ICP-MS at SGS Laboratories (Toronto).

2.3 Separation of Strontium

Separation of Sr was achieved using SrSpec ion resin (Horwitz et al., 1992), contained in a modified 5ml pipette tip (Charlier et al., 2006). Dissolved samples were centrifuged for 30 minutes at 5000rpm and loaded on columns equilibrated to 1M HNO_3. 1ml of 1M HNO_3, followed by 3ml 8M HNO_3 was added. The eluent was discarded and Sr was eluted using 2ml 0.05M HNO_3. From these eluted samples, 0.1ml (i.e. 5% of the sample) was analysed on a multi-collector ICP-MS at University College Dublin to determine the approximate Sr concentration. This portion was

diluted with 0.9ml of 3% HNO_3 and centrifuged before analysis. The remaining solution containing the eluted Sr was dried down. 1ml of concentrated HNO_3 was added and these solutions were dried down again.

2.4 Quadrupole ICP-MS (TCD)

An aliquot of each of the solutions was sub-sampled for trace element analysis using solution quadrupole ICP-MS on the Thermo Scientific™ iCAP Qs™ at the Geochemistry Laboratories at Trinity College Dublin. The machine was calibrated by using United States Geological Survey (USGS) W-2a (diabase from Bull Run quarry near Centreville, Virginia). The experiment design followed that outlined by Eggins et al. (1997), with some adaptions to the method which have been documented in detail by Kamber et al. 2003 and Babechuk et al. 2010). The main methods are summarised below:

The aliquot of stock solution was diluted to produce a 2% HNO_3 solution. Internal standard was added to this, which is composed of a mixture of ^{6}Li, Rh, Re, Bi and ^{235}U and was used for drift correction and signal suppression. Before each set of trace element runs on the unknowns, two prep-experiments were carried out. The first measured the U and Li isotopes in the standards JR-1 (GSJ) and BHVO-2 (USGS) in order to get the pre-enriched, natural contribution to the unknowns (Eggins et al., 1997). The second experiment estimated the rate of production of oxides by analysing solutions with Ba, Nd, Dy and Zr (Ulrich et al., 2010). Following the analysis of procedural blanks, standards and unknowns were bracketed with a drift monitor solutions between each ~7 samples for the purpose of drift correction.

2.5 Thermal Ionisation Mass Spectrometry (TIMS)

A Thermo Scientific Triton Thermal Ionisation Mass Spectrometer (TIMS) was used for Sr isotope analyses. 500ng of Sr was loaded onto outgassed Re filaments with 1µl of a TaF_5 activator. Four filaments were loaded with SRM-987. Sr isotopes were measured in static mode using Faraday cups, which were calibrated immediately

before each batch of analyses to reduce bias from the Faraday amplifiers. A rotation of the Faraday amplifiers was also carried out during the analysis to further eliminate any bias. The cup configuration was as follows; 84 in L1; 85 in C; 86 in H1; 87 in H2 and 88 in H3.

^{87}Sr values were corrected for ^{87}Rb interference and data were normalised to the long-term mean standard SRM-987 $^{87}Sr/^{86}Sr$ value of 0.710246 ± 0.000011 (2SE). Analyses of the NBS SRM 987 reference material gave $^{87}Sr/^{86}Sr$ values of 0.710247, 0.710251, 0.710245 and 0.710245 in good agreement with the long-term mean stated above. Total procedural blanks were on average 1.5 ng and thus, were too low to have any significant effect on the results. Procedural blanks for streamwater samples were <80 pg.

2.6 Equations

Contribution of sea-salt in Tellus topsoils was estimated using an ocean enrichment factor (EF_o) relative to sea-salt-sodium (ssNa), chosen for being the major constituent of sea salt (Weller et al., 2008; Dixon et al., 2013), using the following equation (Osterberg, 2007):

$$EF_O = \left(\frac{Sr_{soil}/Na_{soil}}{Sr_{ref}/Na_{ref}} \right) \qquad \text{Eqn. (1)}$$

Where Sr_{soil} and Na_{soil} are the Sr and Na concentration in the soil sample and Sr_{ref} and Na_{ref} are the Sr and Na concentration in the reference material which was average composition of ocean water (Lide, 2003).

These Tellus data were examined before sampling and analysing plant transects to gauge the extent of the coastal buffer zone which can be characterised by high Sr concentration.

In a two-component system, the contribution of Sr from component$_1$ (seawater) to a mixture is calculated using a simple proportional calculation between the isotopic ratios of the mixture and the end-members. The relative contribution of Sr from sea-

spray/rainfall (component$_1$) and soil mineral weathering products (component$_2$) was calculated using the equation below (Capo et al., 1998; Miller et al., 1993):

$$\% \text{ contribution} = \left(\frac{^{87}Sr/^{86}Sr_{MIXTURE} - ^{87}Sr/^{86}Sr_2}{^{87}Sr/^{86}Sr_1 - ^{87}Sr/^{86}Sr_2} \right) * 100 \qquad \text{Eqn. (2)}$$

$^{87}Sr/^{86}Sr$ of the mixture is calculated using the following equation from Hosono et al., (2007):

$$(^{87}Sr/^{86}Sr)_x = (^{87}Sr/^{86}Sr)_1 (Sr_1/Sr_x) f + (^{87}Sr/^{86}Sr)_2 (Sr_2/Sr_x)(1 - f) \qquad \text{Eqn. (3)}$$

where *f is* the % contribution and Sr_1, Sr_2 and Sr_x are the concentrations of component 1 and 2 and the mixture respectively.

$^{87}Sr/^{86}Sr$ were normalised to seawater composition for ease of comparison and to identify more readily the amount each sample deviates from the $^{87}Sr/^{86}Sr$ seawater value, reported as per mil (‰) deviations from modern seawater of 0.70918 (Stewart et al., 1998; McArthur et al., 2001) using the following equation:

$$\delta^{87}Sr = 10^3 \left[\frac{^{87}Sr/^{86}Sr_{SAMPLE}}{^{87}Sr/^{86}Sr_{SEAWATER}} - 1 \right] \qquad \text{Eqn. (4)}$$

This method also emphasises small but significant variations in $^{87}Sr/^{86}Sr$.

3 Results and Discussion

3.1 Sr variability of coastal transect samples

Large variations in both $^{87}Sr/^{86}Sr$ and Sr concentrations exist between sample sites (Table 1). Bulk soil $^{87}Sr/^{86}Sr$ ranges from 0.7089 to 0.7326, soil leachates range from 0.7093 to 0.7180 and vegetation $^{87}Sr/^{86}Sr$ range from 0.7082 to 0.7142. Sr concentrations range from 58.1 to 177.4 mg/kg for soil, whereas the vegetation samples display a wider range from 65.2 to 356.3 mg/kg (Table 1). The diverse $^{87}Sr/^{86}Sr$ and Sr concentrations reflect the complex mixing of Sr from the range of underlying bedrock types and marine contributions. Whilst geographic variability in $^{87}Sr/^{86}Sr$ across Ireland was noted (Table 1), $^{87}Sr/^{86}Sr$ variability also exists between sample media collected above the same lithology. When comparing vegetation and bulk soil samples collected over the study area, it is evident that they have widely dispersed $^{87}Sr/^{86}Sr$ values with vegetation samples having a much smaller range compared to soil samples. The standard deviation of the bulk soil $^{87}Sr/^{86}Sr$ (0.00742) was more than 5.5 times greater than that of the plant material (0.00134), with vegetation collectively falling much closer to seawater $^{87}Sr/^{86}Sr$.

Sample I.D.[a]	Tellus I.D.	Publish-ed I.D.	Age bracket	Unit label	Geological Formation	Sample Type	Sample Locality	Easting[b]	Northing[b]	Distance from coast(m)	[Sr] (ppm)	$^{87}Sr/^{86}Sr$[c]	Std Err 2σ	Lab I.D.	$\delta^{87}Sr_{seawater}$[d]
1S	581029		Caledonian (Silurian - Devonian)	7	Caledonian Appinite suite	Soil	Donegal	178936	391450	-	148.5	0.724093	0.000004	UCD	21.0
DL1V	588318					Shrub	Donegal	179618	403257	100	206.0	0.709678	0.000004	UCD	0.7
DL1S	580957					Soil	"	179000	405001	100	114.0	0.711019	0.000005	UCD	2.6
DL1L						Soil leach	"	179000	405001	100	-	0.709270	0.000010	BGS	0.1
DL2V	588387					Shrub	"	191549	410963	16000	183.0	0.709635	0.000004	UCD	0.6
DL2S	581004					Soil	"	192705	411380	16000	113.1	0.710494	0.000005	UCD	1.9
DL2L						Soil leach	"	192705	411380	16000	-	0.709325	0.000010	BGS	0.2
2S	580829					Soil	"	196762	416433	16000	165.1	0.711112	0.000004	UCD	2.7
3V						Tree	Wexford	312554	105177	-	-	0.710386	0.000010	BGS	1.7
4V						Tree	"	312554	105177	-	-	0.710401	0.000010	BGS	1.7
5V						Tree	Carlow	275037	165687	-	-	0.714195	0.000010	BGS	7.1
G(A)1V						Tree	Galway	95195	237187	300	-	0.709712	0.000012	ULB	0.8
G(A)2V						Tree	"	97246	236595	2400	-	0.709873	0.000011	ULB	1.0
G(A)3V						Tree	"	99234	237343	3500	-	0.709817	0.000009	ULB	0.9
G(A)4V			Caledonian		Caledonian	Tree	"	102445	233506	5500	-	0.709355	0.000010	ULB	0.2
G(A)5V			(Silurian -		granite,	Tree	"	105150	234785	8300	-	0.709605	0.000011	ULB	0.6
G(A)6V			Devonian)	8	granodiorite	Tree	"	107133	236071	10500	-	0.712269	0.000009	ULB	4.4
6V	585336				Tertiary	Shrub	Down	311263	319103	-	184.6	0.709761	0.000007	UCD	0.8
7V	559056		Palaeogene	9	granite	Shrub	"	330413	322767	-	65.2	0.711800	0.000004	UCD	3.7
8S	560101		Palaeogene	10	Tertiary	Soil	Antrim	319120	393140	-	59.6	0.710105	0.000005	UCD	1.3
DL3V	584944		Neoproterozoic	23	Dalradian	Shrub	Donegal	200222	410090	25000	67.9	0.714236	0.000004	UCD	7.1

Sample I.D.[a]	Tellus I.D.	Publish-ed I.D.	Age bracket	Unit label	Geological Formation	Sample Type	Sample Locality	Easting[b]	Northing[b]	Distance from coast(m)	[Sr] (ppm)	$^{87}Sr/^{86}Sr$[c]	Std Err 2σ	Lab I.D.	$\delta^{87}Sr_{seawater}$[d]
DL3S	581090				Appin Grp schist & marble	Soil	"	199273	409728	25000	153.7	0.717569	0.000004	UCD	11.8
DL3L						Soil leach	"	199273	409728	25000	-	0.713163	0.000010	BGS	5.6
9S	580496		Neoproterozoic	26	Dalradian Argyll Gp quartzite	Soil	Donegal	217402	432888	-	66.3	0.732572	0.000004	UCD	33.0
10V	587672		Neoproterozoic	27	Caledonian appinite suite	Shrub	Donegal	172518	385443	-	128.9	0.709981	0.000004	UCD	1.1
11V						Tree	Wexford	299471	126488	-	-	0.711189	0.000010	BGS	2.8
WW1V						Tree	Wicklow	331705	203729	500	97.9	0.709717	0.000004	UCD	0.8
WW1S						Soil	"	331772	203702	500	121.9	0.717739	0.000004	UCD	12.1
WW1L						Soil leach	"	331772	203702	500	-	0.709510	0.000010	BGS	0.5
WW2V						Tree	"	328981	204192	2100	98.0	0.709389	0.000004	UCD	0.3
WW2S						Soil	"	328996	204196	2100	68.0	0.722440	0.000004	UCD	18.7
WW2L						Soil leach		328996	204196	2100	-	0.711261	0.000010	BGS	2.9
WW3V						Tree	"	325529	205676	4700	79.6	0.709880	0.000004	UCD	1.0
WW3S			Palaeozoic,		Cambrian greywacke,	Soil	"	325644	205735	4700	58.1	0.725652	0.000004	UCD	23.2
WW3L			Cambrian	32	sandst, qtzite	Soil leach	"	325644	205735	4700	-	0.717983	0.000010	BGS	12.4
12V	585837		Palaeozoic, Mid - Up Ordovician	38	Ordovician acid volcanics	Shrub	Louth	303537	284265	-	87.2	0.712133	0.000006	UCD	4.2
13V	585723		Palaeozoic, Mid - Up Ordovician	40	Derryveeny Fm conglom.	Shrub	Monag.	274471	331852	-	75.9	0.710067	0.000004	UCD	1.3
14V	585457		Palaeozoic,	49	Silurian	Shrub	Louth	290113	300920	-	356.3	0.710891	0.000004	UCD	2.4

Sample I.D.[a]	Tellus I.D.	Publish-ed I.D.	Age bracket	Unit label	Geological Formation	Sample Type	Sample Locality	Easting[b]	Northing[b]	Distance from coast(m)	[Sr] (ppm)	$^{87}Sr/^{86}Sr$[c]	Std Err 2σ	Lab I.D.	$\delta^{87}Sr_{seawater}$[d]
L1(A)V		I20*	Silurian		sandstone, g'wacke, shale	Grass	"	315818	281293	30	-	0.709177	0.000010	ULB	0.0
L1(B)V		I20*				Grass	"	315818	281293	30	-	0.709179	0.000009	ULB	0.0
L1(C)V		I20*				Grass	"	315818	281293	30	-	0.709397	0.000007	ULB	0.3
L2(A)V		I91*				Grass	"	312843	283956	3500	-	0.711300	0.000009	ULB	3.0
L2(B)V		I91*				Grass	"	312843	283956	3500	-	0.711027	0.000008	ULB	2.6
L2(C)V		I91*				Shrub	"	312843	283956	3500	-	0.711445	0.000011	ULB	3.2
L3(A)V		I92*				Grass	"	311139	283371	5100	-	0.710293	0.000009	ULB	1.6
L4(A)V		I19*				Grass	"	307529	284836	7300	-	0.711762	0.000007	ULB	3.6
L4(B)V		I19*				Grass	"	307529	284836	7300	-	0.710486	0.000008	ULB	1.8
15V	586607		Palaeozoic,	52	Siluruian -	Shrub	Sligo	169287	300838	-	257.4	0.709407	0.000004	UCD	0.3
KY1V						Tree	Kerry	40575	77007	150	-	0.710171	0.000009	ULB	1.4
KY2V						Tree	"	41442	76344	1015	-	0.709581	0.000009	ULB	0.6
KY3V						Tree	"	45567	75733	600	-	0.709749	0.000012	ULB	0.8
KY4V					Mid	Tree	"	47872	75429	2730	-	0.709951	0.000010	ULB	1.1
KY5V			Palaeozoic,		Devonian	Tree	"	49882	76958	5000	-	0.710099	0.000007	ULB	1.3
KY6V			Middle Devonian	53	ORS	Tree	"	55085	75541	9960	-	0.710946	0.000009	ULB	2.5
W1V						Tree	Waterf.	225329	81017	10	-	0.709378	0.000010	ULB	0.3
W2V						Tree	"	224742	81698	900	-	0.710689	0.000010	ULB	2.1
W3V						Tree	"	223786	82705	2300	-	0.710946	0.000011	ULB	2.5
W4V						Tree	"	222674	83973	4000	-	0.709906	0.000009	ULB	1.0
W5V			Palaeozoic, Up.		Up Dev-Lr	Tree	"	221665	85635	5860	-	0.711531	0.000013	ULB	3.3
W6V			Devonian - Carb.	54	Carb ORS	Tree	"	220774	88842	9000	-	0.712920	0.000013	ULB	5.3

Sample I.D.[a]	Tellus I.D.	Publish-ed I.D.	Age bracket	Unit label	Geological Formation	Sample Type	Sample Locality	Easting[b]	Northing[b]	Distance from coast(m)	[Sr] (ppm)	$^{87}Sr/^{86}Sr$[c]	Std Err 2σ	Lab I.D.	$\delta^{87}Sr_{seawater}$[d]
16S	580008		Palaeozoic, Carb., Mississippian	59	Courceyan basal clastics	Soil	Donegal	247282	424662	-	142.2	0.730015	0.000005	UCD	29.4
17V	585640		Palaeozoic,			Shrub	Cavan	237971	306805	-	96.2	0.708701	0.000005	UCD	-0.7
18S	554977		Carb.,		Courceyan	Soil	Ferma.	242475	322610	-	98.1	0.719118	0.000005	UCD	14.0
19S			Mississippian	61	limestone	Soil	Wexford	304681	124530	-	65.7	0.727429	0.000005	UCD	25.7
20S						Soil	Wexford	305730	122680	-	177.4	0.714120	0.000005	UCD	7.0
21S						Soil	"	305728	122677	-	68.2	0.726138	0.000005	UCD	23.9
G(B)1V			Palaeozoic,		Marine shelf	Tree	Galway	141985	219715	1140	-	0.708991	0.000009	ULB	-0.3
G(B)2V			Carb.,		facies	Tree	"	148118	219015	7300	-	0.708680	0.000008	ULB	-0.7
G(B)3V			Mississippian	64	limestone	Tree	"	151879	225039	12200	-	0.708165	0.000008	ULB	-1.4
CE(A)1						Tree	Clare	99750	168365	590	-	0.710271	0.000011	ULB	1.5
CE(A)2						Tree	"	101642	167556	2760	-	0.710862	0.000008	ULB	2.4
CE(A)3						Tree	"	109373	169781	4840	-	0.710434	0.000010	ULB	1.8
CE(A)4						Tree	"	107064	170582	7100	-	0.710826	0.000010	ULB	2.3
CE(A)5						Tree	"	103941	168059	9450	-	0.713871	0.000009	ULB	6.6
CE(A)6						Tree	"	111302	170169	11330	-	0.714023	0.000008	ULB	6.8
CE(B)1		I65**				Grass	"	103541	177654	80	-	0.709241	0.000010	ULB	0.1
CE(B)2		I64**				Grass	"	102065	173433	2440	-	0.711017	0.000010	ULB	2.6
CE(B)3		I63**				Grass	"	108987	179853	5410	-	0.710159	0.000009	ULB	1.4
CE(B)4		I62**				Grass	"	113039	181903	9730	-	0.710820	0.000012	ULB	2.3
CE(B)5		I61**				Grass	"	120308	180791	16500	-	0.709796	0.000010	ULB	0.9
CE(B)1		I65**	Palaeozoic,		Namurian	Shrub	"	103541	177654	80	-	0.709412	0.000009	ULB	0.3
CE(B)2		I64**	Carb.,		sandstone,	Shrub	"	102065	173433	2440	-	0.710774	0.000008	ULB	2.2
CE(B)3		I63**	Pennsylvanian	71	shale	Shrub	"	108987	179853	5410	-	0.711837	0.000011	ULB	3.7

Sample I.D.[a]	Tellus I.D.	Publish-ed I.D.	Age bracket	Unit label	Geological Formation	Sample Type	Sample Locality	Easting[b]	Northing[b]	Distance from coast(m)	[Sr] (ppm)	$^{87}Sr/^{86}Sr$[c]	Std Err 2σ	Lab I.D.	$\delta^{87}Sr_{seawater}$[d]
CE(B)4		I62**				Shrub	"	113039	181903	9730	-	0.710544	0.000014	ULB	1.9
CE(B)5		I61**				Shrub	"	120308	180791	16500	-	0.709871	0.000014	ULB	1.0
CE(B)1T		I65**				Tree	"	103541	177654	80	-	0.709265	0.000009	ULB	0.1
CE(B)2T		I64**				Tree	"	102065	173433	2440	-	0.709836	0.000010	ULB	0.9
CE(B)4T		I62**				Tree	"	113039	181903	9730	-	0.710495	0.000008	ULB	1.9
CE(B)5T		I61**				Tree	"	120308	180791	16500	-	0.709516	0.000009	ULB	0.5
22V	5664		Palaeozoic, Carb.,		Westphalian	Tree	Monag.	280768	303294	-	171.1	0.714097	0.000004	UCD	6.9
23V			Pennsylvanian	72	shale, sandst	Tree	Kilkenny	261034	172118	-	-	0.710854	0.000010	BGS	2.4
24S	561247		Mesozoic, Triassic	75	Triassic sandstone	Soil	Tyrone	280198	354596	-	61.2	0.723563	0.000004	UCD	20.3
25S	559598		Cenozoic, Palaegene	79	Lower Basalt Formation	Soil	Derry	292621	404748	-	162.0	0.708929	0.000004	UCD	-0.4
26S	561538		Cenozoic, Palaeogene	83	Oligocene clay, sand	Soil	Armagh	300683	352618	-	83.9	0.717338	0.000005	UCD	11.5

[a] (S),(L) and (V) are abbreviations of bulk soil, soil leachate and vegetation respectively

[b] location data easting and northing are in Irish National Grid

[c] corrected for instrumental mass fractionation

[d] deviation of the $^{87}Sr/^{86}Sr$ from the seawater value = 0.70918

*=published in Snoeck et al., (2016). **=published in Snoeck, (2014)

Table 1. $^{87}Sr/^{86}Sr$ and Sr concentrations of modern biosphere samples (bulk soil, soil leachates and vegetation) collected along coastal transects.

3.2 Marine influence on coastal transects

For samples collected across the selected coastal transects (Figure 2), the isotopic composition of Sr is presented both as a ratio of $^{87}Sr/^{86}Sr$ and as $\delta^{87}Sr_{seawater}$ for the vegetation samples (V) and for the soil leachates (L) and bulk soil (S), where applicable. Based on the $\delta^{87}Sr_{seawater}$ values, most bulk soil samples deviate an order of magnitude away from the seawater value compared to associated soil leach and vegetation samples. The relative contribution from seawater and bedrock/soil sources (mineral weathering) were quantified and vary significantly between sample sites (Table 1). Vegetation samples from sites closest to the coast, from almost every transect have $^{87}Sr/^{86}Sr$ values which closely resemble that of seawater ($\delta^{87}Sr_{seawater}$ = 1). Systematically, these values diverge from seawater progressively inland, with the sample furthest inland generally displaying the most divergent $^{87}Sr/^{86}Sr$ from seawater (higher $\delta^{87}Sr_{seawater}$). Where soils were collected, both bulk and leached soils also have progressively more radiogenic values inland.

Notably there is a clear trend of increasing $^{87}Sr/^{86}Sr$ values with distance from the coast for most transects with marine $^{87}Sr/^{86}Sr$ representing the lower limit of biosphere $^{87}Sr/^{86}Sr$ variation. Samples collected above Visean limestone (G(B) transect) displayed the opposite trend of decreasing $^{87}Sr/^{86}Sr$ with increasing distance from the coast. This aligns with expected values for Lower Carboniferous seawater which had $^{87}Sr/^{86}Sr$ below that of present day seawater, ranging between ~0.7076-0.7082; (Burke et al., 1982; McArthur et al., 2001; Woodard et al., 2013). Visean limestone can thus be differentiated from modern seawater signatures with sufficient distance from the coast. In areas such as these with less radiogenic lithologies, seawater $^{87}Sr/^{86}Sr$ can therefore represent the upper limit of variation within the biosphere.

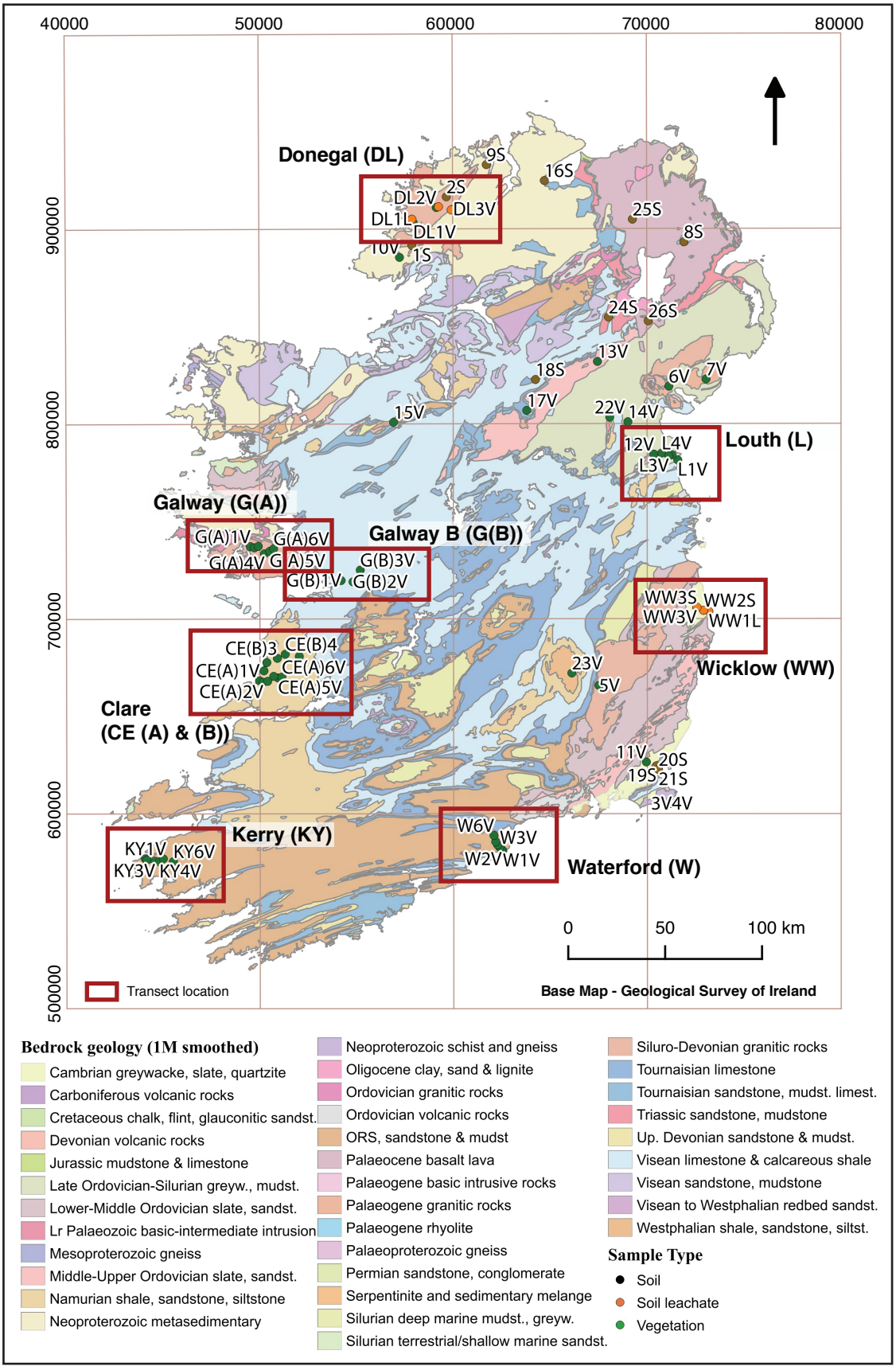


Figure 2. Spatial distribution of sampling sites. The units are coordinates in the Irish Transverse Mercator Grid.

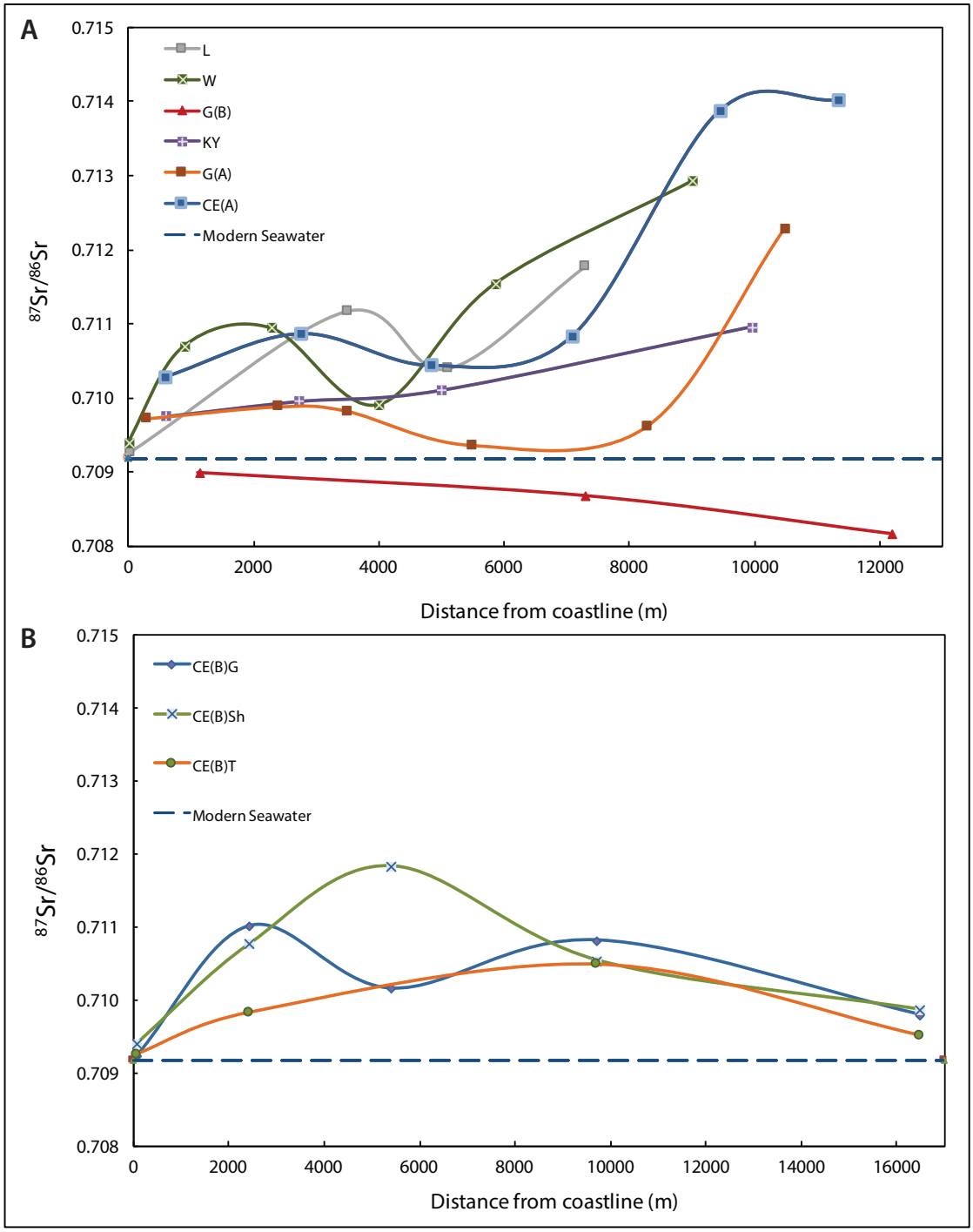


Figure 3 A. $^{87}Sr/^{86}Sr$ of plant coastal transects within 13 km from the coastline. **B.** $^{87}Sr/^{86}Sr$ of one transect in Co. Clare compares grass (CE(B)G), shrub (CE(B)Sh) and tree (CE(B)T) samples (data from Snoeck, 2014). Key: CE = Co. Clare - Namurian sandstone and shale, W = Co. Waterford – Old Red Sandstone, L = Co. Louth – Silurian sandstone, G(A) = Co. Galway – Caledonian granite, G(B) = Co. Galway – Visean limestone, KY – Co. Kerry – Old Red Sandstone, WW= Co. Wicklow, Cambrian greywacke (see Table 1 for further site details)

The sources of Sr can be constrained by the relationships between the $^{87}Sr/^{86}Sr$ composition of the endmembers and inform on mixing processes (Négrel and Roy, 2002; Hogan et al., 2000; Négrel et al., 2004; Hosono et al., 2007; Miller et al., 1993; Capo et al., 1998; Stewart et al., 1998). There is an overall trend of increasing $^{87}Sr/^{86}Sr$ plant values with distance from the coast, mostly notably for Clare (CE(A)), Louth (L), Kerry (KY), Waterford (W), whilst there is a decreasing trend observed for the transect over Visean limestone (G(B)) (Fig. 3 A). For one transect (CE(B)) grass, shrub and tree were collected and analysed to assess differences between vegetation type at the same location (Snoeck, 2014). There is good agreement between the different plant samples, particularly at the coast where there is a definite marine signal and more variability is induced further inland due to local heterogeneities in bedrock and/or soil composition (Fig. 3 B).

A simple two-endmember mixing scenario of $^{87}Sr/^{86}Sr$ in coastal plants was produced using the $^{87}Sr/^{86}Sr$ of seawater (0.70918) as one endmember and the most radiogenic terrestrial plant $^{87}Sr/^{86}Sr$ of each transect as the other. This permits an estimation for the marine-derived Sr fraction of the plant $^{87}Sr/^{86}Sr$ values which is plotted against distance from the coastline (Fig. 4), where '% marine-derived Sr' = -0.01(d) + 80.34, where d = distance from the coastline. The plants from the coastal transects plot along this trend line with a somewhat scattered array. This relationship between marine fraction of $^{87}Sr/^{86}Sr$ and distance demonstrates that 47% of the $^{87}Sr/^{86}Sr$ variation in the measured plants can be assigned to the input of the seawater/marine aerosol end-member. Marine chemical contribution to vegetation is strongest within 1 km of the coastline, with an average marine-derived fraction of ~84% (n=5) as plants growing adjacent to the coast have the most highly marine-influenced $^{87}Sr/^{86}Sr$, likely from direct input of marine-aerosols, sea-spray and sea-splash. However, establishing precisely how far inland the sea-spray effect acts is difficult and will vary between environments. This approach demonstrates that high contributions (>40% Sr of marine origin) occurs within a 9 kilometre range from the coast and decreases progressively inland.

Whilst there is a correlative relationship between the $^{87}Sr/^{86}Sr$ values of plants and their location relative to the coast, it is not a strictly linear one. Within the first 1-2 kilometres, vegetation progressively retains a more radiogenic Sr value, with further

subsequent peaks and depressions of the marine-fingerprint at most distal, terrestrial sites. The most radiogenic peaks are generally observed at a distance greater than 7km inland. These peaks and troughs represent the local scale heterogeneities that exist and demonstrate that the natural coastal environment will not fit a linear trend.

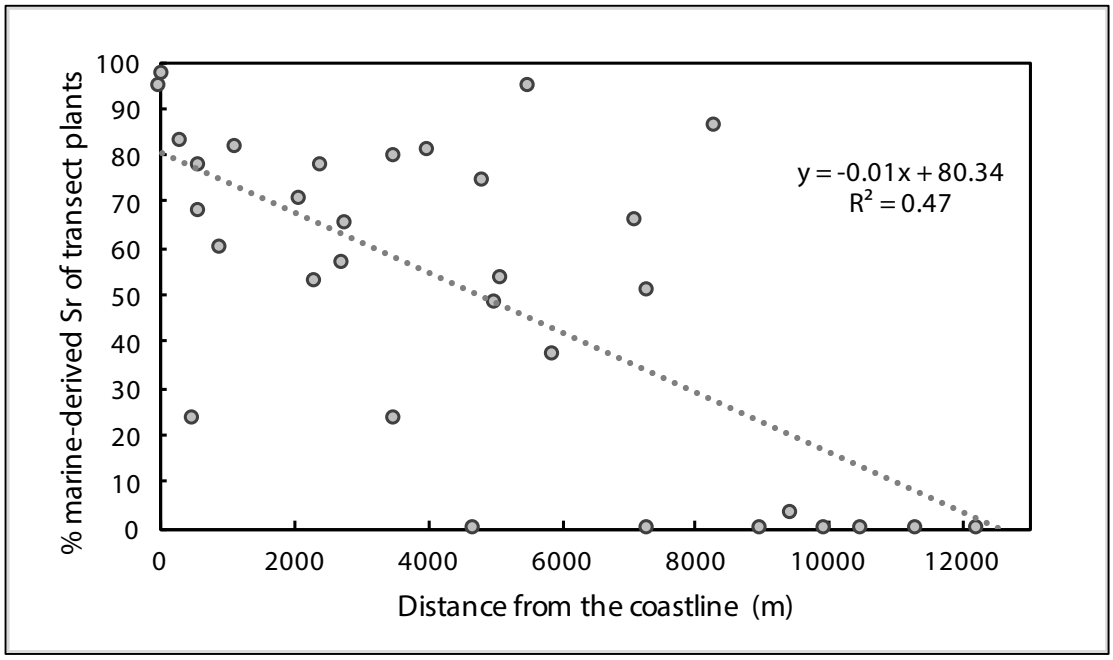


Figure 4. Proportional calculation of % marine-contribution to the $^{87}Sr/^{86}Sr$ budget of plants along coastal transects.

Rainwater is a proxy for average atmospheric Sr input (Montgomery et al., 2007) and the $^{87}Sr/^{86}Sr$ value of rainwater can vary based on the incorporation of terrestrial dust aerosols and contaminants as precipitation moves progressively inland (Capo et al., 1998; Faure and Mensing, 2009; Bailey et al., 1996; Dijkstra et al., 2003; Miller et al., 1993; Négrel et al., 2001). For example, the $^{87}Sr/^{86}Sr$ of rainwater ranged between 0.709-0.713 in France (Négrel and Roy, 1998; Probst et al., 2000; Négrel et al., 2001, 2007). Rainfall samples across this coastal trajectory would need to be analysed to assess if these contributions have a significant effect in this environment. This has been tested in Australia where the $^{87}Sr/^{86}Sr$ of rainfall in central and western Victoria became progressively more radiogenic inland due to incorporation of atmospheric dust (Raiber et al., 2009); Nevertheless, near the coast, values were close to modern seawater 0.709339 (20km), 0.709406 (60km) and 0.709677 (70km) continuing to 0.710608 (310 km). Therefore, the scale over which the addition of dust changes the Sr isotope composition of rainwater is on the order of hundreds of kilometres. The

long-term $^{87}Sr/^{86}Sr$ of precipitation in Ireland is likely to be very close to that of seawater given the direct Atlantic weather fronts, prevailing south westerly winds and high levels of rainfall. Notably, the marine influence on the $^{87}Sr/^{86}Sr$ of plants is not limited to the west coast, as the transects in both the south and east of Ireland also corresponded with a marine-terrestrial trend with progressive distance from seawater.

3.3 Bioavailability of strontium in soils

Bulk soil is unlikely to be in equilibrium with the soil solution from which plants absorb Sr. Thus, soil leaching was carried out for selected sites to determine the $^{87}Sr/^{86}Sr$ of the exchangeable cation fraction. Deionised H_2O was used to leach the bulk soil in an attempt to mirror natural soil pore water. Compared to other common salt solutions used for leaching, H_2O does not excessively dissolve carbonate minerals and therefore can be a representative $^{87}Sr/^{86}Sr$ value of the soil solution (Warham, 2012). Most soil leachates analysed (WW1L, DL1L, DL2L, DL3L) have lower $^{87}Sr/^{86}Sr$ than corresponding vegetation, more closely resembling the value of seawater. It is possible that the H_2O leach did not accurately replicate the leaching process in the natural environment. Alternatively, the lower $^{87}Sr/^{86}Sr$ of the soil leaches may indicate that the $^{87}Sr/^{86}Sr$ of these soil extracts, which are less radiogenic than both the vegetation and bulk soil, is largely supplied by marine salts/aerosols. The seawater-like $^{87}Sr/^{86}Sr$ and $\delta^{87}Sr_{seawater}$ leachate values could reflect that the soils receive inputs of marine Sr by direct wet deposition in the form of sea spray. This is based on the assumption that the soil leachates analysed here effectively resemble those of natural pore waters.

Contrastingly, the other soil extracts analysed from Co. Wicklow (WW2L and WW3L) fall intermediately between the vegetation and bulk soil $^{87}Sr/^{86}Sr$. Several studies have shown that plants demonstrate the same or very close $^{87}Sr/^{86}Sr$ to the cation extracts of the soil taken from the main root zone of the soil profile in which the plants were growing (Green et al., 2004; Bailey et al., 1996; Kennedy et al., 1998). Such a relationship indicates a strong link between Sr in the soil exchange pool and that taken up by plants. Whilst the leachates analysed here have $^{87}Sr/^{86}Sr$ closer to that of the vegetation than the bulk soil, there is no direct correlation and

therefore a straightforward relationship between these biosphere components has not been found, although this is likely a procedural artefact.

3.4 Molar cation ratios in topsoils

The cation concentration of soils collected by the regional Tellus Survey (Young et al., 2016; Young and Donald, 2013) are extremely useful for examining the distribution and bioavailability of strontium. The atmospheric influx of an element to the terrestrial environment is the product of the element's concentration in precipitation/seaspray and the absolute amount of precipitation/seaspray. As both concentrations of marine elements and quantity of rainfall are highest near the coast, it corresponds that soils at coastal sites are subject to elevated amounts of "marine"-elements, such as Cl, Na, Mg, S and Sr.

Selected molar cation concentrations, LOI and the oceanic Sr enrichment factor ($SrEF_O$) are plotted geographically using the QGIS 2.8.2-Wien for Mac with a bedrock geology map of Ireland for comparison (Geological Survey of Ireland, 2016) (Figure 5). Quantile-based (equal length) colour and symbol scales are used here to present the geochemical data and illustrate the observed patterns. Due to the issues that arise from the compositional nature of geochemical concentration data (McKinley et al., 2016), Sr concentrations are illustrated here both in absolute molar cation concentrations (mol/kg) and log-normalised to Ca (Fig 5. D & F). Absolute quantile classification maps tend to highlight outliers (McKinley et al., 2016) and here, more Sr-concentrated topsoils are dotted continuously along the north-western coast of Ireland (Fig 5. D) and a gradient is evident with decreasing concentrations as distance from the coast increases. A similar pattern is observed for Na, suggesting a marine source of both these cations. High concentrations would not be predicted from the Dalradian metasediments in this north-west area but high values are noted consistently along the north-western coastline. High Sr concentrations are also distinctly noted in the north-east region of Palaeogene flood basalts, which is largely accounting for the most Sr-enriched topsoil values. This is observed in the molar cation concentrations of SrO and CaO in topsoils (Fig 5. D & E). High Na_2O, CaO and SrO in these soils likely arise from the presence of relatively unweathered calcic plagioclase feldspar derived from the basalts; Leaching of these elements from silicates can be relatively slow.

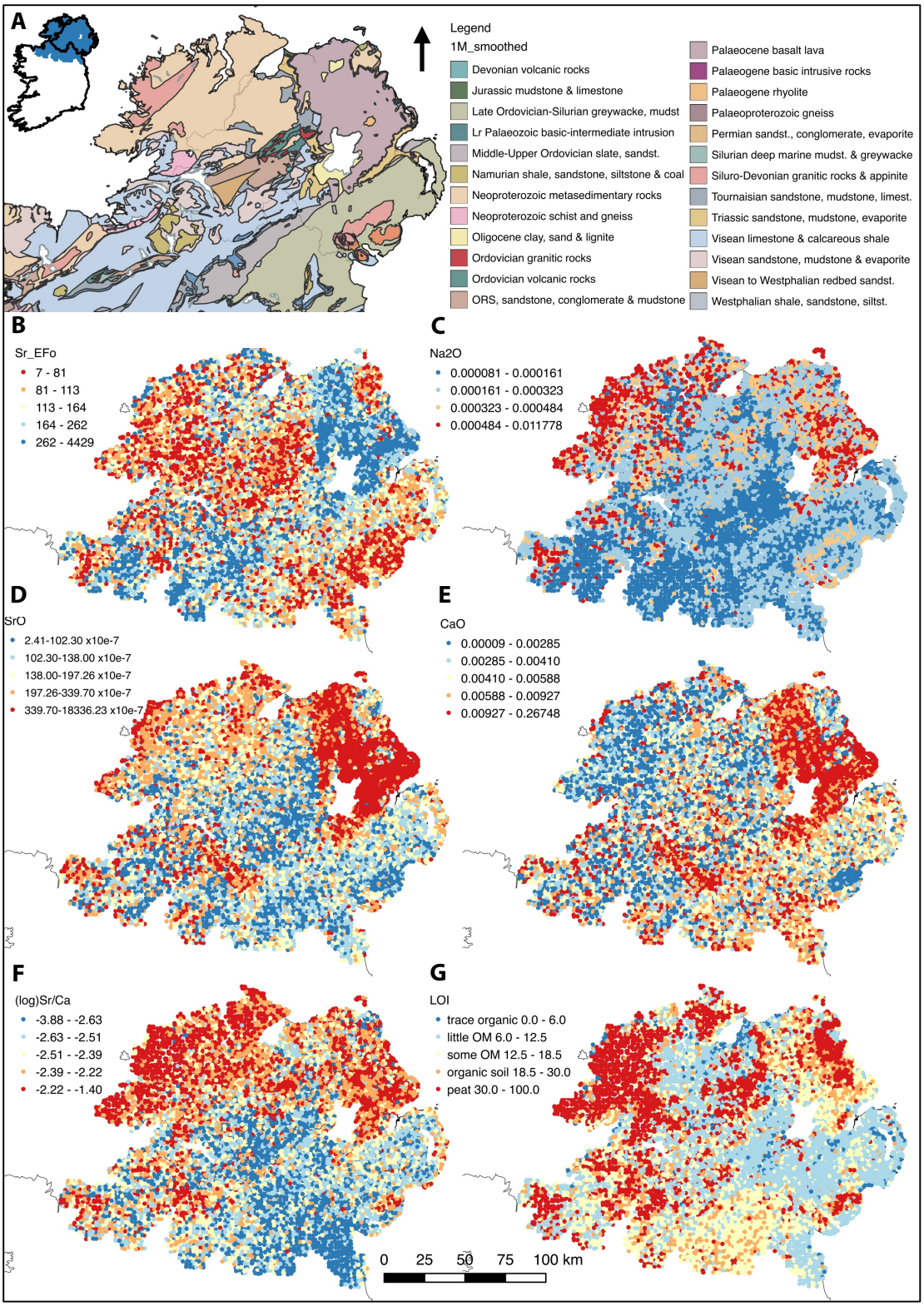


Figure 5. Cation distribution across the Tellus and Tellus Border sampling area. **A.** Geological map of the sampling area (Geological Survey of Ireland). **B.** Ocean Sr enrichment factor (SrEFo). **C.** Na_2O distribution in topsoils. **D.** SrO distribution in topsoils. **E.** CaO distribution in topsoils. **F.** Molar (log-) Sr/Ca. **G.** LOI of topsoils, highlights regions of peat coverage.

Correction of the strong geologic control over their distribution can be carried out by log normalisation of the Sr to Ca concentrations. As the variation in geochemical maps can be influenced by dilution and/or enrichment in other elements, (log-)ratios can be more informative of the processes specific to an element of interest (McKinley et al., 2016). The (log-)ratio map of Sr/Ca (Fig. 5 F), confirms that the coastal enrichment patterns observed are not simply an artefact of the compositional nature of these data. Rather, the higher Sr concentrations noted at the coastal sites are a result of marine aerosol input and the extent of the west coast enrichment is observed to be much more extensive using this method of mapping compared to absolute concentrations. The (log-)ratio Sr/Ca reduces the prominence of the Antrim Basalt and illustrates a greater delimitation of the coastal enrichment than the single component maps of Sr and Ca cation concentrations.

Low oceanic Sr enrichment factors ($SrEF_O$), i.e. Sr/Na ratios normalised to the seawater standard, are noted in soils along the west coast, again reflecting marine-derived contributions. There is also a correspondence between low $SrEF_O$ and regions of peat coverage, which contain high volatiles (represented by Loss on Ignition, LOI of 30-100%; criteria based on Huang et al., (2009); Fig. 5 G). This geographical correspondence suggests that there is a considerable geochemical contribution from the marine environment to these regions and that the peat is acting as a long-term sink for these elements, thus providing a time-integrated signature, over the Holocene. Therefore, LOI can be used as an indicator of areas that are more likely to be affected isotopically by marine geochemical signals. Soil organic matter is an important factor in the distribution of Sr. In Norway, atmospheric input of sea-salt cations result in a net accumulation of Sr in the organic top-layer relative to the C horizon (Steinnes and Njastad, 1995). In another Norwegian based study, soil samples from the organic horizon show a clear south-north trend of decreasing Na concentrations (Reimann et al., 2007). This is likely because ombrogenous peat soils tend to be more dependent on the composition of the precipitation than podzol soils or brown earths (Låg, 1968). This effect was also noted on a much larger scale on the Kola Peninsula (Reimann et al., 2000); In the organic soil horizon, Sr and Na exhibit elevated, but sharply decreasing concentrations in the first 100–150 km from coast. Peat deposits have previously been considered to mask the bedrock-sourced, due to

their high rainwater content (Evans et al., 2009). The enrichment of Sr along the west coast of Ireland and in peat covered regions is conceivably derived from marine salts which are preferentially bound to organic material in the upper soil horizon, combined with the fact that peat has a high water content, largely from stored precipitation.

For the purposes of biosphere mapping, (log-)ratio and molar cation concentrations can identify regions of high Sr concentrations. From this, it can be inferred that the $^{87}Sr/^{86}Sr$ budget of the identified regions will be more inclined to have $^{87}Sr/^{86}Sr$ deviating away from local geogenic signatures and will thus be less informative for provenancing. The marine influence on biosphere samples also highlights the need to collect bioavailable $^{87}Sr/^{86}Sr$ data rather than relying solely on geological proxies.

3.5 Geogenic and atmospheric mixing of Sr in surface water

The $^{87}Sr/^{86}Sr$ values of water samples collected from the River Main and associated tributaries in Co. Antrim range from 0.704973 to 0.707981 with a mean of 0.7060 ± 8 (1SD, n =20) (see supplementary Table S1 for all Antrim surface water $^{87}Sr/^{86}Sr$ and multi-element concentration data). Figure 6 illustrates the sample site locations and $^{87}Sr/^{86}Sr$ ratios in relation to other site parameters, including bedrock and surficial geology, pH, Sr concentration and Sr/Ca ratio. The strontium contents vary by almost a factor of eight, ranging from 4.6 to 38.2 µg/L with an average Sr concentration of 18.6 ± 10.2 (n=21). Values vary in a consistent manner between upstream and downstream with less concentrated water in the upland regions – Both $^{87}Sr/^{86}Sr$ ratios and Sr concentrations are correlated with elevation (Fig. 7). Sr content in surface water are correlated with Ca ($R^2 = 0.54$) and to an even greater degree with Na ($R^2 = 0.67$) (Fig. 8). This indicates a common origin and implies that Sr content is influenced by atmospheric/marine-derived inputs. Figure 8 illustrates the positive correlation between Al/Na ratios and $^{87}Sr/^{86}Sr$ values of surface waters. This relationship further signifies the derivation of Sr from two predominant sources, namely a minerogenic source (surface run-off which has interacted with weathering mineral products and is characterised by low Al/Na and low $^{87}Sr/^{86}Sr$ ratios) and a marine sea salt/rainfall source (with elevated Al/Na and elevated $^{87}Sr/^{86}Sr$ values).

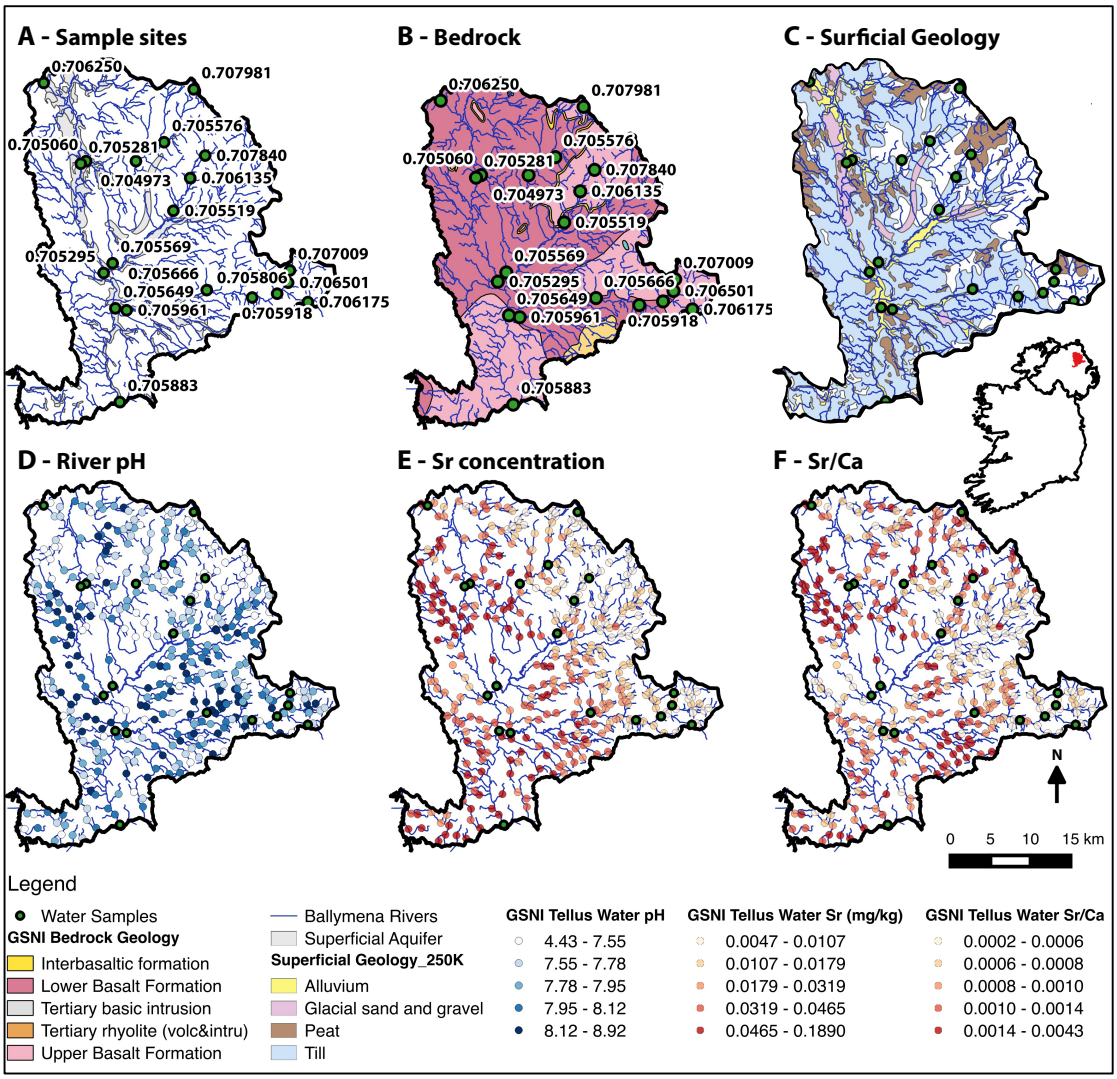


Figure 6. River Main Catchment and Tributaries. **A.** Water sample sites with associated $^{87}Sr/^{86}Sr$ values. **B.** Bedrock geology **C.** Surficial geology. **D.** Water pH. **E.** Sr concentration (mg/L) and **F.** Sr/Ca ratio. Data displayed in D, E and F were collected as part of the Tellus survey sampling.

The over-abundance of Y relative to HREE is expressed numerically using the deviation of the Y/Ho ratio from that of shale, i.e. greater than 27 (average upper continental crust and chondrite Y/Ho value is ~26 (Kamber et al., 2005)). Surface waters here are characterised by superchondritic Y/Ho ratios ranging from 28.25 to 34.01 (mean 30.96 ± 1.48; n = 21), which are all above the average upper continental crust and chondrite Y/Ho value but significantly lower than the average ratio of seawater (Y/Ho=105) (Zhang and Liu, 2004). This further suggests mixing processes between oceanic and continental element sources, although only a weak correlation is observed between Y/Ho and $^{87}Sr/^{86}Sr$ ($R^2 = 0.39$) and no correlation is noted with Sr concentrations ($R^2 = 0.14$).

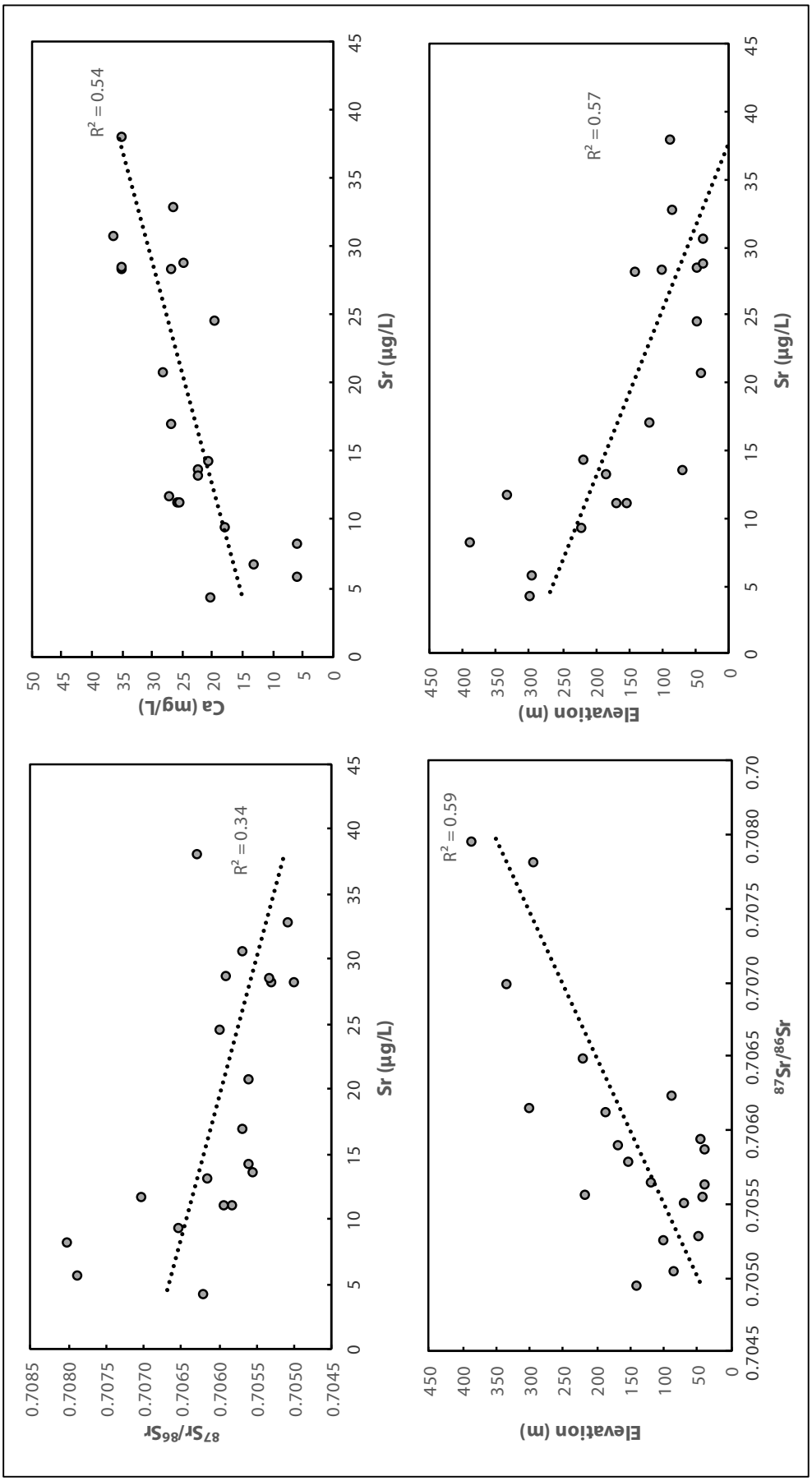


Figure 7. $^{87}Sr/^{86}Sr$, elevation and Ca concentration (linear) relationships.

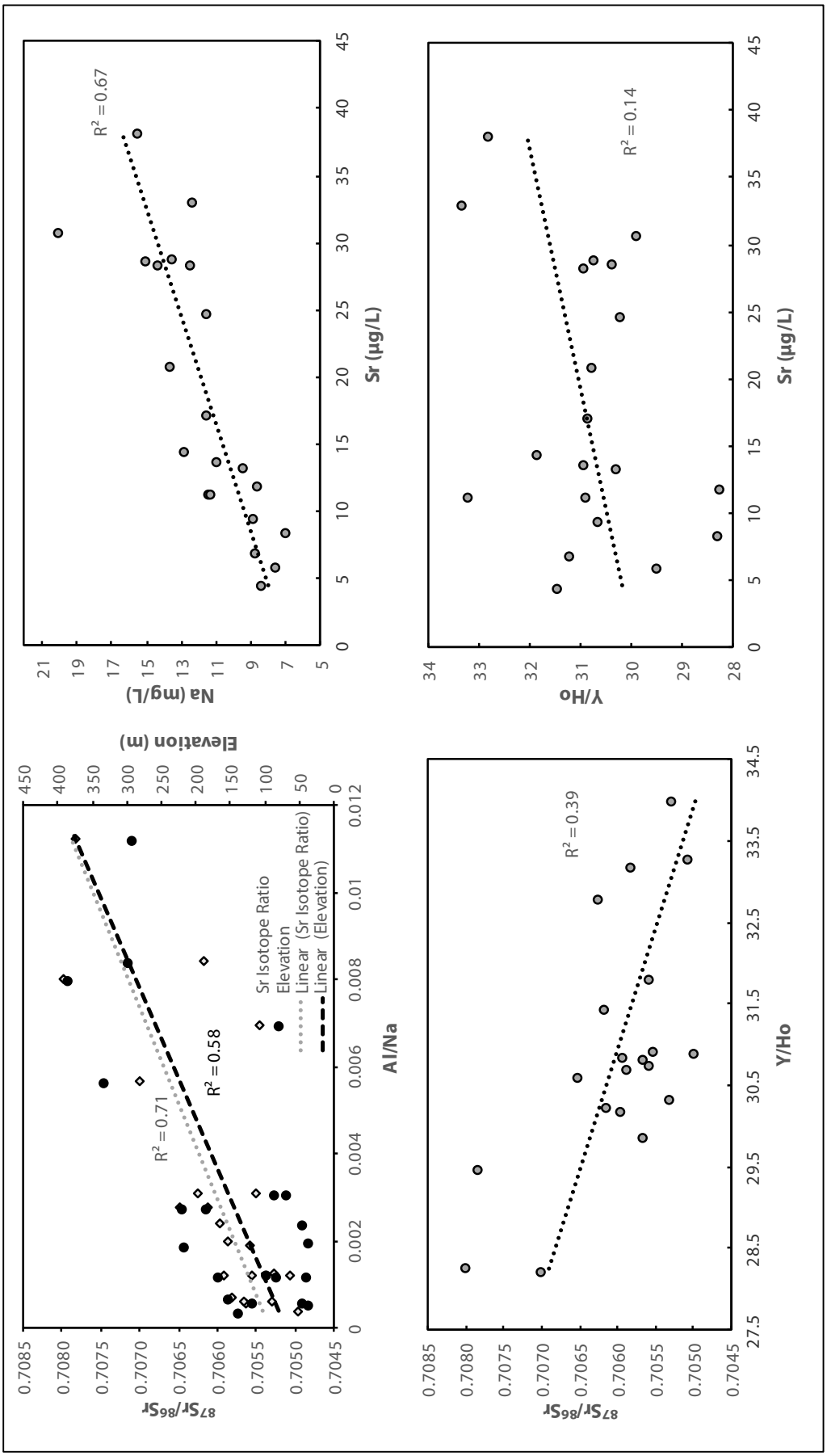


Figure 8. Relationship between $^{87}Sr/^{86}Sr$ and Sr concentrations with Na concentrations, Al/Na and Y/Ho ratios.

A mixing model was used to understand the role of atmospheric-derived Sr in the hydrological system. For this calculation, the $^{87}Sr/^{86}Sr$ composition of rainwater and the local bedrock-interacted runoff were used as the endmember compositions and the Sr concentration of these endmembers were calculated based on the equation of the trend line for the river water sample set. The $^{87}Sr/^{86}Sr$ values for the Upper and Lower Basalt Formations in this catchment have been measured with a mean of 0.7049 ± 0.001 (1SD, n=21) (Wallace et al., 1994). The modelled mixing relationship between the Sr isotopic composition and Sr concentration produces straight lines (Faure, 1986). Figure 9 illustrates the relationship between end-member Sr sources with a $^{87}Sr/^{86}Sr$ vs. 1/Sr graph. The binary mixing trend connecting a bedrock-interacted runoff water composition to a rainfall endmember, shows a close fit between $^{87}Sr/^{86}Sr$ and Sr concentration of the river water along this trend line. This demonstrates that rainfall is a highly influential source of Sr in this system. From this mixing model, >80% rainwater Sr-contribution is associated with high $^{87}Sr/^{86}Sr$ values and low Sr concentrations in the water, indicating that rainfall is a major contributor of Sr to river tributaries, particularly upland water where the streams are originating. Surface water runoff from agricultural land may also be contributing to this mixing scenario but a distinctive third endmember mixing vector is not evident.

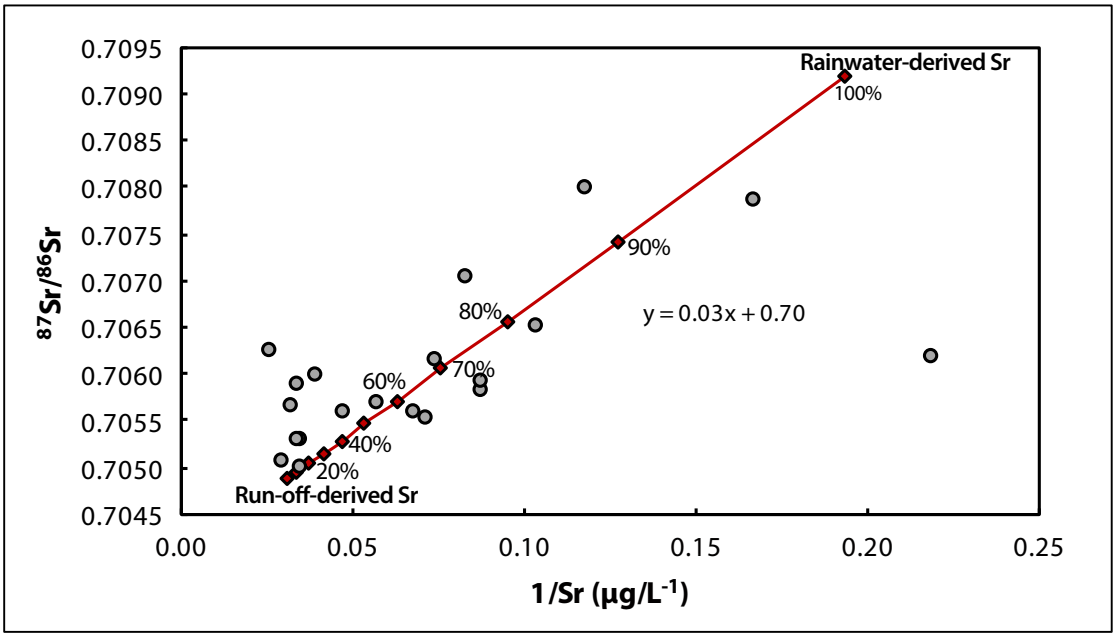


Figure 9. Two component end-member mixing of river water between rainwater and run-off endmembers.

3.6 Implications for biosphere mapping

An extensive data compilation by Evans et al., (2012) shows that the $^{87}Sr/^{86}Sr$ composition of human tooth enamel in Britain ranges between 0.7078 and 0.7165 (n = 614). Moreover, ~80% of the individuals from Britain and Ireland range within 0.7090 - 0.7110 (Montgomery et al 2014). These values have been aptly coined the "strontium of doom" range (Montgomery et al., 2014) and the authors highlight that data falling within this range arise from a combination of factors including (i) cultivation and excavation bias, (ii) carbonate minerals are more easily weathered than more radiogenic silicate minerals, (iii) these values are characteristic of widespread sedimentary rocks, limestones, and surficial deposits (Evans et al., 2010; Frei and Price, 2012; Price et al., 2014) and (iv) the effect of sea-spray. This latter point is corroborated here with evidence that values within this range also result from marine/precipitation input, which act to superimpose their distinct values on that of the geological $^{87}Sr/^{86}Sr$ range. This is demonstrated by three lines of evidence, trends in: (i) $^{87}Sr/^{86}Sr$ of coastal plant transects and (ii) topsoil cations concentrations, demonstrating coastal enrichment of Sr and associated $^{87}Sr/^{86}Sr$ deviations towards a seawater value and (iii) binary mixing is observed in river waters between atmospheric and minerogenic endmembers.

$^{87}Sr/^{86}Sr$ of human dental enamel that resemble closely the value of seawater or fall within the 'strontium of doom' range (0.7090–0.7110) (Montgomery et al., 2014) are prevalent in Ireland and Britain due to the Island setting and high precipitation/onshore winds. Because precipitation and sea-spray alter the terrestrial $^{87}Sr/^{86}Sr$ signature of coastal areas by masking the minerogenic local values with their distinctive maritime Sr composition, this further reduces the capacity to use local environmental baseline values in coastal regions to provenance individuals. Biosphere values around that of seawater are not geographically characteristic and thus, $^{87}Sr/^{86}Sr$ cannot be used effectively as a tool to trace geographic origins by means of comparison with local baseline biosphere ranges in coastal environments. Moreover, using bedrock geology maps for the interpretation of human and/or faunal material is strongly inadvisable in regions proximal to the coast. The degree to which the maritime contribution affects terrestrial values will however depend on distance from

the coastline and susceptibility to precipitation and wind fronts and will therefore vary depending on the specific environment.

3.7 $^{87}Sr/^{86}Sr$ variability in the biosphere through time

Tree core ring width is compared to the annual rainfall patterns for Northern Ireland (Fig. 10). There is a correspondence between the tree cores from two different trees and rainfall indicating that rainfall amount is an important controlling factor on tree growth in this region. The differences in the growth rate between the two beech trees sampled (*Fagus sylvatica L.*), particularly in the oldest section of the core, can result from several site-specific factors such a soil nutrient availability and drainage. Moreover, the growth rate of tree rings tends to naturally decline with age resulting in an overall decreasing trend in both cores.

It should also be noted that the $^{87}Sr/^{86}Sr$ values and element content measured in tree cores are time-averaged: first, the annual ring is a somewhat biased record of annual element availability as it mostly represents the high-growth season, secondly, soil mixing processes, which can occur on a timescale much longer than a year, mean that the $^{87}Sr/^{86}Sr$ values of the soil are a mélange of past and present atmospheric deposition, anthropogenic addition and mineral input so tree growth and rainfall patterns are unlikely to directly correspond.

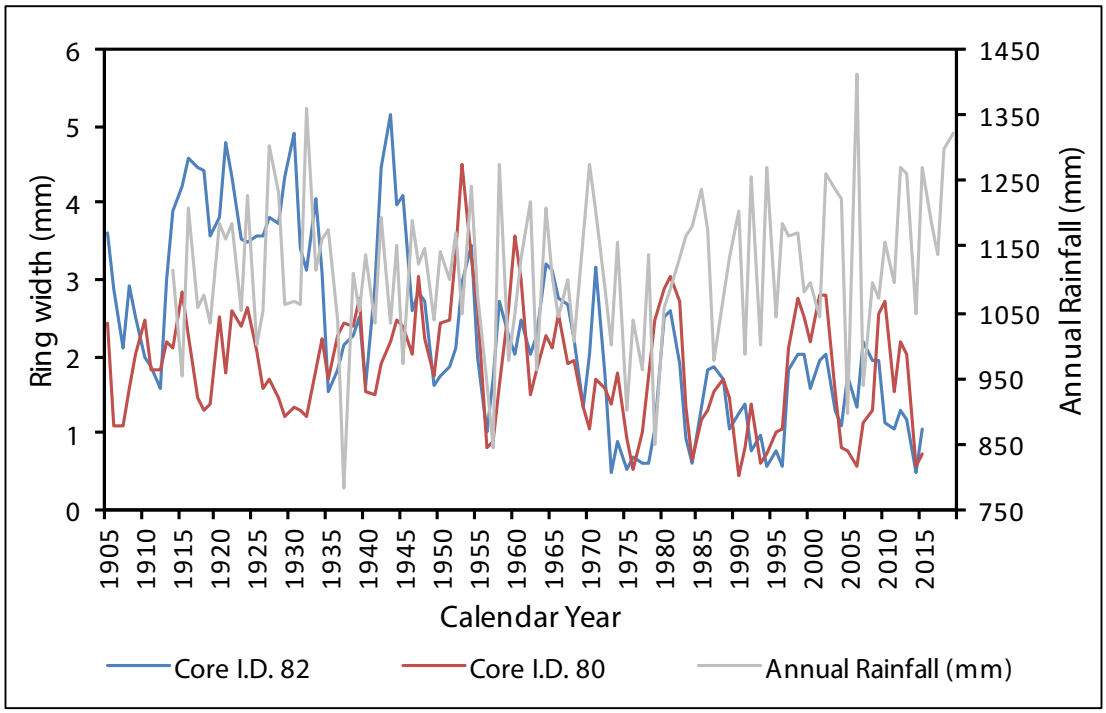


Figure 10. Annual tree ring width between 1905 – 2016 and annual rainfall record for Northern Ireland (Met Office, 2015).

$^{87}Sr/^{86}Sr$ of the two tree cores analysed are plotted against the time over which the tree rings grew (1916-2016) (Fig. 11). Given that average $^{87}Sr/^{86}Sr$ values for the Upper Basalt Formation underlying the tree bedrock are characterised by a mean of 0.7047 ± 0.0009 (1 SD, n = 8) (Wallace et al., 1994), the $^{87}Sr/^{86}Sr$ value of the tree core has likely received an input from other sources in order to explain the more radiogenic values (mean of 0.7063 for Core 80 and mean of 0.7060 for Core 82) (see supplementary Tables S2 and S3 for isotope and element data relating to the tree cores). As Core 82 was taken from a tree growing in a remote woodland, it should reflect natural geochemical changes over time. $^{87}Sr/^{86}Sr$ remain remarkably consistent over this century-long time window and despite temporal changes in Sr concentrations in the tree, the isotopic ratio is consistently around 0.7060 with some very minor variations. Even the most recent sample i.e. the bark of the tree has an almost identical $^{87}Sr/^{86}Sr$ value (0.706130).

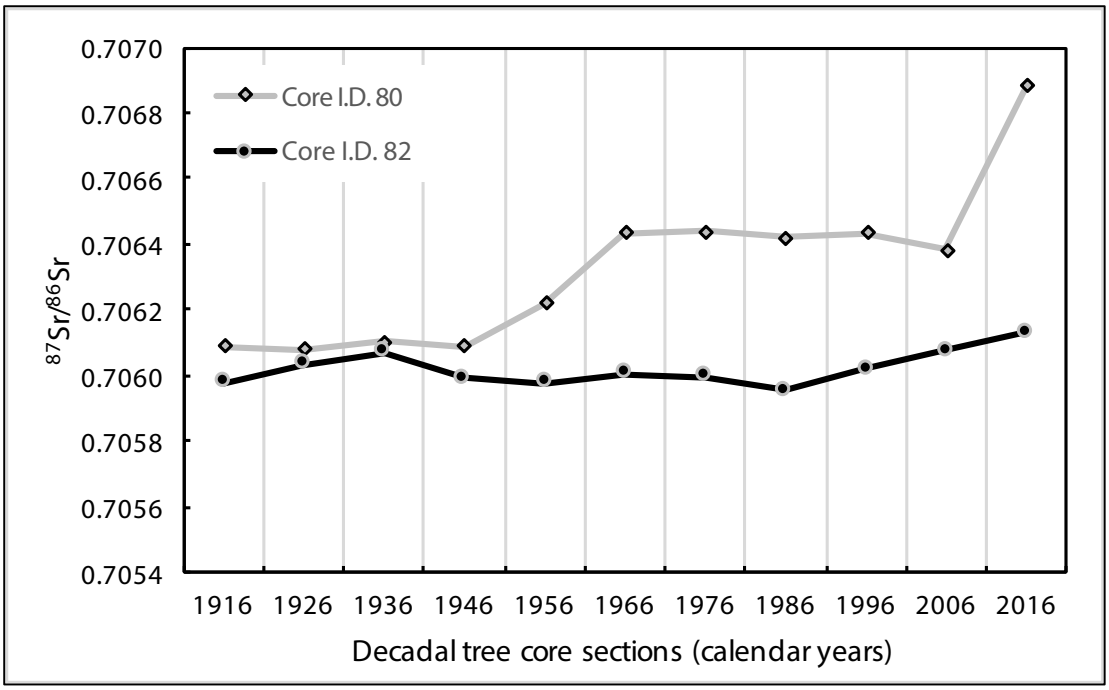


Figure 11. $^{87}Sr/^{86}Sr$ values of two tree cores – 10-year incremental samples representing period from 1916 to 2016. Core 80 was sampled from a beech free growing on agricultural soils whilst core 82 was taken from a beech tree growing in undisturbed woodland.

Although the contemporary biosphere $^{87}Sr/^{86}Sr$ values can be extrapolated into the past for use in science based archaeology, particularly for tracing studies, modern anthropogenic influences can hinder this extrapolation (Bentley, 2006; Maurer et al., 2012). Given that modern samples are used for the purposed of biosphere mapping, anthropogenic contributions may skew the current biosphere composition away from pre-industrial 'natural' values. Here the degree to which anthropogenic inputs of Sr have changed the biosphere $^{87}Sr/^{86}Sr$ values over time are examined by measuring $^{87}Sr/^{86}Sr$ from the two tree cores, one growing on modern agricultural soils and the other from an undisturbed woodland. The agricultural-influenced core $^{87}Sr/^{86}Sr$ values appear to reflect a slight increase (0.5‰) between the first and latter half of the 20th century. This small but marked increase in $^{87}Sr/^{86}Sr$ coincides with the decade beginning 1956. Historical records of fertiliser consumption (nitrogenous, potash, and phosphate fertilisers) begin in 1967 and show a dramatic increase, with peak consumption in 1994, after which fertiliser use declines (Trading Economics, 2016). The increasing $^{87}Sr/^{86}Sr$ in the tree core from the agricultural site may thus reflect this proliferation in fertiliser use. Site-specific factors such as selective element uptake by roots, ion solubility, soil type and the quantity of macronutrients versus metals can

affect element concentration absorbed and recorded in tree rings. Thus, these factors and potential anthropogenic inputs can overprint natural climate variability (Rediske and Selders, 1953; Cutter and Guyette, 1993; Padilla and Anderson, 2002).

In the case of seaweed, which has been used extensively as a fertiliser throughout Ireland in the past, it's $^{87}Sr/^{86}Sr$ value generally corresponds with that of seawater. For modern fertilisers, there is a much greater variability in the isotopic signature, ranging from 0.7034 to 0.7152 (Vitòria et al., 2004; Hosono et al., 2007) but most fertilisers have $^{87}Sr/^{86}Sr$ that range between 0.7080-0.709l. Studies such as Böhlke and Horan (2000) and Négrel and Deschamps (1996) showed that fertiliser can provide a significant contribution of Sr to local groundwater and soil solutions. Contrastingly, there are many studies that illustrate that fertiliser has little or no effect to the $^{87}Sr/^{86}Sr$ of soil solute/surface waters (Frei and Frei, 2011; Frei and Price, 2012). Therefore, the influence of fertiliser on any specific land area will depend on many factors including the amount of fertiliser applied and the $^{87}Sr/^{86}Sr$ value of the fertiliser. The effect of fertiliser in an Irish context is not well known but these results show that pre- and post-modern fertiliser introduction show a relatively minor change in the $^{87}Sr/^{86}Sr$ composition measured in *Fagus sylvatica L.*

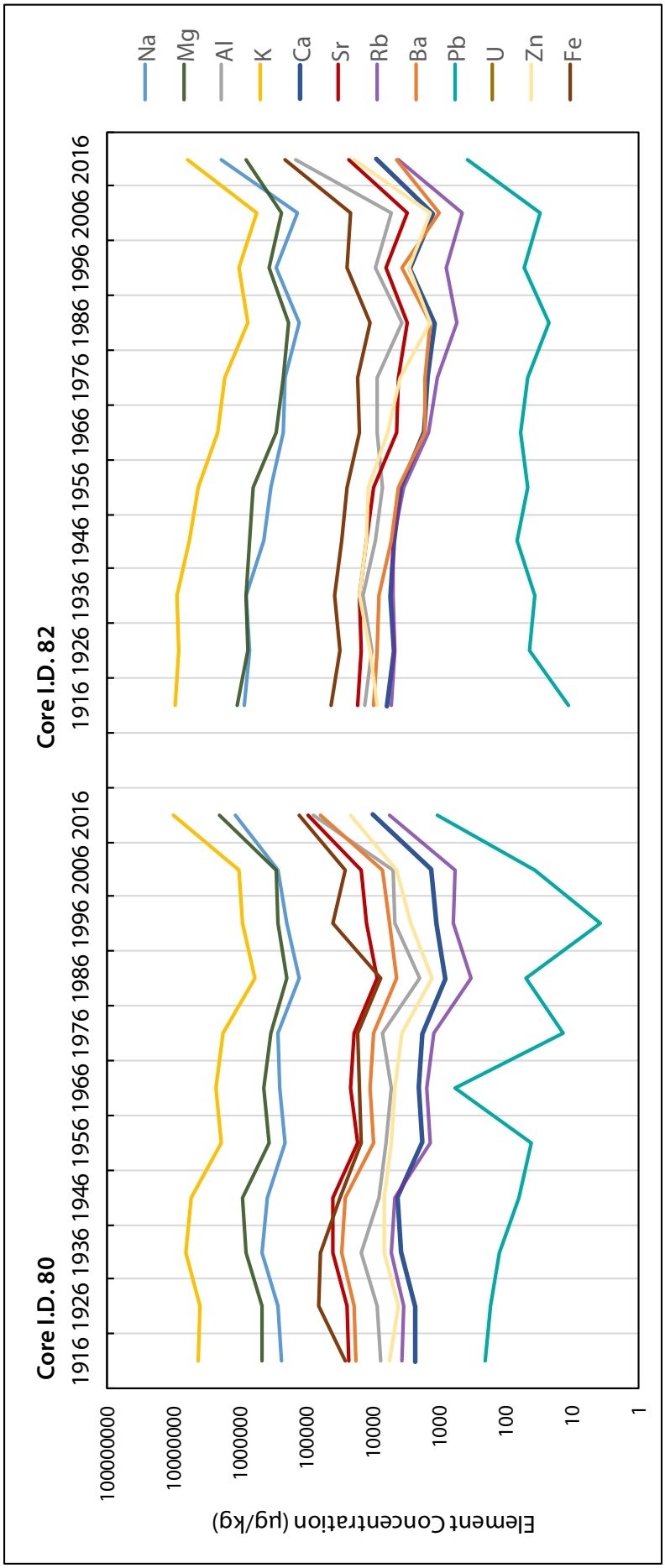


Figure 12. Selected major and trace element concentrations over 10-year averaged incremental sections representing the period from 1916 to 2016. Core 80 was sampled from a beech tree growing on agricultural soils whilst core 82 was taken from a beech tree growing in undisturbed woodland.

The measurement of major element concentrations such as Ca, Na, Mg, Al, K and Y/Ho ratios further distinguish bedrock vs. atmospheric-derived element inputs. Pb concentrations in the agricultural tree core are notably more variable than the non-agricultural counterpart. A large peak is noted for the decade beginning in 1996. This could be the result of increased infrastructure-building and a rise in petroleum combustion and vehicle use at this time. Declining element concentrations over the last 100 years are noted in both tree cores for a wide suite of major and trace elements, including Na Mg Al, K, Ca Ba, Sr and Rb. This pattern has also been reported by other tree-ring studies (Baes and McLaughlin, 1984; Hasanen and Huttunen, 1989; Bondietti et al., 1990). In the present study, the cations, strontium and calcium, have decreased over the last 100 years by 36% and 42% respectively for the tree core taken at the agricultural site and 81% and 80% respectively from the non-agricultural site (see Fig. 12). Such decreases may be interpreted as reduced nutrient availability from the soil cation pool which can result from leaching of element following extended period of intensified mobilisation.

Anthropogenic acid rain may account for enhanced element mobility as lower soil pH increases element solubility and plant uptake (Tyler et al., 1987 Baes and McLaughlin, 1984; Bondietti et al., 1990). Thus, exposure of soils to acid rain over prolonged periods can deplete the local ecosystem, resulting in decreasing element concentration patterns in the tree (Hedin and Likens, 1999). At present, there is no comprehensive record for acid rain deposition in Ireland spanning the last century. Average surface water pH in the catchment was 7.80 ± 0.44 (n=359). Average rainwater pH collected from a rainwater harvesting facility in the south east of Ireland gave a mean of 7.24, from 19 monthly samples (McCarton et al., 2009), thus, acid rain is unlikely to be affecting the element depletion observed in this study. Given the apparent net loss of major elements over the last century, which are seemingly not being replenished by bedrock weathering, one could hypothesise that atmospheric inputs of elements will become a progressively more significant element source.

4 Conclusion

For $^{87}Sr/^{86}Sr$ to be used effectively in biosphere provenance studies, a better understanding of the interaction between different $^{87}Sr/^{86}Sr$ reservoirs is needed. In the case of bulk soil, soil cation extracts and vegetation samples taken from coastal transects in NW and E Ireland, it is apparent that there is a decoupling between soil and vegetation $^{87}Sr/^{86}Sr$ resulting from marine-derived wet deposition. Within 100m from the coastline, marine-derived Sr contributed on average ~84% of the $^{87}Sr/^{86}Sr$ present in the vegetation, corroborating that sea-spray/precipitation has a significant control on the bio-available Sr composition in certain coastal regions.

Establishing precisely how far inland the sea-spray effect acts is difficult but a simple binary-mixing equation estimates that at ~9km distance from the coast, the marine influence on the $^{87}Sr/^{86}Sr$ values of vegetation becomes less pronounced (<40% marine fraction) and decreases progressively inland. For more distal vegetation from the coast, the minerogenic Sr becomes an increasingly more influential source of $^{87}Sr/^{86}Sr$. The results verify the dominant marine influence on the Sr budget in these coastal environments and that comparable coastline-adjacent sites will likely be characterised by a marine signature.

Molar Sr, Ca and Na cation concentrations, oceanic Sr enrichment factors (SrEFo) and (log-) Sr/Ca ratios further demonstrate that higher concentrations reflect both underlying bedrock geology and marine inputs in western coastal regions. There is also a correspondence between low SrEFo and regions of peat coverage (LOI > 30%). This geographical correlation indicated a considerable geochemical contribution from the marine environment to these regions, as the peat is acting as a long-term store of labile elements. Higher Sr concentrations in topsoil can thus be used to infer regions where $^{87}Sr/^{86}Sr$ are more likely to deviate away from geogenic signatures. These results highlight that sources of bioavailable Sr other than bedrock need to be considered in biosphere studies and demonstrate the complexity of attaining a single biosphere signature for any given area.

Mixing models of the contribution of different Sr sources to a region river catchment in a basaltic region, Co. Antrim, provides information about the relative contributions of rainfall and bedrock to Sr in the hydrological system. Rainfall was identified as a major source of Sr for surface waters, particularly in the upland regions where the streamwater tributaries originate and bedrock contributions from runoff are less influential. Time-resolved concentration values measured from tree cores show that element availability, including strontium, calcium and several other major and trace elements, has decreased over the past 100 years. $^{87}Sr/^{86}Sr$ values remain almost constant in the tree core taken from natural woodland over this timespan and small changes (on the order of ~0.0003) to the $^{87}Sr/^{86}Sr$ values of the tree growing on agricultural land pre-and post-modern fertiliser introduction are observed.

The findings of this study demonstrate that sea-spray, rainfall and potentially anthropogenic activity have a notable influence on terrestrial biosphere values in soils, plants and surface water. It is concluded that biosphere maps inferred primarily from bedrock $^{87}Sr/^{86}Sr$ are of limited use in coastal regions or areas with considerable rainfall. Intensive agricultural areas where fertiliser is used and whose $^{87}Sr/^{86}Sr$ deviates substantially from local geogenic sources, may create non-natural variability in biosphere signatures. Provenance studies utilising $^{87}Sr/^{86}Sr$ of environmental sample media as reference data should take atmospheric and anthropogenically-derived Sr into account.

Acknowledgements

This project was supported by a Geological Survey of Ireland (GSI) shortcall grant awarded to Q.G.C. We thank Prof. Stephen Daly of the National Centre for Isotope Geochemistry, UCD, for the use of this geochemical facility and for the suggestions for improvement of the manuscript. Dr. Kate Knights and Dr. Mairead Glennon of the Geological Survey of Ireland are thanked for facilitating the use of TELLUS border samples. Thanks also to Mr. Mick Murphy of the National Centre for Isotope Geochemistry, UCD. Geological Survey of Ireland (GSI). Geological Survey of Northern Ireland (GSNI) are gratefully acknowledged for the use of the Tellus Project dataset. The Tellus dataset used here is available free for academic use from Geological Survey of Northern Ireland.

References

Åberg, G., Jacks, G., and Hamilton, P.J., 1989, Weathering rates and $^{87}Sr/^{86}Sr$ ratios: An isotopic approach: Journal of Hydrology, v. 109, p. 65–78.

Åberg, G., Jacks, G., Wickman, T., and Hamilton, P.J., 1990, Strontium isotopes in trees as an indicator for calcium availability: Catena, v. 17, p. 1–11.

Aherne, J., and Farrell, E.P., 2002, Deposition of sulphur, nitrogen and acidity in precipitation over Ireland: Chemistry, spatial distribution and long-term trends: Atmospheric Environment, v. 36, p. 1379–1389.

Andersson, P., Löfvendahl, R., and Åberg, G., 1990, Major element chemistry, δ^2H, $\delta^{18}O$ and $^{87}Sr/^{86}Sr$ in a snow profile across central Scandinavia: Atmospheric Environment. Part A. General Topics, v. 24, p. 2601–2608.

Babechuk, M.G., Kamber, B.S., Greig, A., Canil, D., and Kodolányi, J., 2010, The behaviour of tungsten during mantle melting revisited with implications for planetary differentiation time scales: Geochimica et Cosmochimica Acta, v. 74, p. 1448–1470.

Baes, C.F., and Mclaughlin, S.B., 1984, Trace Elements in Tree Rings: Evidence of Recent and Historical Air Pollutants: Science, v. 224, p. 495–496.

Bailey, S.W., Hornbeck, J.W., Driscoll, C.T., and Gaudette, E., 1996, Calcium inputs and transport in a base-poor forest ecosystem as interpreted by sr isotopes: Water Resources Research, v. 32, p. 707–719.

Bain, D.C., and Bacon, J.R., 1994, Strontium isotopes as indicators of mineral weathering in catchments: Catena, v. 22, p. 201–214.

Bain, D.C., Midwood, A.J., and Miller, J.D., 1998, Strontium isotope ratios in streams and the effect of flow rate in relation to weathering in catchments: Catena, v. 32, p. 143–151.

Barnes, D., Hamadah, M.A., and Ottaway, J.M., 1976, The lead, copper and zinc content of tree rings and bark A measurement of local metallic pollution: Science of the Total Environment, v. 5, p. 63–67.

Bataille, C.P., and Bowen, G.J., 2012, Mapping $^{87}Sr/^{86}Sr$ variations in bedrock and water for large scale provenance studies: Chemical Geology, v. 304–305, p. 39–52.

Bataille, C.P., Brennan, S.R., Hartmann, J., Moosdorf, N., Wooller, M.J., and Bowen, G.J., 2014, A geostatistical framework for predicting variations in strontium concentrations and isotope ratios in Alaskan rivers: Chemical Geology, v. 389, p. 1–15.

Beard, B.L., and Johnson, C.M., 2000, Strontium isotope composition of skeletal material can determine the birth place and geographic mobility of humans and animals: Journal of Forensic Sciences, v. 45, p. 1049–1061.

Bentley, R.A., 2006, Strontium Isotopes from the Earth to the Archaeological Skeleton: A Review: Journal of Archaeological Method and Theory, v. 13, p. 135–187.

Bentley, R.A., Krause, R., Price, T.D., and Kaufmann, B., 2003, Human mobility at the early Neolithic settlement of Vaihingen, Germany: Evidence from strontium isotope analysis: Archaeometry, v. 45, p. 471–486.

Beramendi-Orosco, L.E., Rodriguez-Estrada, M.L., Morton-Bermea, O., Romero, F.M., Gonzalez-Hernandez, G., and Hernandez-Alvarez, E., 2013, Correlations between metals in tree-rings of Prosopis julifora as indicators of sources of heavy metal contamination: Applied Geochemistry, v. 39, p. 78–84.

Berner, K.B., and Berner, R.A., 1987, Global environment: Water, air, and geochemical cycles: Princeton University Press. 488 pp.

Blum, J.D., Erel, Y., and Brown, K., 1993, $^{87}Sr/^{86}Sr$ ratios of Sierra Nevade stream waters: Implications for relative mineral weathering rates: Geochimica et Cosmochimica Acta, v. 58, p. 5019–5025.

Böhlke, J.K., and Horan, M., 2000, Strontium isotope geochemistry of groundwaters and streams affected by agriculture, Locust Grove, MD: Applied Geochemistry, v. 15, p. 599–609.

Burke, W.H., Denison, R.E., Hetherington, E. a, Koepnick, R.B., Nelson, H.F., and Otto, J.B., 1982, Variation of seawater $^{87}Sr/^{86}Sr$ throughout Phanerozoic time: Geology, v. 10, p. 516–519.

Cahill Wilson, J., and Standish, C.D., 2016, Mobility and migration in late Iron Age and early Medieval Ireland: Journal of Archaeological Science: Reports, v. 6, p. 230–241.

Capo, R.C., Stewart, B.W., and Chadwick, O.A., 1998, Strontium isotopes as tracers of ecosystem processes: Theory and Methods: Geoderma, v. 82, p. 197–225.

Chadwick, O.A., Derry, L.A., Vitousek, P.M., Huebert, B.J., and Hedin, L.O., 1999, Changing sources of nutrients during four million years of ecosystem development: Nature, v. 397, p. 491–497.

Charlier, B.L. a., Ginibre, C., Morgan, D., Nowell, G.M., Pearson, D.G., Davidson, J.P., and Ottley, C.J., 2006, Methods for the microsampling and high-precision analysis of strontium and rubidium isotopes at single crystal scale for petrological and geochronological applications: Chemical Geology, v. 232, p. 114–133.

Chayes, F., 1960, On Correlation between Variables of Constant Sum: Journal of Geophysical Research, v. 65, p. 4185–4193.

Clarke, I.D., and Fritz, P., 1997, Environmental Isotopes in Hydrogeology: CRC Press 260 pp.

Cui, M., He, X., Davi, N., Chen, Z., Zhang, X., Peng, J., and Chen, W., 2013, Evidence of century-scale environmental changes: Trace element in tree-ring from Fuling Mausoleum Shenyang, China: Dendrochronologia, v. 31, p. 1–8.

Cutter, B.E., and Guyette, R.P., 1993, Anatomical, Chemical, and Ecological Factors Affecting Tree Species Choice in Dendrochemistry Studies: Journal of Environment Quality, v. 22, p. 611.

Dijkstra, F. a, Breemen, N. Van, Jongmans, A.G., Davies, G.R., and Likens, G.E., 2003, Calcium Weathering in Forested Soils and the Effect of Different Tree Species Calcium weathering in forested soils and the effect of different tree species: Biogeochemistry, v. 62, p. 253–275.

Dixon, D.A., Mayewski, P.A., Korotkikh, E., Sneed, S.B., Handley, M.J., Introne, D.S., and Scambos, T.A., 2013, Variations in snow and firn chemistry along US ITASE traverses and the effect of surface glazing: The Cryosphere, v. 7, p. 515–535.

Drouet, T., Herbauts, J., Gruber, W., and Demaiffe, D., 2005, Strontium isotope composition as a tracer of calcium sources in two forest ecosystems in Belgium: Geoderma, v. 126, p. 203–223.

Eggins, S.M., Woodhead, J.D., Kinsley, L.P.J., Mortimer, G.E., Sylvester, P.J., McCulloch, M.T., Hergt, J.M., and Handler, M.R., 1997, A simple method for the precise determination of >40 trace elements in geological samples by ICPMS using enriched isotope internal standardisation: Chemical Geology, v. 1, p. 311–326.

English, N.B., Betancourt, J.L., Dean, J.S., and Quade, J., 2001, Strontium isotopes reveal distant sources of architectural timber in Chaco Canyon, New Mexico: Proceedings of the National Academy of Sciences of the United States of America, v. 98, p. 11891–11896.

Ettler, V., Mihaljevic, M., Sebek, O., and Nechutny, Z., 2007, Antimony availability in highly polluted soils and sediments - A comparison of single extractions: Chemosphere, v. 68, p. 455–463.

Evans, J.A., and Bullman, R., 2009, $^{87}Sr/^{86}Sr$ isotope fingerprinting of Scottish and Icelandic migratory shorebirds: Applied Geochemistry, v. 24, p. 1927–1933.

Evans, J.A., Chenery, C.A., and Montgomery, J., 2012, A summary of strontium and oxygen isotope variation in archaeological human tooth enamel excavated from Britain: Journal of Analytical Atomic Spectrometry, v. 27, p. 754.

Evans, J.A., Montgomery, J., and Wildman, G., 2009, Isotope domain mapping of $^{87}Sr/^{86}Sr$ biosphere variation on the Isle of Skye, Scotland: Journal of the Geological Society, London, v. 166, p. 617–631.

Evans, J.A., Montgomery, J., Wildman, G., and Boulton, N., 2010, Spatial variations in biosphere 87Sr/86Sr in Britain: Journal of the Geological Society, London, v. 167, p. 1–4.

Faure, G., and Mensing, T.M., 2009, Isotopes: Principles and Applications: Wiley; Third edition, 897 pp.

Faure, G., and Powell, J.L., 1972, Strontium Isotope Geology: New York, Springer-Verlag.

Frei, R., and Frei, K.M., 2013, The geographic distribution of Sr isotopes from surface waters and soil extracts over the island of Bornholm (Denmark) – A base for provenance studies in archaeology and agriculture: Applied Geochemistry, v. 38, p. 147–160.

Frei, K.M., and Frei, R., 2011, The geographic distribution of strontium isotopes in Danish surface waters – A base for provenance studies in archaeology, hydrology and agriculture: Applied Geochemistry, v. 26, p. 326–340.

Frei, K.M., and Price, T.D., 2012, Strontium isotopes and human mobility in prehistoric Denmark: Archaeological and Anthropological Sciences, v. 4, p. 103–114.

García-Suárez, A.M., Butler, C.J., and Baillie, M.G.L., 2009, Climate signal in tree-ring chronologies in a temperate climate: A multi-species approach: Dendrochronologia, v. 27, p. 183–198.

Geological Survey of Ireland, 2016, GSI Spatial Resources Viewer: http://dcenr.maps.arcgis.com/apps/MapSeries/index.html?appid=a30af518e87a4c0ab2fbde2aaac3c228.

Gosz, J.R., and Moore, D.I., 1989, Strontium isotope studies of atmospheric inputs to forested in New Mexico watersheds: Biogeochemistry, v. 8, p. 115–134.

Graustein, W.C., 1989, $^{87}Sr/^{86}Sr$ ratios measure the sources and flow of strontium in terrestrial ecosystems: Stable isotopes in ecological research, p. 491–512.

Graustein, W.C., and Armstrong, R., 1983, The use of $^{87}Sr/^{86}Sr$ to measure atmospheric transport into forested watersheds: Science, v. 219, p. 289–292.

Green, G.P., Bestland, E.A., and Walker, G.S., 2004, Distinguishing sources of base cations in irrigated and natural soils: Evidence from strontium isotopes: Biogeochemistry, v. 68, p. 199–225.

Grupe, G., Von Carnap-Bornheim, C., and Sollner, F., 2011, Stable strontium isotope mapping for provenance studies in archaeology–different material, different signals? Bulletin de la Société Suisse d'Anthropologie, v. 17, p. 67–76.

Guelle, W., Schulz, M., Balkanski, Y., and Dentener, F., 2001, Influence of the source formulation on modeling the atmospheric global distribution of sea salt aerosol: Journal of Geophysical Research, v. 106, p. 27509.

Hagemeyer, J., 1993, Plants as Biomonitors: Indicators for Heavy Metals in the Terrestrial Environment: Bernd Markert, New york, p. 541–563.

Hess, J., Bender, M.L., and Schilling, J.G., 1986, Evolution of the ratio of strontium-87 to strontium-86 in seawater from cretaceous to present: Science (New York, N.Y.), v. 231, p. 979–984.

Hodell, D., Quinn, R.L., Brenner, M., and Kamenov, G., 2004, Spatial variation of strontium isotopes ($^{87}Sr/^{86}Sr$) in the Maya region: a tool for tracking ancient human migration: Journal of Archaeological Science, v. 31, p. 585–601.

Hogan, J.F., Blum, J.D., Siegel, D.I., and Glaser, P.H., 2000, $^{87}Sr/^{86}Sr$ as a tracer of groundwater discharge and precipitation recharge in the Glacial Lake Agassiz Peatlands, northern Minnesota: Water Resources Research, v. 36, p. 3701–3710.

Horwitz, E.P., Chiarizia, R., and Dietz, M.L., 1992, A Novel Strontium-Selective Extraction Chromatographic Resin*: Solvent Extraction and Ion Exchange, v. 10, p. 313–336.

Hosono, T., Nakano, T., Igeta, A., Tayasu, I., Tanaka, T., and Yachi, S., 2007, Impact of fertilizer on a small watershed of Lake Biwa: Use of sulfur and strontium isotopes in environmental diagnosis: Science of the Total Environment, v. 384, p. 342–354.

Huang, P.-T., Patel, M., Santagata, M.C., and Bobet, A., 2009, Classification of Organic Soils: Soil Science Society of America Journal, v. B7, p. 108.

Johnson, C., Breward, N., Ander, E.L., and Ault, L., 2005, G-BASE: baseline geochemical mapping of Great Britain and Northern Ireland: Geochemistry: Exploration, Environment, Analysis, v. 5, p. 347–357.

Kador, T., Fibiger, L., Cooney, G., and Fullagard, P., 2014, Movement and diet in early Irish prehistory: first evidence from multi-isotope analysis: The Journal of Irish Archaeology, v. XXIII, p. 83–96.

Kamber, B.S., Greig, A., and Collerson, K.D., 2005, A new estimate for the composition of weathered young upper continental crust from alluvial sediments, Queensland, Australia: Geochimica et Cosmochimica Acta, v. 69, p. 1041–1058.

Kamber, B.S., Greig, A., Schoenberg, R., and Collerson, K.D., 2003, A refined solution to Earth's hidden niobium: implications for evolution of continental crust and mode of core formation: Precambrian Research, v. 126, p. 289–308.

Kennedy, M.J., Chadwick, O.A., Vitousek, P.M., Derry, L.A., and Hendricks, D.M., 1998, Changing sources of base cations during ecosystem development, Hawaiian Islands: Geology, v. 26, p. 1015–1018.

Kennedy, M.J., Hedin, L.O., and Derry, L., 2002, Decoupling of unpolluted temperate forests from rock nutrient sources revealed by natural $^{87}Sr/^{86}Sr$ and ^{84}Sr tracer addition.: Proceedings of the National Academy of Sciences of the United States of America, v. 99, p. 9639–9644.

Knudson, K.J., O'Donnabhain, B., Carver, C., Cleland, R., and Price, T.D., 2012, Migration and Viking Dublin: Paleomobility and paleodiet through isotopic analyses: Journal of Archaeological Science, v. 39, p. 308–320.

Laffoon, J.E., Davies, G.R., Hoogland, M.L.P., and Hofman, C.L., 2012, Spatial variation of biologically available strontium isotopes ($^{87}Sr/^{86}Sr$) in an archipelagic setting: a case study from the Caribbean: Journal of Archaeological Science, v. 39, p. 2371–2384.

Låg, J., 1968, Relationships between the Chemical Composition of the Precipitation and the Contents of Exchangeable Ions in the Humus Layer of Natural Soils: Acta Agriculturae Scandinavica, v. 18, p. 148–152.

Lide, D.R., 2003, CRC Handbook of Chemistry and Physics, 84th Edition, 2003-2004: Handbook of Chemistry and Physics, v. 53, p. 2616.

Likens, G.E., Driscoll, C.T., and Buso, D.C., 1996, Long-Term Effects of Acid Rain: Response and Recovery of a Forest Ecosystem: Science, v. 272, p. 244–246.

Maurer, A.-F., Galer, S.J.G., Knipper, C., Beierlein, L., Nunn, E. V, Peters, D., Tütken, T., Alt, K.W., and Schöne, B.R., 2012, Bioavailable $^{87}Sr/^{86}Sr$ in different

environmental samples - Effects of anthropogenic contamination and implications for isoscapes in past migration studies.: The Science of the Total Environment, v. 433, p. 216–29.

McArthur, J.M., Howarth, R., and Bailey, T., 2001, Strontium isotope stratigraphy: LOWESS version 3: Best fit to the marine Sr-isotope curve for 0–509 Ma and accompanying look-up table for deriving: The Journal of Geology, v. 109, p. 155–170.

McCarton, L., Ohogain, S., Reid, A., McIntyre, N., and Pender, J., 2009, Pilot Rainwater Harvesting Study, Ireland: IRCSA Conference, on Aug.3-6, 2009 at Kuala Lumpur, Malaysia, p. 1–8.

McKinley, J.M., Hron, K., Grunsky, E.C., Reimann, C., de Caritat, P., Filzmoser, P., van den Boogaart, K.G., and Tolosana-Delgado, R., 2016, The single component geochemical map: Fact or fiction? Journal of Geochemical Exploration, v. 162, p. 16–28.

Met Office, 2015, Time-series of monthly, seasonal and annual values: http://www.metoffice.gov.uk/climate/uk/summaries/datasets.

Miller, E., Blum, J.D., and Friedland, A., 1993, Determination of soil exchangeable-cation loss and weathering rates using Sr isotopes: Nature, v. 362, p. 438–441.

Miller, O.L., Solomon, D.K., Fernandez, D.P., Cerling, T.E., and Bowling, D.R., 2014, Evaluating the use of strontium isotopes in tree rings to record the isotopic signal of dust deposited on the Wasatch Mountains: Applied Geochemistry, v. 50, p. 53–65.

Millero, F.J., and Sohn, M.J., 1992, Chemical Oceanography: CRC Press; Boca Raton; London, 531 p.

Montgomery, J., 2010, Passports from the past: Investigating human dispersals using strontium isotope analysis of tooth enamel: Annals of Human Biology, v. 37, p. 325–46.

Montgomery, J., Evans, J.A., and Cooper, R.E., 2007, Resolving archaeological populations with Sr-isotope mixing models: Applied Geochemistry, v. 22, p. 1502–1514.

Montgomery, J., Evans, J.A., and Neighbour, T., 2003, Sr isotope evidence for population movement within the Hebridean Norse community of NW Scotland: Journal of the Geological Society, v. 160, p. 649–653.

Montgomery, J., Evans, J.A., and Wildman, G., 2006, $^{87}Sr/^{86}Sr$ isotope composition of bottled British mineral waters for environmental and forensic purposes: Applied Geochemistry, v. 21, p. 1626–1634.

Montgomery, J., Grimes, V., Buckberry, J., Evans, J.A., Richards, M.P., and Barrett, J.H., 2014, Finding Vikings with isotope analysis: The view from wet and windy islands: Journal of the North Atlantic, v. 7, p. 54–70.

Nafplioti, A., 2011, Tracing population mobility in the Aegean using isotope geochemistry: a first map of local biologically available $^{87}Sr/^{86}Sr$ signatures: Journal of Archaeological Science, v. 38, p. 1560–1570.

Négrel, P., 2006, Water-granite interaction: Clues from strontium, neodymium and rare earth elements in soil and waters: Applied Geochemistry, v. 21, p. 1432–1454.

Négrel, P., Casanova, J., and Aranyossy, J.F., 2001, Strontium isotope systematics used to decipher the origin of groundwaters sampled from granitoids: The Vienne Case (France): Chemical Geology, v. 177, p. 287–308.

Négrel, P., and Deschamps, P., 1996, Natural and anthropogenic budgets of a small watershed in the massif central (France): Chemical and strontium isotopic characterization of water and sediments: Aquatic Geochemistry, v. 2, p. 1–27.

Négrel, P., Giraud, E.P., and Widory, D., 2004, Strontium isotope geochemistry of alluvial groundwater: a tracer for groundwater resources characterisation: Hydrology and Earth System Sciences Discussions, v. 8, p. 959–972.

Négrel, P., Guerrot, C., Cocherie, A., Azaroual, M., Brach, M., and Fouillac, C., 2000, Rare earth elements, neodymium and strontium isotopic systematics in mineral waters: evidence from the Massif Central, France: Applied Geochemistry, v. 15, p. 1345–1367.

Négrel, P., and Roy, S., 1998, Chemistry of rainwater in the Massif Central (France): A strontium isotope and major element study: Applied Geochemistry, v. 13, p. 941–952.

Négrel, P., and Roy, S., 2002, Investigating the sources of the labile fraction in sediments from silicate-drained rocks using trace elements, and strontium and lead isotopes: Science of the Total Environment, v. 298, p. 163–181.

Ojiambo, S.B., Lyons, W.B., Welch, K.A., Poreda, R.J., and Johannesson, K.H., 2003, Strontium isotopes and rare earth elements as tracers of groundwater-lake water interactions, Lake Naivasha, Kenya: Applied Geochemistry, v. 18, p. 1789–1805.

Osterberg, E.C., 2007, North Pacific Late Holocene Climate Variability and Atmospheric Composition: Ph.D. Thesis. The University of Maine.

Padilla, K.L., and Anderson, K.A., 2002, Trace element concentration in tree-rings biomonioring centuries of environmental change: Chemosphere, v. 49, p. 575–585.

Poszwa, A., Wickman, T., Dambrine, E., Ferry, B., Dupouey, J.L., Helle, G., Schleser, G., and Breda, N., 2003, A retrospective isotopic study of spruce decline in the Vosges mountains (France): Water, Air, and Soil Pollution: Focus, v. 3, p. 201–222.

Price, T.D., Frei, K.M., and Naumann, E., 2014, Isotopic Baselines in the North Atlantic Region: Journal of the North Atlantic, v. 7, p. 103–136.

Probst, A., El Gh'mari, A., Aubert, D., Fritz, B., and McNutt, R., 2000, Strontium as a tracer of weathering processes in a silicate catchment polluted by acid atmospheric inputs, Strengbach, France, in Chemical Geology, v. 170, p. 203–219.

Raiber, M., Webb, J.A., and Bennetts, D.A., 2009, Strontium isotopes as tracers to delineate aquifer interactions and the influence of rainfall in the basalt plains of southeastern Australia: Journal of Hydrology, v. 367, p. 188–199.

Rediske, J.H., and Selders, A.A., 1953, The Absorption and Translocation of Strontium by Plants 1: Plant physiology, v. 28, p. 594–605.

Reimann, C., 2005, Geochemical mapping: technique or art? Geochemistry: Exploration, Environment, Analysis, v. 5, p. 359–370.

Reimann, C., Arnoldussen, A., Englmaier, P., Filzmoser, P., Finne, T.E., Garrett, R.G., Koller, F., and Nordgulen, Ø., 2007, Element concentrations and variations along a 120-km transect in southern Norway - Anthropogenic vs. geogenic vs. biogenic element sources and cycles: Applied Geochemistry, v. 22, p. 851–871.

Reimann, C., Banks, D., and De Caritat, P., 2000, Impacts of airborne contamination on regional soil and water quality: The Kola Peninsula, Russia: Environmental Science and Technology, v. 34, p. 2727–2732.

Rich, S., Manning, S.W., Degryse, P., Vanhaecke, F., and Van Lerberghe, K., 2012, Strontium isotopic and tree-ring signatures of Cedrus brevifolia in Cyprus: Journal of Analytical Atomic Spectrometry, v. 27, p. 796.

Roy, S., Gaillardet, J., and Allègre, C.J., 1999, Geochemistry of dissolved and suspended loads of the Seine river, France: Anthropogenic impact, carbonate and silicate weathering: Geochimica et Cosmochimica Acta, v. 63, p. 1277–1292.

Schmid, I., 2002, The influence of soil type and interspecific competition on the fine root system of Norway spruce and European beech: Basic and Applied Ecology, v. 3, p. 339–346.

Semhi, K., Abdalla, O.A.E., Al Khirbash, S., Khan, T., Asaidi, S., and Farooq, S., 2009, Mobility of rare earth elements in the system soils-plants-groundwaters: A case study of an arid area (Oman): Arabian Journal of Geosciences, v. 2, p. 143–150.

Semhi, K., Clauer, N., and Probst, J.L., 2000, Strontium isotope compositions of river waters as records of lithology-dependent mass transfers: The Garonne river and its tributaries (SW France): Chemical Geology, v. 168, p. 173–193.

Shand, P., Darbyshire, D.P.F., Love, A.J., and Edmunds, W.M., 2009, Sr isotopes in natural waters: Applications to source characterisation and water–rock interaction in contrasting landscapes: Applied Geochemistry, v. 24, p. 574–586.

Shaw, B.J., Summerhayes, G.R., Buckley, H.R., and Baker, J.A., 2009, The use of strontium isotopes as an indicator of migration in human and pig Lapita populations in the Bismarck Archipelago, Papua New Guinea: Journal of Archaeological Science, v. 36, p. 1079–1091.

Sheridan, J.A., Jay, M., Montgomery, J., Pellegrini, M., and Cahill Wilson, J., 2013, "Tara Boy": local hero or international man of mystery?, in M. O' Sullivan, M. Doyle, and C. Scarre, (Eds.), Tara-from the past to the future, Wordwell: Dublin.

Sholkovitz, E.R., Landing, W.M., and Lewis, B.L., 1994, Ocean particle chemistry: The fractionation of rare earth elements between suspended particles and seawater: Geochimica et Cosmochimica Acta, v. 58, p. 1567–1579.

Smyth, D., 2007, Methods used in the Tellus Geochemical Mapping of Northern Ireland, in British Geological Survey Open Report, OR/07/022, p. 1–89.

Snoeck, C., 2014, Impact of strontium sea spray effect on the isotopic ratio ($^{87}Sr/^{86}Sr$) of plants in coastal Ireland: Quaternary Newsletter, v. 134, p. 37–39.

Snoeck, C., Lee-Thorp, J.A., Schulting, R.J., de Jong, J., Debouge, W., and Mattielli, N., 2015, Calcined bone provides a reliable substrate for strontium isotope ratios as shown by an enrichment experiment: Rapid Communications in Mass Spectrometry, v. 29, p. 107–114.

Snoeck, C., Pouncett, J., Ramsey, G., Meighan, I.G., Mattielli, N., Goderis, S., Lee-Thorp, J.A., and Schulting, R.J., 2016, Mobility during the Neolithic and Bronze Age in Northern Ireland explored using strontium isotope analysis of cremated human bone: American Journal of Physical Anthropology, v. 160, p. 397–413.

Steinnes, E., and Njastad, O., 1995, Enrichment of Metals in the Organic Surface Layer of Natural Soil: Identification of Contributions from Different Sources: Analyst, v. 120, p. 1479–1483.

Stewart, B.W., Capo, R.C., and Chadwick, O.A., 1998, Quantitative strontium isotope models for weathering, pedogenesis and biogeochemical cycling: Geoderma, v. 82, p. 173–195.

Stille, P., Schmitt, A.-D., Labolle, F., Pierret, M.C., Gangloff, S., Cobert, F., Lucot, E., Guéguen, F., Brioschi, L., Steinmann, M., and Chabaux, F., 2012, The suitability of annual tree growth rings as environmental archives: Evidence from Sr, Nd, Pb and Ca isotopes in spruce growth rings from the Strengbach watershed: Comptes Rendus - Geoscience, v. 344, p. 297–311.

Tolosana-Delgado, R., and van den Boogaart, K.G., 2013, Joint Consistent Mapping of High-Dimensional Geochemical Surveys: Mathematical Geosciences, v. 45, p. 983–1004.

Trading Economics, 2016, http://www.tradingeconomics.com (accessed November 2016).

U.S. EPA, 1996, Method 1669 Sampling Ambient Water for Trace Metals at EPA Water Quality Criteria Levels: U.S. Environmental Protection Agency, p. 37.

Ulrich, T., Kamber, B.S., Woodhead, J.D., and Spencer, L. a., 2010, Long-Term Observations of Isotope Ratio Accuracy and Reproducibility Using Quadrupole ICP-MS: Geostandards and Geoanalytical Research, v. 34, p. 161–174.

de Villiers, S., and Nelson, B., 1999, Detection of low-temperature hydrothermal fluxes by seawater Mg and Ca anomalies: Science (New York, N.Y.), v. 285, p. 721–3.

Vitòria, L., Otero, N., Soler, A., and Canals, A., 2004, Fertilizer characterization: isotopic data (N, S, O, C, and Sr): Environmental Science & Technology, v. 38, p. 3254–3262.

Vitousek, P.M., Kennedy, M.J., Derry, L.A., and Chadwick, O.A., 1999, Weathering versus atmospheric sources of strontium in ecosystems on young volcanic soils: Oecologia, v. 121, p. 255–259.

Voerkelius, S., Lorenz, G.D., Rummel, S., Quétel, C.R., Heiss, G., Baxter, M., Brach-Papa, C., Deters-Itzelsberger, P., Hoelzl, S., Hoogewerff, J., Ponzevera, E., Van Bocxstaele, M., and Ueckermann, H., 2010, Strontium isotopic signatures of natural mineral waters, the reference to a simple geological map and its potential for authentication of food: Food Chemistry, v. 118, p. 933–940.

Wallace, J., Ellam, R.M., and Meighan, I.G., 1994, Sr isotope data for the Tertiary lavas of Northern Ireland: evidence for open system petrogenesis: Journal of the Geological Society, London, v. 151, p. 869–877.

Wallace, A., Montgomery, J., and Grimes, V., 2010, Excavation of an Early Medieval cemetery at Ratoath, Co. Meath., in C. Corlett and M. Potterton (Eds.) Death and burial in Early Medieval Ireland in the light of recent archaeological excavations, Bray: Wordwell, p. 335–359.

Warham, J.O., 2012, Mapping biosphere strontium isotope ratios across major lithological boundaries: PhD Thesis. University of Bradford.

Weller, R., Wöltjen, J., Piel, C., Resenberg, R., Wagenbach, D., König-Langlo, G., and Kriews, M., 2008, Seasonal variability of crustal and marine trace elements in the aerosol at Neumayer station, Antarctica: Tellus, Series B: Chemical and Physical Meteorology, v. 60 B, p. 742–752.

Werner, M., Kryza, M., Dore, A.J., Blaś, M., Hallsworth, S., Vieno, M., Tang, Y.S., and Smith, R.I., 2011, Modelling of marine base cation emissions, concentrations and deposition in the UK: Atmospheric Chemistry and Physics, v. 11, p. 1023–1037.

West, J.B., Hurley, J.M., Dudás, F.Ö., and Ehleringer, J.R., 2009, The stable isotope ratios of marijuana. II. strontium isotopes relate to geographic origin: Journal of Forensic Sciences, v. 54, p. 1261–1269.

Whipkey, C.E., Capo, R.C., Chadwick, O.A., and Stewart, B.W., 2000, The importance of sea spray to the cation budget of a coastal Hawaiian soil: a strontium isotope approach: Chemical Geology, v. 168, p. 37–48.

Willmes, M., Mcmorrow, L., Kinsley, L., Armstrong, R.A., Aubert, M., Eggins, S., Falgueres, C., Maureille, B., Moffat, I., and Grun, R., 2014, The IRHUM (Isotopic Reconstruction of Human Migration) database - bioavailable strontium isotope ratios for geochemical fingerprinting in France: Earth System Science Data, v. 6, p. 117–122.

Woodard, S.C., Thomas, D.J., Grossman, E.L., Olszewski, T.D., Yancey, T.E., Miller, B. V., and Raymond, A., 2013, Radiogenic isotope composition of Carboniferous seawater from North American epicontinental seas: Palaeogeography, Palaeoclimatology, Palaeoecology, v. 370, p. 51–63.

Woodcock, A.H., 1953, Salt Nuclei in marine air as a function of altitude and wind force: Journal of Meteorology, v. 10, p. 362–371.

Young, M.E., and Donald, A.E., 2013, A Guide to the Tellus Data. Geological Survey of Northern Ireland: Geological Survey of Northern Ireland. Belfast.

Young, M.E., Knights, K., Smyth, D., Scanlon, R., and Gallagher, V., 2016, The Tellus geochemical surveys, results and applications, in M. Young, (Ed.), Unearthed: impacts of the Tellus surveys of the north of Ireland, Royal Irish Academy, p. 33–52.

Yu, K.-F., Kamber, B.S., Lawrence, M.G., Greig, A., and Zhao, J.-X., 2007, High-precision analysis on annual variations of heavy metals, lead isotopes and rare earth elements in mangrove tree rings by inductively coupled plasma mass spectrometry: Nuclear Instruments and Methods in Physics Research Section B: Beam Interactions with Materials and Atoms, v. 255, p. 399–408.

Zazzo, A., Monahan, F.J., Moloney, A.P., Green, S., and Schmidt, O., 2011, Sulphur isotopes in animal hair track distance to sea: Rapid communications in mass spectrometry: RCM, v. 25, p. 2371–2378.

Zhang, J., and Liu, C.-Q., 2004, Major and rare earth elements in rainwaters from Japan and East China Sea: Natural and anthropogenic sources: Chemical Geology, v. 209, p. 315–326.

5 Supplementary Tables

ID		SR103	SR104	SR105	SR106	SR107	SR108	SR109	SR110	SR111	SR112	SR113	SR114
Easting		309276	315502	317309	305561	319084	323958	326639	329937	308019	314509	311486	328013
Northing		397297	407766	411277	412812	399250	398457	398866	397968	401088	415123	414091	401366
$^{87}Sr/^{86}Sr$		0.705649	0.705519	0.706135	0.705281	0.705666	0.705806	0.705918	0.706175	0.705295	0.705576	0.704973	0.707009
Std Err 2σ		0.000004	0.000006	0.000003	0.000006	0.000008	0.000005	0.000004	0.000006	0.000003	0.000007	0.000004	0.000003
Elevation (m)		36	66	182	96	117	150	165	296	45	214	137	330
Na	mg/L	19.95	10.84	9.40	14.23	11.43	11.39	11.19	8.290	15.00	12.68	12.40	8.554
Mg	"	17.27	10.43	11.98	17.23	14.33	13.73	13.05	10.87	17.04	9.30	13.39	15.10
Al	"	0.011	0.033	0.026	0.018	0.007	0.008	0.014	0.070	0.009	0.024	0.005	0.048
K	"	2.257	0.782	0.455	0.949	0.722	0.539	0.485	0.189	1.049	0.278	0.675	0.331
Ca	"	36.26	22.23	22.12	34.77	26.65	25.65	25.39	20.01	34.91	20.33	26.69	26.97
Rb	ng/L	1584.5	502.6	362.9	599.2	615.8	460.8	452.7	126.9	634.2	229.5	432.9	363.8
Sr	µg/L	30.87	13.81	13.40	28.5	17.23	11.39	11.38	4.550	28.69	14.50	28.48	11.91
Y	ng/L	47.1	40.8	27.8	50.0	31.0	30.3	24.5	119.2	46.5	29.2	20.8	38.9
Ba	"	479.4	306.1	167.6	389.4	211.9	172.4	173.6	210.2	438.4	626.1	379.0	952.4
La	"	3.4	5.0	2.1	4.4	3.0	2.8	2.0	12.5	3.5	2.6	1.9	3.2
Ce	"	6.0	8.4	3.0	8.5	4.6	4.7	2.7	21.4	6.1	3.2	2.9	6.3
Pr	"	1.3	2.0	0.8	1.7	1.1	1.1	0.8	5.4	1.4	1.1	0.7	1.5
Nd	"	6.9	9.9	4.8	9.6	6.2	5.9	4.4	28.3	7.4	6.4	4.2	7.7
Sm	"	2.4	3.3	1.7	3.1	2.1	2.1	1.4	8.7	2.2	2.1	1.5	2.3
Eu	"	0.9	1.1	0.6	1.2	0.8	0.9	0.6	4.1	0.9	0.9	0.6	1.1
Tb	"	0.7	0.7	0.4	0.8	0.5	0.5	0.4	2.0	0.7	0.6	0.4	0.7
Gd	"	4.7	4.4	2.5	4.8	2.8	2.9	2.3	12.8	3.9	3.1	2.0	3.6
Dy	"	5.3	5.3	3.3	5.8	3.8	3.7	2.9	14.5	5.0	3.7	2.5	4.9
Ho	"	1.6	1.3	0.9	1.5	1.0	0.9	0.8	3.8	1.5	0.9	0.7	1.4
Er	"	6.1	4.3	3.1	5.1	3.4	3.3	2.6	12.5	6.0	3.0	2.2	4.4
Tm	"	1.2	0.7	0.5	0.9	0.5	0.5	0.4	2.0	1.2	0.5	0.4	0.7
Yb	"	9.6	4.8	3.6	6.6	4.0	3.9	3.1	13.7	9.3	3.2	2.9	5.5
Lu	"	2.1	0.9	0.7	1.3	0.8	0.8	0.6	2.5	2.0	0.6	0.6	1.0
Hf	"	0.5	0.5	0.3	0.5	0.4	0.3	0.3	0.8	0.5	0.2	0.2	0.6
Pb	"	18.1	43.9	6.9	32.5	18.5	7.3	4.8	41.9	21.9	33.8	8.7	17.3
Th	"	0.1	0.3	0.1	0.1	0.1	0.1	0.0	0.3	0.1	0.0	0.0	0.1
U	"	64.8	38.2	21.9	68.5	32.3	26.0	29.7	49.5	64.9	84.3	33.4	27.1
Sr/Ca	-	0.85	0.62	0.61	0.82	0.65	0.44	0.45	0.23	0.82	0.71	1.07	0.44
Y/Ho	-	29.89	30.93	30.27	34.01	30.84	33.19	30.88	31.45	30.35	31.84	30.91	28.25

Table S1. $^{87}Sr/^{86}Sr$ values and selected major and trace element concentrations of Antrim waters

ID		P717-17	P717-18	P717-19	P717-20	P717-21	P717-22	P717-23	P717-24	P717-25
Easting		301585	318919	306139	317682	327818	308980	329633	310484	309754
Northing		421485	413692	413096	420797	400049	402134	398091	397085	387236
$^{87}Sr/^{86}Sr$		0.706250	0.707839	0.705060	0.707981	0.706501	0.705569	-	0.705961	0.705883
Std Err 2σ		0.000010	0.000010	0.000010	0.000010	0.000010	0.000010	0.000010	0.000010	0.000010
Elevation (m)		84	292	82	384	217	39		43	35
Na	mg/L	15.38	7.431	12.25	6.884	8.768	13.50	8.614	11.40	13.46
Mg	"	16.90	4.03	13.49	4.487	9.370	13.52	8.018	10.27	12.24
Al	"	0.05	0.08	0.01	0.055	0.024	0.016	0.097	0.028	0.027
K	"	1.471	0.590	1.010	0.366	0.395	0.975	0.156	1.149	1.528
Ca	"	34.96	5.62	26.30	5.584	17.68	28.04	13.03	19.37	24.62
Rb	ng/L	728.7	538.3	645.4	353.2	366.8	557.8	146.3	926.4	919.8
Sr	µg/L	38.24	5.967	33.05	8.435	9.552	20.94	6.937	24.77	28.96
Y	ng/L	303.7	103.4	77.8	67.4	48.6	65.0	171.2	128.4	127.9
Ba	"	1002.0	417.3	467.6	252.9	254.0	457.4	410.8	1125.5	722.0
La	"	24.1	14.1	6.0	11.4	5.9	6.3	24.6	21.6	16.5
Ce	"	49.9	38.3	10.8	20.4	8.3	10.4	45.2	37.1	29.6
Pr	"	10.4	5.8	2.6	4.3	2.4	2.5	9.8	8.3	6.5
Nd	"	58.7	28.5	14.2	20.0	11.7	13.1	48.7	41.2	33.7
Sm	"	19.6	8.6	4.6	5.9	3.7	4.2	14.5	11.9	10.6
Eu	"	7.3	3.1	1.7	2.1	1.6	1.6	6.0	3.3	3.7
Tb	"	5.2	2.1	1.3	1.4	0.9	1.1	3.2	2.6	2.5
Gd	"	29.8	11.8	7.5	8.2	5.4	6.1	19.4	16.4	14.8
Dy	"	35.6	14.1	8.8	9.8	6.5	7.6	22.2	17.2	16.6
Ho	"	9.3	3.5	2.3	2.4	1.6	2.1	5.5	4.3	4.2
Er	"	29.9	10.8	7.9	7.1	5.1	7.3	17.4	13.6	13.4
Tm	"	4.9	1.7	1.3	1.2	0.8	1.3	2.8	2.2	2.2
Yb	"	34.4	11.5	8.9	8.1	5.6	10.4	19.0	15.5	15.4
Lu	"	6.2	1.9	1.6	1.3	1.0	2.2	3.3	2.8	2.8
Hf	"	5.9	1.2	0.6	0.7	0.5	0.6	1.4	1.2	1.5
Pb	"	20.6	542.2	34.3	48.6	59.2	33.6	114.0	118.9	72.2
Th	"	1.1	0.7	0.1	0.3	0.1	0.1	0.7	0.5	0.3
U	"	39.9	1.3	35.2	2.4	9.8	31.6	20.0	41.8	32.3
Sr/Ca	-	1.09	1.06	1.26	1.51	0.54	0.75	0.53	1.28	1.18
Y/Ho	-	32.81	29.48	33.30	28.30	30.62	30.77	31.21	30.20	30.72

Table S1. continued.

CORE I.D. 80		SR 801	SR 802	SR 803	SR 804	SR 805	SR 806	SR 807	SR 808	SR 809	SR 8010	SR 8011
Decade start year		1916	1926	1936	1946	1956	1966	1976	1986	1996	2006	2016
$^{87}Sr/^{86}Sr$		0.706090	0.706082	0.706104	0.706090	0.706222	0.706433	0.706437	0.706420	0.706434	0.706385	0.706886
Std Err 2σ		0.000004	0.000004	0.000003	0.000004	0.000005	0.000003	0.000004	0.000004	0.000003	0.000003	0.000003
Na	mg/kg	238.3	274.6	469.1	387.2	217.2	257.7	268.6	133.0	202.0	277.2	1184
Mg	mg/kg	489.9	488.2	806.1	920.7	360.7	449.7	357.0	199.6	276.9	287.6	2060
Al	mg/kg	7.758	9.044	15.41	8.181	6.366	5.361	7.245	2.048	4.708	5.103	77.77
K	mg/kg	4304	4197	6491	5407	1899	2320	1869	620.9	957.9	1054	10314
Ca	mg/kg	2274	2337	3769	4346	1813	2069	1780	800.9	1149	1318	10489
Mn	mg/kg	113.8	113.6	178.2	190.1	72.88	92.03	94.26	43.05	60.90	85.84	305.1
Fe	mg/kg	26.02	66.02	60.98	30.99	15.37	16.23	17.00	7.727	40.10	25.79	132.8
Co	µg/kg	230.8	312.7	452.7	432.7	239.0	274.3	227.5	101.8	150.5	238.3	377.8
Ni	µg/kg	1608	2249	2704	1942	929.3	1152	1411	736.7	1279	1000	3876
Cu	µg/kg	4834	4428	7185	5329	9461	4957	5118	4300	12841	19468	11129
Zn	µg/kg	5697	4168	6941	6717	5462	4807	3644	1322	2700	4351	22152
Sr	mg/kg	24.13	25.65	41.67	41.91	17.07	21.73	19.28	8.818	12.39	15.36	98.08
Rb	µg/kg	3693	3477	5470	4669	1425	1618	1225	343.0	619.4	597.2	5640
Y	µg/kg	8.321	8.577	11.07	12.62	5.010	3.910	4.453	1.640	2.135	2.488	138.4
Ba	µg/kg	18023	19911	29802	25755	9916	10990	9983	4550	5873	7481	62380
La	µg/kg	6.935	6.287	8.899	9.677	3.526	3.255	3.881	1.525	1.669	1.816	98.34
Ce	µg/kg	9.742	8.977	11.78	13.35	4.950	4.391	5.297	2.130	2.234	2.574	154.9
Pr	µg/kg	1.079	0.962	1.286	1.506	0.546	0.478	0.567	0.234	0.231	0.277	19.96
Nd	µg/kg	3.884	3.472	4.468	5.544	2.058	1.686	2.026	0.857	0.826	1.058	81.84
Sm	µg/kg	0.891	0.860	1.057	1.287	0.488	0.365	0.478	0.178	0.192	0.246	19.24
Eu	µg/kg	0.223	0.205	0.276	0.358	0.141	0.067	0.117	0.017	0.036	0.053	5.709
Tb	µg/kg	0.167	0.182	0.221	0.249	0.102	0.081	0.096	0.028	0.043	0.043	3.872
Gd	µg/kg	1.126	1.097	1.410	1.577	0.639	0.455	0.543	0.195	0.261	0.282	24.63
Dy	µg/kg	1.009	1.100	1.399	1.501	0.605	0.442	0.535	0.179	0.243	0.310	21.64
Ho	µg/kg	0.198	0.214	0.265	0.292	0.126	0.089	0.102	0.036	0.046	0.060	4.158
Er	µg/kg	0.505	0.560	0.637	0.754	0.322	0.214	0.236	0.083	0.122	0.135	9.795
Tm	µg/kg	0.067	0.083	0.083	0.101	0.045	0.028	0.031	0.011	0.016	0.018	1.209
Yb	µg/kg	0.452	0.535	0.594	0.663	0.290	0.177	0.201	0.071	0.095	0.098	6.490
Lu	µg/kg	0.065	0.074	0.087	0.093	0.042	0.024	0.031	0.011	0.013	0.013	0.839
Hf	µg/kg	0.327	0.647	1.262	1.229	0.551	0.429	0.346	0.073	0.221	0.182	2.056
Pb	µg/kg	204.8	174.7	128.0	63.39	42.52	578.5	13.57	50.20	3.909	36.52	1059
Th	µg/kg	0.430	0.475	0.505	0.618	0.208	0.189	0.074	0.102	0.053	0.120	7.298
U	µg/kg	0.149	0.215	0.375	0.511	0.127	0.119	0.142	0.042	0.068	0.154	6.635
Y/Ho	-	41.96	40.15	41.76	43.23	39.70	44.09	43.73	46.14	45.97	41.81	33.28
Sr/Ca	-	0.09	0.09	0.09	0.10	0.11	0.10	0.09	0.09	0.09	0.09	0.11

Table S2. $^{87}Sr/^{86}Sr$ values and selected major and trace element concentrations of tree core I.D. 80.

CORE I.D. 82		SR 821	SR 822	SR 823	SR 824	SR 825	SR 826	SR 827	SR 828	SR 829	SR 8210	SR 8211
Decade start year		1916	1926	1936	1946	1956	1966	1976	1986	1996	2006	2016
$^{87}Sr/^{86}Sr$		0.705976	0.706032	0.706069	0.705994	0.705976	0.706004	0.705995	0.705955	0.706019	0.706075	0.706130
Std Err 2σ		0.000003	0.000006	0.000003	0.000003	0.000003	0.000003	0.000004	0.000004	0.000004	0.000004	0.000003
Na	mg/kg	890.7	729.7	820.0	440.0	354.8	222.8	218.3	134.9	292.6	136.6	1908
Mg	mg/kg	1133	760.2	826.2	742.9	642.5	284.5	225.1	189.7	380.7	244.1	826.7
Al	mg/kg	13.52	10.65	14.29	9.513	7.522	8.956	8.842	3.633	9.095	5.452	152.4
K	mg/kg	9443	8634	9288	5935	4412	2146	1684	797	1063	568.0	6338
Ca	mg/kg	6264	4814	5626	4956	3795	1758	1502	1208	2793	1264	8937
Mn	mg/kg	116.9	105.8	116.4	88.53	64.11	21.25	19.79	17.47	39.83	16.69	33.01
Fe	mg/kg	43.55	31.98	37.25	30.37	25.66	15.91	16.86	11.54	24.50	22.39	209.3
Co	µg/kg	166.5	122.9	139.1	114.8	101.7	52.41	53.70	27.61	48.05	25.86	125.1
Ni	µg/kg	2739	2751	3390	2315	2024	1432	1345	880.9	1873	703.0	2563
Cu	µg/kg	5278	5143	5668	3766	3042	2628	2508	1121	2316	1596	5623
Zn	µg/kg	9043	10944	16481	12489	12210	5893	4025	1407	2920	1381	19048
Sr	mg/kg	17.37	14.91	16.52	12.56	9.739	4.365	4.222	3.118	6.625	3.093	24.07
Rb	µg/kg	5414	4650	5141	5015	3453	1485	1114	566.3	797.7	460.5	4120
Y	µg/kg	4.378	3.605	5.143	3.303	3.120	2.443	2.066	0.741	1.988	1.208	66.89
Ba	µg/kg	9995	8544	8299	5531	4161	1649	1701	1393	3671	1016	4585
La	µg/kg	8.968	7.378	9.729	5.529	4.912	2.926	2.468	1.208	3.031	2.002	45.93
Ce	µg/kg	11.90	9.925	13.09	8.015	6.220	4.309	3.683	1.834	4.371	2.918	82.01
Pr	µg/kg	1.095	0.860	1.169	0.746	0.613	0.471	0.384	0.152	0.390	0.280	10.69
Nd	µg/kg	3.535	2.956	4.045	2.607	2.232	1.793	1.462	0.535	1.446	0.993	45.08
Sm	µg/kg	0.706	0.613	0.796	0.519	0.461	0.342	0.301	0.101	0.290	0.208	10.28
Eu	µg/kg	0.170	0.135	0.207	0.120	0.119	0.098	0.069	0.020	0.060	0.037	3.209
Tb	µg/kg	0.103	0.095	0.111	0.083	0.065	0.060	0.047	0.017	0.042	0.033	1.823
Gd	µg/kg	1.140	0.584	0.792	0.523	0.474	0.390	0.290	0.101	0.291	0.193	11.53
Dy	µg/kg	0.584	0.490	0.647	0.450	0.415	0.324	0.276	0.093	0.257	0.172	10.80
Ho	µg/kg	0.112	0.094	0.128	0.088	0.078	0.065	0.058	0.018	0.055	0.033	2.241
Er	µg/kg	0.281	0.247	0.350	0.229	0.206	0.197	0.155	0.056	0.143	0.096	6.063
Tm	µg/kg	0.040	0.034	0.048	0.032	0.026	0.026	0.022	0.007	0.019	0.012	0.851
Yb	µg/kg	0.304	0.214	0.304	0.207	0.177	0.174	0.147	0.039	0.103	0.067	5.222
Lu	µg/kg	0.044	0.038	0.051	0.036	0.029	0.026	0.023	0.006	0.016	0.009	0.773
Hf	µg/kg	1.723	1.585	2.263	1.717	1.402	1.104	1.035	0.287	0.669	0.427	3.225
Pb	µg/kg	11.27	44.89	37.44	68.37	46.50	59.44	47.68	22.60	53.31	30.22	393.8
Th	µg/kg	0.272	0.518	0.521	0.495	0.381	0.325	0.284	0.118	0.257	0.183	4.387
U	µg/kg	0.533	0.425	1.541	0.418	0.343	0.261	0.196	0.094	0.254	0.154	4.642
Y/Ho	-	39.15	38.35	40.10	37.36	40.20	37.55	35.76	40.80	36.39	36.34	29.84
Sr/Ca	-	0.36	0.32	0.34	0.39	0.39	0.40	0.36	0.39	0.42	0.41	0.37

Table S3. $^{87}Sr/^{86}Sr$ values and selected major and trace element concentrations of tree core I.D. 82.

Chapter 3: $^{87}Sr/^{86}Sr$ and trace element mapping of geosphere-hydrosphere-biosphere interactions: A case study in Ireland

Co-authors: Christophe Snoeck, Quentin G. Crowley and Michael G. Babechuk

Abbreviations:

REE = Rare earth elements, comprising the lanthanides as well as La and Y
LREE = Light rare earth element (from La to Eu)
HREE = Heavy rare earth element (from Gd to Lu)
BASr = Biologically available strontium
BAC = Biological absorption coefficient
MUQ = Mud from Queensland (trace element normalisation)
[Sr] = Sr concentration

Abstract

Geochemical mapping of biosphere variation has wide application to geological, environmental, forensic and archaeological research. The extent to which trace elements may be used to complement strontium isotopes ($^{87}Sr/^{86}Sr$) for biosphere characterisation is unclear and uncertainties exist regarding the most suitable sample media for this purpose. Here, the variation in $^{87}Sr/^{86}Sr$ and trace elements, predominantly rare earth elements and yttrium (REE), are measured in soil leachates, vegetation and streamwaters. These independent tracers are employed to define geochemical reservoirs and quantify soil-plant-water interactions in a geologically diverse and archaeologically significant area of Ireland, County (Co.) Meath. This integrated isotope and element approach produces the first combined dataset for this temperate environment.

Biological absorption coefficients (BAC) are used to assess bio-uptake of selected elements and demonstrate a preferential uptake of Y relative to HREE. High Y/Ho ratios (65.3-465.1) are exhibited in ash tree samples (*Fraxinus excelsior L.*), regardless of geological setting, indicating a potential species-specific preference. Aerial portions of ash trees do not directly reflect the REE in the bioavailable portion of the soil, indicating selectivity from the soil reservoir or fractionation during plant uptake.

Streamwater REE patterns have a consistent and seawater-like pattern inherited from marine carbonate bedrock, surficial marine carbonate-derived till, agricultural fertiliser or a combination of all three. By contrast, distinct variation in sources of $^{87}Sr/^{86}Sr$ to streamwaters is evident. Therefore, unlike $^{87}Sr/^{86}Sr$, REE in streamwater could not be used for correlation to a specific source lithology, since they do not reflect small-scale differences in underlying bedrock.

The $^{87}Sr/^{86}Sr$ range of vegetation for the study area is 0.7081 to 0.7130. Soil and streamwater samples collected at proximal locations to the vegetation demonstrated a range of 0.7086 to 0.7133 for soil leachates and 0.7081 to 0.7107 for streamwaters. Statistically significant ($p<0.05$) differences between the spatial distribution of $^{87}Sr/^{86}Sr$ in plants and certain underlying bedrock/Quaternary sediment were identified, even in a region without an extreme range in $^{87}Sr/^{86}Sr$ values. Careful selection of appropriate soil leaching protocols is necessary for an informative estimate of the natural ranges that exist within the pedosphere, supporting the notion that plant material is the most suitable sample medium for mapping bioavailable Sr. The high degree of spatial variability in $^{87}Sr/^{86}Sr$ and differences between reservoirs can only be accurately represented by relatively high-density sampling of plants. These data complement both national and European-wide initiatives to produce large-scale $^{87}Sr/^{86}Sr$ biosphere maps.

1 Introduction

Mapping geochemical variations of local biosphere values has wide application to geological, environmental, archaeological, forensic and food authenticity research (eg. Bataille and Bowen, 2012; Beard and Johnson, 2000a; Bentley, 2006; Capo et al., 1998; Evans et al., 2012, 2010; Laffoon, 2012; Laffoon et al., 2017, 2012; Maurer et al., 2012; Montgomery, 2010; Price, 2015; Sealy et al., 1991; Sillen and Kavanagh, 1982; Vinciguerra et al., 2016). Spatially defined biosphere geochemical maps can elucidate elemental and isotope reservoirs and their interactions at the Earth's surface. Strontium isotope ratios ($^{87}Sr/^{86}Sr$) have been used extensively as a geographical discriminant and as a geochemical tracer of weathering processes, in some cases, in combination with rare earth elements (REE) and other trace elements (Tricca et al., 1999; Aubert et al., 2001).

Within the last 15 years there have been numerous large scale Sr isoscapes developed using biosphere samples (e.g. Åberg et al. 1998; Bentley & Knipper 2005; Evans et al. 2009; Evans et al. 2010; Frei & Frei 2011; Frei & Frei 2013; Hartman & Richards 2014; Hedman et al. 2009; Hodell et al. 2004; Knudson & Torres-Rouff 2009; Kootker et al. 2016; Laffoon et al. 2012; Nafplioti 2011; Porder et al. 2003; Price and Naumann, 2015; Sjögren et al. 2009; Thornton 2011; Voerkelius et al. 2010; Willmes et al. 2014; Zitek et al. 2015), however none of these has specifically dealt with detailed Sr isoscapes in Ireland. At present, there are relatively few published data dealing with spatial variation of $^{87}Sr/^{86}Sr$ in the Irish biosphere using environmental samples (Knudson et al., 2012; Voerkelius et al., 2010; Snoeck et al., 2016; Cahill Wilson and Standish, 2016), despite the fact that $^{87}Sr/^{86}Sr$ are commonplace as a provenance tool applied to archaeological studies (e.g. Montgomery, Evans, and Chenery, 2006; Wallace et al., 2010; Montgomery and Grimes, 2010; Montgomery et al., 2014; Kador et al., 2014; Sheridan et al., 2013). For $^{87}Sr/^{86}Sr$ to be applicable to Irish case studies, a baseline reference dataset is imperative, especially in areas of archaeological significance. The context of this study, Co. Meath, is a storehouse of archaeology; the Hill of Tara, the Norman settlement of Trim, the Megalithic sites of the Boyne Valley, Loughcrew and many other sites have been extensively studied but await extended investigation using environmental $^{87}Sr/^{86}Sr$ isotope data. This study provides baseline

$^{87}Sr/^{86}Sr$ data for use in future archaeological studies in this region and in cases where ancient human mobility associated with the locality is in question.

This research aims to geochemically characterise the degree of biosphere variation between specific element reservoirs and investigate geosphere-biosphere-hydrosphere interactions using $^{87}Sr/^{86}Sr$ and REE proxies. To document the spatial variability in geochemical signatures, three sample media were used; vegetation, streamwaters and surface soils. A sampling density of >1 sample per 20km^2 was used here to examine spatial geochemical heterogeneity, with implications for $^{87}Sr/^{86}Sr$ values inferred from larger-scale biosphere maps. REE are naturally present in soils and are important in calculating material fluxes/geochemical budgets within catchments (Aubert, Probst, et al., 2002). Due to the REE variability between geological and hydrological environments, smaller-scale studies on REE systematics are of significant merit (Noack et al., 2014) and are key to interpreting regional natural REE variability. Their abundances are used here to elucidate the origin and mobility behaviour of lanthanides and yttrium in soil-plant-water systems, with emphasis on possible substrate-vegetation fractionation. The distribution of REE from substrate into the dissolved load of streams is also examined to test the degree of inheritance from rock-soil-water interactions.

1.1 Estimating element bioavailability in soil

The $^{87}Sr/^{86}Sr$ of a particular bedrock depends on both its age and geochemical composition (Faure and Powell, 1972). Whilst it is assumed on a larger scale that biosphere values will generally correspond with major lithological boundaries (Beard and Johnson, 2000), this is not always the case. Biosphere $^{87}Sr/^{86}Sr$ ranges do not usually directly resemble whole-rock values because bioavailable Sr originates from rock-weathering products, non-local glaciogenic material and atmospheric and anthropogenic inputs in varying combinations, often with distinctive isotopic fingerprints (Ericson, 1985). Furthermore, plants preferentially source certain elements from soils that have been progressively enriched in more stable minerals, with respect to underlying geology due to preferential weathering (Bain and Bacon, 1994). Although geochemical vectoring using plants is relatively commonplace in economic geology when spatially defining ore bodies or geochemical anomalies (Brooks, 1972;

Dunn, 2007), the relationship between the trace element chemistry of plants and underlying soil, Quaternary deposits and bedrock is not always clear (Capo et al., 1998; Bentley, 2006).

In terms of bedrock and mineral composition, Sr is likely to occur in elevated concentrations in intermediate igneous rocks, calcareous sediments and sulphate rich deposits and its distribution within minerals is most strongly controlled by Ca (Kabata-Pendias, 2001). Sorption and desorption processes such as precipitation, complexation, and ion exchange largely control the behaviour of Sr in soils which in turn are controlled by pH, ionic strength, solution speciation, mineral composition, organic matter, biological organisms, and temperature (Kabata-Pendias, 2001). Sr ions can sorb as hydrated ions on iron oxides and clay minerals (Sahai et al., 2000) and therefore argillaceous sediments tend to be enriched in Sr. However, generally, Sr is easily mobilised and readily exchangeable (Bunker et al., 2000). Organic matter in soils can strongly fix Sr and so it too has a major effect on the mobility of Sr from soils into groundwater (Wiche et al., 2017). The mean Sr concentration of soils across the United States of America, for instance, is on average around 120 mg/kg (Shacklette and Boerngen, 1984), whereas for Ireland this is estimated to be approximately 80 mg/kg for bulk soils and 30 mg/kg for quasi-bulk soils (Young et al., 2016; Young and Donald, 2013). High concentrations of Sr are expected in loamy, calcareous or industrial soils whilst soils that have low organic matter and clay content, such as more sandy soils, generally have lower Sr content (Kabata-Pendias, 2001).

The REE are another useful tracer of element cycling at the soil-plant interface. In contrast to Sr content, ultramafic igneous and calcareous rocks have the lowest concentrations of REE. In soils, REE are mobile and specifically, light REE (LREE) are more mobile than heavy REE (HREE) (Kabata & Pendias 2001), although their mobility is dependent on site specific soil parameters. Generally, LREE are more enriched in labile soils relative to HREE as the latter tend to be concentrated in the clay and amorphous Fe-oxide-bound fraction (Hu et al., 2006). REE also have an affinity to organic compounds and thus, they are more abundant in humus horizons, soil litter, and peat. Like Sr, sandy soils tend to have the lowest concentrations of REE, with loamy soils having the highest. Typically most parent materials have REE concentrations ranging from 0.1 to 100 mg/kg (Aide and Aide, 2012).

The bulk concentration of trace elements and Sr in soils resides in the unleachable detritus rather than the leachable pool (Sholkovitz et al., 1994), but it is only the latter that is immediately bioavailable for plants. REE concentrations of soil pore fluids and soil leaches are generally controlled by the solubility of REE bearing minerals and therefore do not directly reflect the REE concentrations of the bulk soil (Braun et al., 1998). Leaching of soils in order to estimate the bioavailability of REE has been extensively studied – see Hu et al., (2006) and references for multiple examples contained therein. To empirically assess the bioavailability of Sr and the REE in soils, a common strategy is the use of leaching experiments. There is some debate about how successfully leaching experiments replicate the bioavailability of elements within a natural system because REE and Sr in soil can be found in numerous soil fractions and can thus be defined by the chosen extraction method. The key fractions are: the water-soluble, the exchangeable, the carbonate, the amorphous oxides, the manganese oxide bound (Fe-Mn oxides), the organically bound, the crystalline oxide, and the residual fraction. The water soluble and/or exchangeable fractions are usually targeted for studying biogeochemical cycling.

1.2 REE translocation to plants

Examining the biogeochemical relationship between soil and plants enables distinction of key geochemical anomalies and their significance for element transfer between these environmental media. The potential effect of REE on plant growth and their mechanisms for entering into biomass is of growing interest, particularly the uptake, distribution and accumulation of REE in plants (Wyttenbach et al. 1998; Tyler 2004; Tyler & Olsson 2005; Brioschi et al. 2013; Wen et al. 2001; Fu et al. 2001; Censi et al. 2014; Miao et al. 2008; Miao et al. 2011; Lima e Cunha et al. 2014; Ding et al. 2006; Hu et al. 2006). Despite this, the REE content of wild-growing plants in natural ecosystems is much less studied. Both organic and inorganic processes play a role in the uptake of elements by plant roots from the rhizosphere, but generally, plant REE are controlled by the type of soils on which they grow and the plant species in question (Miekeley et al., 1994; Fu et al., 2001). The biomass signature is an end-member in a mixing system of soil/water/rock. Direct rhizospheric acidification of the mineral particles (mostly Fe-oxyhydroxide and clay particles) is the suggested physicochemical process by which REE are made soluble and available for uptake by

plants (Brioschi et al., 2013). In terms of the correspondence between soils and plant REE signatures, complex relationships between concentrations in these media have been demonstrated (Laul et al. 1979; Robinson et al. 1958; Tyler and Olsson 2005). This complexity is due to differing REE concentrations within soil horizons and species-dependent absorption capabilities (Lima e Cunha et al., 2014). The Biological Absorption Coefficient (BAC), the ratio of an element concentration in a plant to that in the soil, or soil fraction, can be used to quantify and predict the relative difference in bioavailability of elements in the soil-plant system (Ebong et al., 2007).

1.3 REE in the hydrological system

Examining the relationship between REE characteristics of soil/plant and small streams is of growing interest for understanding element cycling (Aubert, Stille, et al., 2002; Brioschi et al., 2013; Miao et al., 2008; Cidu et al., 2013). The dissolved REE composition of local streams is controlled to some degree by the local catchment geology and weathering conditions, providing a snapshot of the flux to the hydrosphere. However, in any given drainage basin, physio-chemical parameters such as pH, dissolved organic carbon (DOC) concentration, aquatic chemistry processes, weathering of individual mineral phases and land use can also influence the measured REE chemistry of river waters (Byrne & Sholkovitz 1996; Tricca et al. 1999; Lawrence & Kamber 2006), in addition to REE complexation with organic and inorganic ligands (Millero, 1992; Johannesson et al., 1999; Johannesson and Zhou, 1999).

REE patterns of many large rivers are relatively flat when normalised to shale (Elderfield et al., 1990), demonstrating their similar pattern with the average upper continental crust (often approximated with shale composites) and assumed to be a broad representation of the original REE source (Piper and Bau, 2013). In such cases, this similarity indicates that the relative abundances of the REE are not markedly fractionated during weathering and aqueous transport. However, at a finer scale the REE patterns of smaller streams or rivers often broadly reflect the predominant lithology in the catchments and allow these elements to be exploited as a tracer of water source and mixing (Sadeghi et al., 2013; Lawrence, Greig, et al., 2006; Lawrence, Jupiter, et al., 2006; Zhang et al., 2003). Groundwater and river/streamwater associated with marine-derived carbonate-rich catchments often exhibit LREE depleted patterns

that resemble seawater (e.g. Elderfield et al. 1990; Smedley 1991; Johannesson & Lyons 1994; Sholkovitz 1995; Johannesson et al. 1999; Johannesson & Hendry 2000; Leybourne et al. 2000; Négrel et al. 2000). In this study, REE in immature streams from small drainage catchments in Co. Meath were measured to determine the origin and behaviour of REE and better understand the connection between the dissolved load REE distribution patterns with the principle underlying lithologies and overlying sediments.

1.4 Study site

Co. Meath is located in the east midlands of Ireland between 53° 21' W and 53° 55' W and 6° 12' N and 7° 20' N (Fig. 1). The field area of Co. Meath and proximal surrounding areas, covers approximately 2,500km^2 and has a typical temperate oceanic climate that is subject to south-westerly prevailing winds. Despite some small-scale variation in temperature and rainfall throughout the area, it can essentially be classified as a single bio-climatic zone. The region has a relatively flat topography due to glacial erosion and an extensive blanket of glacial sediments. Aside from a small area in northwest Co. Meath, all rivers drain eastwards towards the Irish Sea, including, Dee, Boyne and Nanny (Finch et al., 1983).

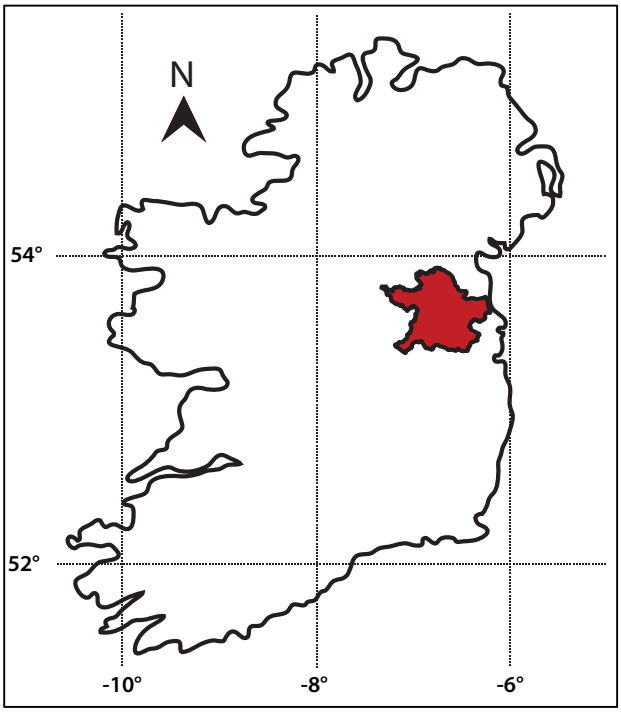


Figure 1. Map of the study site - Co. Meath, Ireland, indicated by the red highlighted region.

The study area encompasses a high degree of bedrock variability over a relatively small area. The bedrock geology consists largely of marine-derived sediments, primarily basinal facies and argillaceous and cherty limestone and shale that are late Palaeozoic in age (Geological Survey of Ireland, 2009). Bedrock can be grouped into three dominant rock types: (1) Ordovician and Silurian lithologies, (2) Upper Carboniferous shale and (3) Carboniferous limestone (Finch et al., 1983). Further details on the geological history and formation of the regional bedrock can be found in Clarke et al., (2007), McConnell et al., (2001) and Meehan and Warren, (1999).

The bedrock geology is variably covered by Quaternary sediments, mostly deposited during the Pleistocene (McCabe, 2007). These sediments include till, fluvioglacial gravels and sands of varying provenance including local bedrock as well as more distal clasts from the Irish Sea and Scandinavia (McCabe, 2007). Owing to the contribution from this source, the bioavailable $^{87}Sr/^{86}Sr$ may not directly reflect bedrock Sr compositions and therefore, the underlying bedrock geology, is not a straightforward proxy for bioavailable Sr. Here, the extent to which distinct geological units can be characterised over the study area by regionally unique $^{87}Sr/^{86}Sr$ values or REE patterns is examined.

2 Materials and Methods

2.1 Sampling strategy

Sampling density and location were organised around distribution of principal chrono-stratigraphic units on the 1:500 000 geological map of Co. Meath (Geological Survey of Ireland, 2016). A plant sample was collected at each site and at four additional representative sites, selected on their distinct bedrock and/or Quaternary deposits, surface soils and streamwater were collected in addition to the plant samples. To avoid contamination by modern day fertilisers, samples were taken from forested, non-agricultural land. The sampling methods followed in this study were adapted from those outlined by the British Geological Survey (BGS) (Smyth, 2007; Johnson et al., 2005) and adhere to the proposed standardised field methods specifically for $^{87}Sr/^{86}Sr$ (Grimstead et al., 2017).

Vegetation samples consisted mainly of grass, fern, heather, ash and other twiggy deciduous material (woody twigs of mature shrubby trees). All plant samples for which REE concentrations were measured are of the species ash, *Fraxinus excelsior L.* and the terminal branches were sampled.

Soil was taken at proximal locations to the vegetation from the surface A-horizon (5-20cm). Soil mineral particles close to the plant roots (in the rhizospheric zone) are more likely to be the main REE source for plants and it is for this reason that the upper horizon of the soil was leached in this study. Moreover, ash trees have an abundance of surface roots with intensive superficial root systems that are far-reaching and dominate the upper 0–5 cm of the soil profile (Rust and Savill, 2000). Soil samples were collected from five points at the corners and the centre of a 20 x 20 m square, combined to form a composite sample of ~1 kg. The bedrock and/or Quaternary substrate on which the collected soils developed is defined in Table 1.

Streamwater was collected from the active portions of small first- and second-order catchment locations that integrate material from an area of no more than a few square kilometres. The ‘clean hands, dirty hands’ sampling procedure (U.S. EPA, 1996) was adopted. Sites were at least 50m upstream of roads, reducing the risk of anthropogenic

runoff contamination. Water samples were collected in acid-cleaned polypropylene bottles filtered immediately by 0.45 μm pore size Millipore HDPE membranes, acidified with ultrapure HNO_3 (to 1% v/v) and stored refrigerated (~4°C) until analysis. The fraction that passed through this filter is considered as the 'dissolved load' and is known to consist of colloids less than 0.45 μm in addition to the truly dissolved fraction. Both the syringe and water filter were rinsed several times in the streamwater and the first portion of the filtration was discarded to clean the membrane.

2.2 Sample preparation and digestions

Sample preparation and digestion were carried out in two different laboratories: in the Geochemistry Laboratory at Trinity College Dublin (TCD), Ireland and in the G-Time Laboratory at the Université Libre de Bruxelles (ULB), Belgium. All reagents were prepared using triple-distilled HNO_3 and ultrapure water. At TCD, plant samples were placed in quartz glass crucibles and ashed in a furnace at 600°C for 8 hours. A 0.1 g aliquot of each sample was digested in 1mL ultrapure concentrated HNO_3 for at least 1 hour before evaporating to dryness and being redissolved in 2 mL 2 mol/L HNO_3.

To separate the water soluble and the exchangeable/labile soil fractions of the soil and hence characterise the origin and bioavailability of Sr and REE that can be desorbed by natural solutions in the soil, separate leaching experiments were performed using either ultra-pure H_2O (Pierson-Wickmann et al., 2009; Maurer et al., 2012) or 1 mol/L NH_4NO_3 (DIN:ISO (German Institute for Standardization) ISO (International Organization for Standardization); Loell et al. 2011; Willmes et al. 2014; Zhai et al., 1999). Using these reagents provided a best estimate of (1) the cations available for plants via ion-exchange in the soil (NH_4NO_3), and (2) the cations leachable with water flowing through the soil (ultra-pure H_2O). These solutions do not extract elements bound to organics (Caporale and Violante, 2016). According to Pearcy et al. (2000), the particular salt solution chosen does not significantly affect the amount of ions extracted, as in any case, nearly all exchangeable cations are released into solution. An extensive sequential leach is therefore not generally necessary. The soil samples were dried in an oven for 48 hours at 60°C. Two 1 g aliquots were used for the two different leaching methods. The first method used 2.5 mL of 1 mol/L NH_4NO_3 and was

constantly agitated for 8 hours. The second leaching method used 10 mL of MilliQ H_2O and was constantly agitated for 24 hours. Extractions were conducted at room temperature. All samples were then centrifuged at 3000 rpm for 20 minutes. The supernatant fluid was extracted and evaporated to dryness and then redissolved in 2 mL 2 mol/L HNO_3. To prepare the streamwaters for chemical analysis, 15 mL of sample was evaporated in PMP beakers to which 1 mL of concentrated HNO_3 was subsequently added and left to react for approximately 12 hours in order to attack organics and convert to nitrate for loading on the column. The concentrated HNO_3 was then evaporated and the sample was redissolved in 2 mL of 2 mol/L HNO_3.

At ULB, additional plant samples were placed in porcelain crucibles and ashed by step heating in a muffle furnace at 650 ºC. The entire acid digestion process and subsequent Sr purification was carried out under a class 100 laminar flow hood in a class 1000 clean room (Université Libre de Bruxelles, Belgium). 50 mg of sample was digested in sub-boiled HNO_3 at 120 ˚C for 24 hours. All samples analysed for $^{87}Sr/^{86}Sr$ were purified through Sr separation columns using Sr-Spec resin (Horwitz et al., 1992). Dissolved samples were centrifuged for 30 minutes at 5000rpm and loaded on columns equilibrated to 1 mol/L HNO_3. Following this, 0.05 mol/L HNO_3 eluants were used to collect Sr.

2.3 Quadrupole ICP-MS determination of trace elements

Trace element abundances were measured via quadrupole ICP-MS (Q-ICP-MS) on a Thermo Scientific™ iCAP Q at the Geochemistry Laboratories at Trinity College Dublin. In preparation for analysis, a 0.1 ml aliquot of each of the solutions was sub-sampled and diluted to produce a 2% (v/v) HNO_3 solution bearing a mixed internal standard with ^{6}Li, Rh, Re, Bi and ^{235}U for the purpose of correcting instrument drift and signal suppression during analysis. Experiments were run following the method outlined initially by Eggins et al. (1997), with some adaptations to the method for different sample matrices and instrument configurations as reported elsewhere (Kamber et al., 2003; Babechuk et al., 2010; Lawrence, Greig, et al., 2006). Long-term measurement of trace element abundances in standards reproduce at 3% RSD (1σ) or better for the analytes of interest. Additional consideration of the method accuracy and

precision has been published elsewhere (e.g., Babechuk and Kamber, (2011)). A notable exception is that in waters bearing a significant abundance of Ba and very little Eu (i.e., a high Ba/Eu ratio), the final determination of Eu may be hindered from BaO^+ production (Lawrence et al., 2006); in these cases, Eu data are not reported. The procedural blank contribution to measured unknowns (plants, soil leaches and sampled waters) was typically well below 1% of the measured intensity, with the exception of the most trace element-depleted stream water (SR39), where the contribution of blanks reached a maximum of 10-15% for some analytes. The NH_4NO_3 REE blank was less <1% (mostly <0.2%). The H_2O blank was <0.02 for all REE, so a significant blank contribution can be ruled out.

It is common practice for REE concentrations to be normalised to that of a composite of the average upper continental crust, such as the so-called Post-Archean Australian Shale composite (Taylor and McLennan, 1985). Here, an alternative normalisation dataset known as MuQ (Mud from Queensland), a sediment composite produced by Kamber et al. (2005) is employed. From the normalised patterns, well-established REE anomalies (REE_n/REE_n*), i.e., deviations from an otherwise smooth pattern from the geogenic source or otherwise resulting from a weathering or aqueous reaction, are calculated. Here, REE_n* is the expected normalised concentration when interpolated from a neighbouring element, which does not exhibit anomalous behaviour. The specific projections employ the geometric calculations from Lawrence, Greig, et al., (2006) for La, Ce, Eu, Gd, and Lu. The magnitude of LREE over HREE depletion, i.e., the slope of the overall normalised REE pattern, is expressed as the Pr_n/Yb_n ratio (Pr/Yb ratio: $(Pr/Yb)_n = (Pr/Yb)_{sample}/(Pr/Yb)_{MuQ}$) with values >1 indicating light enrichment, and values <1 indicating heavy enrichment relative to the normalising values. The Dy_n/Yb_n is used in an analogous manner to define MREE/HREE slopes. The over-abundance of Y relative to HREE is expressed numerically using the deviation of the un-normalised Y/Ho ratio from that of shale i.e. greater than 27 (average upper continental crust and chondrite Y/Ho value is ~26 (Kamber et al., 2005)).

2.4 TIMS

Post-elution Sr concentrations were determined to assess the Sr content prior to loading on the filament. Approximately 200 ng of Sr was loaded onto outgassed Re filaments together with 1 μL of a TaF_5 activator to enhance Sr ionisation (Birck, 1986). Sr isotope analyses were performed on a Thermo Scientific Triton Thermal Ionisation Mass Spectrometer (TIMS) with a 5-cup Faraday multi-collector at University College Dublin (UCD). The instrument was tuned for maximum signal strength, stability and peak shape. Sr isotopes were measured in static mode using Faraday cups, which were calibrated immediately before each batch of analyses. A rotation of the Faraday amplifiers was also done during the analysis to eliminate any bias. The cup configuration was as follows; 84 in L1; 85 in C; 86 in H1; 87 in H2 and 88 in H3. To ensure data precision, accuracy, reproducibility and comparability to other international data sources, blank and standard analyses were analysed with each batch of analyses. ^{87}Sr values were corrected for any ^{87}Rb interference and data normalised to a long-term mean standard NBS SRM 987 $^{87}Sr/^{86}Sr$ value of 0.710260 ± 10 (2SE).

2.5 MC-ICP-MS

$^{87}Sr/^{86}Sr$ of additional plant samples were measured by Multi-Collector Induced-Coupled-Plasma Mass-Spectrometry (MC-ICP-MS) following the procedure detailed in Snoeck et al. (2015). The isotope ratios of the purified Sr samples were then measured on a Nu Plasma MC-ICP Mass Spectrometer (Nu015 from Nu Instruments, Wrexham, UK) at ULB. During the course of this study, repeated measurements of the NBS SRM 987 standard yielded $^{87}Sr/^{86}Sr = 0.710214 \pm 40$ (2SE for 15 analyses). All sample measurements were normalised using a sample-standard bracketing method with the recommended value of $^{87}Sr/^{86}Sr = 0.710248$ (Weis et al., 2006).

2.6 Statistical analysis

Plant data were processed using a one-way ANOVA (Welch's ANOVA, IBM SPSS Statistics for Macintosh, Version 23.0, Armonk, NY: IBMCorp.) to test the null hypotheses that $^{87}Sr/^{86}Sr$ of vegetation, soil leachates and streamwater varies based on (1) underlying bedrock geology and (2) surficial geology.

Further evaluation of statistical outliers, distribution of the variables and resultant trimming of data was conducted as per outlined in Kootker et al. (2016). Six different geological formation based groups and seven different Quaternary geology based groups were used, identified by formation number and Quaternary sediment code, respectively (Table. 1). Extreme outliers, values that deviate more than three times the interquartile range (IQR) from the median, were removed from the dataset. Shapiro–Wilk's normality test was conducted to assess the distribution of $^{87}Sr/^{86}Sr$ in each group. Tukey's schematic boxplot was generated to display the intra- and inter-group variations in $^{87}Sr/^{86}Sr$. Levene's test for equality of variances was used to test the null hypothesis of equal variances between the groups.

2.7 Biological Absorption Coefficient (BAC)

The relationship between REE content of the soil extracts and plants is examined using the biological absorption coefficient (BAC) to quantify the natural process of element transfer and translocation rates. This provides an estimate of their individual availability to the plant. The BAC is defined as follows (Miao et al., 2008):

$$\mathrm{BAC} = \mathrm{Lx} / \mathrm{Nx}$$

where, Lx = REE concentration in the dry plant sample and Nx = REE concentration in soil leachate.

This ratio can also be described as a transfer factor ratio (Brioschi et al., 2013). The results were categorised into 5 groups based on the magnitude of the coefficient: BAC > 1000 – very strongly accumulated; from 100 to 1000 – strongly accumulated; from 10 to 100 – moderate absorption; from 1 to 10 – weak absorption, and from 0.1 to 1 – very weak absorption. This follows the structure outlined by Kabata-Pendias, (2001) and Lima e Cunha et al., (2014) but has been altered by a factor of one hundred to compensate for the fact that soil leachate compositions were used rather than bulk soils.

3 Results

3.1 Sr isotopic and concentration data

$^{87}Sr/^{86}Sr$ and Sr concentration ([Sr]) are presented in Table 1 in stratigraphic sequence, based upon the geological formation above which each sample was located. The range in vegetation $^{87}Sr/^{86}Sr$ for the study area is 0.7080 to 0.7130. At four sites, with differing lithologies: (1) Devonian basalt, (2) Ordovician/Silurian shale, (3) Permian sandstone and (4) Carboniferous limestone, soil and streamwater samples were collected at proximal locations to the vegetation and demonstrated a range of 0.7086 to 0.7133 for soil leachates and 0.7081 to 0.7107 for streamwaters. This comparative approach is used to examine the relationship between the chemical and isotope compositions of plants and the soil/lithology of their growth location. When the two soil leachates (H_2O and NH_4NO_3) are compared, in each case the H_2O leachate has a more radiogenic $^{87}Sr/^{86}Sr$ than the corresponding NH_4NO_3 leachate. The concentration of Sr measured in ashed woody plant material ranged from 14-48 mg/kg. Streamwaters ranged from 81-554 µg/L (Table 1). [Sr] of soil leachates is given as the leachable fraction normalised to the amount of dry mass used and ranged from 5 to 8180 µg/L.

Age	Lithology	Fm No.	Quaternary Sediment	Sample I.D.	Sample Type	Easting[a]	Northing	[Sr] (µg/kg)[b]	$^{87}Sr/^{86}Sr$ ratio	2SE	Lab
Lower - Middle Ordovician	Rhyolite and rhyolitic tuff	34	TLPSsS - Till (Lower Palaeozoic sandstone and shale)	SR23	Tree	308772	267470	20340	0.709892	0.000005	UCD
Ordovician - Silurian (416–488 Ma)	Moffat shale facies; Shale and greywacke	42	TLPSsS	SR20	Tree	290215	275794	13890	0.711931	0.000006	UCD
			"	I24	Grass	292556	275409		0.710787	0.000008	ULB
			Rck - Bedrock outcrop	SR19	Tree	291514	278768	17030	0.710697	0.000006	UCD
			"	SR29	H_2O Soil	"	"	5.509	0.711837	0.000042	"
			"	SR34	NH_4NO_3 Soil	"	"	205.1	0.711616	0.000037	"
			TLPSsS	SR39	Streamwater	290858	278747	138.2	0.709856	0.000006	"
Silurian (416–444 Ma)	Deep marine turbidite sequence; mudstone, sandstone, greywacke, shale and conglomerate	49	Rck	I19 - 1*	Grass	307529	284836		0.711762	0.000007	ULB
			"	I19 - 2*	"	"	"		0.710486	0.000008	"
			Ws - windblown sands	I20 - 1*	"	315817	281292		0.709397	0.000007	"
			"	I20 - 2*	"	"	"		0.709177	0.000010	"
			"	I20 - 3*	"	"	"		0.709179	0.000009	"
			GLPSsS -Gravel (Lower Palaeozoic sandstone and shale)	I27 - 1*	"	262733	283186		0.710315	0.000007	"
			"	I27 - 2*	"	"	"		0.708119	0.000008	"
			"	I27 - 3*	Shrub	"	"		0.708328	0.000012	"
			Rck	I35 - 1	"	311401	263848		0.709302	0.000014	"
			"	I35 - 2	Tree	"	"		0.709377	0.000009	"
			TLPSsS	I91 - 1*	Grass	312843	283959		0.711300	0.000009	"
			"	I91 - 2*	"	"	"		0.711027	0.000008	"
			"	I91 - 3*	Shrub	"	"		0.711445	0.000011	"

Age	Lithology	Fm No.	Quaternary Sediment	Sample I.D.	Sample Type	Easting[a]	Northing	[Sr] (µg/kg)[b]	$^{87}Sr/^{86}Sr$ ratio	2SE	Lab
			"	I92 - 1*	Grass	311143	283373		0.714687	0.000011	"
			"	I92 - 2*	"	"	"		0.710293	0.000009	"
			"	SR18	Tree	293090	284654	21910	0.712990	0.000005	UCD
Devonian	Basalt, andesite, basaltic & andesitic tuff	50	Rck	SR21	Tree	293412	273574	24890	0.708415	0.000005	UCD
			"	SR30	H_2O Soil	"	"	5.632	0.713345	0.000044	"
			"	SR35	NH_4NO_3 Soil	"	"	588.3	0.709520	0.000009	"
			GLPSsS	SR40	Streamwater	294125	274150	187.5	0.709761	0.000005	"
Carboniferous, Mississippian	Marine shelf & ramp facies; Argillaceous dark-grey bioclastic limestone, subsidiary shale	61	TLs - Limestone till	SB8	Tree	288768	287451		0.709867	0.000011	ULB
			"	SW7	Streamwater	"	"		0.708336	0.000007	"
Carboniferous, Mississippian	Waulsortian mudbank; Pale-grey massive limestone	62	TLs	SB11	Tree	274108	244665		0.708417	0.000008	ULB
			"	SW6	Streamwater	"	"		0.708119	0.000007	"
Carboniferous Mississippian (299–359 Ma)	Marine shelf facies; Limestone & calcareous shale	64	Ws	I21 - 1	Shrub	314747	277580		0.709235	0.000015	ULB
			"	I21 - 2	Tree	"	"		0.709566	0.000008	"
			A - Alluvium	I22 - 1	Shrub	303860	276113		0.709521	0.000014	"
			"	I22 - 2	Tree	"	"		0.709682	0.000005	"
			GLs	Bettystown**	H_2O Soil	315076	271501		0.709004	0.000027	-
			GLs	Bettystown**	Vegetation	"	"		0.709010	0.000087	-
			TLs	SB4	Tree	301279	265682		0.708438	0.000012	ULB
			"	SW5	Streamwater	"	"		0.708910	0.000009	"
Carboniferous Mississippian	Marine basinal facies; Dark-grey argillaceous	65	TLs	I26 - 1*	Shrub	287445	288471		0.709575	0.000009	ULB
			"	I26 - 2*	Tree	"	"		0.709248	0.000006	"

Age	Lithology	Fm No.	Quaternary Sediment	Sample I.D.	Sample Type	Easting[a]	Northing	[Sr] (µg/kg)[b]	$^{87}Sr/^{86}Sr$ ratio	2SE	Lab
(299–359 Ma) Visean	and cherty limestone & shale		Cut - cutover raised peat	I28 - 1*	Grass	244235	281550		0.708228	0.000007	"
			"	I28 - 2*	Shrub	"	"		0.708305	0.000013	"
			TNSSs - Till (Namurian sandstones and shales)	I37	"	309440	255596		0.708884	0.000008	"
			TLs	SR24	Tree	304678	250183	48150	0.708589	0.000006	UCD
			"	SR31	H_2O Soil	"	"	84.33	0.708672	0.000005	"
			"	SR36	NH_4NO_3 Soil	"	"	4360	0.708622	0.000005	"
			"	SR41	Streamwater	304146	252118	555.1	0.708281	0.000005	"
			"	Tara**	H_2O Soil	289926	259048		0.708333	0.000028	-
			"	Tara**	Vegetation	"	"		0.708421	0.000035	-
			Rck	Cadbury Hill**	H_2O Soil	268749	234702		0.707979	0.000028	-
			TLs	SB2	Shrub	296620	259360		0.709317	0.000012	ULB
			"	SB6	"	"	"		0.708365	0.000013	"
			"	SW2	Streamwater	"	"		0.708632	0.000007	"
			"	SB3	Tree	304678	250183		0.708347	0.000013	"
			"	SB5	"	277046	240041		0.708376	0.000013	"
			"	SB10	Shrub	"	"		0.708737	0.000012	"
			"	SW1	Streamwater	"	"		0.708417	0.000006	"
Carboniferous (299–359 Ma) Namurian	Sandstone, shale; Fluvio-deltaic & basinal marine (Turbiditic); Shale, sandstone, siltstone & coal	71	TLs	I96 - 1	Grass	300282	271704		0.708677	0.000010	ULB
			"	I96 - 2	Shrub	"	"		0.708911	0.000014	"
			"	I96 - 3	Tree	"	"		0.708937	0.000007	"
			"	Knowth - K1	Grass	299690	273439		0.710756	0.000014	"
			"	Knowth - K2	Shrub	"	"		0.708692	0.000008	"
			"	Newgrange	Grass	300743	272727		0.709201	0.000008	"
			"	SR22	Tree	298981	263940	28590	0.708125	0.000005	UCD

Age	Lithology	Fm No.	Quaternary Sediment	Sample I.D.	Sample Type	Easting[a]	Northing	[Sr] (µg/kg)[b]	$^{87}Sr/^{86}Sr$ ratio	2SE	Lab
			"	New Grange**	H_2O Soil	300889	273030		0.709435	0.000035	-
			"	New Grange**	Vegetation	"	"		0.709210	0.000062	-
			"	Knowth**	H_2O Soil	299445	273587		0.709700	0.000290	-
			"	Knowth**	Vegetation	"	"		0.709372	0.000027	-
			"	Knowth**	H_2O Soil	299427	273586		0.709535	0.000032	-
			"	Knowth**	Vegetation	"	"		0.709224	0.000054	-
			"	SB7	Tree	284377	247292		0.709222	0.000012	ULB
			"	SB9	Shrub	"	"		0.709227	0.000013	"
			"	SW3	Streamwater	"	"		0.708578	0.000009	"
Permian	Redbed facies, sandstone, conglomerate, magnesian limestone, marl evaporite	73	TLPSsS	SR17	Tree	279654	290855	43210	0.709084	0.000005	UCD
			"	SR28	H_2O Soil	"	"	86.53	0.709073	0.000005	"
			"	SR33	NH_4NO_3 Soil	"	"	8180	0.709016	0.000009	"
			"	SR38	Streamwater	279761	290904	82.08	0.710651	0.000008	"
Triassic (200–251 Ma)	Sandstone and mudstone with evaporite; Continental redbed facies, lagoonal & shallow marine	75	A - Alluvium	I31 - 1*	Grass	279680	296247		0.710008	0.000008	ULB
			"	I31 - 2*	Shrub	"	"		0.708955	0.000008	"

Table 1. $^{87}Sr/^{86}Sr$ and Sr concentrations of plant, soil leachates and streamwaters as per geological formation. * (Snoeck et al., 2016), ** (Cahill Wilson and Standish, 2016).[a] location data easting and northing are in Irish National Grid, [b] concentration determined by Q-ICP-MS.

3.2 Statistical assessment of spatial $^{87}Sr/^{86}Sr$ variation

The $^{87}Sr/^{86}Sr$ values of plants were categorised into groups based on underlying (1) bedrock and (2) Quaternary geology. The variance of each group was assessed by the Shapiro–Wilk's normality test and demonstrates that the data are normally distributed. Tukey's schematic boxplot in Figure 2 displays the intra- and inter-group variations in $^{87}Sr/^{86}Sr$. Based on Levene's test for equality of variances, the null hypothesis of equal variances can be rejected as there are differences between the variances in the groups (Table 3). Despite the fact that most groups show an overlap in the range of $^{87}Sr/^{86}Sr$, the mean values of certain groups are statistically different ($p<0.05$) (Table 3), indicating noteworthy differences in the spatial variation of $^{87}Sr/^{86}Sr$ in Co. Meath. Namely, the bedrock formation 42 (slate) ≠ 65 (argillaceous limestone) and 49 (mudstone) ≠ 65 (argillaceous limestone), 71 (Carboniferous sandstone). Quaternary deposit ‘Sandstone and shale till’ ≠ ‘Cut peat’, ‘Limestone till’, ‘Windblown sands’ (see Table 3).

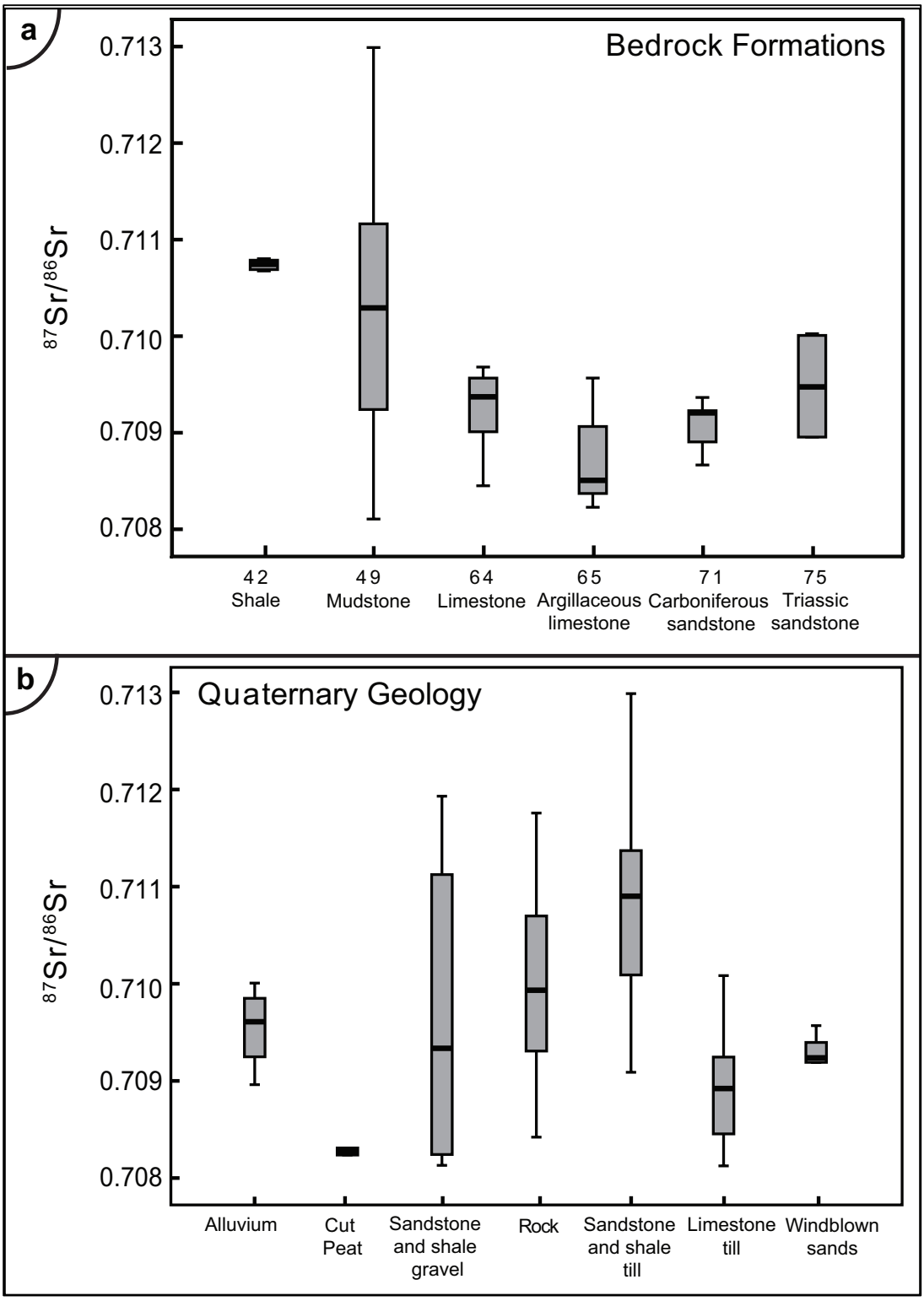


Figure 2. Tukey's schematic boxplot showing $^{87}Sr/^{86}Sr$ variation of each group in Co. Meath. The boxes represent the interquartile range (IQR: Q3–Q1), the central line indicates the median. The whiskers represent Q1−1.5*IQR and Q3+1.5*IQR. For both bedrock and Quaternary geology, there are certain significantly different groups.

Bedrock Formation Statistics	42 - shale	49 - mudstone	49 (w/o outliers)	64 - limestone	65 - argillaceous limestone	71 - Carboniferous sandstone	71 (w/o outliers)	75 - Triassic sandstone
N	2	16	15	6	12	12	10	2
Mean $^{87}Sr/^{86}Sr$	0.710742	0.710449	0.710449	0.709242	0.708699	0.709130	0.709067	0.709482
Standard deviation (1σ)	6.37E-05	1.73E-03	1.36E-03	4.64E-04	4.57E-04	3.85E-07	2.45E-04	7.45E-04
Variance	4.06E-09	3.00E-06	2.00E-06	2.15E-07	2.08E-07	6.20E-04	6.00E-08	5.54E-07
Minimum	0.710697	0.708119	0.708119	0.708438	0.708228	0.708125	0.708677	0.708955
Maximum	0.710787	0.714687	0.71299	0.709682	0.709575	0.710756	0.709372	0.710008
Range	0.000090	0.006568	0.004871	0.001244	0.001347	0.002631	0.000695	0.001053
Median	0.710742	0.710304	0.710293	0.709378	0.708505	0.709205	0.709205	0.709482
Shapiro-Wilk *p* value	-	0.244	0.705	0.340	0.053	0.020	0.058	-

Quaternary Geology Statistics	Alluvium	Cut Peat	Sandstone and shale gravel	Rock	TLPSsS - Sandstone and shale till	TLPSsS (w/o outliers)	TLs - Limestone till	TLs (w/o outliers)	Windblown sands
N	4	2	4	6	9	8	24	23	5
Mean $^{87}Sr/^{86}Sr$	0.709542	0.708266	0.709673	0.710006	0.711278	0.710852	0.708977	0.708900	0.709311
Standard deviation (1σ)	4.40E-04	5.40E-05	1.80E-03	1.20E-03	1.68E-03	1.17E-03	6.08E-04	4.86E-04	1.69E-04
Variance	1.94E-07	2.96E-09	3.00E-06	1.00E-06	3.00E-06	1.00E-06	3.70E-07	2.37E-07	2.84E-08
Minimum	0.708955	0.708228	0.708119	0.708415	0.709084	0.709084	0.708125	0.708125	0.709177
Maximum	0.710008	0.708305	0.711931	0.711762	0.714687	0.71299	0.710756	0.71007	0.709566
Range	0.001053	7.7E-05	0.003812	0.003347	0.005603	0.003906	0.002631	0.001945	0.000389
Median	0.709602	0.708266	0.709321	0.709931	0.711027	0.710907	0.708924	0.708911	0.709235
Shapiro-Wilk *p* value	0.830	-	0.403	0.873	0.468	0.926	0.026	0.185	0.202

Table 2. Descriptive statistics of $^{87}Sr/^{86}Sr$ from plants, for the complete and outlier-trimmed datasets per group.

Bedrock		42 Shale	49 Mudstone	64 Limestone	65 Argillaceous limestone	71 Carboniferous sandstone	75 Triassic sandstone
42 Shale	Mean diff.	-	0.00058	0.00150	0.00204	0.00161	0.00126
	Sig.	-	0.947	0.289	0.002	0.143	0.687
49 Mudstone		-0.00058	-	0.00092	0.00147	0.00110	0.00069
		0.95	-	0.248	0.001	0.035	0.895
64 Limestone		0.00150	0.00092	-	0.00054	0.00018	-0.00024
		0.289	0.248	-	0.80	1.00	1.00
65 - Argillaceous limestone		0.0020	0.00147	0.0005	-	-0.0004	-0.0008
		0.002	0.001	0.803	-	0.915	0.838
71 - Carboniferous sandstone		0.00161	0.00110	0.00018	-0.00037	-	-0.00041
		0.143	0.035	0.999	0.915	-	0.989
75 - Triassic sandstone		0.00126	0.00097	-0.00024	-0.00078	-0.00041	-
		0.687	0.895	0.999	0.838	0.989	-

Quaternary		Alluvium	Cut Peat	Sandstone and shale gravel	Rock	Sandstone and shale till	Limestone till	Windblown sands
Alluvium	Mean diff.	-	0.00128	-0.00013	-0.00047	-0.00131	0.00064	0.00023
	Sig.	-	0.596	1.000	0.978	0.175	0.801	1.000
Cut Peat		0.00128	-	-0.00141	-0.00174	-0.00259	-0.00063	-0.00104
		0.596	-	0.481	0.179	0.006	0.948	0.760
Sandstone and shale gravel		-0.00013	-0.00141	-	-0.00033	-0.00118	0.00077	0.00036
		1.000	0.481	-	0.996	0.281	0.630	0.995
Rock		-0.00047	-0.00174	-0.00033	-	-0.00085	0.00111	0.00070
		0.978	0.179	0.996	-	0.525	0.088	0.822
Sandstone and shale till		-0.00131	-0.00259	-0.00118	-0.00085	-	0.00195	0.00154
		0.175	0.006	0.281	0.525	-	0.000	0.039
Limestone till		0.00064	-0.00063	0.00077	0.00111	0.00195	-	0.00041
		0.801	0.948	0.630	0.088	0.000	-	0.955
Windblown sands		0.00023	-0.00104	0.00036	0.00070	0.00154	0.00041	-
		1.000	0.760	0.995	0.822	0.039	0.955	-

=The mean difference is significant at the 0.05 level

Table 3. Results of the independent sample t-tests comparing mean $^{87}Sr/^{86}Sr$ ratios between the groups. Mean values that are statistically different (p=<.05) are highlighted in grey.

3.3 REE

All pertinent REE ratios are reported along with the abundances in Table 4. The sum REE concentrations vary considerably between sites and between sample media and are given in the order of concentration (see Table 4 for details):

Streamwater: Sandstone >Basalt >Shale >Limestone;
H_2O soil leachate: Basalt >Sandstone >Limestone >Shale;
NH_4NO_3 soil leachate: Basalt >Sandstone >Shale >Limestone;
Plant: Shale>Sandstone>Basalt>Limestone.

Sample Medium	H_2O soil leachate								NH_4NO_3 soil leachate							
Sample I.D.	**SR28**		**SR29**		**SR30**		**SR31**		**SR33**		**SR34**		**SR35**		**SR36**	
Comparative Site	Sandstone		Shale		Basalt		Limestone		Sandstone		Shale		Basalt		Limestone	
		BAC		BAC		BAC		BAC		BAC		BAC		BAC		BAC
(µg/kg)																
Li	2.974	26.9	6.108	60.4	7.201	14.9	1.782	247	13.84	5.77	29.71	12.4	21.70	4.94	3.133	140
Sr	86.53	499	5.509	3090	5.632	4420	84.33	571	8180	5.28	205.1	83.0	588.3	42.3	4360	11.0
Rb	2.376	523	3.751	219	7.685	317	4.392	221	33.05	37.6	94.04	8.74	116.1	21.0	50.06	19.4
Mo	2.115	3.01	0.241	21.5	0.489	562	3.866	8.89	BDL	-	BDL	-	BDL	-	BDL	-
Ba	128.6	857	24.40	5370	73.94	202	118.7	140	20990	5.25	5426	24.2	10520	1.42	16400	1.01
U	3.872	0.32	0.446	7.18	0.695	3.85	1.212	0.99	3.187	0.39	0.435	7.36	0.445	6.00	1.185	1.01
La	5.960	6.48	2.400	37.0	9.178	7.17	6.989	3.70	48.14	0.80	31.55	2.82	308.0	0.21	6.209	4.16
Ce	9.858	5.44	7.906	15.1	42.72	1.75	14.18	2.23	50.35	1.07	59.00	2.02	454.2	0.17	8.158	3.87
Pr	2.205	2.23	0.878	16.6	3.922	2.96	2.139	1.88	9.251	0.53	4.842	3.01	52.65	0.22	1.120	3.58
Nd	10.60	1.77	3.981	13.7	16.58	2.55	9.352	1.57	40.66	0.46	18.80	2.91	188.1	0.23	4.656	3.16
Sm	3.025	1.45	1.042	11.1	3.221	2.28	2.251	1.30	9.834	0.45	3.919	2.96	26.81	0.27	1.032	2.84
Eu	0.842	-	0.268	-	0.760	-	0.542	-	2.616	-	0.960	-	6.025	-	0.176	-
Gd	3.739	1.61	1.119	9.26	2.365	2.74	2.441	1.18	13.57	0.44	4.731	2.19	21.44	0.30	1.028	2.79
Tb	0.563	1.59	0.165	9.11	0.307	2.72	0.372	1.10	1.901	0.47	0.689	2.18	2.569	0.33	0.138	2.96
Dy	3.322	1.53	0.906	8.99	1.590	2.80	2.211	1.01	10.90	0.47	3.772	2.16	12.42	0.36	0.786	2.84
Y	21.22	9.17	4.061	26.0	7.162	12.1	14.80	4.21	109.4	1.78	28.84	3.67	98.71	0.88	6.846	9.10
Ho	0.711	1.51	0.172	9.42	0.297	3.00	0.466	1.00	2.354	0.46	0.731	2.22	2.277	0.39	0.170	2.74
Er	2.036	1.28	0.442	9.42	0.769	2.92	1.267	0.96	6.324	0.41	1.763	2.36	5.306	0.42	0.459	2.64
Tm	0.307	1.05	0.061	9.23	0.107	2.88	0.181	0.93	0.861	0.38	0.218	2.58	0.644	0.48	0.063	2.68
Yb	2.105	0.84	0.362	9.03	0.643	2.76	1.104	0.90	5.263	0.34	1.145	2.86	3.216	0.55	0.380	2.63
Lu	0.347	0.79	0.049	9.90	0.090	3.01	0.162	0.94	0.847	0.33	0.152	3.19	0.426	0.64	0.059	2.59
ΣREE	66.83		23.81		89.71		58.46		264.1		129.6		874.9		25.07	
Ratios:																
Rb/Sr	0.03		0.68		1.36		0.05		0.00		0.41		0.16		0.01	
Ba/Sr	5.92		19.1		56.0		5.98		1.51		23.5		14.9		3.15	
Y/Ho	29.8		23.6		24.2		31.8		46.5		39.4		43.4		40.3	
La/La_n*	1.08		0.97		0.72		1.07		1.73		1.69		1.28		1.65	
Ce/Ce_n*	0.66		1.25		1.41		0.89		0.73		1.45		0.94		0.93	
Eu/Eu_n*	1.04		1.01		1.07		0.98		1.08		1.08		1.19		0.73	
Gd/Gd_n*	1.13		1.09		1.05		1.07		1.23		1.14		1.14		1.13	
Lu/Lu_n*	1.02		0.97		0.98		1.01		1.11		1.07		1.12		1.10	
Dy_n/Yb_n	0.87		1.38		1.36		1.11		1.14		1.82		2.13		1.14	
Pr_n/Yb_n	0.40		0.93		2.34		0.74		0.68		1.63		6.29		1.13	

Table 4. Key trace element concentrations with instructive ratios, and Biological Absorption Coefficients (BAC). BDL: below detection limit.

Sample Medium	Vegetation								Streamwater			
Sample I.D.	**SR17**	**SR18**	**SR19**	**SR20**	**SR21**	**SR22**	**SR23**	**SR24**	**SR38**	**SR39**	**SR40**	**SR41**
Comparative Site	Sandstone	Mudstone	Shale	Shale	Basalt	Sandstone	Rhyolite	Limestone	Sandstone	Shale	Basalt	Limestone
(µg/kg)									**(µg/L)**			
Li	79.85	135.6	368.8	176.6	107.1	50.91	143.9	439.7	0.302	0.659	1.894	1.867
Sr	43210	21910	17030	13890	24890	28590	20340	48150	82.08	138.2	187.5	555.1
Rb	1242	1484	822.0	1032	2438	459.2	1276	970.6	0.673	0.220	0.984	1.037
Mo	6.369	6.965	5.188	3.605	274.8	21.39	3.763	34.38	0.527	0.040	0.217	2.544
Ba	110200	33200	131100	154000	14960	12290	102600	16560	65.79	65.35	114.5	69.96
U	1.251	0.400	3.200	2.024	2.672	1.153	1.088	1.195	0.122	0.159	0.507	1.827
									(ng/L)			
La	38.61	30.76	88.9	100.8	65.84	13.84	51.72	25.85	158.1	14.3	12.7	8.8
Ce	53.64	28.05	119.0	131.7	74.93	24.13	66.48	31.55	128.2	BDL	17.7	11.2
Pr	4.923	4.762	14.58	17.83	11.59	2.956	8.253	4.010	52.3	4.0	3.3	2.3
Nd	18.71	17.52	54.7	65.83	42.34	11.72	31.38	14.71	258.1	19.0	15.5	11
Sm	4.376	3.861	11.60	14.81	7.332	2.367	6.579	2.928	64.9	4.5	4.3	3.2
Eu	-	-	-	-	-	-	-	-	15.7	BDL	BDL	BDL
Gd	6.030	4.691	10.36	15.72	6.481	2.266	6.621	2.870	75.1	5.6	4.5	3.5
Tb	0.896	0.655	1.503	2.249	0.835	0.320	0.921	0.408	9.8	0.8	0.7	0.5
Dy	5.068	3.19	8.142	11.19	4.453	1.882	4.956	2.233	56.2	5.0	4.4	3.9
Y	194.6	75.9	105.7	223.3	86.34	210.5	81.42	62.32	414.1	43.5	45.3	44.0
Ho	1.075	0.566	1.620	2.048	0.892	0.453	0.986	0.465	12.4	1.1	1.1	1.0
Er	2.614	1.169	4.163	4.813	2.245	1.184	2.418	1.211	36.8	3.3	3.3	3.1
Tm	0.323	0.132	0.563	0.616	0.308	0.183	0.307	0.169	5.6	0.5	0.5	0.5
Yb	1.776	0.671	3.269	3.531	1.772	1.207	1.708	0.998	39.9	3.2	3.5	3.7
Lu	0.275	0.098	0.485	0.540	0.271	0.210	0.252	0.153	7.5	0.5	0.6	0.7
ΣREE	332.1	172.4	424.6	595.7	307.1	273.6	264.1	150.3	1335	105.7	117.4	97.3
Ratios:												
Rb/Sr	0.01	0.03	0.02	0.04	0.05	0.01	0.02	0.02	0.06	0.01	0.04	0.01
Ba/Sr	0.87	0.64	2.40	5.19	0.31	0.18	1.75	0.30	6.01	3.54	4.58	0.95
Y/Ho	181	134	65.3	109	96.8	465	82.6	134	33.4	39.8	41.1	45.0
La/La_n^*	1.95	1.50	1.47	1.33	1.30	1.27	1.56	1.49	1.26	1.39	1.47	1.42
Ce/Ce_n^*	1.27	0.66	0.94	0.83	0.72	0.99	0.94	0.88	0.37	0.25	0.78	0.69
Eu/Eu_n^*	-	-	-	-	-	-	-	-	0.97	-	-	-
Gd/Gd_n^*	1.18	1.18	1.04	1.11	1.12	1.08	1.11	1.08	1.21	1.18	1.09	1.13
Lu/Lu_n^*	1.19	1.22	1.08	1.13	1.12	1.12	1.12	1.10	1.12	1.13	0.99	1.12
Dy_n/Yb_n	1.58	2.62	1.37	1.75	1.39	0.86	1.60	1.24	0.78	0.86	0.70	0.58
Pr_n/Yb_n	1.07	2.73	1.71	1.94	2.51	0.94	1.86	1.54	0.50	0.48	0.36	0.24

Table 4. Continued.

3.3.1 Soil leachates

The H_2O leachate of the soils exhibit variable total REE concentrations (23.81-89.71 µg/kg), as well as distinct REE patterns and anomalies (Fig. 5). Y/Ho of the soil associated with shale and basalt are lower at 23.59-24.15 compared to the sandstone and limestone with higher values of 29.84-31.76. The latter trend is mirrored by a negative Ce anomaly in the shale and basalt soil (0.66-0.89) and a positive Ce anomaly in the sandstone and limestone soils (1.25-1.41). The La, Eu, and Lu anomalies are near uniform (0.95-1.05) for most samples, apart from a slight positive Eu anomaly (1.07) and negative La anomaly (0.72) in the basalt soil. A minor Gd anomaly is present in all soils (1.05-1.13). The slope of the REE patterns are variable with Dy_n/Yb_n ranging from 0.87 to 1.38, increasing in the order of shale>basalt>limestone>sandstone soils and Pr_n/Yb_n ranging from 0.40 to 2.34, increasing in the order of basalt>shale>limestone>sandstone.

The NH_4NO_3 leachate of the soils also exhibit highly variable total REE concentrations (25.07-874.9 µg/kg) (Fig. 5). Y/Ho of the soils range from 39.42-46.46 and those associated with shale and basalt are lower at 23.59-24.15 compared to the sandstone and limestone (29.84-31.76). The Ce anomalies in the basalt and limestone soils are minor (0.93 and 0.94 respectively), negative in the sandstone (0.73), and positive in the shale (1.45). The Eu anomaly is minor, ranging from 1.08-1.19, with the highest recorded in the basalt soil. All soils record positive La, Gd, and Lu anomalies, ranging from 1.28-1.73, 1.13-1.24, and 1.07-1.12, respectively. The MREE/HREE slope is only slightly positive in the limestone and sandstone with Dy_n/Yb_n both at 1.14, but higher in the shale (1.82) and basalt (2.13). The overall LREE/HREE slope ranges from 0.68 to 6.29, increasing in the order of basalt>shale>limestone>sandstone. Relative to the H_2O leaches (Figure 5c), the NH_4NO_3 leachates release more of the exchangeable/bioavailable REE, as indicated by the higher REE concentrations, with the exception of the limestone soil leachate (lower in NH_4NO_3 leached sample). Moreover, the NH_4NO_3 leachates from the same soils exhibit greater LREE/HREE enrichment with patterns increasing gradually from Lu to La and higher anomalies (preferential leaching) of the La, Ce, Gd, Y, and Lu.

3.3.2 Vegetation

The total REE concentrations of selected vegetation samples (SR17-SR24) ranged from 150.3 to 595.7 µg/kg, with a mean of 315.0 µg/kg ± 142.9 (n=8). The MREE/HREE slopes are generally consistent with Dy_n/Yb_n a mean of 1.55 ± 0.51 (n=8), with the exceptions of one mudstone/shale sample (SR18 = 2.62) and one sandstone sample (SR22 = 0.86). The overall REE pattern slopes are flat to LREE/HREE enriched with Pr_n/Yb_n ranging from 0.94 to 2.72 with a mean Pr_n/Yb_n ratio of 1.709 ± 0.602 (n=8). All vegetation samples exhibit positive La, Gd, and Lu anomalies (>1.05) and negative Ce (mean of 0.90, n=8). The most striking feature of the vegetation samples is the strong enrichment in Y relative to Ho, with Y/Ho ranging from 65.28-465.1 (Table 4).

The REE and [Sr] can be separated quite readily based on the BAC classification scheme as the latter is strongly to very strongly concentrated in most the studied plants relative to the H_2O soil leachates and weakly to moderately concentrated relative to the NH_4NO_3 soil leachates (BAC ranges from 0.32-5370 for H_2O leach and from 0.17-140 for NH_4NO_3 leach). Relatively high BAC of Y is evident from both H_2O (range: 4.21-26.0) and NH_4NO_3 soil leachates (range: 0.88-9.10).

3.3.3 Dissolved load in streamwater

The total dissolved REE concentrations (ΣREE) of streamwaters are low and variable, ranging from 0.10 to 1.33 µg/L. The highest concentrations (sample SR38) are observed in streamwater that drains terrain overlying Permian sandstone whilst the sample with the lowest sum REE concentration (sample SR41) drains carbonate terrain. This is the inverse of [Sr] for the same samples. All streamwater samples are notably depleted in LREE relative to HREE, with a $(Pr/Yb)_n$, range from 0.24 to 0.50 (Table 4; Figure 7). Moreover, all streamwater samples are characterised by negative Ce anomalies (0.25-0.78, n = 4) and superchondritic Y/Ho ratios ranging from 33.43 to 44.96 (mean 39.83 ± 4.80; n = 4). The majority of streamwaters exhibit positive La (1.26-1.47), Gd (1.09-1.21), and subtly positive Lu (0.99-1.13) anomalies. The Eu abundance was only detectable in the most REE enriched streamwater sample (SR38) and does not exhibit an Eu anomaly ($Eu/Eu_n^* = 0.97$).

4 Discussion

4.1 Sr isotope and concentration data

The range in $^{87}Sr/^{86}Sr$ of modern plants over the study area is 0.7080 to 0.7130. There is a lack of agreement between the $^{87}Sr/^{86}Sr$ measured in different sample media overlying basalt, shale and sandstone (Figure 3). However, vegetation, soil leachates and streamwater associated with limestone bedrock (Formations 64 and 65) have a much smaller range in $^{87}Sr/^{86}Sr$ (0.7082-0.7097), fitting closely with the relatively narrow range of previously measured biosphere samples in Carboniferous limestone regions of Britain: 0.7089 (soil leach n=5), 0.7092 (plant n=11), 0.7099 (water n=7) (Evans et al., 2010). The Waulsortian (upper Tournaisian – lower Visean) limestone underlying much of Co. Meath has an average $^{87}Sr/^{86}Sr$ of 0.7079 (±0.0009, n=23)(Douthit et al., 1993). This value reflects Visean seawater composition which is inferred from the analysis of well-preserved marine fossils (0.7075-0.7082) (Burke et al., 1982; McArthur et al., 2001). Similarly, Visean limestones on the Isle of Man yielded $^{87}Sr/^{86}Sr$ of 0.7079 (n=2) (Hendry et al., 2015). The mean of all limestone-associated biosphere values in this study, 0.7089 ± 0.011 (n=11), is higher than these published whole rock values, indicating an additional more radiogenic source. This can result from the leaching of more silicate-rich fractions in the surficial sediments or the input of contemporary rainfall with values generally close to that of seawater but which can be higher (ca. 0.7095) depending on dust contribution (Bain and Bacon, 1994; Négrel et al., 2007). Moreover, the naturally leachable fraction of bedrock likely does not equate to that of the bulk rock $^{87}Sr/^{86}Sr$. The water-soluble Sr of carbonates were found to vary from 0.23% to 1.3% of the total rock composition (Bailey et al., 2000). Both the water soluble and 1 mol/L ammonium acetate leached fractions produced higher $^{87}Sr/^{86}Sr$ than the bulk rock due to the dissolution of groundwater salts, contaminant Sr on ion-exchange sites and a weak dissolution of calcite (Bailey et al., 2000).

Devonian basalt provides the highest range of $^{87}Sr/^{86}Sr$ values across all sample media, 0.7084 (vegetation) - 0.7133 (H_2O soil leachate) (Fig. 3). The large range is somewhat misleading as the H_2O leach provides an exceptionally high $^{87}Sr/^{86}Sr$ value that is a statistical outlier. Biosphere values above basalt formations within Britain and Ireland

generally do not demonstrate comparably radiogenic values. The range of previously measured biosphere samples (soil, plant, water) overlying basalt in the UK is 0.7061 – 0.7105 (Evans et al., 2010) and in Northern Ireland, which hosts expansive basalts, overlying modern plant samples have been found to have an average value of 0.7089 ± 0.0037 2SD (Snoeck et al 2016). The vegetation and streamwater $^{87}Sr/^{86}Sr$ from the basalt in this study region have much less radiogenic values; 0.7084 and 0.7098 respectively, which are more likely representative of the local biosphere values.

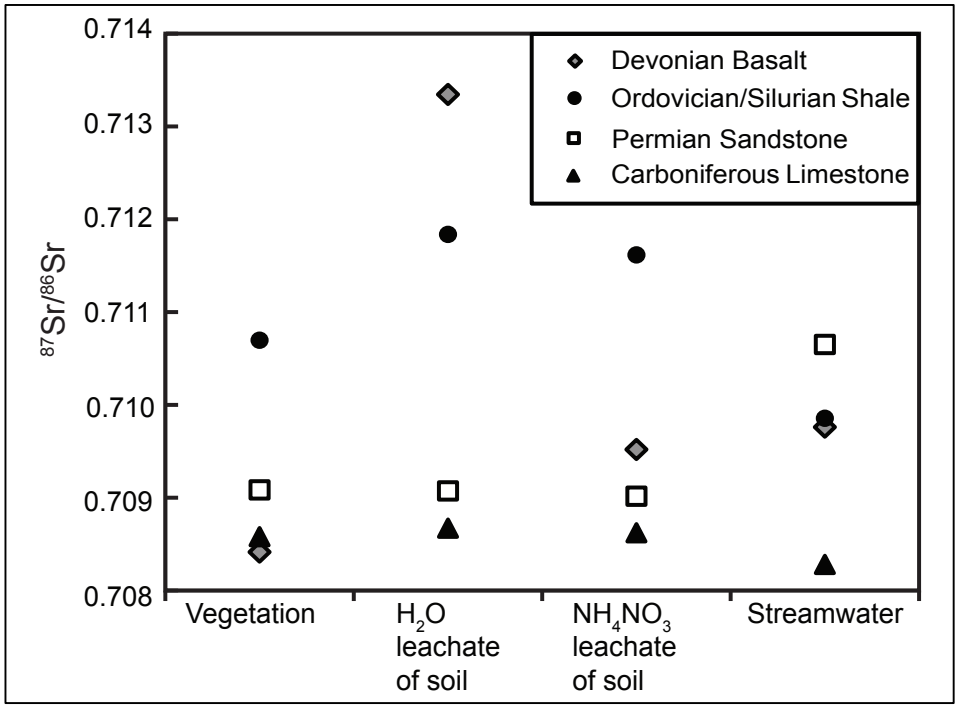


Figure 3. $^{87}Sr/^{86}Sr$ for sample media at four comparative sites in Co. Meath with differing underlying geology. Whilst the $^{87}Sr/^{86}Sr$ of each sample medium overlying the limestone bedrock is relatively invariable, the $^{87}Sr/^{86}Sr$ of different samples at the other three sites show more variation, highlighting a higher degree of complexity in Sr transfer.

Streamwater [Sr] in the region displays a wide spread of values (ranged between 81-554 µg/L), highlighting the complex nature of Sr in the hydrological system of Co. Meath. These concentration data correspond with probable values for the underlying lithology, with concentrations increasing from sandstone < shale < basalt < limestone bedrock. The Quaternary deposit types also correspond with measured streamwater [Sr], showing that streams draining limestone rich tills are the most concentrated in Sr and have the least radiogenic isotope values. Conversely, those draining Lower Palaeozoic sandstone tills have lower concentrations and more radiogenic $^{87}Sr/^{86}Sr$.

The streamwater draining an area with only very thin Lower Palaeozoic sandstone till coverage with outcrops of Permian sandstone bedrock has the lowest concentrations and the highest $^{87}Sr/^{86}Sr$ of the sampled streamwaters. Therefore, both the $^{87}Sr/^{86}Sr$ and [Sr] reflect mixing of bedrock and surficial sediments.

4.2 Suitability of sample media used for bioavailable Sr mapping

Establishing geochemical relationships between soil/plants and streamwater geochemistry makes it possible to determine which sample media are most informative for geographical discrimination studies. Both soil and plants have been employed in previous studies for producing biosphere isoscapes (Evans et al., 2010; Frei and Frei, 2013; Hartman and Richards, 2014; Hodell et al., 2004; Laffoon et al., 2012; Nafplioti, 2011; Porder et al., 2003; Price et al., 2014; Price and Naumann, 2015; Sjögren et al., 2009; Willmes et al., 2014) but it is not agreed which sample medium is most appropriate for this purpose. Most of the debate centers on soils and their disposition for variability. Owing to the fact that the mineral components of soils are inherited from geological parent materials that have been weathered to varying degrees, the bioavailable soil solution is not always in equilibrium with the soil-mineral component (Kabata-Pendias, 2001).

$^{87}Sr/^{86}Sr$ of natural mineral waters have demonstrated a good correlation with estimated values based on the local geology (Montgomery, Evans, and Wildman, 2006; Voerkelius et al., 2010). Correspondence between plant $^{87}Sr/^{86}Sr$ and other media such as snails and small home-range fauna have also been noted (Blum et al., 2000; Laffoon et al., 2012). NH_4NO_3 soil leachates and plants collected across France (Willmes et al., 2014) are correlated (R^2 = 0.89). Warham (2011) also made comparisons between vegetation, H_2O soil leachates and streamwater from different geological settings. Again, there is a strong correlation between the mean values of each sample type in their geological group (n = 30 plant, 30 streamwater, 26 soil leaches), but within each of the chronostratigraphic groups, the standard deviation of the soil data is almost an order of magnitude greater than the associated plant and streamwater values, with the soil leaches giving consistently more radiogenic values than both plants and waters.

Here, when two soil leachates (H_2O and NH_4NO_3) of the same soil are compared, in each case the H_2O leach has more radiogenic $^{87}Sr/^{86}Sr$ than its NH_4NO_3 counterpart (Fig. 3). This finding suggests the latter leaches relatively more Sr from less radiogenic carbonate minerals due to the increased aggressiveness of the NH_4NO_3 towards such mineral weathering products (cf. Frei and Frei, 2013; Warham 2011). The deionised H_2O leach was potentially not aggressive enough to replicate natural dissolution of primary and secondary carbonate minerals and therefore does not achieve values similar to those seen in plant and streamwater and does not represent the bioavailable fraction of the soil. Overall, the $^{87}Sr/^{86}Sr$ range in soil leachates is determined by the specific leaching method chosen and therefore, careful selection of an appropriate leaching protocol, in this case NH_4NO_3, is necessary for informative estimates of the natural ranges that exist within the pedosphere. Based on results from this study, soil leachates provide a larger range of $^{87}Sr/^{86}Sr$ than vegetation and are thus less effective at estimating local bioavailable $^{87}Sr/^{86}Sr$ ranges. This is in agreement with others studies (Evans et al., 2010; Evans and Tatham, 2004; Maurer et al., 2012; Poszwa et al., 2002; Montgomery et al., 2003) that also conclude soil leachates are a poor material for mapping local $^{87}Sr/^{86}Sr$ as they can produce more variable $^{87}Sr/^{86}Sr$, that are inconsistent with the associated plant data. Thus, plant material provides a more direct estimate of bio-available $^{87}Sr/^{86}Sr$ and can average out short-term or seasonal variations in the soil composition.

4.3 Relationship between bedrock/Quaternary geology and biosphere

Thick glacial deposits (>10 m depth in most areas) of differing composition are extensive across Co. Meath. Consequently, there is strong potential for these surficial glacial deposits to contribute to the Sr biosphere budget. Both the underlying bedrock (Figure 4 a) and Quaternary surficial geology (Figure 4 b) are examined as controlling factors of biosphere $^{87}Sr/^{86}Sr$.

Based on discriminant analysis, using $^{87}Sr/^{86}Sr$ as descriptors, there were significant differences ($p>0.05$) in the mean $^{87}Sr/^{86}Sr$ of plants between both the different bedrock formations (n=47, categorised into 6 groups) and Quaternary geology (n=52, categorised into 7 groups). Notably, formation 49, Silurian mudstone was significantly different statistically ($p<0.05$) from both Formations 65 (Visean limestone) and 71 (Carboniferous shale/sandstone). In addition, the mean difference of biosphere samples

overlying the two primary Quaternary geology groups (limestone till (n=24) and Lower Palaeozoic sandstone and shale till (n=8)) was statistically significant (Table 3). The $^{87}Sr/^{86}Sr$ signature of these samples therefore reflects both the underlying geology and, to a significant degree, the superficial Quaternary geology. The surficial deposits in this region homogenise with the local bedrock signatures and thus, the measured signatures reflect the averaging of these two prominent geochemical reservoirs.

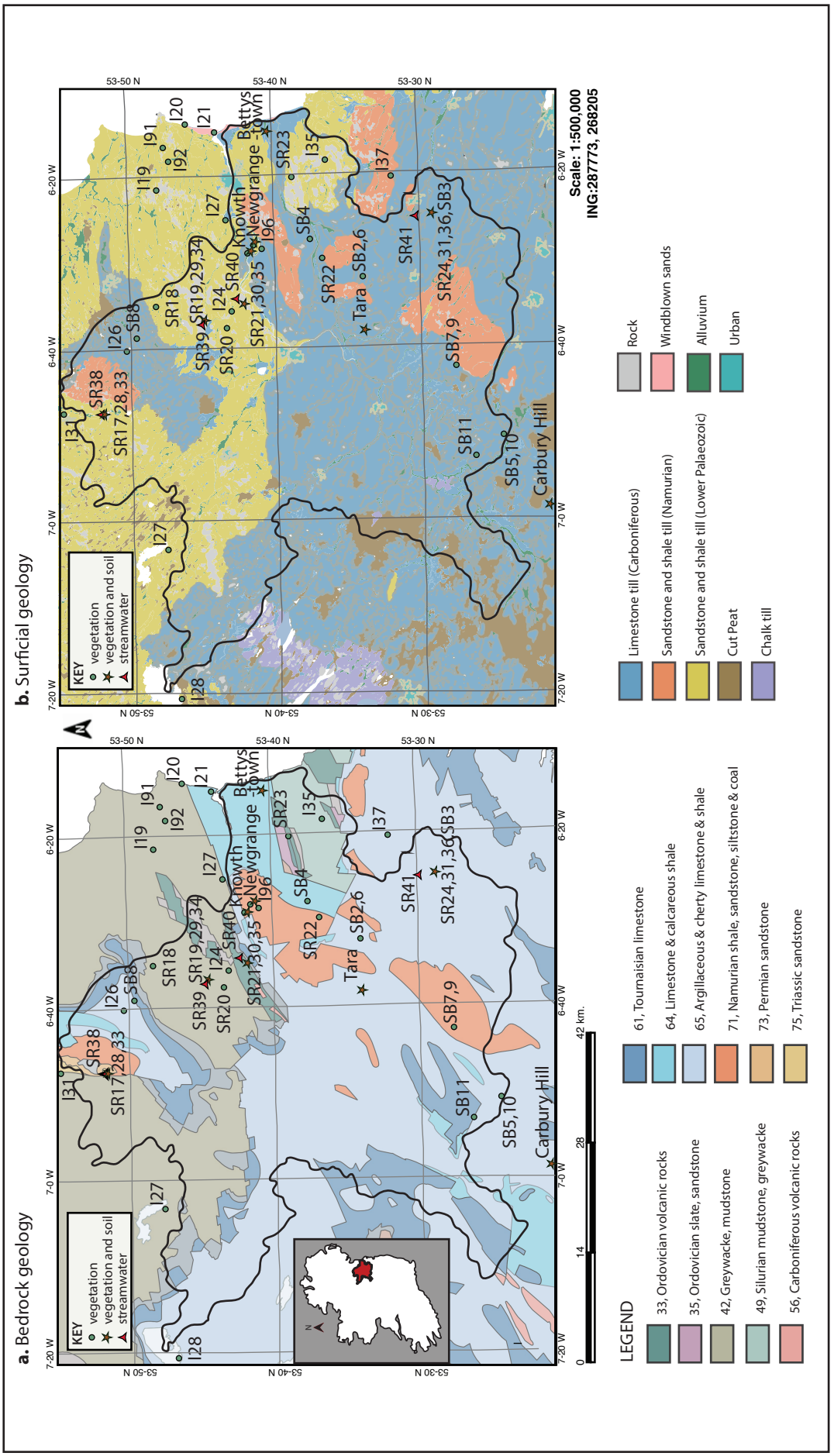


Figure 4. (a) Bedrock and (b) Quaternary geology of Co. Meath with sample sites and corresponding $^{87}Sr/^{86}Sr$. Basemap from the Geological Survey of Ireland, (2016).

4.4 Archaeological implications

Element cycling from bedrock through to the biosphere underpins isotopic geographical discrimination. Characterising the distribution of Sr in the biosphere of Co. Meath and the surrounding area is of particular interest owing to the region's rich archaeological heritage, with internationally renowned sites such as Newgrange, Tara and Knowth. Based on the statistical and observed results of this study, Co. Meath has distinct $^{87}Sr/^{86}Sr$ packages within the local biosphere that correlate, to varying degrees, with both underlying bedrock and superficial sediments. Therefore, it is possible to use this isotope system as a provenance indicator for archaeological case studies based within this region, with caution not to base interpretations on bedrock geology composition alone.

Whilst the overall $^{87}Sr/^{86}Sr$ range (0.7080 to 0.7130) of plants across the entire studied region is not geographically unique when compared with values already known for Ireland and to the more regionally comprehensive database for Britain, there are nonetheless distinctive divisions of the biosphere. For comparison, plants collected across Britain have a range of 0.7077 (chalk bedrock) to 0.7266 (granite bedrock) (Evans et al., 2010; Montgomery, Evans, and Wildman, 2006). $^{87}Sr/^{86}Sr$ of modern plants from the north of Ireland demonstrate a range of 0.7067 (basalt bedrock) to 0.7195 (granite bedrock), excluding those values deemed as outliers (Snoeck et al. 2016). This highlights that there are regions of Ireland which have measured biosphere $^{87}Sr/^{86}Sr$ lower and higher than the range in Co. Meath (0.7080 to 0.7130).

Granite and a combination of Lower Palaeozoic and late Pre-Cambrian metamorphic rocks are found in the West of Ireland (Fay et al., 2007). Due to the extensive age of these rocks, they are likely to have higher $^{87}Sr/^{86}Sr$ that other parts of the country. Northern Ireland comprises schists and quartzites and high $^{87}Sr/^{86}Sr$ values are exhibited in granitic gneisses (0.7603-0.7676), shales (0.7196-0.7273) and diorites (0.7126-0.7217) in south east Ireland (Davies et al., 1985). Tertiary basalts in the northeast of Ireland are relatively young and low in Rb and therefore exhibit less radiogenic $^{87}Sr/^{86}Sr$, ~0.703-0.708 (O'Connor, 1988; Wallace et al., 1994) and a porcellanite from the north of Ireland was found to have mean $^{87}Sr/^{86}Sr$ values of 0.7044

(± 0.0004, n=12)(Curran et al., 2001). $^{87}Sr/^{86}Sr$ of modern plants collected across Northern Ireland ranged between 0.7067 (above basalt bedrock) to 0.7195 (above granite bedrock) (Snoeck et al., 2016).

Although these values are measured from whole rocks, they indicate that the biosphere components can source Sr from rock reservoirs with $^{87}Sr/^{86}Sr$ values both below and above the range exhibited in Co. Meath. This allows archaeological remains of individuals local to this area to be distinguished from those originating from such isotopically distinct regions of Ireland or from further afield. Using $^{87}Sr/^{86}Sr$ for geographic discrimation of regions to trace origin can also be informative when compared with more radiogenic environments such as Scandinavia. The higher $^{87}Sr/^{86}Sr$ values that characterise parts of Northern European regions, and hence the people who inhabited them, allow such individuals to be discerned from those who were local to Co. Meath or the surrounding area (cf. Knudson et al. 2012).

Dentine can exchange varying proportions (15-100%) of biogenic Sr with soil from its burial environment making it unreliable as a reservoir of biogenic Sr (Budd et al., 2000). It is because of this exchangeability of Sr with soil that measured dentine $^{87}Sr/^{86}Sr$ values are sometimes used as a proxy for the local range in biosphere $^{87}Sr/^{86}Sr$ values (Evans et al., 2010; Montgomery et al., 2007). In such cases, dentine $^{87}Sr/^{86}Sr$ valuesare used in combination with the co-genetic enamel and Sr concentrations to define a diagenetic vector. The inconsistency of soil leachates with vegetation data in this study suggest that using dentine, derived from archaeological dental remains that were buried and equilibrated with surrounding soil, may be erroneous for establishing such a vector towards biologically available Sr (BASr) and determining local ranges. The local leached soil does not directly reflect BASr and by inference, neither would exchanged tooth dentine. Plant material is the most appropriate and informative sample type for estimating BASr in this region but owing to small-scale variations, high-density sampling is required.

4.5 REE in the biosphere

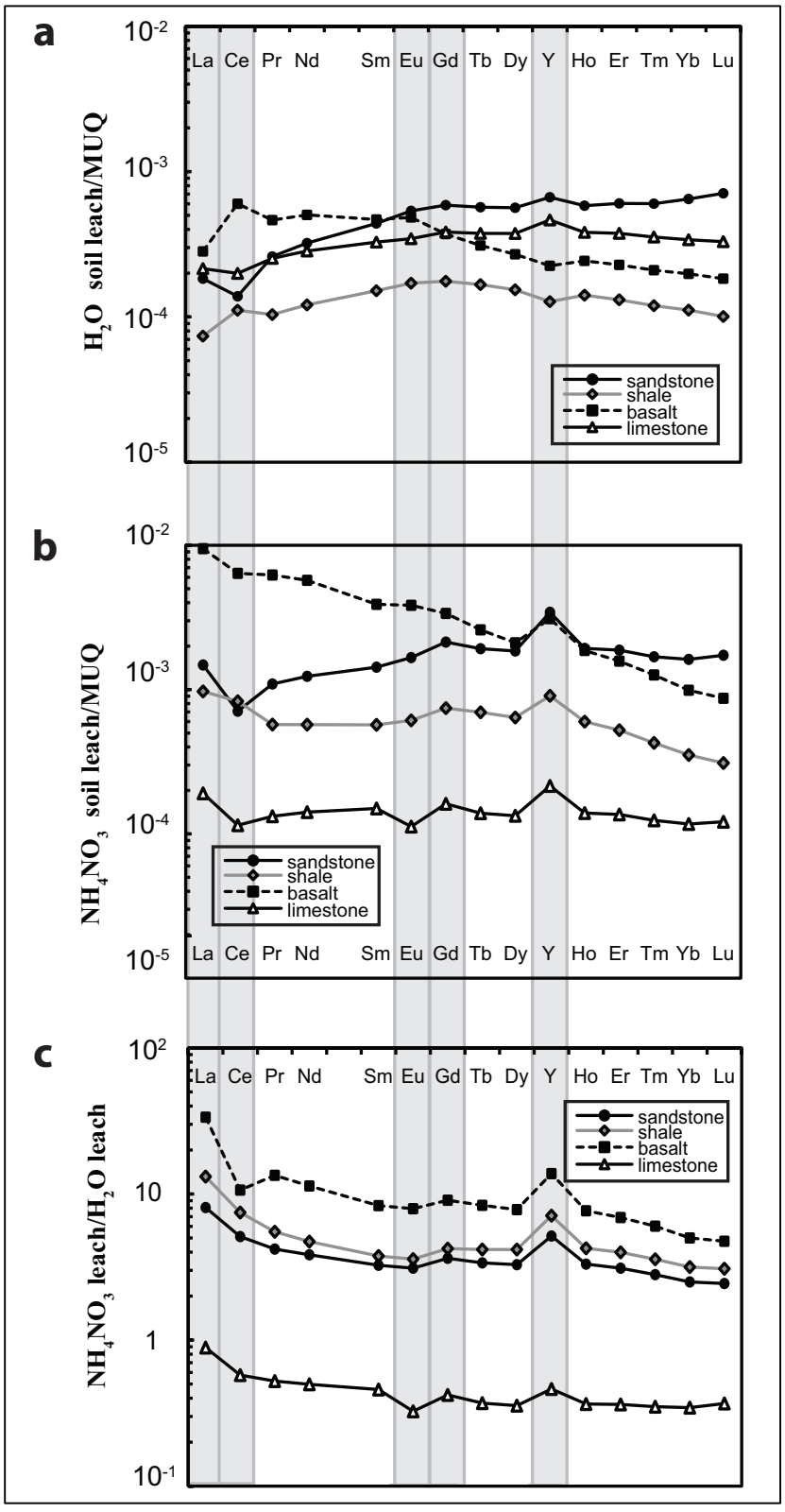


Figure 5. Soil REE of (a) H_2O leachate, (b) NH_4NO_3 leachate and (c) leachates normalised to one another. Key features of REE patterns are highlighted with grey backgrounds. Normalisation value is the modern alluvial sediment composite MUQ (Mud from Queensland) of Kamber et al. (2005).

4.5.1 Translocation of REE from soil to biomass

Just as for the [Sr], there are notable differences between the two leaching methods employed, both in terms of REE concentration and overall pattern (Figure 5). The main comparative bedrock types in this catchment (sandstone, mudstone, basalt and limestone), should have distinct REE and [Sr] based on mineral composition as the distribution of both Sr and REE in various soils typically reflects the geological origin of parent rocks and their mineral composition (Kabata & Pendias 2001). Thus, one might expect the REE pattern and $^{87}Sr/^{86}Sr$ of the soils that have developed on these rocks to reflect, at least to some extent, their geochemical fingerprint. When comparing total concentration of REE in soils on the basis of geographical location, those developed on basalt bedrock have relatively higher REE concentrations than the soil developed on sandstone, shale and limestone lithologies. It follows that generally, soils originating from igneous rock, sandstone, and shale have higher REE contents than soils developed from loess and calcareous rock (Hu et al., 2006; Loell et al., 2011). Apatite ($Ca_5(PO_4)_3(OH,Cl,F)$) is a conceivable major source of REE in basalt-derived soils due to their weatherability and high abundance of REE and often a characteristic LREE enrichment (Giero and Stille, 2004). Accordingly, the greatest enrichment of LREE/HREE in the soil from basalt-dominated areas could arise from the preferential leaching of REE from its carrier apatite. The NH_4NO_3 leached-soils that developed on the limestone bedrock had the lowest ΣREE. Calcareous soils tend to have relatively low REE contents; carbonate bears relatively low REE concentrations and any non-carbonate phases in limestone (minor amounts of phyllosilicate detritus) would be poorly leachable (Bailey et al., 2000).

The presence of positive Ce anomalies in the H_2O leaches of the basalt and shale-derived soils suggest that more easily exchangeable Ce was present and likely reflects a higher abundance of Fe/Mn oxy(hydroxides). In contrast, a negative anomaly was present for the NH_4NO_3 leachate of the basalt soil which may reflect dilution by LREE released from other phases. The overall stronger LREE enrichment of NH_4NO_3 over H_2O soil leachates suggests that mineral phases abundant in LREE, are more susceptible to dissolution with the more aggressive leach and thus, NH_4NO_3 preferentially releases LREE adsorbed to soil particulate surfaces. Particularly, mudstones and argillaceous sediments exhibit greater LREE concentrations over HREE

(Aide and Aide, 2012) and bulk soils tend to have higher LREE concentrations with respect to HREE (Kabata-Pendias, 2001). It is thus likely that NH_4NO_3 is acting to leach the bulk soil more intensively, and in doing so mirrors more closely the slope that would be present for the bulk soil itself.

By comparing REE patterns of soil leachates and trees accessing this nutrient pool, it is possible to address whether the observed REE anomalies in *Fraxinus excelsior L.* are a function of those in soil. The distribution of individual REE in plants showed some agreement with that in the soil extracts but no clear trends were observed (Figure 6). Generally, REE extracted with the H_2O and NH_4NO_3 extraction procedures were poor indicators of REE uptake in plants, with a slightly closer correspondence between the REE of plants with those of the NH_4NO_3 leach, which have relatively flat REE slopes when normalised to one another (mean slope=1.10, n=4). LREE enrichment is consistent in the plants above that of the H_2O leachates (Figure 6b). Notably, the Gd, and Lu anomalies are near uniformity when normalised to the H_2O leachate, indicating that the plants capture these anomalies from the water soluble portion of the soils. Exceptions are the variability in the Ce anomalies (Ce/Ce_n* range from 0.65 - 1.73) that appear to be only represented by the leachates of the limestone. The strong over-abundance of Y in all vegetation samples beyond what was released by the NH_4NO_3 or H_2O leached soils. Whilst the water-soluble and exchangeable fraction are operationally defined, they are nonetheless useful for obtaining an estimate of REE bioavailability. As such, it cannot be explicitly deduced that the specific anomalies present in the leached soils are a precursor of those in the terminal branches of *Fraxinus excelsior L*. Nonetheless, the discrepancy between the REE patterns of the sample media indicates that the aerial portion of ash trees do not directly reflect the REE in the bioavailable portion of the soil.

Fractionation of Ce results from changes in oxidation state whilst fractionation of the other REE may be due to differences between plant species or even variations between individual plants of the same species (Wyttenbach et al., 1998). Under oxic conditions Ce(III) is oxidised to Ce(IV) which is less mobile, due to its adsorption by Fe/Mn oxides and resulting in a preferential uptake of the trivalent REE (Bau, 1999; Laveuf and Cornu, 2009). Two soil leachate samples (from above shale and basalt) and all plants display a negative Ce anomaly. This is consistent with previous studies demonstrating

lesser uptake of Ce(IV) in vascular plants, such as spruce and blackberry (Wyttenbach et al., 1998; Fu et al., 2001). The penetrability of ions through plant membranes decreases with the increase of its valency and therefore even simple ions of Ce(IV) are less penetrable than Ce(III) and thus, dissolved REEs typically exhibit a Ce-depletion (Fu et al., 2001). The negative Ce anomalies in *Fraxinus excelsior L.* supports findings that REE behaviour in aerial portions of plants is mainly partitioned in the dissolved phase as it is preferentially scavenged on the roots and is thus less mobile than the other REE, cf. Censi et al. (2014). Therefore, REE are absorbed and/or are likely to have been transported within the plant tissues as free ions rather than complex ions.

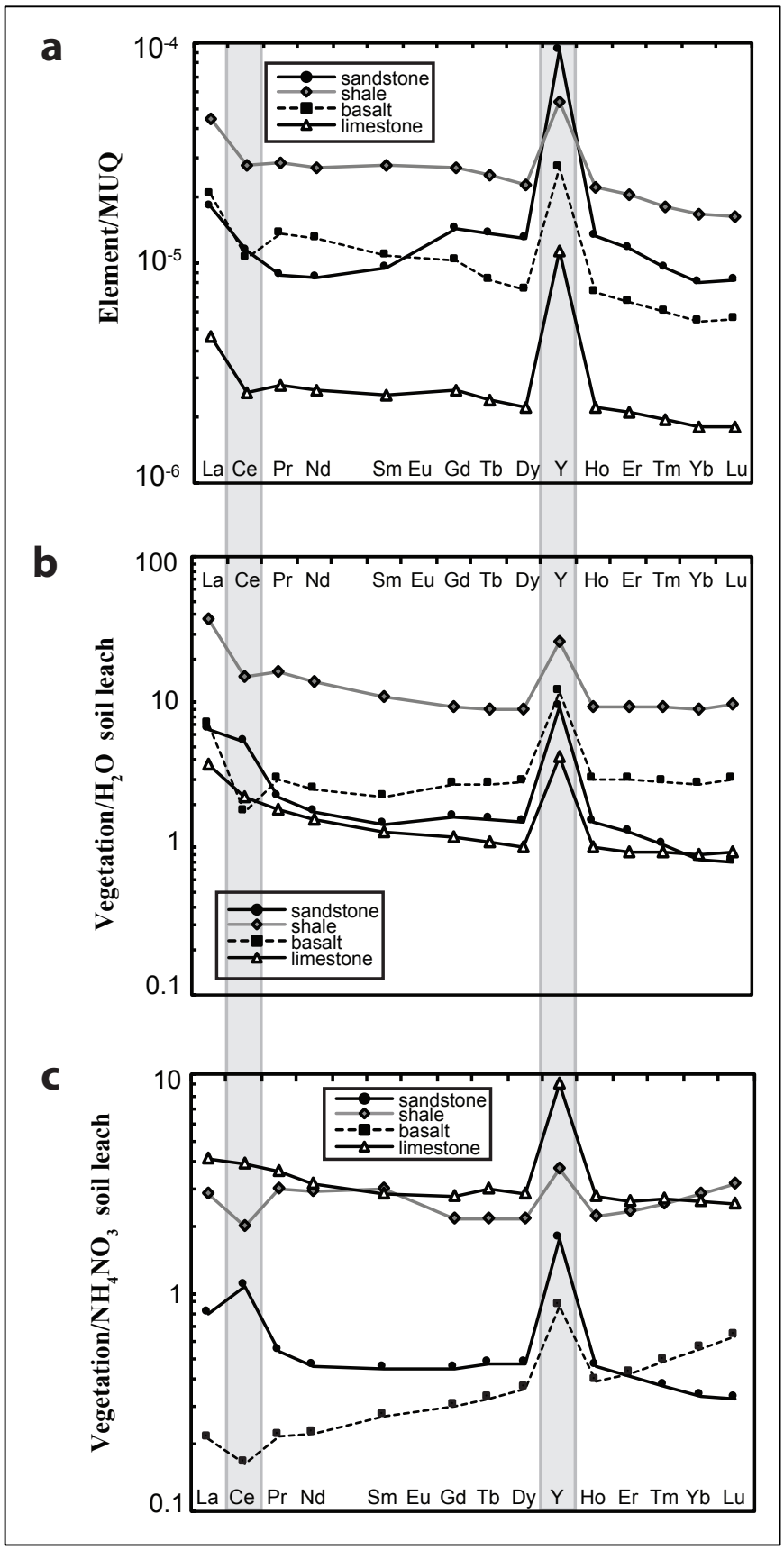


Figure 6. REE of vegetation from comparative sites (n=4) normalised to (a) MUQ, (b) H_2O leachate and (c) NH_4NO_3 leachate.

The REE patterns of the trees illustrate an overall similarity to each other, where generally LREE are being fractionated from HREE during migration from the soil and uptake into the plant system and as a result, the BAC is higher for LREE (except for Ce) than HREE. This fractionation was not noted for the bark from *Fraxinus excelsior L.* from environments across France (Agnan et al., 2014). There is a natural tendency for the preferential uptake of available LREE relative to HREE with decreasing transfer of REE with increasing atomic mass. The high abundance of LREE relative to HREE has been widely observed but whether this fractionation occurs during the process of absorption or within the plant tissues themselves is still an ongoing subject of research. Rather than the plants indiscriminately absorbing REE, the LREE enrichment of plants may result from plant roots preferentially solubilising LREE in soil surrounding the plant roots over HREE. This LREE enrichment has been taken to reflect the presence of organic acids, ligands, the dissolution of the phosphate phase in the soil and complexation of REE in the rhizosphere (Ding et al., 2006; Fu et al., 1998,2001; Miao et al., 2008; Wang et al., 1997; Wei et al., 2001; Wyttenbach et al., 1998; Zhang et al 2002). Additionally, REE bound to Fe-oxyhydroxides include HREE in their mineral structure and as a result, LREE are relatively more mobile, and thus are more likely to enrich soil water pool (Brioschi et al., 2013).

REE mostly have very weak to weak absorption coefficients (BAC ranges from 0.84-37.03 for H_2O leach and from 0.17-4.16 for NH_4NO_3 leach), with the exception of Y and La, which are enriched in these plants (Table 4). The high Y/Ho ratio is the most striking characteristic of the REE patterns of tree samples (Figure 6a). Notably, the topsoils are dominantly developed on carbonate-rich tills and the preferential Y enrichment may be consistent with the chemical composition of the local carbonate lithology, which already bears an over-abundance of Y (relative to Ho). However, although the anomaly may in part be attributed to a transfer of the geogenic signature during biouptake, the Y/Ho anomaly in all biomass is much higher than all measured soil leachates and would appear to require a preferential uptake mechanism of Y. At what stage and for what purpose this occurs is speculative (Kastori et al., 2010), but the enhanced aqueous mobility of Y due to its contrasting complexation behaviour in comparison to the lanthanides (Bau et al., 1996) is probably a contributor to the elevated uptake from the soil element budget.

Elevated Y/Ho ratios have also been recorded by Yu et al., (2007) in mangrove tree rings with Y/Ho ratios ranging from 70-229, averaging 124. These values are much higher than expected seawater or shale Y/Ho ratios. Yu et al., (2007) speculated that the relative enrichment of Y to Ho and the other REE is due to the difference in its transportation in the metabolic pathway or its bioavailability in ambient seawater. In another case study, Loell et al., (2011), measured the total REE contents (aqua regia digestion), potentially plant-available (EDTA) and mobile (NH_4NO_3) in loess soils. The authors found that the EDTA fraction represented on average 10.1% of the total REE soil contents with a notably high available proportion of Y (mean 24.8%, max 39%). In addition, Ce was the most abundant REE in the bulk digests but was least abundant in the EDTA fraction emphasising its poor bioavailability. The mobile (NH_4NO_3) fraction had mostly undetectable amounts of REE, with only ~0.018% of the total REEs measured in this mobile fraction. These findings corroborate the REE patterns found in the present study, with depleted Ce and elevated Y concentrations in the plants reflecting their respective lower and higher bioavailability in the potentially-available soil fraction.

The general geochemical distinction between soils and plants associated with different parent materials is observed within other diagnostic trace elements that concentrate in different minerals/rock types. For example, the soils developed on shale and basalt have higher Rb/Sr and Ba/Sr ratios than those from sandstone or limestone catchments. Generally, Rb/Sr is comparatively higher in all sample media overlying basalt bedrock, whilst the inverse is true for samples overlying limestone, although plants and streamwater seem to have more variable trace element ratios and ΣREE than the soil leachates. Streamwater draining sandstone bedrock has a relatively high Ba/Sr and Rb/Sr whilst streamwater draining limestone bedrock displays a much lower Ba/Sr than the other three comparative samples. This is likely due to the high concentration of Sr being sourced from the limestone, or in general a greater contribution from a Sr-rich carbonate source. Moreover, Y/Ho is highest in this sample and has the lowest Pr_n/Yb_n (steepest slope), which would be consistent with the inferred higher source of carbonate weathering contributing to the signature. For all streamwater samples, there is a strong correlation between [Sr] and Pr_n/Yb_n (R^2=0.87), Y/Ho (R^2=0.69) and U concentrations (R^2=0.99). Pr_n/Yb_n and U concentrations are highly correlated (R^2=0.90) for waters in

the order of: sandstone (0.122 µg/L) <shale (0.159 µg/L) <basalt (0.507 µg/L) <limestone (1.827 µg/L) which illustrates the complex sourcing of this element.

4.5.2 Dissolved load in streamwater

Individual REE patterns of sampled streams are remarkably similar, whilst having diverse concentrations. The MUQ normalised REE patterns of the streamwaters exhibit a strong resemblance to those of seawater or groundwater (Figure 7), of which the characterising features are a steep LREE/HREE depleted pattern, negative Ce anomaly, and over-abundance of La, Gd, and, to a lesser extent, Lu (see Kamber et al., (2014) for a discussion of these features). The expression of each of these features in the streamwaters is noteworthy, since it suggests that the predominant source of the REE in all areas is carbonate (either bedrock or surficial sediments), which reflect the palaeo-ocean chemistry from which they were precipitated. As rainwater percolates through the soil and carbonate-rich sediments and enters the streams by means of run-off, the freshwater flowing off these small catchment systems manages to obtain the seawater-like trace element geochemical fingerprint. This finding is in agreement with the conclusions of several other investigations analysing terrestrial waters, showing that rivers, groundwater and lakes can have HREE enriched patterns that resemble those of modern seawater (e.g. Elderfield et al. 1990; Smedley 1991; Johannesson & Lyons 1994; Sholkovitz 1995; Johannesson et al. 1999; Tricca et al. 1999; Johannesson & Hendry 2000; Johannesson et al. 2006). The degree of fractionation in river water is not as pronounced as seawater, implying that the processes that give rise to this HREE enrichment pattern of seawater (solution and surface complexation reactions) have been partially overprinted by dissolved REE derived from the weathering of other, siliciclastic or igneous rocks in the area, indicated also by a flatter slope (Pr_n/Yb_n).

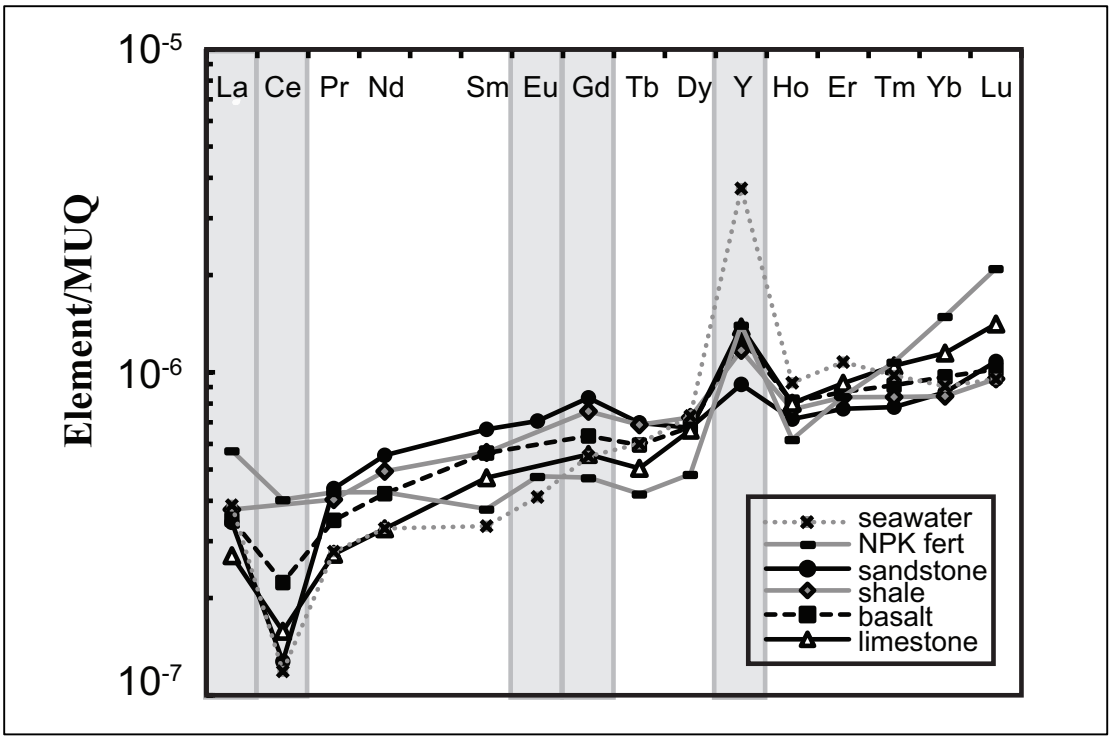


Figure 7. REE distribution of streamwater. Average REE pattern of NPK fertilisers (N=3) and fodder phosphate (n=1)((Hu et al., 1998) and shallow seawater REE (n=12)(Alibo and Nozaki, 1999; Hongo et al., 2006) are also plotted. For visual comparison, the patterns have been scaled to a constant concentration (Lawrence, Greig, et al., 2006). Note that negative Ce and positive Y anomalies are seen in the streamwater, shallow seawater and NPK fertiliser REE distribution.

The negative Ce anomaly reflects the redox-induced separation of Ce^{4+} relative to remaining redox-insensitive (strictly trivalent) LREE. This separation is well-documented to occur in soils prior to REE leaching or during aqueous transport (Wang and Liang, 2014) or, alternatively, can arise as a feature inherited from the weathering of a source rock already exhibiting a Ce anomaly as would be expected from the carbonates. Ce and Y are not expected to fractionate significantly in freshwater (Lawrence, Jupiter, et al., 2006; Lawrence, Greig, et al., 2006; Möller et al., 2003) and therefore aquatic fractionation alone is unlikely to explain the high Y/Ho ratios in the range of 33-45. The elevated ratios in these waters are instead an indication that there has been inheritance from overlying till or carbonate rock. Möller et al. (2003) also attributed elevated Y/Ho ratios and strongly negative Ce anomalies to these interactions. Many authors (Armand et al., 2015; Pourret et al., 2010) have demonstrated that the magnitude of Ce anomalies in both groundwaters and river waters decreases downslope as REE become bound to organic colloids at low topographies. With low organic carbon/Fe(Mn) ratios in the soil, a negative Ce anomaly exists in soil

solutions (Pédrot et al., 2015). Armand et al., (2015) measured the REE concentrations of 119 streamwater samples across France and the authors stress that topography, residence time, wetlands and pH play a key role in the speciation of REE in river systems. Pourret et al., (2010) also found topography to be a main controlling factor on the spatial distribution of Ce anomalies. As first and second order upland streams were samples here, this may have also contributed to the negative Ce anomalies noted.

Whilst groundwater and mature river water can have prolonged contact with the host aquifer rock, it is evident in this study area that the distinctive seawater-like REE pattern can occur from preferential weathering of marine carbonate sources in a complex bedrock and tillite bearing catchment. An additional factor is the potential contribution from anthropogenic sources in the form of fertilisers with high marine phosphate composition, which is difficult to differentiate based on their similar REE pattern to seawater. The average REE pattern of NPK fertilisers (n=3) and fodder phosphate (n=1) (Hu et al., 1998) and shallow seawater REE (n=12) (Alibo and Nozaki, 1999; Hongo et al., 2006) are plotted with the streamwater REE from this study for the purpose of visual comparison (Fig. 7) and illustrate their overall similarity. The source and composition of the phosphate fertiliser(s) applied to this region would need to be established and without adequate contrast between those and the carbonate within the catchment, these sources cannot be discerned. However, it is noted that the $^{87}Sr/^{86}Sr$ reflect differences in bedrock without obvious evidence for a fertiliser contribution. Unlike Sr, REE cannot be used to directly correlate a solute to a specific source lithology as the signature in this case is overwhelmed by the carbonate fraction/fertiliser input and therefore REE patterns do not reflect small-scale differences in underlying bedrock within this region and instead reflect a more homogenised signature.

Plants have very distinct REE patterns when compared with streamwaters. This can be interpreted as a selective transfer of REE between these environmental compartments, with streamwater inheriting the same REE signature from the carbonate in the catchment whilst the signature of the plants is controlled by other factors, as previously discussed. Stille et al., (2006), demonstrated that LREE are preferentially absorbed by plants in a forested setting, which results in LREE depletion in surface run off and streams in a forested catchment. This may also be contributing to the similar trend observed here. In the context of this study, the REE chemistry of streams does not

directly reflect the availability in the sampled soils, despite also exhibiting evidence for the preferential release of HREE/LREE, Gd, Y, and La. This overall lack of agreement between the REE signature of the leached soils and the streams is likely a result of REE being sourced from the wider preferential dissolution of carbonate in till, fertiliser input, the catchment itself being underlain by carbonate, or any combination of the above.

REE and Sr have different aqueous characteristics and mineral sources and thus, have different capabilities as tracers. Whilst the REE pattern is remarkably similar between all waters suggesting that the carbonate/fertiliser dominates this REE budget, [Sr] and $^{87}Sr/^{86}Sr$ are highly variable and reflect a mixed contribution from different geogenic/biospheric processes. Thus REE, within this study site, are less diagnostic of source input than $^{87}Sr/^{86}Sr$, but both tracers are valuable for revealing different information about element mobility within the catchment. REE are more sensitive to site specific parameters such as pH, organic matter content and topography whilst $^{87}Sr/^{86}Sr$ act to average reservoir sources.

5 Conclusion

This study has taken a systematic sampling approach to trace the distribution and movement of $^{87}Sr/^{86}Sr$ and trace elements, namely REE, in streamwater, soils and plants to enhance our understanding of the dispersal of these elements through the biosphere. The complexity of sources highlights several challenges to elemental mapping in such an environment. Streamwater REE patterns have a consistent and seawater-like pattern that appears to be inherited from marine carbonate bedrock, interaction with surficial marine carbonate-derived till, anthropogenic fertiliser input or a combination of all three. By contrast, a spatial variation in streamwater $^{87}Sr/^{86}Sr$ is evident. Therefore, unlike $^{87}Sr/^{86}Sr$, REE could not be used for correlation to a specific source lithology, since they do not reflect small-scale differences in underlying bedrock within this region and instead reflect a more homogenised signature derived from the preferential leaching of REE from carbonate rock with possible additions from anthropogenic fertilisers.

A significant fractionation phenomenon among individual REE was observed during transport from the exchangeable soil to both plants and streamwater. Plants show a general tendency of decreasing transfer of REE with increasing atomic mass, resulting in a LREE-enrichment. The biological absorption coefficient (BAC) of REE reveals that plants from geologically discrete regions differ in absorption capacity but a striking preferential biouptake of Y is noted in all ash tree (*Fraxinus excelsior L.*) samples. The transportation of individual REE in plants shows some agreement with that of the soil extracts, mostly those leached with H_2O, which captured the apparent preferential release of La, Gd, Lu, and preferential release of LREE, but overall, both NH_4NO_3 and H_2O leaches were poor indicators of REE uptake in plants. Further work is necessary to understand the behaviour of the anomalous REE elements in soil reservoirs (e.g., complexation, preferential release during weathering, uptake mechanisms).

The $^{87}Sr/^{86}Sr$ of soil leachates is procedurally defined and is therefore not accurately informative of the natural values that exist within the pedosphere. This finding attests to the view that plant material is most suitable for the purpose of constructing biosphere Sr isoscapes. In contrast to some of the larger Sr biosphere mapping studies to date that

have taken a more generalised regional approach, this research has spatially resolved variation at a resolution that allows for more detailed local geochemical differences to be observed. Use of discriminant analysis successfully classified certain bedrock lithologies and Quaternary deposits as isotopically coherent biosphere packages. Namely, there are significant ($p<0.05$) differences in biosphere values between sandstone/shale tills and those composed primarily of limestone. These distinguishable biosphere units demonstrate that the presence of soil-parent materials derived from both bedrock and Quaternary sediments control the $^{87}Sr/^{86}Sr$ distribution within this region. Even without a large range in $^{87}Sr/^{86}Sr$ biosphere values, significant spatial variations in $^{87}Sr/^{86}Sr$ have been characterised. Furthermore, there is sufficient $^{87}Sr/^{86}Sr$ variation within this region to give critical geographic perspective to archaeological provenance investigations.

Acknowledgments

S.E.R. was funded by a Trinity Postgraduate Studentship. C.S. was supported by the Philippe Wiener-Maurice Anspach Foundation. We thank the technical and scientific staff at University College Dublin, in particular Mr. Michael Murphy, who provided invaluable help with the analyses. Nadine Mattielli, Jeroen de Jong and Wendy Debouge from the G-Time laboratory of the Université Libre de Bruxelles are also thanked for their help with strontium isotope analyses.

References

Åberg, G., Fosse, G., and Stray, H., 1998, Man, nutrition and mobility: A comparison of teeth and bone from the Medieval era and the present from Pb and Sr isotopes: Science of the Total Environment, v. 224, p. 109–119.

Agnan, Y., Séjalon-Delmas, N., and Probst, A., 2014, Origin and distribution of rare earth elements in various lichen and moss species over the last century in France: Science of the Total Environment, v. 487, p. 1–12.

Aide, M.T., and Aide, C., 2012, Rare Earth Elements: Their Importance in Understanding Soil Genesis: ISRN Soil Science, v. 2012, p. 1–11.

Alibo, D.S., and Nozaki, Y., 1999, Rare earth elements in seawater: Particle association, shale-normalization, and Ce oxidation: Geochimica et Cosmochimica Acta, v. 63, p. 363–372.

Armand, R., Cherubini, C., Tuduri, J., Pastore, N., and Pourret, O., 2015, Rare earth elements in French stream waters — Revisiting the geochemical continental cycle using FOREGS dataset: Journal of Geochemical Exploration, v. 157, p. 132–142.

Aubert, D., Probst, A., Stille, P., and Viville, D., 2002, Evidence of hydrological control of Sr behavior in stream water (Strengbach catchment, Vosges mountains, France): Applied Geochemistry, v. 17, p. 285–300.

Aubert, D., Stille, P., and Probst, A., 2001, REE fractionation during granite weathering and removal by waters and suspended loads: Sr and Nd isotopic evidence: Geochimica et Cosmochimica Acta, v. 65, p. 387–406.

Aubert, D., Stille, P., Probst, A., Gauthier-Lafaye, F., Pourcelot, L., and Del Nero, M., 2002, Characterization and migration of atmospheric REE in soils and surface waters: Geochimica et Cosmochimica Acta, v. 66, p. 3339–3350.

Babechuk, M.G., and Kamber, B.S., 2011, An estimate of 1.9 Ga mantle depletion using the high-field-strength elements and Nd-Pb isotopes of ocean floor basalts, Flin Flon Belt, Canada: Precambrian Research, v. 189, p. 114–139.

Babechuk, M.G., Kamber, B.S., Greig, A., Canil, D., and Kodolányi, J., 2010, The behaviour of tungsten during mantle melting revisited with implications for planetary differentiation time scales: Geochimica et Cosmochimica Acta, v. 74, p. 1448–1470.

Bailey, T.R., McArthur, J.M., Prince, H., and Thirlwall, M., 2000, Dissolution methods for strontium isotope stratigraphy: Whole rock analysis: Chemical Geology, v. 167, p. 313–319.

Bain, D.C., and Bacon, J.R., 1994, Strontium isotopes as indicators of mineral weathering in catchments: Catena, v. 22, p. 201–214.

Bataille, C.P., and Bowen, G.J., 2012, Mapping $^{87}Sr/^{86}Sr$ variations in bedrock and water for large scale provenance studies: Chemical Geology, v. 304–305, p. 39–52.

Bau, M., 1999, Scavenging of dissolved yttrium and rare earths by precipitating iron oxyhydroxide: Experimental evidence for Ce oxidation, Y-Ho fractionation, and lanthanide tetrad effect: Geochimica et Cosmochimica Acta, v. 63, p. 67–77.

Bau, M., Koschinsky, A., Dulski, P., and Hein, J.R., 1996, Comparison of the partitioning behaviours of yttrium, rare earth elements, and titanium between hydrogenetic marine ferromanganese crusts and seawater: Geochimica et Cosmochimica Acta, v. 60, p. 1709–1725.

Beard, B.L., and Johnson, C.M., 2000, Strontium isotope composition of skeletal material can determine the birth place and geographic mobility of humans and animals: Journal of forensic sciences, v. 45, p. 1049–1061.

Bentley, R.A., 2006, Strontium Isotopes from the Earth to the Archaeological Skeleton: A Review: Journal of Archaeological Method and Theory, v. 13, p. 135–187.

Bentley, R.A., and Knipper, C., 2005, Geographical patterns in biologically available strontium, carbon and oxygen isotope signatures in prehistoric SW Germany: Archaeometry, v. 47, p. 629–644.

Birck, J.L., 1986, Precision K-Rb-Sr isotopic analysis: Application to Rb-Sr chronology: Chemical Geology, v. 56, p. 73–83.

Blum, J.D., Taliaferro, E.H., Weisse, M.T., and Holmes, R.T., 2000, Changes in Sr/Ca, Ba/Ca and $^{87}Sr/^{86}Sr$ ratios between trophic levels in two forest ecosystems in the northeastern U.S.A.: Biogeochemistry, v. 49, p. 87–101.

Bowen, G.J., Maibauer, B.J., Kraus, M.J., Röhl, U., Westerhold, T., Steimke, A., Gingerich, P.D., Wing, S.L., and Clyde, W.C., 2014, Two massive, rapid releases of carbon during the onset of the Palaeocene–Eocene thermal maximum: Nature Geoscience, v. 8, p. 44–47.

Braun, J.-J., Viers, J., Dupré, B., Polvé, M., Ndam, J., and Muller, J.-P., 1998, Solid/Liquid REE Fractionation in the Lateritic System of Goyoum, East Cameroon: The Implication for the Present Dynamics of the Soil Covers of the Humid Tropical Regions: Geochimica et Cosmochimica Acta, v. 62, p. 273–299.

Brioschi, L., Steinmann, M., Lucot, E., Pierret, M.C., Stille, P., Prunier, J., and Badot, P.M., 2013, Transfer of rare earth elements (REE) from natural soil to plant systems: Implications for the environmental availability of anthropogenic REE: Plant and Soil, v. 366, p. 143–163.

Brooks, R.R., 1972, Geobotany and Biogeochemistry in Mineral Exploration: New York: Harper & Row, 1-292 p.

Budd, P., Montgomery, J., Barreiro, B., and Thomas, R.G., 2000, Differential diagenesis of strontium in archaeological human dental tissues: Applied Geochemistry, v. 15, p. 687–694.

Bunker, D.J., Smith, J.T., Livens, F.R., and Hilton, J., 2000, Determination of radionuclide exchangeability in freshwater systems: Science of the Total Environment, v. 263, p. 171–183.

Burke, W.H., Denison, R.E., Hetherington, E. a, Koepnick, R.B., Nelson, H.F., and Otto, J.B., 1982, Variation of seawater $^{87}Sr/^{86}Sr$ throughout Phanerozoic time: Geology, v. 10, p. 516–519.

Byrne, R.H., and Sholkovitz, E.R., 1996, Marine chemistry and geochemistry of the lanthanides., in K.A. Jr., Gschneidner and L., Eyring (Eds.), Handbook on the Physics and Chemistry of Rare Earths., Elsevier, Amsterdam, p. 497–593.

Cahill Wilson, J., and Standish, C.D., 2016, Mobility and migration in late Iron Age and early Medieval Ireland: Journal of Archaeological Science: Reports, v. 6, p. 230–241.

Capo, R.C., Stewart, B.W., and Chadwick, O.A., 1998, Strontium isotopes as tracers of ecosystem processes: Theory and Methods: Geoderma, v. 82, p. 197–225.

Caporale, A.G., and Violante, A., 2016, Chemical Processes Affecting the Mobility of Heavy Metals and Metalloids in Soil Environments: Current Pollution Reports, v. 2, p. 15–27.

Censi, P., Saiano, F., Pisciotta, A., and Tuzzolino, N., 2014, Geochemical behaviour of rare earths in Vitis vinifera grafted onto different rootstocks and growing on several soils: The Science of the Total Environment, v. 473–474, p. 597–608.

Cidu, R., Vittori Antisari, L., Biddau, R., Buscaroli, A., Carbone, S., Da Pelo, S., Dinelli, E., Vianello, G., and Zannoni, D., 2013, Dynamics of rare earth elements in water-soil systems: The case study of the Pineta San Vitale (Ravenna, Italy): Geoderma, v. 193–194, p. 52–67.

Clarke, A., Parkes, M., and Gatley, S., 2007, The Geological Heritage of Meath: An audit of County Geological Sites in Meath. Geological Survey of Ireland. Unpublished Report.

Curran, J.M., Meighan, I.G., Simpson, D.D.A., Rogers, G., and Fallick, A.E., 2001, $^{87}Sr/^{86}Sr$: a New Discriminant for Provenancing Neolithic Porcellanite Artifacts from Ireland: Journal of Archaeological Science, v. 28, p. 713–720.

Davies, G., Gledhill, A., and Hawkesworth, C., 1985, Upper crustal recycling in southern Britain: evidence from Nd and Sr isotopes: Earth and Planetary Science Letters, v. 75, p. 1–12.

DIN: ISO 19730 (2009) Soil quality – Extraction of trace elements from soil using ammonium nitrate solution (ISO 19730:2008), DIN, 2009.

Ding, S., Liang, T., Zhang, C., Wang, L.J., and Sun, Q., 2006, Accumulation and fractionation of rare earth elements in a soil-wheat system: Pedosphere, v. 16, p. 82–90.

Douthit, T.L., Meyers, W.J., and Hanson, G.N., 1993, Nonmonotonic Variation of Seawater $^{87}Sr/^{86}Sr$ Across the Ivorian/Chadian Boundary (Mississippian, Osagean): Evidence from Marine Cements within the Irish Waulsortian Limestone: Journal of Sedimentary Research, v. Vol. 63, p. 539–549.

Dunn, C., 2007, Biogeochemistry in Mineral Exploration Volume 9: Elsevier, Amsterdam, 460 p.

Ebong, G.A., Etuk, H.S., and Johnson, A.S., 2007, Heavy Metals Accumulation by Talinum triangulare grown on Waste Dumpsites in Uyo Metropolis, Akwa Ibom State, Nigeria: Journal of Applied Sciences, v. 7, p. 14.

Eggins, S.M., Woodhead, J.D., Kinsley, L.P.J., Mortimer, G.E., Sylvester, P.J., McCulloch, M.T., Hergt, J.M., and Handler, M.R., 1997, A simple method for the precise determination of >40 trace elements in geological samples by ICPMS using enriched isotope internal standardisation: Chemical Geology, v. 1, p. 311–326.

Elderfield, H., Upstill-Goddard, R., and Sholkovitz, E.R., 1990, The rare earth elements in rivers, estuaries, and coastal seas and their significance to the composition of ocean waters: Geochimica et Cosmochimica Acta, v. 54, p. 971–991.

Ericson, J.E., 1985, Strontium isotope characterization in the study of prehistoric human ecology: Journal of Human Evolution, v. 14, p. 503–514.

Evans, J.A., Chenery, C.A., and Montgomery, J., 2012, A summary of strontium and oxygen isotope variation in archaeological human tooth enamel excavated from Britain: Journal of Analytical Atomic Spectrometry, v. 27, p. 754.

Evans, J.A., Montgomery, J., and Wildman, G., 2009, Isotope domain mapping of $^{87}Sr/^{86}Sr$ biosphere variation on the Isle of Skye, Scotland: Journal of the Geological Society, London, v. 166, p. 617–631.

Evans, J.A., Montgomery, J., Wildman, G., and Boulton, N., 2010, Spatial variations in biosphere $^{87}Sr/^{86}Sr$ in Britain: Journal of the Geological Society, London, v. 167, p. 1–4.

Evans, J.A., and Tatham, S., 2004, Defining “local signature” in terms of Sr isotope composition using a tenth- to twelfth-century Anglo-Saxon population living on a Jurassic clay-carbonate terrain, Rutland, UK: Geological Society, London, Special Publications, v. 232, p. 237–248.

Faure, G., and Powell, J.L., 1972, Strontium Isotope Geology: New York, Springer-Verlag.

Fay, D., Kramers, G., and Zhang, C., 2007, Soil Geochemical Atlas of Ireland: Teagasc and Environmental Protection Agency Ireland, 120 p.

Finch, T.F., Gardiner, M., Comey, A., Radford, T., and Taluntais, A.F., 1983, Soil of Co. Meath: National Soil Survey of Ireland: An Foras Taluntais.

Frei, R., and Frei, K.M., 2013, The geographic distribution of Sr isotopes from surface waters and soil extracts over the island of Bornholm (Denmark) – A base for provenance studies in archaeology and agriculture: Applied Geochemistry, v. 38, p. 147–160.

Frei, K.M., and Frei, R., 2011, The geographic distribution of strontium isotopes in Danish surface waters – A base for provenance studies in archaeology, hydrology and agriculture: Applied Geochemistry, v. 26, p. 326–340.

Fu, F., Akagi, T., and Shinotsuka, K., 1998, Distribution pattern of rare earth elements in fern: Biological trace element research, v. 64, P. 13-26.

Fu, F., Akagi, T., Yabuki, S., and Iwaki, M., 2001, The variation of REE (rare earth elements) patterns in soil-grown plants: A new proxy for the source of rare earth elements and silicon in plants: Plant and Soil, v. 235, p. 53–64.
Geological Survey of Ireland, 2009, Energy and Natural Resources: Bedrock Geology.

Geological Survey of Ireland, 2016, GSI Spatial Resources Viewer: Retrieved from URL: http://dcenr.maps.arcgis.com/home/webmap/viewer.html?useExisting=1.

Giero, R., and Stille, P., 2004, Energy, waste and the environment - a geochemical perspective: introduction: Geological Society, London, Special Publications, v. 236, p. 1–5.

Grimstead, D.N., Nugent, S., and Whipple, J., 2017, Why a Standardization of Strontium Isotope Baseline Environmental Data Is Needed and Recommendations for Methodology: Advances in Archaeological Practice, p. 1–12.

Hartman, G., and Richards, M.P., 2014, Mapping and defining sources of variability in bioavailable strontium isotope ratios in the Eastern Mediterranean: Geochimica et Cosmochimica Acta, v. 126, p. 250–264.

Hedman, K.M., Curry, B.B., Johnson, T.M., Fullagar, P.D., and Emerson, T.E., 2009, Variation in strontium isotope ratios of archaeological fauna in the Midwestern United States: a preliminary study: Journal of Archaeological Science, v. 36, p. 64–73.

Hendry, J.P., Gregg, J.M., Shelton, K.L., Somerville, I.D., and Crowley, S.F., 2015, Origin, characteristics and distribution of fault-related and fracture-related dolomitization: Insights from Mississippian carbonates, Isle of Man: Sedimentology, v. 62, p. 717–752.

Hodell, D., Quinn, R.L., Brenner, M., and Kamenov, G., 2004, Spatial variation of strontium isotopes ($^{87}Sr/^{86}Sr$) in the Maya region: a tool for tracking ancient human migration: Journal of Archaeological Science, v. 31, p. 585–601.

Hongo, Y., Obata, H., Alibo, D.S., and Nozaki, Y., 2006, Spatial Variations of Rare Earth Elements in North Pacific Surface Water: Journal of Oceanography, v. 62, p. 441–455.

Horwitz, E.P., Chiarizia, R., and Dietz, M.L., 1992, A Novel Strontium-Selective Extraction Chromatographic Resin: Solvent Extraction and Ion Exchange, v. 10, p. 313–336.

Hu, Z., Haneklaus, S., Sparovek, G., and Schnug, E., 2006, Rare Earth Elements in Soils: Communications in Soil Science and Plant Analysis, v. 37, p. 1381–1420.

Hu, Y., Vanhaecke, F., Moens, L., Dams, R., Del Castilho, P., and Japenga, J., 1998, Determination of the aqua regia soluble content of rare earth elements in fertilizer, animal fodder phosphate and manure samples using inductively coupled plasma mass spectrometry: Analytica Chimica Acta, v. 373, p. 95–105.

Johannesson, K.H., Farnham, I.M., Guo, C., and Stetzenbach, K.J., 1999, Rare earth element fractionation and concentration variations along a groundwater flow path within a shallow, basin-fill aquifer, southern Nevada, USA: Geochimica et Cosmochimica Acta, v. 63, p. 2697–2708.

Johannesson, K.H., Hawkins, D.L., and Cortés, A., 2006, Do Archean chemical sediments record ancient seawater rare earth element patterns?: Geochimica et Cosmochimica Acta, v. 70, p. 871–890.

Johannesson, K.H., and Hendry, M.J., 2000, Rare earth element geochemistry of groundwaters from a thick till and clay-rich aquitard sequence, Saskatchewan, Canada: Geochimica et Cosmochimica Acta, v. 64, p. 1493–1509.

Johannesson, K.H., and Lyons, W.B., 1994, The rare earth element geochemistry of Mono Lake water and the importance of carbonate complexing: Limnology and Oceanography, v. 39, p. 1141–1154.

Johannesson, K.H., and Zhou, X., 1999, Origin of middle rare earth element enrichments in acid waters of a Canadian High Arctic lake: Geochimica et Cosmochimica Acta, v. 63, p. 153–165.

Johnson, C., Breward, N., Ander, E.L., and Ault, L., 2005, G-BASE: baseline geochemical mapping of Great Britain and Northern Ireland: Geochemistry: Exploration, Environment, Analysis, v. 5, p. 347–357.

Kabata-Pendias, A., 2001, Trace elements in soils and plants: CRC Press; Boca Raton; London, 3rd Edition, 331 p.

Kador, T., Fibiger, L., Cooney, G., and Fullagard, P., 2014, Movement and diet in early Irish prehistory: first evidence from multi-isotope analysis: The Journal of Irish Archaeology, v. XXIII, p. 83–96.

Kamber, B.S., Greig, A., and Collerson, K.D., 2005, A new estimate for the composition of weathered young upper continental crust from alluvial sediments, Queensland, Australia: Geochimica et Cosmochimica Acta, v. 69, p. 1041–1058.

Kamber, B.S., Greig, A., Schoenberg, R., and Collerson, K.D., 2003, A refined solution to Earth's hidden niobium: implications for evolution of continental crust and mode of core formation: Precambrian Research, v. 126, p. 289–308.

Kamber, B.S., Webb, G.E., and Gallagher, M., 2014, The rare earth element signal in Archaean microbial carbonate: information on ocean redox and biogenicity: v. 171, p. 745–763.

Kastori, R.R., Maksimović, I. V., Zeremski-Škorić, T.M., and Putnik-Delić, M.I., 2010, Rare earth elements: Yttrium and higher plants: Zbornik Matice srpske za prirodne nauke, p. 87–98.

Knudson, K.J., O'Donnabhain, B., Carver, C., Cleland, R., and Price, T.D., 2012, Migration and Viking Dublin: Paleomobility and paleodiet through isotopic analyses: Journal of Archaeological Science, v. 39, p. 308–320.

Knudson, K.J., and Torres-Rouff, C., 2009, Investigating cultural heterogeneity in San Pedro de Atacama, Northern Chile, through biogeochemistry and bioarchaeology: American Journal of Physical Anthropology, v. 138, p. 473–485.

Kootker, L.M., van Lanen, R.J., Kars, H., and Davies, G.R., 2016, Strontium isoscapes in The Netherlands. Spatial variations in $^{87}Sr/^{86}Sr$ as a proxy for palaeomobility: Journal of Archaeological Science: Reports, v. 6, p. 1–13.

Laffoon, J.E., 2012, Patterns of paleomobility in the ancient Antilles : an isotopic approach: Ph.D. Thesis. Leiden University.

Laffoon, J.E., Davies, G.R., Hoogland, M.L.P., and Hofman, C.L., 2012, Spatial variation of biologically available strontium isotopes ($^{87}Sr/^{86}Sr$) in an archipelagic setting: a case study from the Caribbean: Journal of Archaeological Science, v. 39, p. 2371–2384.

Laffoon, J.E., Sonnemann, T.F., Shafie, T., Hofman, C.L., Brandes, U., and Davies, G.R., 2017, Investigating human geographic origins using dual-isotope ($^{87}Sr/^{86}Sr$, ^{18}O) assignment approaches: PLoS ONE, v. 12, p. 1–16.

Laul, J.C., Weimer, W.C., and Rancitelli, L.A., 1979, Biogeochemical distribution of rare earths and other trace elements in plants and soils: Physics and Chemistry of the Earth, v. 11, p. 819–827.

Laveuf, C., and Cornu, S., 2009, A review on the potentiality of Rare Earth Elements to trace pedogenetic processes: Geoderma, v. 154, p. 1–12.

Lawrence, M.G., Greig, A., Collerson, K.D., and Kamber, B.S., 2006, Rare earth element and yttrium variability in South East Queensland waterways: Aquatic Geochemistry, v. 12, p. 39–72.

Lawrence, M.G., Jupiter, S.D., and Kamber, B.S., 2006, Aquatic geochemistry of the rare earth elements and yttrium in the Pioneer River catchment, Australia: Marine and Freshwater Research, v. 57, p. 725–736.

Lawrence, M.G., and Kamber, B.S., 2006, The behaviour of the rare earth elements during estuarine mixing-revisited: Marine Chemistry, v. 100, p. 147–161.

Leybourne, M.I., Goodfellow, W.D., Boyle, D.R., and Hall, G.M., 2000, Rapid development of negative Ce anomalies in surface waters and contrasting REE patterns in groundwaters associated with Zn-Pb massive sulphide deposits: Applied Geochemistry, v. 15, p. 695–723 15.

Lima e Cunha, M. do C., Nardi, L.V.S., Pereira, V.P., Bastos Neto, A.C., and Vedana, L.A., 2014, Evaluation of Biological Absorption Coefficient of Trace Elements in Plants From the Pitinga Mine District, Amazonian Region: Revista do Instituto Geológico, v. 35, p. 19–29.

Loell, M., Reiher, W., and Felix-Henningsen, P., 2011, Contents and bioavailability of rare earth elements in agricultural soils in Hesse (Germany): Journal of Plant Nutrition and Soil Science, v. 174, p. 644–654.

Maurer, A.-F., Galer, S.J.G., Knipper, C., Beierlein, L., Nunn, E. V, Peters, D., Tütken, T., Alt, K.W., and Schöne, B.R., 2012, Bioavailable $^{87}Sr/^{86}Sr$ in different

environmental samples--effects of anthropogenic contamination and implications for isoscapes in past migration studies: The Science of the Total Environment, v. 433, p. 216–29.

McArthur, J.M., Howarth, R., and Bailey, T., 2001, Strontium isotope stratigraphy: LOWESS version 3: Best fit to the marine Sr-isotope curve for 0–509 Ma and accompanying look-up table for deriving: The Journal of Geology, v. 109, p. 155–170.

McCabe, M., 2007, Glacial Geology and Geomorphology. The Landscapes of Ireland: Dunedin, Edinburgh.

McConnell, B., Philcox, M.E., and Geraghty, M., 2001, Geology Of Meath. A Geological Description To Accompany The Bedrock Geology 1:100,000 Scale Map Sheet 13, Meath: Department of Public Enterprise.

Meehan, R.T., and Warren, W.P., 1999, The Boyne Valley in the Ice Age: A field guide to some of the valley's most important glacial geological features: Meath County Council and the Geological Survey of Ireland. 84 p.

Miao, L., Ma, Y., Xu, R., and Yan, W., 2011, Environmental biogeochemical characteristics of rare earth elements in soil and soil-grown plants of the Hetai goldfield, Guangdong Province, China: Environmental Earth Sciences, v. 63, p. 501–511.

Miao, L., Xu, R., Ma, Y., Zhu, Z., Wang, J., Cai, R., and Chen, Y., 2008, Geochemistry and biogeochemistry of rare earth elements in a surface environment (soil and plant) in South China: Environmental Geology, v. 56, p. 225–235.

Miekeley, N., Casartelli, E.A., and Dotto, R.M., 1994, Concentration levels of rare-earth elements and thorium in plants from the Morro do Ferro environment as an indicator for the biological availability of transuranium elements: Journal of Radioanalytical and Nuclear Chemistry Articles, v. 182, p. 75–89.

Millero, F.J., 1992, Stability constants for the formation of rare earth-inorganic complexes as a function of ionic strength: Geochimica et Cosmochimica Acta, v. 56, p. 3123–3132.

Möller, P., Morteani, G., and Dulski, P., 2003, Anomalous Gadolinium, Cerium, and Yttrium contents in the Adige and Isarco River waters and in the water of their tributaries (Provinces Trento and Bolzano/Bozen, NE Italy): Acta Hydrochimica et Hydrobiologica, v. 31, p. 225–239.

Montgomery, J., 2010, Passports from the past: Investigating human dispersals using strontium isotope analysis of tooth enamel.: Annals of Human Biology, v. 37, p. 325–46.

Montgomery, J., Evans, J.A., and Chenery, C.A., 2006, Report of the lead, strontium, and oxygen isotope analysis of the Iron Age burial from Rath, Ireland.: Unpublished report for CRDS Ltd, Dublin, Ireland. 13 p.

Montgomery, J., Evans, J.A., and Cooper, R.E., 2007, Resolving archaeological populations with Sr-isotope mixing models: Applied Geochemistry, v. 22, p. 1502–1514.

Montgomery, J., Evans, J.A., and Neighbour, T., 2003, Sr isotope evidence for population movement within the Hebridean Norse community of NW Scotland: Journal of the Geological Society, v. 160, p. 649–653.

Montgomery, J., Evans, J.A., and Wildman, G., 2006, $^{87}Sr/^{86}Sr$ isotope composition of bottled British mineral waters for environmental and forensic purposes: Applied Geochemistry, v. 21, p. 1626–1634.

Montgomery, J., and Grimes, V., 2010, Appendix 21.1: Report on the isotope analysis of a burial from Ratoath, Co. Meath., in C. Corlett and M. Potterton (Eds.). Death and Burial in Early Medieval Ireland in the Light of Recent Archaeological Excavations. Wordwell, Dublin, Ireland. 316 pp, p. 309–311.

Montgomery, J., Grimes, V., Buckberry, J., Evans, J.A., Richards, M.P., and Barrett, J.H., 2014, Finding Vikings with isotope analysis: The view from wet and windy islands: Journal of the North Atlantic, v. 7, p. 54–70.

Nafplioti, A., 2011, Tracing population mobility in the Aegean using isotope geochemistry: a first map of local biologically available $^{87}Sr/^{86}Sr$ signatures: Journal of Archaeological Science, v. 38, p. 1560–1570.

Négrel, P., Guerrot, C., Cocherie, A., Azaroual, M., Brach, M., and Fouillac, C., 2000, Rare earth elements, neodymium and strontium isotopic systematics in mineral waters: evidence from the Massif Central, France: Applied Geochemistry, v. 15, p. 1345–1367.

Négrel, P., Guerrot, C., and Millot, R., 2007, Chemical and strontium isotope characterization of rainwater in France: influence of sources and hydrogeochemical implications: Isotopes in Environmental and Health Studies, v. 43, p. 179–196.

Noack, C.W., Dzombak, D.A., and Karamalidis, A.K., 2014, Rare earth element distributions and trends in natural waters with a focus on groundwater: Environmental Science and Technology, v. 48, p. 4317–4326.

O'Connor, P.J., 1988, Strontium isotope geochemistry of Tertiary igneous rocks, NE Ireland, in A.C. Morton and L.M. Parson (Eds.), Early Tertiary Volcanism, Geological Society Special Publication No. 39, p. 361–363.

Pearcy, R., Ehleringer, J., Mooney, H.A., and Rundel, P.W. (Eds.), 2000, Plant Physiological Ecology: Field methods and instrumentation: Kluwer Academic Publishers, v. 80, 1785 p.

Pédrot, M., Dia, A., Davranche, M., and Gruau, G., 2015, Upper soil horizons control the rare earth element patterns in shallow groundwater: Geoderma, v. 239, p. 84–96.

Pierson-Wickmann, A.C., Aquilina, L., Weyer, C., Molénat, J., and Lischeid, G., 2009, Acidification processes and soil leaching influenced by agricultural practices revealed by strontium isotopic ratios: Geochimica et Cosmochimica Acta, v. 73, p. 4688–4704.

Piper, D.Z., and Bau, M., 2013, Normalized Rare Earth Elements in Water, Sediments, and Wine: Identifying Sources and Environmental Redox Conditions: American Journal of Analytical Chemistry, v. 2013, p. 69–83.

Porder, S., Paytan, A., and Hadly, E.A., 2003, Mapping the origin of faunal assemblages using strontium isotopes: Paleobiology, v. 29, p. 197–204.

Poszwa, A., Dambrine, E., Ferry, B., Pollier, B., and Loubet, M., 2002, Do deep tree roots provide nutrients to the tropical rainforest? Biogeochemistry, v. 60, p. 97–118.

Pourret, O., Gruau, G., Dia, A., Davranche, M., and Molénat, J., 2010, Colloidal control on the distribution of rare earth elements in shallow groundwaters: Aquatic Geochemistry, v. 16, p. 31–59.

Price, T.D., 2015, An Introduction to the Isotopic Studies of Ancient Human Remains: Journal of the North Atlantic, v. 7, p. 71–87.

Price, T.D., Burton, J.H., Sharer, R.J., Buikstra, J.E., Wright, L.E., Traxler, L.P., and Miller, K.A., 2010, Kings and commoners at Copan: Isotopic evidence for origins and movement in the Classic Maya period: Journal of Anthropological Archaeology, v. 29, p. 15–32.

Price, T.D., Frei, K.M., and Naumann, E., 2014, Isotopic Baselines in the North Atlantic Region: Journal of the North Atlantic, v. 7, p. 103–136.

Price, T.D., and Naumann, E., 2015, The Peopling of the North Atlantic: Isotopic Results from Norway: Journal of the North Atlantic, v. 7, p. 88–102.

Robinson, W.O., Bastron, H., and Murata, K.J., 1958, Biogeochemistry of the rare-earth elements with particular reference to hickory trees: Geochimica et Cosmochimica Acta, v. 14, p. 55–67.

Rust, S., and Savill, P.S., 2000, The root systems of Fraxinus excelsior and Fagus sylvatica and their competitive relationships: Forestry, v. 73, p. 499–508.

Sadeghi, M., Morris, G.A., Carranza, E.J.M., Ladenberger, A., and Andersson, M., 2013, Rare earth element distribution and mineralization in Sweden: An application of principal component analysis to FOREGS soil geochemistry: Journal of Geochemical Exploration, v. 133, p. 160–175.

Sahai, N., Carroll, S.A., Rocberts, S., and O'Day, P.A., 2000, X-Ray Absorption Spectroscopy of Strontium(II) Coordination: Journal of Colloid and Interface Science, v. 222, p. 184–197.

Sealy, J.C., van der Merwe, N.J., Sillen, A., Kruger, F.J., and Krueger, H.W., 1991, $^{87}Sr/^{86}Sr$ as a dietary indicator in modern and archaeological bone: Journal of Archaeological Science, v. 18, p. 399–416.

Shacklette, H.T., and Boerngen, J.G., 1984, Element concentrations in soils and other surficial materials of the conterminous United States: U.S. Geological Survey Professional Paper 1270, p. 1–63.

Sheridan, J.A., Jay, M., Montgomery, J., Pellegrini, M., and Cahill Wilson, J., 2013, "Tara Boy": local hero or international man of mystery?, in M. O' Sullivan, M. Doyle and C. Scarre (Eds.), Tara-from the past to the future, Wordwell: Dublin.

Sholkovitz, E.R., 1995, The aquatic chemistry of rare earth elements in rivers and estuaries: Aquatic Geochemistry, v. 1, p. 1–34.

Sholkovitz, E.R., Landing, W.M., and Lewis, B.L., 1994, Ocean particle chemistry: The fractionation of rare earth elements between suspended particles and seawater: Geochimica et Cosmochimica Acta, v. 58, p. 1567–1579.

Sillen, A., and Kavanagh, M., 1982, Strontium and paleodietary research: A review: American Journal of Physical Anthropology, v. 25, p. 67–90.

Sjögren, K.G., Price, T.D., and Ahlström, T., 2009, Megaliths and mobility in south-western Sweden. Investigating relationships between a local society and its neighbours using strontium isotopes: Journal of Anthropological Archaeology, v. 28, p. 85–101.

Smedley, P.L., 1991, The geochemistry of rare earth elements in groundwater from the Carnmenellis area, southwest England: Geochimica et Cosmochimica Acta, v. 55, p. 2767–2779.

Smyth, D., 2007, Methods used in the Tellus Geochemical Mapping of Northern Ireland, in British Geological Survey Open Report, OR/07/022, p. 1–89.

Snoeck, C., Lee-Thorp, J.A., Schulting, R.J., de Jong, J., Debouge, W., and Mattielli, N., 2015, Calcined bone provides a reliable substrate for strontium isotope ratios as shown by an enrichment experiment: Rapid Communications in Mass Spectrometry, v. 29, p. 107–114.

Snoeck, C., Pouncett, J., Ramsey, G., Meighan, I.G., Mattielli, N., Goderis, S., Lee-Thorp, J.A., and Schulting, R.J., 2016, Mobility during the Neolithic and Bronze Age in Northern Ireland explored using strontium isotope analysis of cremated human bone: American Journal of Physical Anthropology, v. 160, p. 397-413.

Stille, P., Steinmann, M., Pierret, M.C., Gauthier-Lafaye, F., Aubert, D., Probst, A., Viville, D., and Chabaux, F., 2006, The impact of vegetation on fractionation of rare earth elements (REE) during water-rock interaction: Journal of Geochemical Exploration, v. 88, p. 341–344.

Taylor, S.R., and McLennan, S., 1985, The continental crust: Its composition and evolution: McClennan, Blackwell Scientific Publications, v. 21, p. 85–86.

Thornton, E.K., 2011, Reconstructing ancient Maya animal trade through strontium isotope ($^{87}Sr/^{86}Sr$) analysis: Journal of Archaeological Science, v. 38, p. 3254–3263.

Tricca, A., Stille, P., Steinmann, M., Kiefel, B., Samuel, J., and Eikenberg, J., 1999, Rare earth elements and Sr and Nd isotopic compositions of dissolved and suspended loads from small river systems in the Vosges mountains (France), the river Rhine and groundwater: Chemical Geology, v. 160, p. 139–158.

Tyler, G., 2004, Rare earth elements in soil and plant systems - A review: Plant and Soil, v. 267, p. 191–206.

Tyler, G., and Olsson, T., 2005, Rare earth elements in forest-floor herbs as related to soil conditions and mineral nutrition.: Biological trace element research, v. 106, p. 177–191.

U.S. EPA, 1996, Method 1669 Sampling Ambient Water for Trace Metals at EPA Water Quality Criteria Levels: U.S. Environmental Protection Agency.

Vinciguerra, V., Stevenson, R., Pedneault, K., Poirier, A., Hélie, J.F., and Widory, D., 2016, Strontium isotope characterization of wines from Quebec, Canada: Food Chemistry, v. 210, p. 121–128.

Voerkelius, S., Lorenz, G.D., Rummel, S., Quétel, C.R., Heiss, G., Baxter, M., Brach-Papa, C., Deters-Itzelsberger, P., Hoelzl, S., Hoogewerff, J., Ponzevera, E., Van Bocxstaele, M., and Ueckermann, H., 2010, Strontium isotopic signatures of natural mineral waters, the reference to a simple geological map and its potential for authentication of food: Food Chemistry, v. 118, p. 933–940.

Wallace, A., Montgomery, J., and Grimes, V., 2010. Excavation of an early medieval cemetery at Ratoath, Co. Meath, in C. Corlett and M. Potterton (Eds.) Death and Burial in Early Medieval Ireland in Light of Recent Archaeological Excavations, 335–59. Dublin Wordwell.

Wallace, J., Ellam, R.M., and Meighan, I.G., 1994, Sr isotope data for the Tertiary lavas of Northern Ireland: evidence for open system petrogenesis: Journal of the Geological Society, London, v. 151, p. 869–877.

Wang, L., and Liang, T., 2014, Geochemical fractions of rare earth elements in atmospheric particulates around a mine tailing in Baotou, China: Atmospheric Environment, v. 88, p. 23–29.

Warham, J.O., 2012, Mapping biosphere strontium isotope ratios across major lithological boundaries: PhD Thesis. University of Bradford.

Wei, Z., Yin, M., Zhang, X., Hong, F., Li, B., Tao, Y., Zhao, G., and Yan, C., 2001, Rare earth elements in naturally grown fern Dicranopteris linearis in relation to their variation in soils in South-Jiangxi region (Southern China): Environmental Pollution, v. 114, p. 345–355.

Weis, D., Kieffer, B., Maerschalk, C., Barling, J., de Jong, J., Williams, G.A., Hanano, D., Pretorius, W., Mattielli, N., Scoates, J.S., Goolaerts, A., Friedman, R.M., and Mahoney, J.B., 2006, High-precision isotopic characterization of USGS reference materials by TIMS and MC-ICP-MS: Geochemistry, Geophysics, Geosystems, v. 7, p. 1-30.

Wen, B., Yuan, D.A., Shan, X.Q., Li, F.L., and Zhang, S.-Z., 2001, The influence of rare earth element fertilizer application on the distribution and bioaccumulation of rare earth elements in plants under field conditions: Chemical Speciation and Bioavailability, v. 13, p. 39–48.

Wiche, O., Zertani, V., Hentschel, W., Achtziger, R., and Midula, P., 2017, Germanium and rare earth elements in topsoil and soil-grown plants on different land use types in the mining area of Freiberg (Germany): Journal of Geochemical Exploration, v. 175, p. 120–129.

Willmes, M., Mcmorrow, L., Kinsley, L., Armstrong, R.A., Aubert, M., Eggins, S., Falgueres, C., Maureille, B., Moffat, I., and Grun, R., 2014, The IRHUM (Isotopic Reconstruction of Human Migration) database - bioavailable strontium isotope ratios for geochemical fingerprinting in France: Earth System Science Data, v. 6, p. 117–122.

Wyttenbach, A., Furrer, V., Schleppi, P., and Tobler, L., 1998, Rare earth elements in soil and in soil-grown plants: Plant and Soil, v. 199, p. 267–273.

Xu, Z., and Han, G., 2009, Chemical and strontium isotope characterization of rainwater in Beijing, China: Atmospheric Environment, v. 43, p. 1954–1961.

Young, M.E., and Donald, A.W., 2013, A guide to the Tellus data: Geological Survey of Northern Ireland, Belfast.

Young, M.E., Knights, K., Smyth, D., Scanlon, R., and Gallagher, V., 2016, The Tellus geochemical surveys, results and applications, in Young, M. (Ed.), Unearthed: impacts of the Tellus surveys of the north of Ireland, Royal Irish Academy, p. 33–52.

Yu, K.-F., Kamber, B.S., Lawrence, M.G., Greig, A., and Zhao, J.-X., 2007, High-precision analysis on annual variations of heavy metals, lead isotopes and rare earth elements in mangrove tree rings by inductively coupled plasma mass spectrometry: Nuclear Instruments and Methods in Physics Research Section B: Beam Interactions with Materials and Atoms, v. 255, p. 399–408.

Zhai, H., Yang, Y., Zheng, S., Hu, A., Zhang, S., and Wang, L., 1999, Selection of the extractants for available rare earths in soils: China Environmental Science, p. 67–71.

Zhang, X.C., Nearing, M. a., Polyakov, V.O., and Friedrich, J.M., 2003, Using Rare-Earth Oxide Tracers for Studying Soil Erosion Dynamics: Soil Science Society of America Journal, v. 67, p. 279.

Zitek, A., Tchaikovsky, A., Irrgeher, J., Waidbacher, H., and Prohaska, T., 2015, The $^{87}Sr/^{86}Sr$ river water isoscape of the Danube catchment, in I. Liška, F. Wagner, M. Sengl, K. Deutsch and J. Slobodník (Eds.), Joint Danube Survey 3: A Comprehensive Analysis of Danube Water Quality: ICPDR - International Commission for the Protection of the Danube River, p. 349–354.

Chapter 4: Early Medieval Reliance on the Land and the Local: An Integrated Multi-Isotope Study ($^{87}Sr/^{86}Sr$, $\delta^{18}O$, $\delta^{2}H$, $\delta^{13}C$, $\delta^{15}N$) of Diet and Migration in Co. Meath, Ireland.

Co-authors: Linda M. Reynard, Quentin G. Crowley, Christophe Snoeck and Noreen Tuross.

Abstract

Three early medieval Irish communities within a 30 km radius in Co. Meath, Ireland, have been measured for multiple isotopes ($^{87}Sr/^{86}Sr$, $\delta^{18}O$, $\delta^{2}H$, $\delta^{13}C$, $\delta^{15}N$) to elucidate human and domesticated animal subsistence and provenance. Existing $^{87}Sr/^{86}Sr$ data from geochemical mapping of contemporary soils, plants and streamwater, were compared to human and animal tooth enamel $^{87}Sr/^{86}Sr$ to assess potential past human migration, in combination with $\delta^{18}O$, $\delta^{2}H$, $\delta^{13}C$ and $\delta^{15}N$ from bone collagen.

Oxygen isotope ($\delta^{18}O$) values of bone collagen are notably invariable, 10.0‰ ± 0.6 (n = 36), for the three archaeological sites: Collierstown, Johnstown and Raystown. Nitrogen isotope ($\delta^{15}N$) values for both domesticated animal (9.8 ‰ ± 1.7) and adult human (12.0 ‰ ± 0.8) bone collagen are also tightly constrained suggesting a common diet for humans. A mean carbon isotope ($\delta^{13}C$) value of -21.0 ‰ ± 0.41 for adult humans suggests overwhelming terrestrial sources of foodstuffs. Strontium isotopic ratios ($^{87}Sr/^{86}Sr$) from human dental enamel range from 0.7085-0.7110 with a mean of 0.7091 ± 0.0002 2SD (n = 25). Two individuals (R841 and R854) are statistical outliers based on $^{87}Sr/^{86}Sr$ and $\delta^{13}C$ and are likely migrants to the locality where they were buried. We note that one of these putative migrants met a particularly violent end.

From an analytical perspective, due to the formation of HCN during the measurement of certain organic compounds by High-Temperature Conversion (HTC) with a glassy carbon reactor, hydrogen isotope ($\delta^{2}H$) values can be artificially skewed relative to those analysed using a chromium-packed reactor. Here, the first comparative results using these two methods for human samples are presented. Preliminary results show that 'glassy carbon' $\delta^{2}H$ values are linearly offset by a mean of -12.2‰ ± 4.5 (n = 36) compared to those obtained using a Cr-packed reactor. Such an offset has implications for $\delta^{2}H$ values measured with a glassy C reactor as resulting values may be significantly displaced from true values.

1 Introduction

1.1 Aims and Rationale:

The early medieval period (c AD 500–1100) was a time of frequent migrations and Ireland was no exception. Despite being often referred to as the 'Dark Ages', this was a time of movement, religious conversion and associated cultural change (Hodges, 1989). Relatively sparse material culture from certain communities make isotope studies particularly informative, inferring diet and provenance of otherwise unknown people. Stable and radiogenic isotopes can be used to identify migrants to a specific region. Several recent studies have investigated past mobility in Europe (Bentley and Knipper, 2005; Chenery et al., 2014, 2010; Budd et al., 2004; Hemer et al., 2017; Evans et al., 2012; Shaw et al., 2009, 2016; Eckardt et al., 2009; Buckberry et al., 2014; Montgomery et al., 2014, 2003; Beaumont et al., 2013; Lamb et al., 2014; Hamre and Daux, 2016; Evans and Tatham, 2004) but few have focused on an Irish context (Kador et al., 2014; Snoeck et al., 2016; Sheridan et al., 2013; Knudson et al., 2012; Beaumont et al., 2013; Lynch, 2014; Schulting et al., 2012; Schweitzer, 2009; Montgomery et al., 2006; Montgomery and Grimes, 2010) and even fewer still have specifically investigated early medieval remains (Cahill Wilson and Standish, 2016; Cahill Wilson, 2012, 2010; Novak, 2015; Tobin, 2011; Wallace et al., 2010).

Combined isotope systems are employed here with the aim of reconstructing the diet and potential movements of early medieval populations in the archaeologically-rich region of Co. Meath in Ireland. Biosphere mapping of $^{87}Sr/^{86}Sr$ has been carried out (Chapter 3) and provides comprehensive comparative data, giving geographical context to the individuals whose archaeological remains were the subject of analyses. A better understanding of certain aspects of life from isotope values, combined with excavation records, broadens perspective on the cultural practices during this period, one which marks the transition from the pagan to early Christian period in Ireland at the beginning of the fifth century.

This study has measured a suite of isotopes from individuals (n=38) buried at three different sites, all located within 30 km from one another (Fig. 2):

- Collierstown - a cemetery with inferred high status individuals.
- Johnstown - a multi-period settlement-cemetery and industrial site.
- Raystown - a settlement-cemetery site with evidence for large scale milling and grain production.

Analysing human remains from these three sites provides a representative dataset for expected isotope values and allows for comparison between these three groups buried within such relative proximity.

1.2 Early medieval Farming Practices in Ireland

Agriculture had a major role in the economy and social structure of early medieval Ireland and whilst farming was heavily relied upon for subsistence and livelihood, it also determined the overall structure and hierarchy of society (McCormick, 2008). For both high status and ordinary members of the community, agriculture, both arable and pastoral, determined their rank and for the latter, was the focus of much of the daily life activity (McCormick et al., 2011). There is evidence for a strong emphasis on cattle-farming, with dairying central to farming during early medieval times. Given the zooarchaeological evidence for intensive dairying, milk products were likely of great importance and this was also noted for a comparable site in Atlantic Scotland (Mulville et al., 2005). The late-age slaughter and sex-ratio of cattle further infers the importance of dairying and it is therefore rather unlikely that beef was consumed regularly by commoners (McCormick, 1992). Sheep were of lesser importance as a food source, as sheep were valued mainly for their fleece. The Early Medieval Agriculture Project (EMAP) (McCormick et al., 2011) determined some temporal and regional variation in the record of farming practices but generally in eastern Ireland, where these cemetery-settlements were located, there was a strong importance of cattle over other animal species, highlighting that within this livestock economy, cattle had primary importance.

From about AD 800 onwards, distribution of livestock from various sites became more diverse, and in many places cattle began to lose their dominant role (McCormick, 2008). This change has been tied to the lesser use of cattle as a currency and framework for the wealth system. It is argued that grain was a superior way of generating independent economic wealth than cattle rearing, which gave rise to this expansion in grain production (McCormick and Murray, 2007). The prevalence of mills and other features representative of arable farming, including fields and kilns, are evidence for a mixed pastoral/arable farming economy (Seaver, 2016; Brady, 2006) and is indicative of this expansion in arable farming around the turn of the eighth century. There is also increased evidence for crops during later periods in early medieval Ireland, both in the number of sites where they were recovered and the range of crops cultivated. Barley and oats are confirmed as the primary crops and whilst wheat was present at many sites, it does not appear to have been the primary crop (McCormick et al., 2011). As well as the cereals, evidence was found for other crops, such as flax and legumes. Pollen evidence for early medieval Ireland indicates a landscape of scrubby woodland and mixed farming, almost invariably dominated by pastureland.

Changes to paleo-dietary practices have been proposed and highly debated, notably the replacement of fishing with dairying immediately following the adoption of farming in Neolithic Westernmost Europe (Tauber, 1981, 1982, Schulting and Richards, 2002b, 2002a; Hedges, 2004; Milner et al., 2006, 2004; Woodman, 2004; Sjögren, 2003; Rowley-Conwy, 2004; Cramp et al., 2014; Richards et al., 2003). For the purposes of comparison, there is a limited isotope dataset for early medieval burials excavated in Ireland. Notable contemporaneous sites for which relevant data exists included Owenbristy, Cappogue and Knockrobbin Hill (Geber, 2010 and references therein). $\delta^{15}N$ and $\delta^{13}C$ data exist for some individuals from both Raystown (Fibiger, 2006) and Johnstown (Carlin et al., 2008). We aim to add to the current limited Irish $\delta^{15}N$ and $\delta^{13}C$ database for early medieval burials in order to better understand diet and dietary practises during this period in Ireland and compare these results with other datasets such as the more extensive isotope framework which exists for Britain. Given the wide range of time covered by the selected burials analysed in this study, potential changes in diet throughout the medieval period are also investigated.

1.3 Combined Isotope Analyses of Human Remains

1.3.1 Reconstructing Paleo-diet

Determining the age, diet and movement of an individual is possible through the use of radiocarbon dating and multi-isotope studies from bone and tooth tissue. Dietary reconstruction focuses on the relative importance of marine vs. terrestrial food and the trophic level of a consumer; the relative importance of cereals vs. meat/fish (Schoeninger et al., 1983; Hedges and Reynard, 2007; Sealy et al., 1987; Richards and Trinkaus, 2009). Differences in the isotope composition of archaeological remains reflect these different food sources and trophic levels (Richards and Hedges, 1999; Privat et al., 2002; Richards, 2000).

Plant carbon (C) is controlled by the photosynthetic pathway the plant used to fix carbon fromm the air. C3, C4 and Crassulacean Acid Metabolism (CAM) pathways result in distinct average $\delta^{13}C$ values of -26.5, -12.5 and -19‰, respectively (Deines, 1980). Temperate zones of Europe natively have C3 plants, including wheat, barley and oats (Lee-Thorp and Sponheimer, 2006; Mays and Beavan, 2012). Between plant and herbivore tissue, there is a fractionation of 5‰ in bone collagen and 10‰ in tooth enamel and there is an additional 1.5‰ fractionation in the bone collagen of carnivores (Schoeninger and DeNiro, 1984). Therefore, $\delta^{13}C$ measured in human bone collagen reflects variability in the food source(s) which in turn is controlled by environmental, physiological and dietary processes. $\delta^{13}C$ of plants govern consumer collagen $\delta^{13}C$, either by direct consumption or by indirect meat consumption (Vogel and van der Merwe, 1977; DeNiro and Epstein, 1978).

$\delta^{15}N$ is generally analysed in combination with $\delta^{13}C$ and reveals information about the trophic level of a consumer (Richards and Trinkaus, 2009; Hedges and Reynard, 2007; Sealy et al., 1987; Schoeninger et al., 1983). Plants absorb N from soil and/or the atmosphere, acting as a link into the food chain. The lighter isotope ^{14}N is removed from the body more easily than heavier ^{15}N, thus creating a fractionation process. Herbivores have higher $\delta^{15}N$ values than their plant food source, with carnivores higher again, thus, each consecutive consumer up the food chain will have progressively higher $\delta^{15}N$ values. This ‘trophic level effect’ is estimated at 3‰ to 5‰ enriched in

^{15}N for each trophic level (Sponheimer et al., 2003; Schoeninger and DeNiro, 1984; Sealy et al., 1987; Schoeninger, 1985).

For humans, an exclusive marine diet tends to result in bone collagen $\delta^{13}C$ of -12 ± 1‰, with an exclusive terrestrial C3 diet having a $\delta^{13}C$ value around -21 ± 1‰ (Barrett and Richards, 2004). These values are directly comparable to this study as they are were based on burials from the early medieval (pictish) in Orkney, Scotland but they do not unequivocally demonstrate an exclusive marine or terrestrial diet, respectively. Rather, such values imply that it is unlikely that terrestrial or marine protein was a significant portion of dietary protein. An exclusive marine diet tends to result in higher bone collagen $\delta^{15}N$ than an exclusive terrestrial C3 diet (Schoeninger and DeNiro, 1984) with omnivorous humans normally falling intermediately between these values but these values can overlap due to factors such as physiological stress, manuring, breastfeeding, freshwater fish consumption which can increased $\delta^{15}N$ values.

1.3.2 Reconstructing Mobility

Isotopes are present in dental apatite as carbonate and phosphate ions and reflect the place of residence at the time of mineralisation which varies depending on the tooth (AlQahtani et al., 2010) but broadly reflect childhood to early adolescence. $^{87}Sr/^{86}Sr$ and $\delta^{18}O$ are independent but complementary isotope systems frequently employed to study migration of humans and animals. Their use in this application is based on the premise that the $^{87}Sr/^{86}Sr$ and $\delta^{18}O$ of mineralised tissues reflect those of the diet of the consumer and the geographical region where the food/water was sourced. Detailed summaries of the theory and application of these isotopic methods have been extensively examined by (Montgomery, 2010; Bentley, 2006; Hedges and Reynard, 2007; Lee-Thorp, 2008). Sr is absorbed into the body from food and water sources and follows the pathway of Ca due to their chemical affinity and is thus incorporated into dental and skeletal tissues (Beard and Johnson, 2000). As teeth mineralise at different stages (AlQahtani et al., 2010) it is possible to analyse two or more teeth from one individual to assess migration throughout childhood. For Sr, tooth enamel tends to be the most suitable material as it is less susceptible to digenetic alteration than dentine (Budd et al., 2000). Measured human $^{87}Sr/^{86}Sr$ and $\delta^{18}O$ composition can be compared

to local biosphere baseline values for a given region and potential migrants originating from isotopically distinct environments can be distinguished based on their outlying isotope composition.

$^{87}Sr/^{86}Sr$ of a region is largely controlled by the age and mineral composition of the underlying bedrock, surficial geology, weathering processes (Capo et al., 1998; Bentley, 2006; Slovak and Paytan, 2012) and may also be influenced by external inputs from sea-spray/fertilisers (Price et al., 2002; Bentley, 2006; Evans et al., 2010; Voerkelius et al., 2010; Maurer et al., 2012; Slovak and Paytan, 2012; Frei and Frei, 2013). The complexity of different Sr end-members contributing to a system can complicate the range of bioavailable $^{87}Sr/^{86}Sr$ values originating solely from bedrock. It is therefore best practice to directly sample biosphere components, such as local plants (Price et al., 2002), to determine this range with better confidence, which has been done for the region of Co. Meath (Chapter 3). Archaeological human tooth enamel samples that fall within a narrow range of 0.7090 - 0.7110 (Montgomery et al., 2014) need additional archaeological evidence or isotope measurements to constrain their origins as these values are extremely common geographically throughout Britain and Ireland (Evans et al., 2012). Knudson et al., (2012) analysed both faunal (pig) bones and human tooth enamel samples from a Viking Age site in Ireland. Faunal bones had a mean of 0.7094 ± 0003 (n=11) whilst human tooth enamel gave a mean of 0.71017 ± 0.00074 (n=11). Montgomery et al., (2014) also measured human Viking Age skeletons from Dublin, which demonstrated a range from 0.709 to 0.720. Price et al., (2015) measured archaeological human bone from the south-eastern coast of Ireland in two locations: Waterford - with a mean $^{87}Sr/^{86}Sr$ of 0.7098 ± 0.0002 (n = 3), and Tintern Abbey, Wexford – with a mean $^{87}Sr/^{86}Sr$ also 0.7098 ± 0.0002 (n = 5).

$\delta^{18}O$ and $\delta^{2}H$ vary geographically reflecting the isotope ratio of precipitation which is effected by enrichment or depletion of ^{18}O relative to ^{16}O with evaporation/precipitation. This in turn varies based on other factors including distance from the oceanic source, absolute amount of precipitation, elevation and local/regional temperature (Bowen and Wilkinson, 2002; Dansgaard, 1964; Criss, 1999). These isotopes have a much greater relative mass difference compared to Sr so they are more sensitive to fractionation from environmental and biological processes. In vertebrates,

$\delta^{18}O$ and $\delta^{2}H$ reflect the composition of body water which is governed by that of drinking water, food and atmospheric water (Longinelli, 1984; Luz et al., 1984).

The isotope composition of $\delta^{18}O$ and $\delta^{2}H$ also varies by species, due to differences in metabolic rate and water use (Bryant and Froelich, 1995) and the turnover rate of the sampled tissue (Hobson, 1999; Bowen et al., 2005), seasonal and annual variations in the isotope composition of meteoric water and changes in dietary behaviour and/or cultural practices (such as cooking, breastfeeding) on a seasonal or yearly timescale (Tuross et al., 2017; Brettell et al., 2012; Daux et al., 2008; Royer et al., 2017). These factors must be considered when examining the consumer population. Nonetheless, as $\delta^{18}O$ and $\delta^{2}H$ composition of meteoric water vary systematically by geographic location (Dansgaard, 1964; Rozanski et al., 1993) biochemically inert tissues, such as keratin and bone collagen, can be used to estimate the provenance of organisms by comparison with isotopically characterised regions (Bowen et al., 2005).

Oxygen isotopes have been measured in the modern groundwater and surface water of Ireland and the UK (Diefendorf and Patterson, 2005; Darling et al., 2003; Darling, 2004) (Fig. 1). However, because the $\delta^{18}O$ of human tissues can differ from that of local precipitation (as discussed above), the local meteoric water values are not always suitable for direct comparison. In this case, having a rather large dataset, it is appropriate to determine a local range from measured skeletal values within the area (cf. Cahill-Wilson & Standish 2016). It should be noted that in Ireland, as is the case for many environments, stable $\delta^{18}O$ and $\delta^{2}H$ generally cannot spatially distinguish short distance movements with accuracy, particularly if used independently, as it is generally at a continental scale that pronounced gradients can be noted (Bowen, 2010). This can result in an underestimation of migrants but using combined isotope systems helps to overcome this constraint.

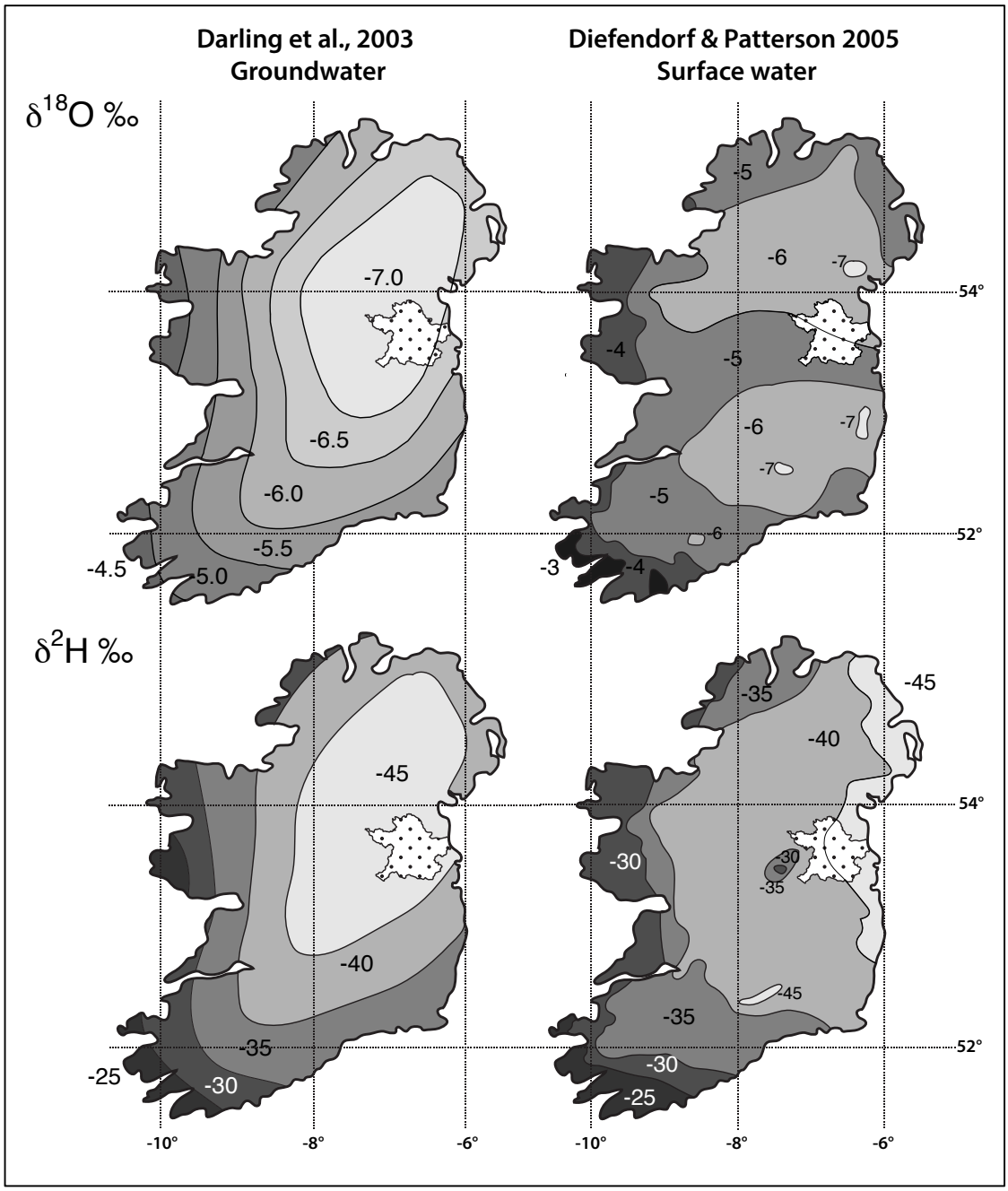


Figure 1. Comparative $\delta^{18}O$ and $\delta^{2}H$ distribution in meteoric waters in Ireland (adapted from Darling et al., 2003; Diefendorf and Patterson, 2005). The study area of Co. Meath is represented by the dotted region.

Whilst oxygen isotopes derived from carbonates and phosphates in bone and tooth apatite are widely used to trace mobility of humans and animals (Chenery et al., 2010; Lamb et al., 2014; Müldner et al., 2011), one of the more novel and experimental areas of stable isotope research deals with the measurement of $\delta^{2}H$ and $\delta^{18}O$ in proteins (mainly collagen). Makarewicz and Sealy (2015) recommend focusing on these "unconventional" analyses in future studies as such data also have the potential to

answer questions regarding seasonality, mobility, food provenance and diet. δ^2H and $\delta^{18}O$ have received less attention due to analytical complications that arise from δ^2H measurement and the associated preparatory work. Approximately 20% of total organic hydrogen in collagen is exchangeable with ambient atmospheric moisture (Cormie et al., 1994). Pre-treating samples by equilibrating them with water of known isotopic composition largely resolves this problem, as it controls for the unknown isotopic composition of exchangeable hydrogen (Chesson et al., 2009; Kelly et al., 2009; Sauer et al., 2009; Wassenaar and Hobson, 2000). However, the δ^2H and $\delta^{18}O$ value of the water used to equilibrate the samples will change slightly over time and geographically between different laboratories. Thus, for inter-laboratory comparisons, standards should be measured in tandem with unknowns to account for any variability (Meier-Augenstein et al., 2013). Oxygen isotopes in collagen are less exchangeable than hydrogen. Moreover, whilst the $\delta^{18}O$ of bone carbonate is susceptible to diagenetic alteration, the measurement of organic oxygen avoids this problem through well-established treatments for diagenetic alteration (Tuross, 2012). Another issue with δ^2H analysis is the accuracy, or lack thereof, associated with certain measurement protocols. Values measured by High-Temperature Conversion (HTC) with a glassy-carbon packed reactor have been shown to result in hydrogen exchange, likely from the formation of HCN (Reynard and Tuross, 2016). Owing to this, different δ^2H of certain N-containing tissues can arise as a function of reactor configuration.

1.4 Geology of Co. Meath

Much of the region is underlain by Carboniferous limestone bedrock with interbedded mudstone, shale and sandstone (Figure 2). The $^{87}Sr/^{86}Sr$ of Carboniferous limestone is generally within the range of 0.7075 to 0.7085 (Shields, 2007; Veizer, 1989) reflecting the value of seawater during this geological period. Lower Palaeozoic rocks are also present; these are mostly represented by argillaceous/cherty limestone and shale (Geological Survey of Ireland, 2009). It is noted by Cahill-Wilson & Standish (2016) that the expected bioavailable range encompassing all bedrock lithologies of the region falls within 0.7075 – 0.7105. An existing dataset, produced by biosphere sampling of the area has identified statistically distinct areas based on plant $^{87}Sr/^{86}Sr$ values (Chapter 3). Some other localised areas have also been sampled for biosphere $^{87}Sr/^{86}Sr$ (Cahill Wilson and Standish, 2016; Snoeck et al., 2016) and these combined datasets will be compared to the $^{87}Sr/^{86}Sr$ of the human remains presented here.

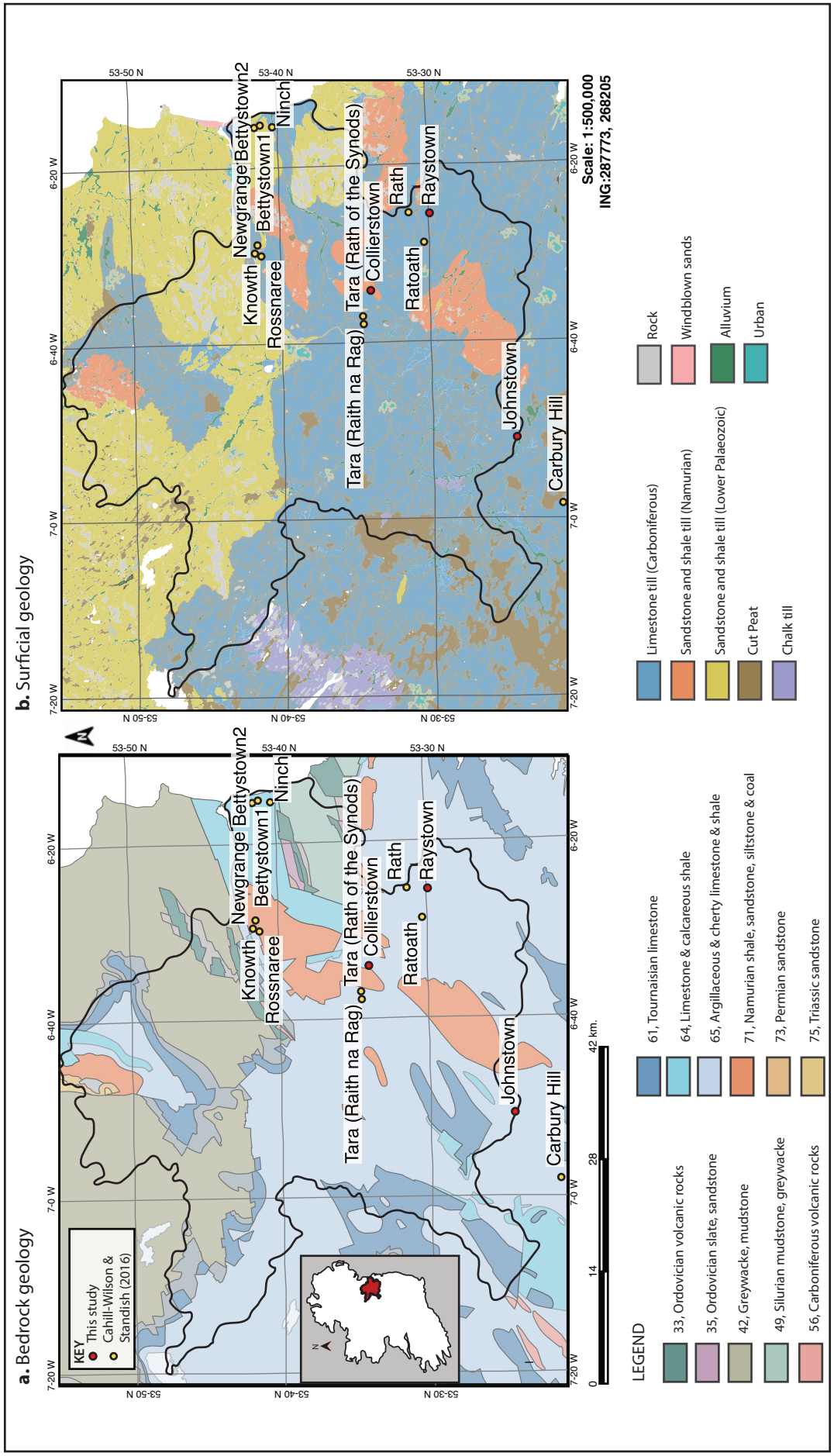


Figure 2. Location of cemetery sites in Co. Meath, Ireland (examined in this study (red points) and in Cahill Wilson and Standish, (2016) (yellow points)) in relation to underlying (a) bedrock and (b) Quaternary geology.

2 Archaeological Sites

2.1 Johnstown

Johnstown was a multi-period settlement-cemetery and industrial site which included a succession of three enclosures centred around a burial mound (Clarke and Carlin, 2008; McCormick et al., 2011). The primary enclosure was dated to 430-650 cal AD, nucleated with the insertion of 3 graves (2 females (J33 dated to 430-680 cal AD and J110 dated 370-640 cal AD) and disarticulated remains of 3 adult individuals in a charnel pit beneath the central mound, possibly all male (J129 dated 370-640 cal AD). The second enclosure was dated between the fifth and seventh centuries and was abandoned before the end of the ninth century. Further burials (J25, J42, J219), all dated to the 6th/8th century, were inserted in and around the mound in the 7th/8th century (including a decapitated male (J25), with skull missing, dated to 580-700 cal AD). The final enclosure is estimated to have been created in the ninth or tenth century and was abandoned sometime between the fifteenth and seventeenth centuries, with the site ultimately used as a cillín (a burial place for unbaptised children) in the post-medieval period. In total, 398 inhumations were found within the enclosures. Evidence for industrial activity in the form of smelting and smithing, and agricultural activity in the form of animal bone and possible milling suggest long term occupation (Carlin et al., 2008).

2.2 Raystown

Raystown developed over a period of 800 years with six developmental phases (Seaver, 2010). Multiple enclosures, a cemetery, kilns, furnaces and the remains of watermills were excavated from these phases. The site was initially a large farming settlement surrounding the cemetery and in the eighth century, it developed into a milling centre which continued in use for another 400 years. Unlike other early medieval mill sites in Ireland that featured a single mill or sometimes two, there were eight water mills at Raystown (Seaver, 2016). The mills were found in association with six grain-drying kilns (all located outside the main enclosures), souterrains and a cemetery and are

suggestive of a specialised, almost industrial scale milling site (Clarke and Carlin, 2008; Seaver, 2006). Burials range from early 5th to late 10th centuries AD (Seaver, 2005). The site was likely occupied for 500 to 600 years (Seaver 2006), being abandoned in the twelfth century, leaving no "historical resonance" (Seaver, 2016).

2.3 Collierstown

Collierstown was a cemetery in use from the mid-fifth to the late-ninth century (O'Hara, 2009). Four main phases of burial were identified. The earliest burial was a female (C48), dated to 420-600 cal AD, with a further eight inhumations extended west-east. A minimum of 61 individuals were buried in a mix of dug, stone-lined and wood-lined graves with almost no associated grave goods. High status artefacts included whalebone sword hilt, a fragment of E ware (mid-sixth/seventh century) and fragments of Late Roman Amphorae (Bii ware) (O'Hara, 2008). Perhaps the most significant find amongst the Collierstown excavation was a sherd from the rim of an imported Phocaean Red Slip Ware (PRSW) pottery vessel, a common type of pottery throughout the eastern Mediterranean from the fifth to seventh centuries AD (Kelly, 2008, 2010). The distribution of late-Roman artefacts (particularly PRSW) was limited in Ireland (to Counties Cork, Tyrone and Dublin) and thus it is inferred that the foreign trade of such items is associated with high-status settlement sites, often interpreted as royal sites (Kelly, 2008); thus, this sherd reflects social prestige at Collierstown. The proximity of Collierstown to the Hill of Tara makes it a possible focal point as a trade networking and distribution centre (Kelly, 2008).

2.4 Excavation Details

Raystown was excavated between the 1st of October 2003 until the 5th of January 2005 by licensee archaeologist Dr. Matthew Seaver. Johnstown was excavated between the 22nd of April until the 16th of October 2002 by archaeologist Dr. Linda Clarke. Collierstown was excavated between the 18th of September 2006 until the 6th of April 2007 under the site director Dr. Robert O'Hara.

3 Materials and Methods

3.1 Rationale for Sampled Tissues

The choice of tissue for isotope analysis is based on the specific research objectives. In this study, the primary objectives are to infer the place of residence during childhood and determine whether this is in agreement with the place of burial. This is inferred by comparison of archaeological dental enamel $^{87}Sr/^{86}Sr$ with the isotope range of the local values. An additional aim is to reconstruct the paleo-diet of these individuals in the latter stages of life in order to gauge cultural practices and customs at these settlements. These objectives rely on the analysis of tissues that provide information about both childhood (teeth) and later life (bone collagen). Therefore, the tissues selected for analysis in this study are: (1) enamel from a third permanent molar, where possible and (2) rib bone.

Teeth follow a rather well constrained chronological mineralisation (Hillson, 1986). The permanent first molars, incisors, and canines begin mineralisation *in utero* and during early infancy and thus, they tend to be influenced by trophic fractionation associated with breastfeeding. Third molars avoid this issue as they begin mineralisation post-weaning, between 7 and 10 years of age. Therefore, they provide an excellent archive of childhood/early adolescent diet. $^{87}Sr/^{86}Sr$ values were measured from dental enamel.

From a small (< 2 mg) sample of bone collagen, it was possible to obtain four different isotope ratios ($\delta^{18}O$, $\delta^{2}H$, $\delta^{13}C$, $\delta^{15}N$) from aliquots of the same sample. Rib bone was selected for analysis in this study as it was available for all individuals and thus was the best choice for consistency in tissue selection. Rib bone is relatively thin and is a cancellous bone (Hill and Orth, 1998) with high turnover rate, giving a shorter-term record of diet, approximately 2-5 years (Cox and Sealy, 1997; Sealy et al., 1995). Only mandible bone was available for animal specimens. The main organic component of bone is collagen, and this tissue reflects the average protein source consumed during the time of bone mineralisation (Sealy, 2001). This period generally corresponds with the latter portion of life as bone is continually remodelled, although remodelling times

vary depending on the specific bone (Ambrose and Norr, 1993). Tuross et al., (2017) highlight the effect of different development regimes for various skeletal components and note that collagen turnover rates decrease with age, which is likely the case for all skeletal elements. Thus, depending on the turnover rate, density and age of the bone selected, the isotopic compositions may vary. Moreover, bone collagen is composed of differing proportions of drinking water and food macronutrients than carbonate and phosphate, (Tieszen and Fagre, 1993; Kirsanow and Tuross, 2011) and bone naturally acts to average isotopic inputs through remodelling, so it is of lower resolution than individual enamel growth layers (Hedges and Reynard, 2007). Other factors can influence the collagen isotope ratios including site-specific environmental variables, soil type and aridity (Heaton, 1987) and these considerations must be taken into account when reviewing the data.

3.2 Bone and Teeth Sample Preparation

All of the sampled archaeological material used in this study is curated by the National Museum of Ireland. Following museum guidelines, only teeth that were loose and could freely be taken from the mandible or maxilla without force were removed for sampling. Fortunately, it was possible to sample 3rd molars (M3) from the majority of individuals. Crown calcification of the M3 begins between the ages of 7 to 10 years old and is generally completed by 12 to 16 years (Hillson, 1986). In some cases, the third molar was either unerupted, not present or firmly rooted in the mandible, and in these instances, other available teeth were sampled (see supplemental Table S4 for details). A sample of tooth enamel was taken from 25 individuals and for three individuals, a second tooth – the first molar, was also sampled to gauge isotope variation through childhood, as this tooth begins calcification in utero and is fully mineralised by the age of 3. Human cortical rib samples from 36 adult humans were selected. See Figure 3 for summarised preparatory and analytical methods. Mandibular bone samples were taken from 15 animals, all from the Raystown site: sheep (n=6), pig (n=6), dog (n=1) and cat (n=2). These bone collagen samples were used to measure $\delta^{18}O$, $\delta^{2}H$, $\delta^{13}C$ and $\delta^{15}N$ values. 7 molars were also selected from a select group of these fauna: sheep (n=3), pig (n=1), dog (n=1) and cat (n=2) and were measured for $^{87}Sr/^{86}Sr$ values. None of the fauna have been radiocarbon dated but they are considered to be contemporaneous with the human remains based on stratigraphy.

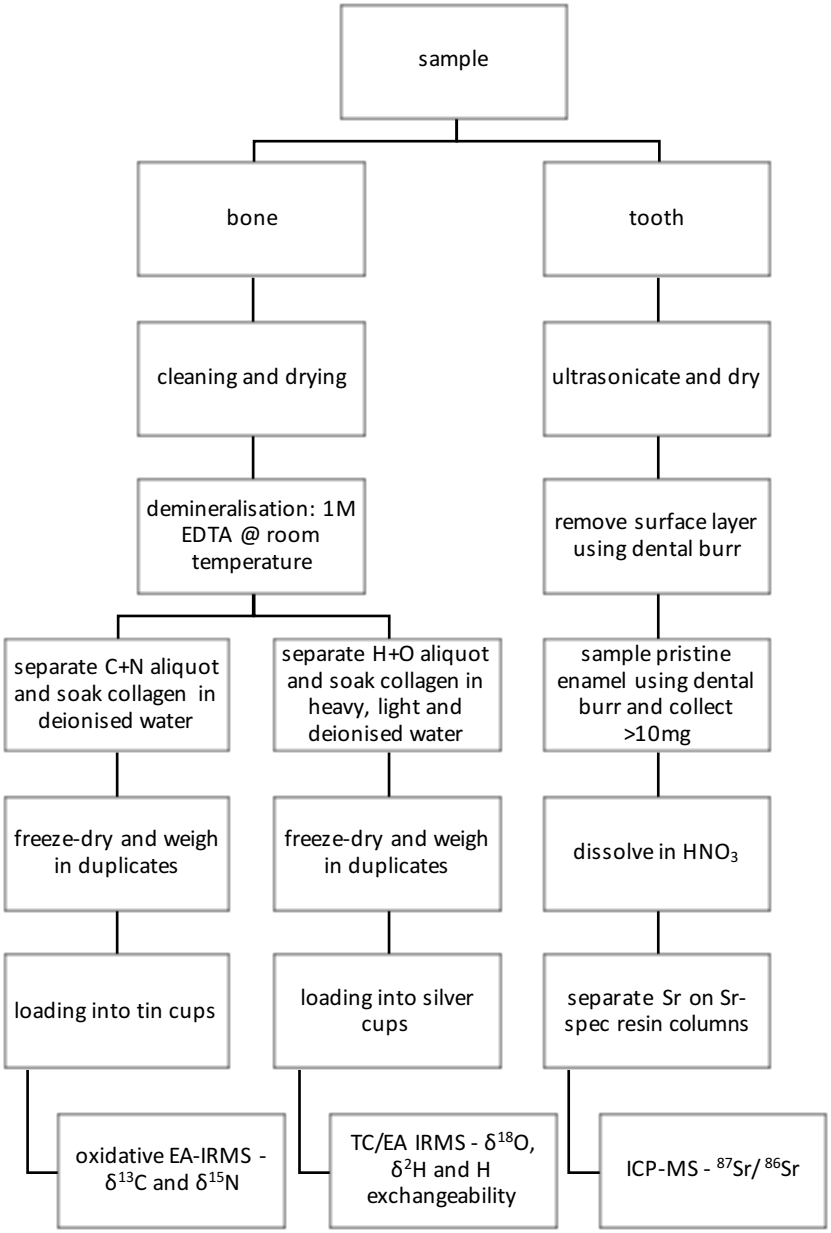


Figure 3. Flow chart of summarised methods (adapted from Topalov et al., (2012).

3.3 Carbon and Nitrogen Isotopes

All stable isotope mass-spectrometric analysis was performed at the Harvard University's Biogeochemistry Facility. $\delta^{13}C$ and $\delta^{15}N$ values are used for dietary reconstruction and were measured from purified collagen extracted from small bone samples. 200–300 mg of bone was cleaned and demineralised at room temperature over several days in 0.5 M EDTA and rinsed in deionised water (Tuross, 2012; Tuross et al., 1988). The collagen was freeze-dried and analysed in duplicate. Isotope ratios were

measured on a Thermo-Finnegan Delta Plus XP, coupled to a Costech 1040 elemental analyser. $\delta^{13}C$ and $\delta^{15}N$ ratios are reported relative to the international standards of Vienna-PDB and AIR respectively. $\delta^{13}C$ and $\delta^{15}N$ ratios were calibrated using USGS 40 and USGS 41 (glutamic acid).

Generally, samples with atomic C/N greater than 3.6 are excluded from further analysis, since this indicates likely diagenetic alteration and thus, poor preservation of the extracted collagen (DeNiro, 1985). The use of O/H ratios has been used as an additional tool to assess the extent of diagenetic alteration (Reynard et al., 2015), and those greater than 0.35 should be excluded. All the measured samples were acceptable based on both discrimination methods (Figure 4).

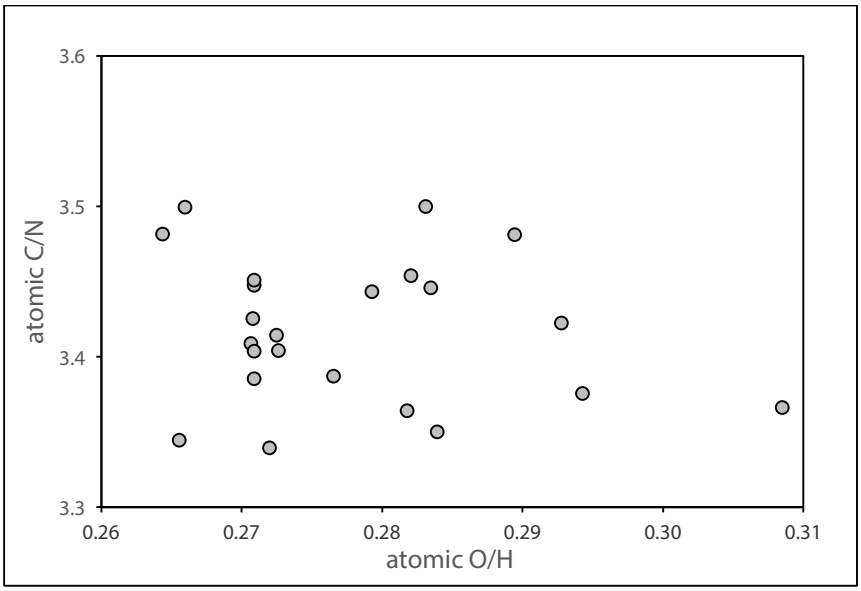


Figure 4. Measures of diagenetic alteration – atomic C/N and atomic O/H - both indicating the collagen is suitably preserved

3.4 Oxygen and Hydrogen Isotopes

Oxygen isotope measurements on each sample were analysed on a Thermo-Finnegan Delta Plus XP, coupled to a Thermo Thermal-Conversion Elemental Analyser (O and H), previously described in detail by Tuross et al., (2008). Samples were mostly analysed in duplicate (details in supplemental Table S3). All $\delta^{18}O$ and $\delta^{2}H$ data are normalised to the SMOW-SLAP scale. The average standard deviation of the duplicated samples for bone collagen was ± 1.2 ‰ for Cr- $\delta^{2}H$, ± 1.8 ‰ for g-C $\delta^{2}H$ and ± 0.2 ‰ for $\delta^{18}O$. Water–collagen exchange experiments were performed on a

subset of samples to determine the influence of environmental water on measured collagen δ^2H. The isotopic value of water used to equilibrate the samples will change slightly over time and geographically between different laboratories, so sample preparation time was kept to a minimum and laboratory standards were run alongside unknowns.

3.5 Strontium Isotopes

All sample preparation was conducted in a clean (class 100, laminar flow) working area. The samples were first washed in deionised water, cleaned ultrasonically, rinsed and dried. The outer enamel surface of each tooth was abraded to a depth of approximately 100 μm using a tungsten carbide dental burr and the residue discarded (Budd et al., 2000). A powdered enamel sample was then collected by abrading the clean enamel surface until a sufficient amount was aquired. Extreme care was taken not to approach the enamel-dentine boundary. The powdered sample was transferred into pre-acid-cleaned microtubes and weighed. The entire acid digestion process and subsequent Sr purification was achieved under a class 100 laminar flow hood in a class 1000 clean room. ±10 mg of sample was pre-treated with acetic acid in Teflon. Samples were purified through Sr separation columns using Sr-Spec resin (Horwitz et al., 1992). The purified solutions were then evaporated, and dried residues were dissolved in 100μl of concentrated HNO_3, evaporated and finally dissolved in 1.5mL of 0.05M HNO_3. $^{87}Sr/^{86}Sr$ compositions were measured on a Nu Plasma MC-ICP Mass Spectrometer at the Vrije Universiteit Brussels (VUB), Belgium. Data were corrected for mass fractionation by internal normalization to $^{86}Sr/^{88}Sr = 0.1194$. All raw data were normalised using a standard-sample bracketing method with the recommended value of $^{87}Sr/^{86}Sr = 0.710248$ (Weis et al., 2006). For each sample the $^{87}Sr/^{86}Sr$ value is reported with a 2 SE. The international standard for $^{87}Sr/^{86}Sr$, NBS987, gave a value of 0.710251 ± .000005 (n=19, 2 SE) during the analysis of these samples. Sr procedural blank values were in the region of 100 pg.

3.6 Statistical Methods

Outliers here are defined as values that fall below Q1 − 1.5*Inter Quartile Range (IQR) or above Q3 + 1.5*IQR and extreme outliers are defined as values that fall below Q1 – 3*IQR or above Q3 + 3*IQR. For boxplots, the highest and lowest occurring value

within this limit are indicated by whiskers of the box, outliers are illustrated as individual points and extreme outliers by an asterisk. These analyses were performed on IBM SPSS Statistics for Macintosh, Version 23.0, Armonk, NY: IBMCorp. Principal component analysis (PCA) was carried out using JMP Pro 12.0.1 for Macintosh, 2015 SAS Institute Inc.

4 Results and Discussion

4.1 Difference in Diet Spatially and Temporally:

Carbon ($\delta^{13}C$) and nitrogen ($\delta^{15}N$) values of individuals from each of the archaeological sites illustrate a terrestrial based diet which included both plant and animal protein, with potential differences in diet as a function of site (Fig. 5; see Table 1 and supplemental Table S2 for further details). There is no statistical difference ($p>0.05$) between the $\delta^{13}C$ values of individuals from the three archaeological sites, Raystown (mean -20.9 ± 0.5 ‰, n=17), Collierstown (mean -20.9 ± 0.2 ‰, n=6) and Johnstown (mean -21.2 ± 0.4 ‰, n=11) (see supplemental Table S6 for detailed statistical results). There is however a small, but significant difference ($p=0.013$) between the $\delta^{15}N$ values of adult populations from Collierstown and Raystown, with Collierstown having a mean $\delta^{15}N$ values of 12.7 ± 0.5 ‰ (n=6) and Raystown having a mean value of 11.7 ± 0.7 ‰ (n=17). Johnstown is not statistically different from either of the other two sites, having an intermediate $\delta^{15}N$ mean of 11.9 ± 0.9 ‰ (n=11).

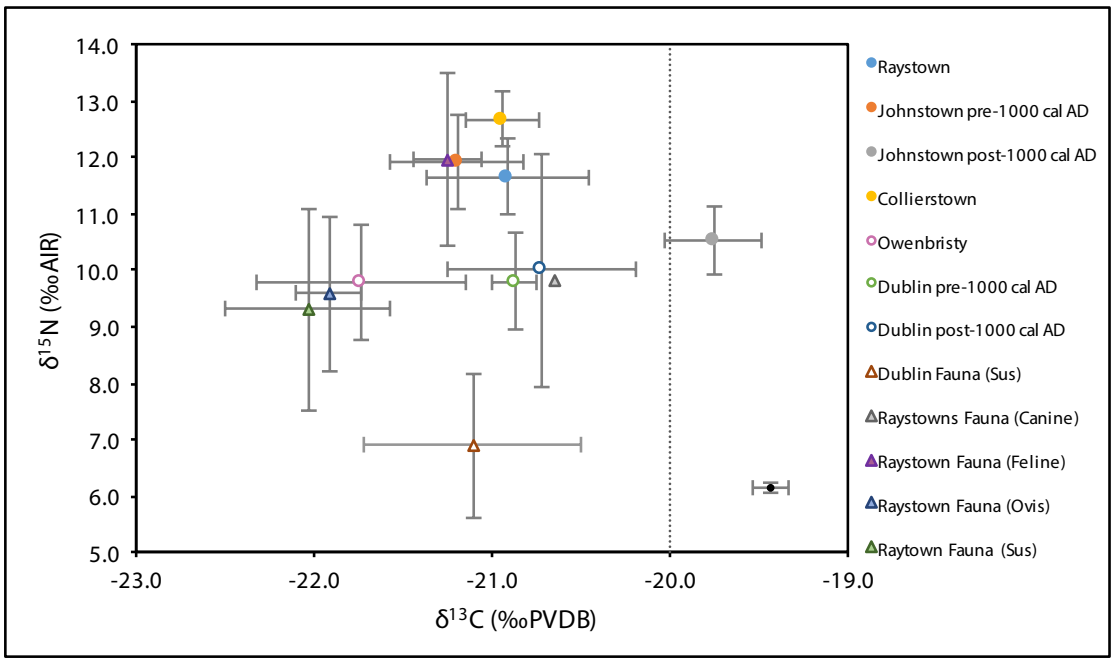


Figure 5. $\delta^{13}C$ and $\delta^{15}N$ values of human and animal remains from cemetery sites in Co. Meath and proximal comparative sites: Viking Dublin (Knudson et al., 2012), Owenbristy (Geber, 2010), Johnstown post-1000 cal AD (Carlin et al., 2008). Dashed line indicates the margin for a solely terrestrial based diet (Barrett and Richards, 2004). The black point in the bottom right-hand corner illustrates the analytical error.

ID	Age Cat.	Sex	Age	Calibrated date (AD) 2 σ	$\delta^{13}C_{VPDB}$	± SD	$\delta^{15}N_{AIR}$	± SD	Cr $\delta^{2}H_{VSMOW}$	± SD	glassy-C $\delta^{2}H_{VSMOW}$	± SD	$\delta^{18}O_{VSMOW}$	± SD	Tooth	Enamel $^{87}Sr/^{86}Sr$	±2 SE
RAYSTOWN																	
R853	Adult	F	36-45	260-540	-20.9		12.4		-6.9	1.3	-15.6		10.2		M3	0.708843	0.000005
R854	Adult	F	36-45	390-550	-21.9		10.4		-18.8	0.8	-32.3		9.3		C	0.711006	0.000013
R820	Adult	F	36-45	400-550	-21.1		11.9		-15.1	1.9	-26.8		10.0		M3	0.708748	0.000003
R841	Adult	M	26-35	430-600	-21.8		10.8		-2.5	2.2	-12.0		10.2		PM2	0.710688	0.000027
R2398	Adult	M	> 25	410-570	-20.9		12.4		-5.6	0.2	-13.2	4.0	10.3	0.3			
R811	Adult	F	45+	430-610	-20.7		12.5		-7.9	0.3	-20.4	0.3	10.3	0.1	M2	0.708789	0.000016
R907	Adult	M	26-35	430-610	-21.1		11.4		-11.5	1.4	-20.3		9.9		M3	0.709395	0.000004
R944	Adult	M	18-25	430-600	-21.1		12.1		-18.1	0.5	-33.8		9.3		M3	0.709330	0.000033
R417	Adult	F	45+	430-640	-20.8		12.1		-19.1	4.6	-30.3		9.2				
R984	Adult	F	45+	440-650	-21.2		12.3		-15.5	0.7	-26.8		10.5				
R848	Adult	M	18-25	550-660	-20.3		10.7		-19.1	0.1	-30.3		9.6				
R954	Adult	U	> 25	550-660	-21.1		12.1										
R1053	Juv.	U	2.2-2.5	570-660	-20.7		13.3		-31.8	0.2	-36.1	0.0	10.2	0.1	M2	0.708684	0.000017
R928	Adult	M	45+	575-665	-20.4		12.2		-16.4	0.2	-30.4		11.6		M3	0.708873	0.000008
R988	Adult	F	45+	430-650	-20.8		11.3		-16.0	0.0	-32.3		10.2		M2	0.708865	0.000004
R1036	Adult	F	18-25	650-780	-20.3		11.4		-18.1	2.8	-29.1		11.0		M3	0.708632	0.000014
R831	Adult	F	36-45	640-780	-20.9		11.0		-15.2	0.2	-29.2		10.4		M3	0.708860	0.000007
R957	Adult	M	36-45	700-950	-20.4		11.3										
R949	Juv.	U	0.8-1.1	780-990	-21.0		13.8		-29.8	0.4	-46.6	5.4	9.2	0.3	M2	0.708547	0.000019
COLLIERSTOWN																	
C48*	Adult	F		420-600											M2	0.709246	0.000010
C58	Adult	F		420-600	-20.8	0.1	13.5	0.0	-9.6	0.9	-20.0		11.8				
C47	Adult	M	20-24	420-610	-20.7	0.1	12.1	0.1	-2.7	1.5	-16.3	0.9	9.8				
C1	Adult	F	35-44	420-600	-21.0	0.1	12.5	0.2	-22.1	0.3	-41.4	0.9	10.2	0.1	M3	0.709030	0.000016
C39	Adult	M	17-25	-					-12.0		-23.0	1.2	9.1	0.4	M3	0.709015	0.000013
C54	Adoles	U	14-17	560-660	-20.9	0.4	12.4	0.1	-10.5	0.9	-20.1	0.3	9.4	0.1	M3	0.709042	0.000013
C18	Adult	M	17-25	540-650	-21.2	0.1	12.6	0.2	-14.0	0.6	-21.2		10.4		M3	0.709003	0.000007
C13	Adult	M	17-25	690-900	-21.1	0.0	13.0	0.2	-17.0	2.5	-26.8		9.5		M3	0.709803	0.000005
JOHNSTOWN																	
J110	Adult	F	45+	370-640	-21.7		12.7		-20.0	1.3	-36.4		9.8				
J129		U		370-640	-21.3		13.2		-17.8	0.6	-25.4	0.6	9.6	0.2			
J33	Adult	F	36-45	430-680	-21.5	0.0	11.8	0.0	-12.3	0.9	-29.4		9.9		M3	0.708755	0.000005
J219	Adult	U		530-660	-21.5	0.0	11.8	0.1	-21.3	0.3	-38.7		10.2		M3	0.708927	0.000010

ID	Age Cat.	Sex	Age	Calibrated date (AD) 2 σ	$\delta^{13}C_{VPDB}$	± SD	$\delta^{15}N_{AIR}$	± SD	Cr $\delta^{2}H_{VSMOW}$	± SD	glassy-C $\delta^{2}H_{VSMOW}$	± SD	$\delta^{18}O_{VSMOW}$	± SD	Tooth	Enamel $^{87}Sr/^{86}Sr$	±2 SE
J25	Adult	M	18-25	580-700	-21.0	0.0	10.3	0.1	-7.0	0.5	-21.7	2.5	9.9	0.1			
J43	Adult	M		545-700	-21.5	0.1	13.0	0.5	-13.4	4.0	-33.2		9.2		M2	0.709624	0.000014
J34	Adult	M	36-45	680-890	-20.4	0.0	10.9	0.0	-13.3	1.6	-32.2		9.4				
J128	Adult	M	45+	680-890	-20.8		11.9		-17.3	2.4	-28.7		9.7		M2	0.708516	0.000004
J166	Adult	F	36-45	650-900	-21.0		11.5		-18.2	0.7	-27.6		10.3				
J249	Adult	F	18-25	680-980	-21.1	0.0	12.5	0.0	-12.2	1.4	-21.4		10.3		M3	0.708463	0.000013
J21	Juv.	U	7	-	-21.1	0.0	11.6	0.0	-18.4	3.0	-33.5	1.2	10.2	0.2			
J42	Adult	M	36-45	-	-21.5		11.7		-15.4	2.1	-31.6		9.4		M3	0.708698	0.000015
J68**				1500-1665	-20.0		10.0										
J295**				1290-1440	-19.7		10.9										
J222**				1290-1410	-19.9		10.5										
J196**				1225-1410	-20.1		9.8										
J145**				1230-1300	-19.3		11.2										
J370**				1230-1300	-19.7		11.3										
J269**				990-1255	-19.6		10.1										
RAYSTOWN FAUNA																	
275 S					-22.3	0.2	8.1	0.2			-32.8	6.1	7.2	0.6			
1 O					-22.1	0.3	10.4	0.5			-61.5	3.6	9.0	0.4			
275 O					-22.1	0.1	9.1	0.1			-57.6	2.1	8.4	0.2	-	0.708837	0.000008
275 2 O					-22.1	0.1	11.3	0.1			-47.1	0.7	8.6	0.1			
1397 O					-21.7	0.1	9.1	0.2			-58.1	1.8	8.7	0.1	-	0.709051	0.000008
263 F					-21.1	0.1	10.9	0.2			-28.2	1.8	6.6	0.6	-	0.708572	0.000003
415 F					-21.4	0.0	13.1	0.0			-31.6	0.4	6.7	0.0	-	0.708443	0.000004
11 S					-21.9	0.0	11.4	0.0			-36.4	1.7	7.1	0.0			
1379 S					-21.3	0.0	11.3	0.0			-30.1	1.3	6.3	0.1			
1406 S					-22.7	0.1	7.2	0.2			-59.1	1.9	6.7	0.0			
1078 O					-21.8	0.0	10.2	0.2			-58.0	4.0	8.8	0.8			
275 2 S					-22.0	0.1	8.1	0.4			-42.5	0.7	7.0	0.2			
1172 O					-21.8	0.1	7.4	0.3			-46.2	2.5	7.9	0.3	-	0.709317	0.000010
803 S					-21.9	0.1	9.8	0.2			-33.4	0.2	6.8	0.3	-	0.708553	0.000007
4 C					-20.6	0.0	9.8	0.1			-36.2	1.4	6.9	0.0	-	0.708545	0.000006

Table 1. Summary table of radiocarbon dates and isotope results from bone collagen and tooth enamel. *$^{87}Sr/^{86}Sr$ value from Cahill Wilson et al., (2014) ** $\delta^{13}C$ and $\delta^{15}N$ for Johnstown from Clarke and Carlin, (2008). Radiocarbon dates from Raystown (Seaver, 2016), Collierstown (O'Hara, 2008) and Johnstown (Clarke & Carlin, 2013), calibrated using Reimer et al., (2004).

Individuals from all three locations have rather tightly clustered $\delta^{13}C$ and $\delta^{15}N$ values suggesting a similar subsistence base by each community. It is difficult to interpret the difference in nitrogen isotopic composition of collagen from Collierstown as animals utilised by the population were not available for this study. It has been suggested that Collierstown was a cemetery reserved for individuals of high social status (Kelly, 2008) and considering this, a diet rich in animal products (or more specifically, more omnivorous animals) corresponds with this suggestion, given that importance of the cow within the economic structure of this period (Kerr et al., 2013). However, two possibilities seem equally likely: either this high-status population ate more animal products or there was a difference in the intensity of manuring practices at Collierstown. It should also be noted that elevated $\delta^{15}N$ values can arise from nutritional or health stress (Beaumont et al., 2015; Beaumont and Montgomery, 2016).

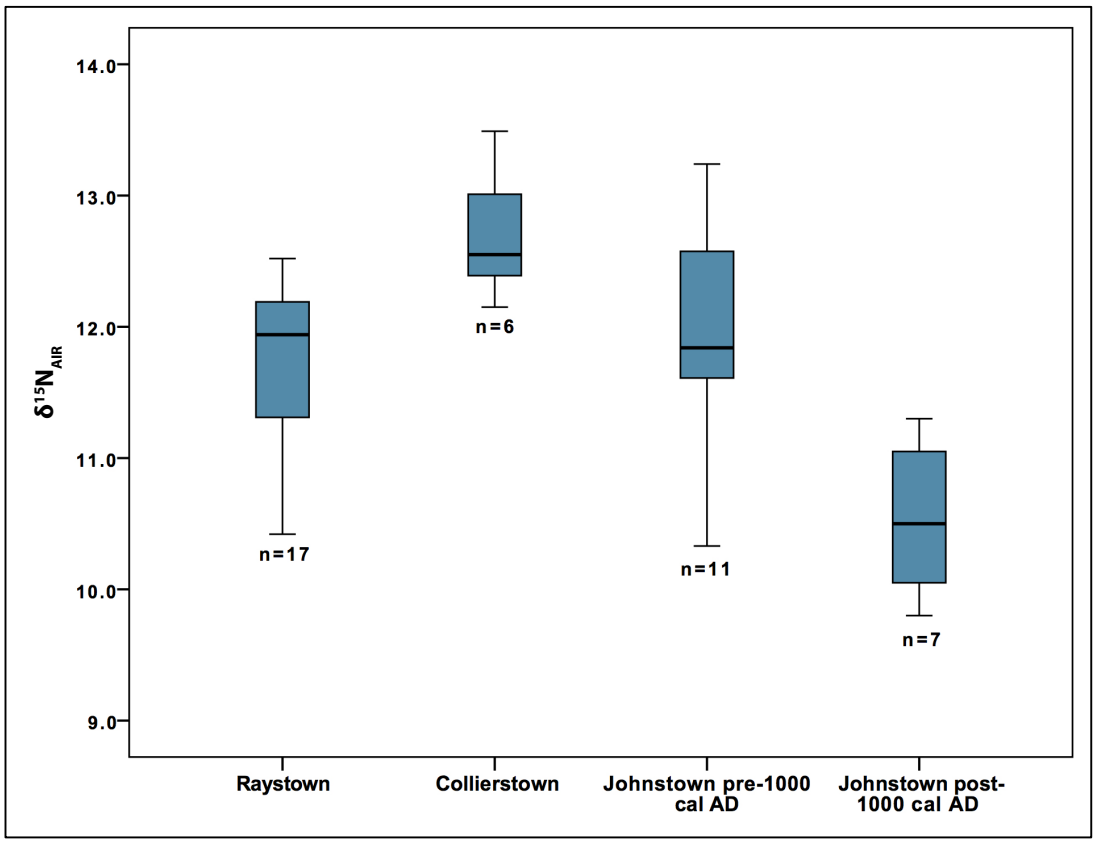


Figure 6. Boxplot of $\delta^{15}N$ values of individuals from each site, with Johnstown subdivided into pre- and post-1000 cal AD. Note that individuals from Collierstown all have $\delta^{13}C$ values > 12‰. Johnstown post-1000 cal AD from Carlin et al. (2008).

Sub-adults from Raystown have expected higher $\delta^{15}N$ values, presumably due to trophic level shift associated with breastfeeding (Fogel et al., 1989). Two individuals (R841, male and R854, female) are statistically defined as outliers with more negative $\delta^{13}C$ (-21.8 ‰, 10.8 ‰ and -21.9 ‰, 10.4 ‰, respectively) compared to the rest of the analysed remains. This is based on their deviation from the IQR while these individuals are not determined to be outliers from the $\delta^{15}N$ dataset based on this discrimination method (Fig. 6). Nonetheless, they do have lower $\delta^{15}N$ values than the rest of the Raystown individuals. One possibility for these lower values is that the man and woman ate less meat and/or dairy than their fellow Raystown inhabitants. These two individuals plot within the same isotope range as the sheep and pigs analysed from this site (Ovis $\delta^{15}N$ range from 7.4 to 11.3 (n=6) and Sus $\delta^{15}N$ range from 7.2 to 11.4 (n=5)), further suggesting they had very little meat/dairy contribution to their diet. Given that meat and dairy was a relative luxury during this period, the lesser contribution of these food sources to their diet potentially indicates a lower social status.

Cats, and the single dog analysed at Raystown, plot within the same $\delta^{13}C$ and $\delta^{15}N$ space on Figure 5 as the majority of human adults, a common observation in archaeological populations. Both pigs and sheep have a large range in $\delta^{13}C$ and $\delta^{15}N$ values, likely because of varying age of the animals (the lingering isotopic effect of suckling is not easy to distinguish) and potentially because of small differences in diet, which could result from a possible range in pasturing locations and animal-management practices.

Individuals from all sites dated to pre-1000 cal AD had $\delta^{13}C$ values <-20.0 ‰ which can be taken as an indicative margin for solely terrestrial based food intake (-21.0 ‰ ± 1) (Barrett and Richards, 2004). It is noteworthy that these people were settled within a small distance from the Irish Sea coastline (Raystown – 16km, Collierstown – 31km, Johnstown - 43km), yet they did not exploit this resource. Likewise, Barrett and Richards, (2004) also noted an emphasis on high terrestrial meat protein, with minor marine protein consumption, even at coastal sites in Orkney, Scotland. This was based on excavation evidence and the associated $\delta^{13}C$ and $\delta^{15}N$ of early medieval people. The potential significance, or lack thereof, of a marine contribution to the diet at these near-coastal sites raises questions about the dietary customs at the time and why there is such little importance placed on fish and other marine-products. Rather than this being a

cultural disregard for marine resources it is likely a question of accessibility through local barter and reciprocal economy; the people who lived in Raystown did not have a client relationship with people from the other túatha (tribes) at or near the coast (M. Seaver, personal communication, 2016).

Bone collagen from Johnstown individuals dated to post-1000 cal AD were previously analysed for $\delta^{13}C$ and $\delta^{15}N$ (Carlin et al., 2008) and there is a noticeable shift in dietary practices over this transition from the early to high medieval period. Both $\delta^{13}C$ and $\delta^{15}N$ values are statistically different ($p<0.05$) from Raystown, Collierstown and pre-1000 cal AD individuals from Johnstown (Fig. 7). The more positive $\delta^{13}C$ values of individuals who lived during the high medieval period suggest that marine and/or estuarine sources such as mussels, contributed to a greater extent to their diet. Lower $\delta^{15}N$ values are inconsistent with consumption of large salt-water fish or mammals.

Archaeological evidence suggests that cattle were a highly important commodity for meat and milk throughout the medieval period in Ireland and Scotland (Alcock, 2003; Ritchie, 1977; Curtis-Summers et al., 2014; Mulville et al., 2005). However, from about AD 800 onwards there seems to have been a steady decline in the central role of cattle (McCormick, 2008). This coincides with a shift to grain production, evidenced by the prevalence of mills around the turn of the eighth century (Brady, 2006). The stark distinction between $\delta^{13}C$ and $\delta^{15}N$ values, noted between pre- and post-1000 cal AD in populations from Johnstown, particularly the lower $\delta^{15}N$ values, may reflect this change in farming practices as well as some use of marine resources. Evidence for a steady increase in fish contribution to diet from the Neolithic to the Viking age has been demonstrated from $\delta^{13}C$ values of individual fatty acids preserved in cooking vessels from Britain (Cramp et al., 2014). It is postulated that an increase in marine food consumption in the mid- to late-medieval period was associated with growing populations and an increase in the fish trade, as well as a widespread adherence to Christian fasting practices (Barrett and Richards, 2004; Müldner and Richards, 2005; Barrett et al., 1983; Müldner and Richards, 2007b, 2007a). There was no significant change in diet noted between pre- and post-1000 cal AD populations excavated from Dublin (Knudson et al., 2012) or from Owenbristy, Co. Galway over the 6th to 10th century (Geber, 2010) (Fig. 5). The individuals excavated from Owenbristy are also compared by Geber (2010) to parallel assemblages excavated at Knockrobbin Hill (Co.

Wicklow) and Cappogue Castle (Co. Dublin), where in each case, there appears to be a strong emphasis on plant-based foods with terrestrial animal protein being consumed to a lesser extent (Geber (2010) and references therein).

The high $\delta^{15}N$ values for both animal (9.8 ‰ ± 1.7) and human (12.0 ‰ ± 0.8) bone collagen from all three sites is likely an indication of ^{15}N enrichment in the biome. One explanation for high $\delta^{15}N$ values of human bone collagen is consumption of manured crops by humans, since manuring increases the $\delta^{15}N$ values of plants (Bogaard et al., 2007). Studies have shown that manuring of crops can increase cereal $\delta^{15}N$ values by as much as 10‰ and that $\delta^{15}N$ values are correlated to the amount of manure applied (Bogaard et al., 2007, 2013). The effect of this increase on crop $\delta^{15}N$ values is the raising of the bone collagen $\delta^{15}N$ value of consumers. In other words, herbivores eating manured crops would have higher $\delta^{15}N$ than herbivores eating unmanured plants (Styring et al., 2015). If the base of the ecosystem started out with high $\delta^{15}N$ values, it would shift both animal and human consumers of manured crops towards more positive $\delta^{15}N$. The effect of manuring has also been noted by Toolis (2008), where elevated $\delta^{15}N$ is taken to imply the manuring of crops with animal dung, but substantial consumption of animal protein is also suggested as a potential factor for the observed ^{15}N enrichment. This uncertainty highlights the difficulty in untangling these contributors.

Without direct measurement of plants at the bottom of the $\delta^{15}N$ hierarchy, it is not possible to know precisely how much manuring has raised, if at all, the baseline $\delta^{15}N$ values in this environment. Measuring the stable isotope composition of plants consumed by humans tends not to be common practice as they are often not preserved or if so, they may be contaminated from prolonged burial and/or altered isotopically by charring, the latter being the process by which most grains remain intact. Another limitation is that one does not know if livestock were being fed manured crops or if they were grazing on unmanured crops, making is more difficult to effectively compare humans and livestock based on the isotope values.

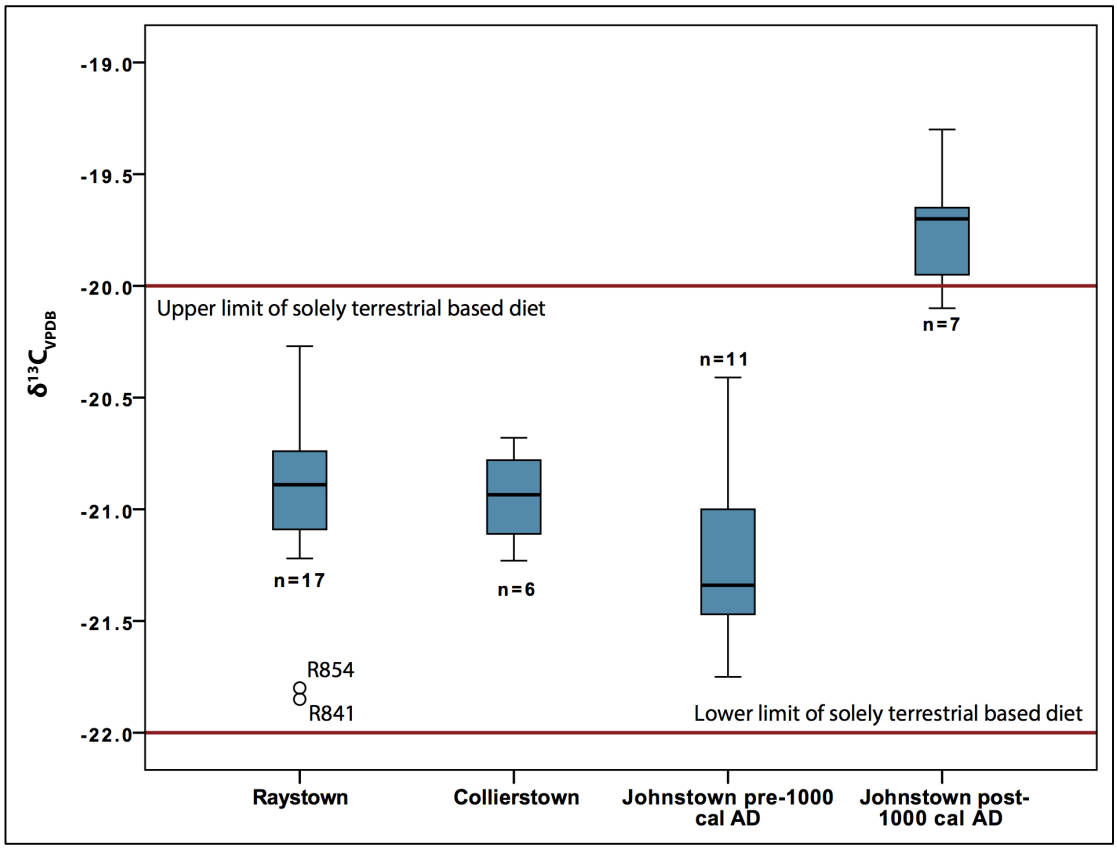


Figure 7. Boxplot of $\delta^{13}C$ values of individuals from each site, with Johnstown subdivided into pre- and post-1000 cal AD. Note that post-1000 cal AD individuals from Johnstown have a statistically distinguishable mean from the other three groups. Johnstown post- 1000 cal AD from Carlin et al. (2008).

4.2 Migration

4.2.1 $^{87}Sr/^{86}Sr$

Human tooth enamel has a range of $^{87}Sr/^{86}Sr$ values of 0.7085-0.7110, with a mean value of 0.7091 ± 0.0002 (2 SD). This value is overlapping modern sea water (0.7092; McArthur et al., (2001)) and above the range of Carboniferous limestone, 0.7075 to 0.7085 (Shields, 2007; Veizer, 1989), which these sites overlie. Present-day seawater-like values can also arise from the cultivation of soils which have been fertilised with seaweed (Hemer et al., 2017) but as discussed above, the sea and its associated products (including seaweed) were unlikely to have been used extensively by these populations.

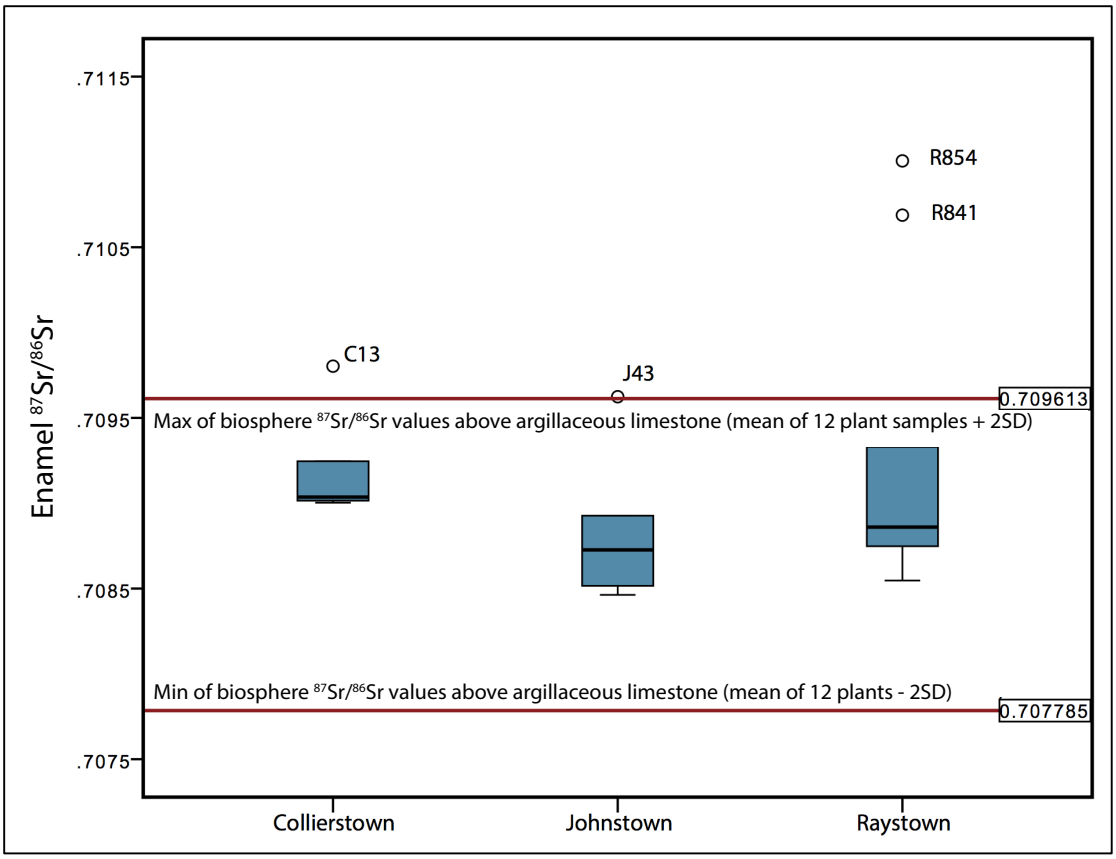


Figure 8. Boxplot of $^{87}Sr/^{86}Sr$ from each of the early medieval cemetery sites. Red lines signify the upper and lower limits of the local biosphere $^{87}Sr/^{86}Sr$ collected from plants overlying limestone bedrock.

Using $^{87}Sr/^{86}Sr$ for the purpose of geographical distinction can be problematic when the areas under study have similar or overlapping isotopic compositions. This generally occurs when there is relatively homogenous bedrock/surficial geology but this is not the case in Co. Meath (Chapter 3). Values for local terrestrial bioavailable $^{87}Sr/^{86}Sr$, determined from soil leachates, vegetation and streamwater, for the entire region of Co. Meath range from 0.7081 to 0.7118. This range excludes three outliers which have more radiogenic values. The mean bioavailable $^{87}Sr/^{86}Sr$ for the region is 0.7095 ± 0.0002 (n=56); This includes biosphere samples that overlie a range of bedrock types across the county, including Devonian basalt, Ordovician-Silurian shale, Permian sandstone and Carboniferous limestone. All three of these archaeological sites lie above the latter and are also dominantly covered by limestone till. The mean of plant samples collected above this bedrock alone was 0.7087 ± 0.0009 (n=12), ranging from 0.7082-0.7096 (Chapter 3) and all human values are in or very near the bioavailable range (mean 0.7087 ± 2 SD), except for two clear outliers (Figure 9).

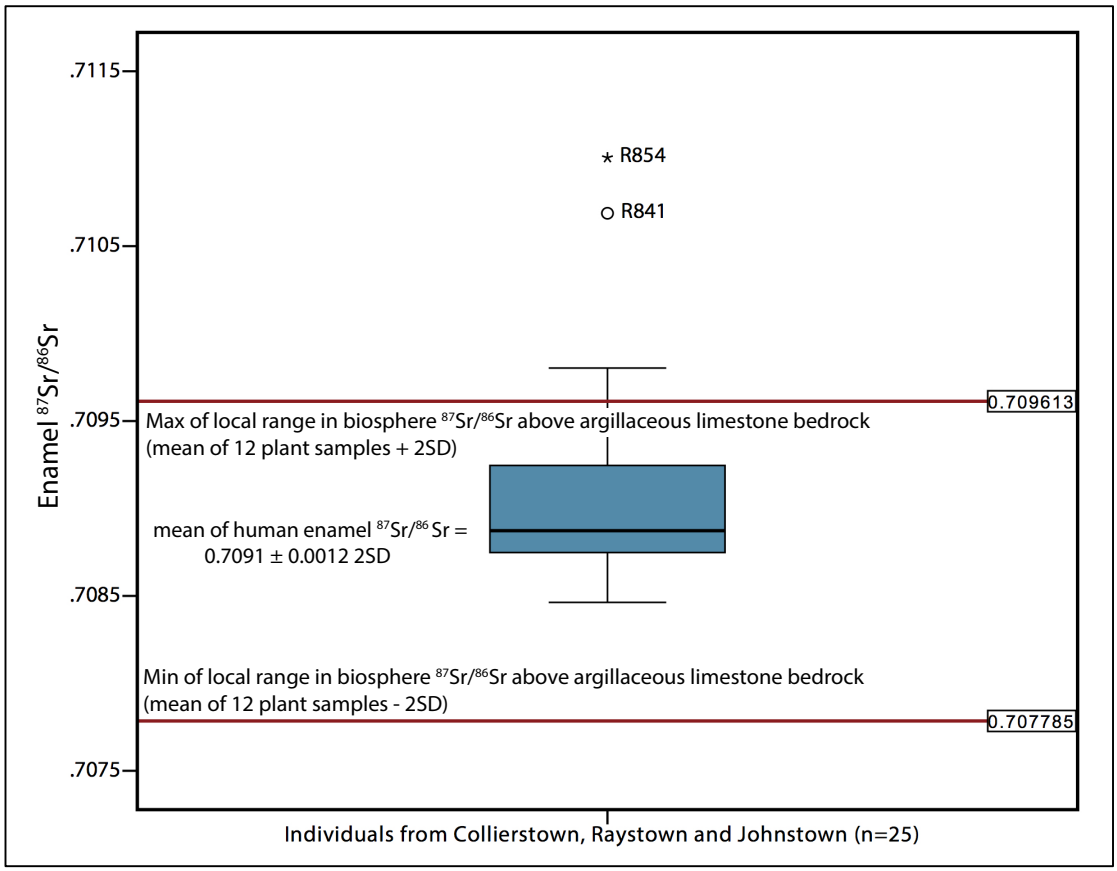


Figure 9. Boxplot of $^{87}Sr/^{86}Sr$ from of all individuals from each early medieval cemetery sites. Red lines signify the upper and lower limits of the local biosphere $^{87}Sr/^{86}Sr$ collected from plants overlying limestone bedrock. Open circle indicates an outlier, whilst a star indicates an extreme outlier.

As for the $\delta^{13}C$ dataset, R841 and R854 (Raystown), are statistically significant outliers, with the former being an extreme outlier from the entire human $^{87}Sr/^{86}Sr$ tooth enamel dataset (Fig. 9); R841 = 0.710688 and R854 = 0.711006. They also fall outside the bioavailable range, noted above, determined for their limestone-dominated burial area. The radiocarbon dates of these individuals are largely within range of one another (R841, 390-550 cal AD and R854 430-600 cal AD) and notably, R854 was a later burial insertion directly on top of R841. These lines of evidence suggest that these people were likely linked in some way, perhaps husband and wife, or some other association.

The skeletal remains of R841 had evidence of multiple (110) peri-mortem blade injuries (Seaver, 2009), a clear sign of violence directed toward him, perhaps a ritual killing or execution. This individual was aged between 26 - 35 years old at the time of death. According to Seaver (2016) this man was the victim of a fierce attack and the extensive

weapon trauma suggesting that there was more than one attacker, potentially occurring in battle or as a targeted killing.

It is not clear where this man and woman came from and whilst they fall above the $^{87}Sr/^{86}Sr$ range for the limestone-dominated local area, they are still within the bioavailable $^{87}Sr/^{86}Sr$ range for all of Co. Meath as noted above (also see Fig. 10). Furthermore $^{87}Sr/^{86}Sr$ values of this order, exist in several areas across Ireland (Chapter 3). It is very possible that they did not migrate over a long distance, a suggestion consistent with oxygen isotopic values in the adult bone collagen (discussed below). Multiple individuals from the greater area of Co. Meath have previously been analysed for their $^{87}Sr/^{86}Sr$ composition (Cahill Wilson and Standish, 2016; Montgomery et al., 2014 and references therein). Using these data in addition to those collected here and within the context of the local bedrock types, a much larger range exists for tooth enamel $^{87}Sr/^{86}Sr$ from areas underlain by Namurian shale/sandstone (Fm. 71) than for enamel from burial sites underlain by limestone (Fm. 65) (Figure 10). Therefore, R854 and R841 can only be considered outliers from their burial population and from the limestone-area. They are within the range of shale/sandstone regions and consequently may have originated from those areas or from further afield. Nonetheless, it seems likely that they moved to Raystown and were somewhat isolated culturally from the 'local' population based on their isotope composition, and R841's violent demise.

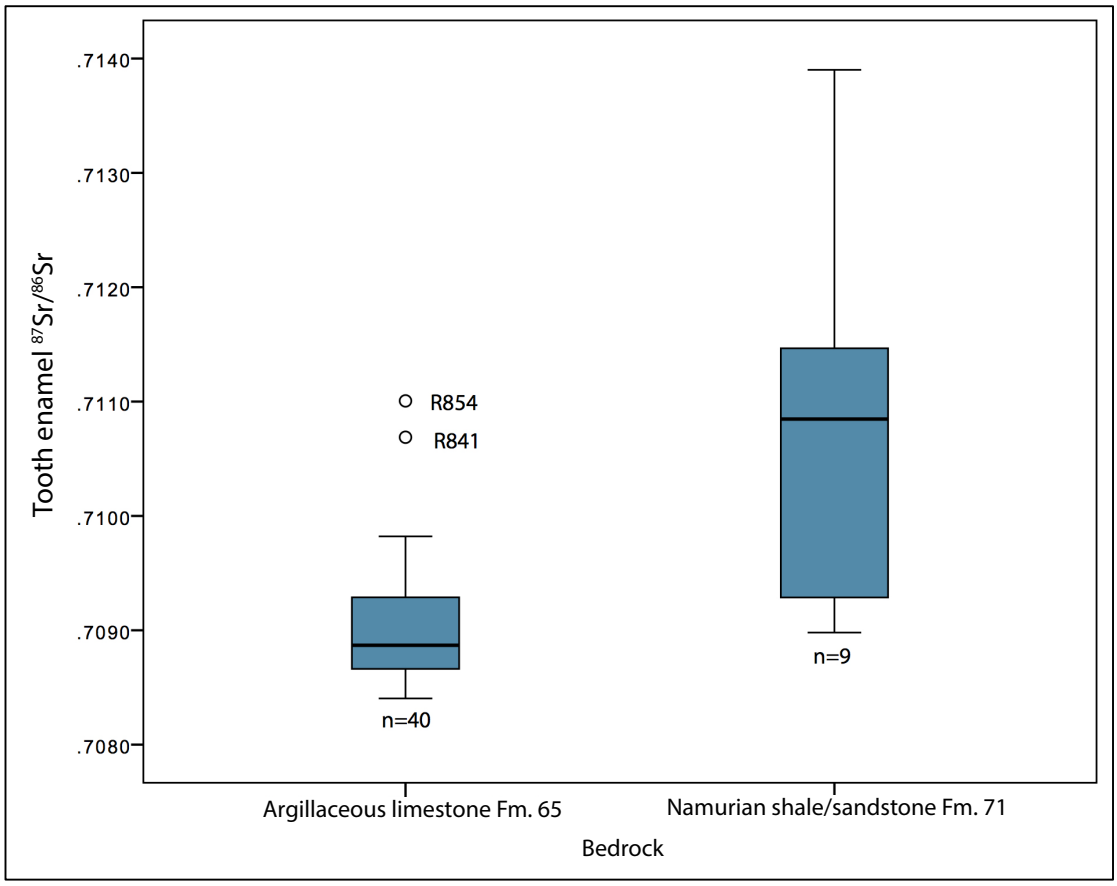


Figure 10. Tooth enamel $^{87}Sr/^{86}Sr$ from individuals buried above limestone (left) and sandstone/shale (right) bedrock. Limestone dataset includes values from Cahill Wilson & Standish (2016) and data from this study. Shale/sandstone values (n=9) are solely from Cahill Wilson & Standish (2016). From 40 individuals, R841 and R854 remain outliers.

For three individuals, in addition to the third molar, a second tooth – the first molar, was also sampled. This was carried out in order to gauge $^{87}Sr/^{86}Sr$ variation through childhood as this tooth begins calcification in utero and is fully mineralised by the age of 3 in comparison to the third molar which completes crown mineralisation in early-mid adolescence (Hillson, 1986). The difference between first and third molar is small for each individual; $\Delta^{87}Sr/^{86}Sr_{M3\text{-}M1}$ = -0.0003 (C39), 0.0001 (C18) and 0.0002 (J219) (Fig. 11), therefore, movement between isotopically contrasting regions over childhood can be deemed unlikely for these three people. Dentine was also analysed and in each case it demonstrates less radiogenic values than associated enamel. These lower $^{87}Sr/^{86}Sr$ arise from exchange between the porous dentine and the local soil water in which they had been buried. It is well established that dentine is highly susceptible to diagenetic alteration and that the degree of biogenic Sr exchangeability is variable

(Budd et al., 2000). Thus, these values show that local labile soil $^{87}Sr/^{86}Sr$ is contributing less radiogenic $^{87}Sr/^{86}Sr$ to the tooth dentine relative to enamel but their $^{87}Sr/^{86}Sr$ values are not directly representative of the local bio-available Sr range that exists within the pedosphere.

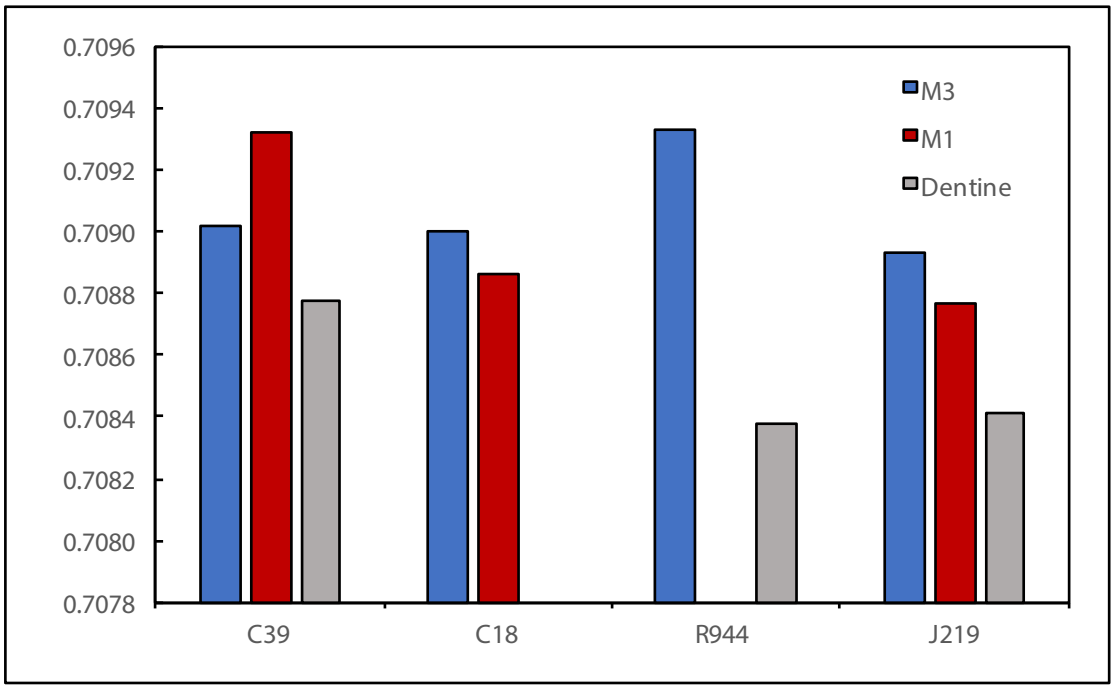


Figure 11. $^{87}Sr/^{86}Sr$ variation between third and first molars and dentine in four individuals.

4.2.2 $\delta^{18}O$

Oxygen ($\delta^{18}O$) and hydrogen ($\delta^{2}H$) ranges for this study area have been produced based on $\delta^{18}O$ and $\delta^{2}H$ values of environmental waters (groundwater or meteoric), denoted as $\delta^{18}O_{DW}$ where $_{DW}$ represents 'drinking water'; In Ireland $\delta^{18}O_{DW}$ ranges from c. −4.5‰ to c. −7‰ and $\delta^{2}H_{DW}$ range from -25‰ to -45‰ (Darling et al., 2003; Diefendorf and Patterson, 2005). Grids/contoured maps of $\delta^{18}O$ and $\delta^{2}H$ environmental data are an extremely useful tool for provenance studies because they can provide accurate point estimates for $\delta^{18}O$ and $\delta^{2}H$ in precipitation that can be compared to biological and animal samples of known or unknown origin (Bowen et al., 2005). Despite this, in most local landscapes, stable isotope maps do not provide the level of spatial accuracy to detect short distance movements, even when multiple isotopes are combined. Thus, comparing environmental stable isotope values with human bone values can result in an underestimation of the true number of individuals who are immigrants. Moreover, whilst there are broad gradients of water $\delta^{18}O$ and $\delta^{2}H$ values from the west to the east

across Ireland, the two main datasets that exist for $\delta^{18}O$ and $\delta^{2}H$ for drinking water in Ireland (Darling et al., 2003; Diefendorf and Patterson, 2005) vary and therefore different interpretations can arise based on the dataset selected for comparison (cf. Sheridan et al., 2013).

Characterised local $\delta^{18}O$ and $\delta^{2}H$ distribution based on interpolated water values can be compared to human and/or animal isotope values if the offset, or diet-tissue discrimination factor, is known (Bowen et al., 2005). Measured $\delta^{18}O$ of bone collagen ($\delta^{18}O_{COLL}$) cannot be directly converted to local water values ($\delta^{18}O_{DW}$) as a conversion for human bone collagen is complicated by the unknown specific controls over $\delta^{18}O$ composition in bone collagen. Nonetheless, Kirsanow and Tuross (2011) found that the isotopic value of drinking water was found to be reflected in the bone collagen of raised rats. Furthermore, terrestrial mammals were found to have collagen that is ^{18}O-depleted relative to coexisting structural carbonate ($\Delta^{18}O_{CARB}$-$^{18}O_{COLL}$= ~13–18‰) (Crowley, 2014). An alternative approach to estimating local $\delta^{18}O$ ranges is to determine a local population range from measured skeletal values within the study area, provided sufficient sample numbers have been analysed. Cahill-Wilson & Standish (2016) found a mean $\delta^{18}O_{CARB}$ of 27.1 ± 1.0‰ (2σ) with a range of 24.7-29.6 ‰ (n=49) for sites located in Co. Meath. Here the mean $\delta^{18}O_{COLL}$ is defined as 10.0‰ ± 0.6 (n=36) with quite a narrow range of collagen $\delta^{18}O$ (9.1 – 11.8 ‰).

Two further individuals, an adult female C58 ($\delta^{18}O$ = 11.8 ‰, $^{87}Sr/^{86}Sr$ = n/a) and an adult male R928 ($\delta^{18}O$ = 11.6 ‰, $^{87}Sr/^{86}Sr$ = 0.708873) are statistical outliers based on their $\delta^{18}O$ values if a discrimination criterion of falling outside two standard deviations (SD) from the mean is used. If three standard deviations from the mean are used, these individuals cannot be categorised as outliers (Fig. 12). Their $\delta^{18}O$ values may indicate a place of origin further afield; However, deviating $\delta^{18}O_{COLL}$ from the population average can arise from other factors such as tissue-specific differences, age of the individual and cooking practices (Tuross et al., 2017). The time discrepancy between tissue mineralisation should also be noted, with $\delta^{18}O$ from bone collagen representing later life and $^{87}Sr/^{86}Sr$ reflecting values from childhood. Therefore, the question of mobility in the intervening period is another variable which complicates the direct comparison of these two isotope values (Fig. 12).

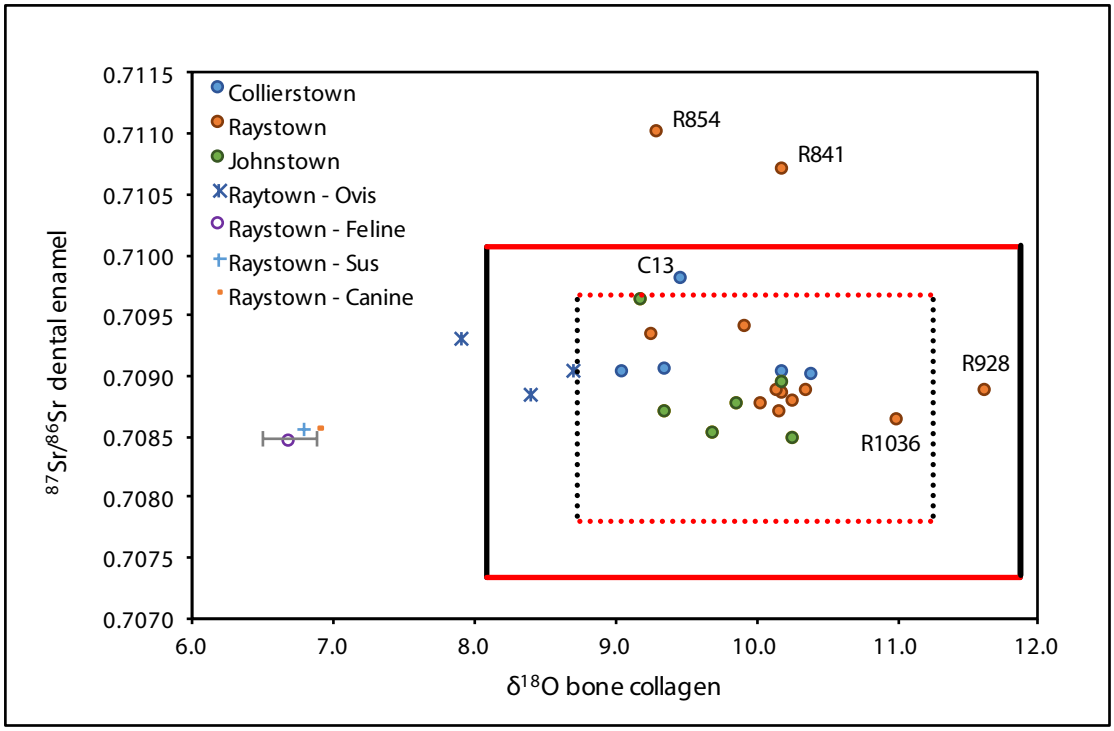


Figure 12. $^{87}Sr/^{86}Sr$ and $\delta^{18}O$ of human dental enamel and bone collagen respectively. Red lines delimit the upper and lower margins of the biologically available (plant) $^{87}Sr/^{86}Sr$ for this limestone-dominated region (mean ±3SD, n=12) (Chapter 3) and dashed red lines signify the mean ± 2SD limits. Black lines delimit 3SD from the mean $\delta^{18}O$ for the entire human dataset (n=36) and dashed blank lines signify the mean ±2SD.

Given that the collective data produced here includes multiple variables, i.e. different isotope systems, principal component analysis is a useful technique to reduce the dimensionality of the entire dataset. Six variables, $^{87}Sr/^{86}Sr$, $\delta^{18}O$, glassy-C $\delta^{2}H$, Cr $\delta^{2}H$, $\delta^{13}C$ and $\delta^{15}N$, can be visualised on a two-dimensional plot (Fig. 13). Before running the PCA, data were standardised so that each variable had a mean of 0, correcting for the different scales of each of the variables. Together, principal component 1 (PC1) and PC2 account for 64% of the variability of the dataset. The red vectors (arrows) in Figure 13 originate at the mean value for the entire dataset and point in the direction associated with each of the individual variables. The results show that R841 and R854 plot distinctly from the central grouping, largely based on $^{87}Sr/^{86}Sr$ values. R1053 and R949 (juveniles) also plot notably to the extreme left of PC1, in the direction on the $\delta^{15}N$ vector and in the direct opposite direction of the two $\delta^{2}H$ vectors. C58 and R928 can be distinguished based on the $\delta^{13}C$ and $\delta^{18}O$ vectors. Overall, the PCA substantiates the observations made from the boxplots and outliers previously determined by falling outside two standard deviations from the mean.

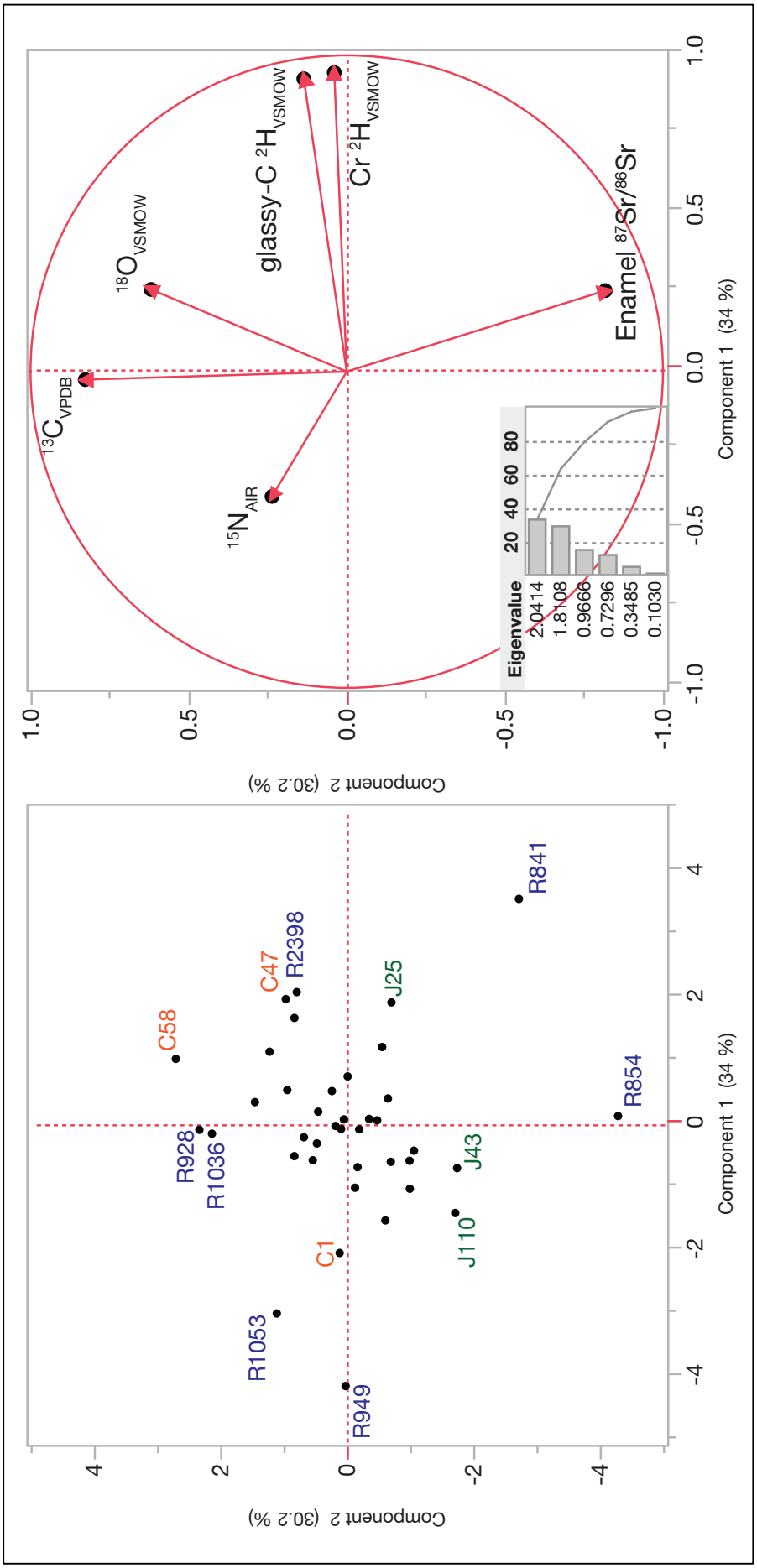


Figure 13. Principal component analysis (PCA) of 6 isotope systems (variables) analysed, $^{87}Sr/^{86}Sr$, $\delta^{18}O$, glassy-C $\delta^{2}H$, Cr $\delta^{2}H$, $\delta^{13}C$ and $\delta^{15}N$, in human remain

4.2.3 δ^2H

As detailed in the introduction of this chapter, one of the more "underutilised" and experimental areas of stable isotope research deals with the measurement of $\delta^{18}O$ and δ^2H in proteins (mainly collagen) (Makarewicz and Sealy, 2015). The exchangeable hydrogen in collagen is accounted for here by equilibration with deionised water of known isotopic composition (see supplemental Table S5 for results). The extent of water exchange was small enough that any variability in environmental water isotopic ratio has a minimal effect on measured collagen δ^2H. A detailed rationale regarding this exchange experiment is detailed in Reynard and Hedges, (2008). Near identical exchange experiments to those carried out in this study are documented in Reynard et al., (2015) with corresponding measured and exchanged collagen δ^2H, indicating linear behaviour. In this instance, the slopes were somewhat flatter, but still behaved in a systematic manner.

δ^2H values measured by High-Temperature Conversion (HTC) with a glassy carbon reactor have been shown to result in hydrogen exchange, likely from the formation of HCN (Reynard and Tuross, 2016). When comparing glassy carbon packed reactor δ^2H values to those obtained using a Cr-packed reactor, there is a clear offset produced by different reactor configurations. Thus, different δ^2H of certain nitrogen-containing tissues can arise as a function of reactor configuration. The offset is linear with an equation of $y=1.08x-11.37$ including two infants (Fig. 14) or $y=1.22x-8.56$, $R^2=0.77$ excluding these two values. This clear offset reinforces the findings of Reynard and Tuross, (2016) and demonstrates that using glassy-C to measure δ^2H values from nitrogen-containing compounds, such as collagen, is not accurate. Fortunately for the vast body of glassy-C δ^2H data produced in the literature, it seems that the linear offset could be used to create a correction factor; However, more comparative data using both packing methods, preferably from a range of N-containing compounds, would need compiling before this can be done with confidence.

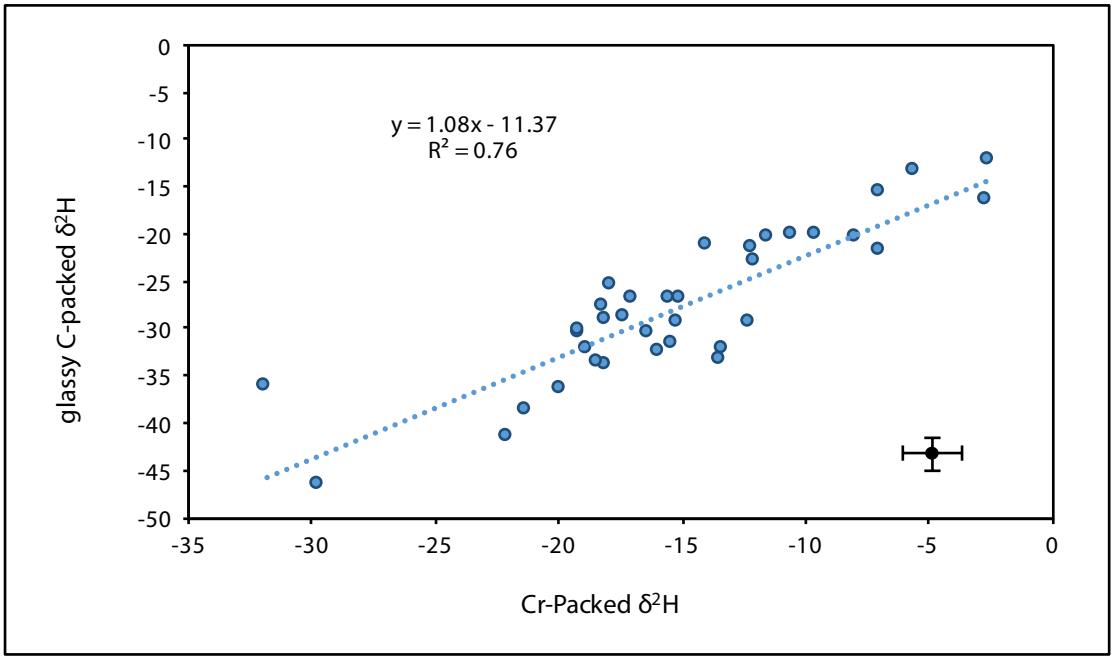


Figure 14. δ^2H values of human rib bone collagen measured with a glassy carbon-packed reactor vs. those obtained using a Cr-packed reactor.

$\delta^{18}O$ and δ^2H values of collagen tend to track one another as they are both strongly related to the composition of ingested water (Cormie et al., 1994; Leyden et al., 2006) and to a lesser extent dietary contributions (Kirsanow et al., 2008; Reynard and Hedges, 2008; Tuross et al., 2008). However, there is an offset here between the $\delta^{18}O$ and δ^2H measured from the same bone collagen and this lack of expected correspondence between these isotope values, when measured from the same individuals suggests that water and diet may be contributing to different extents to the $\delta^{18}O$ and δ^2H of bone collagen (Ehleringer et al., 2008; Kirsanow et al., 2008; Podlesak et al., 2008; Tuross et al., 2008). Trophic level and body weight (metabolism) have also been shown to influence δ^2H composition of animal collagen (Birchall et al., 2005; Kirsanow and Tuross, 2011; Topalov et al., 2012; Hedges and Reynard, 2007; Reynard and Hedges, 2008; Reynard et al., 2015; Pietsch et al., 2011). In this study, the $\delta^{18}O$ and δ^2H of collagen are directly compared (Fig. 15). Some species-specific differences are apparent with sheep (ovis) quite distinct from pigs (sus), cats (feline) and the dog (canine). In general, all fauna have distinct values compared to humans, with the exception of a juvenile from Raystown (R949, aged between 0.8-1.1 years of age at death, making it the youngest of the analysed population) who plots closely to the ovine grouping (Fig. 15).

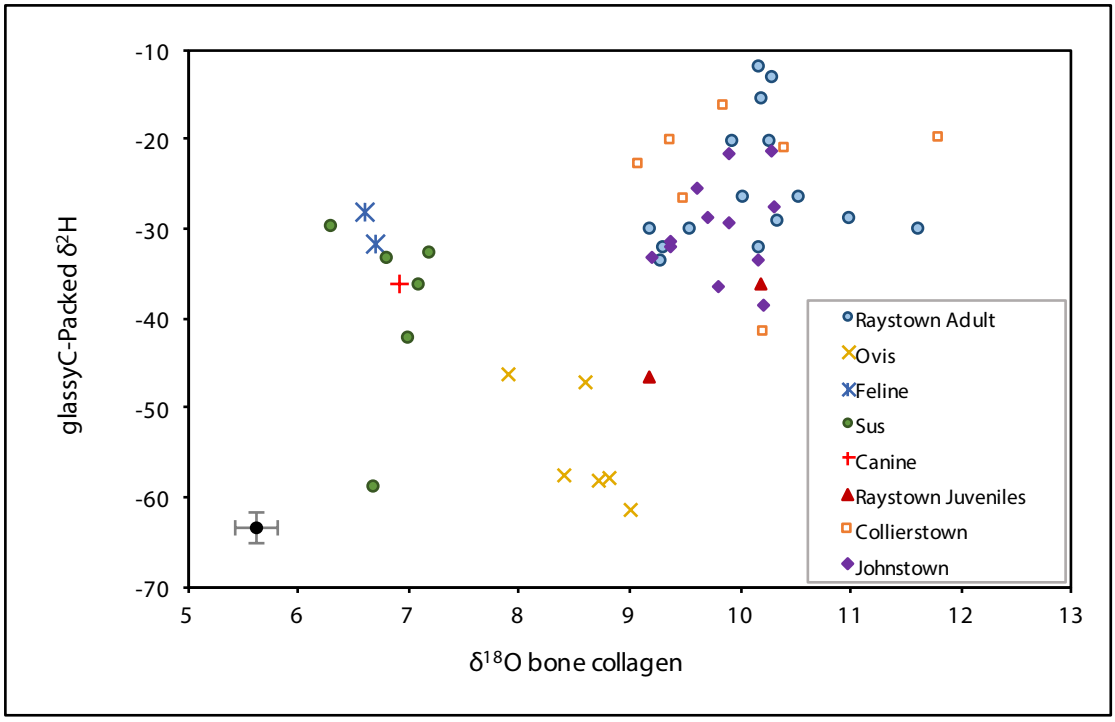


Figure 15. Glassy-C packed δ^2H vs. $\delta^{18}O$ bone collagen in human and animals.

To better distinguish the causal factor(s) of these offsets, controlled feeding experiments would need to be carried out with varied dietary compositions with known isotopic values, i.e., altering the lipids, carbohydrates and protein ratio. This method would allow better determination of what food sources most strongly govern the δ^2H and $\delta^{18}O$ of bone collagen. Adult human and juveniles are measured here which informs on the potential trophic level and metabolic shifts in δ^2H and $\delta^{18}O$ values of organic tissues. Whilst it is known that both δ^2H and $\delta^{15}N$ values increase with trophic level (DeNiro and Epstein, 1978; Birchall et al., 2005; Sealy et al., 1987), it is evident here that Cr-packed δ^2H values effectively separate infants from the entire data, even more distinctly than $\delta^{15}N$ and glassy-C packed δ^2H (see Fig. 16). Cr-packed δ^2H can be deemed as an additional, independent method of studying trophic level, whilst the more commonly used glassy-C δ^2H values are less effective at demonstrating this distinction. Future studies examining the species/metabolic offsets between these isotope systems are advised to use Cr- δ^2H values.

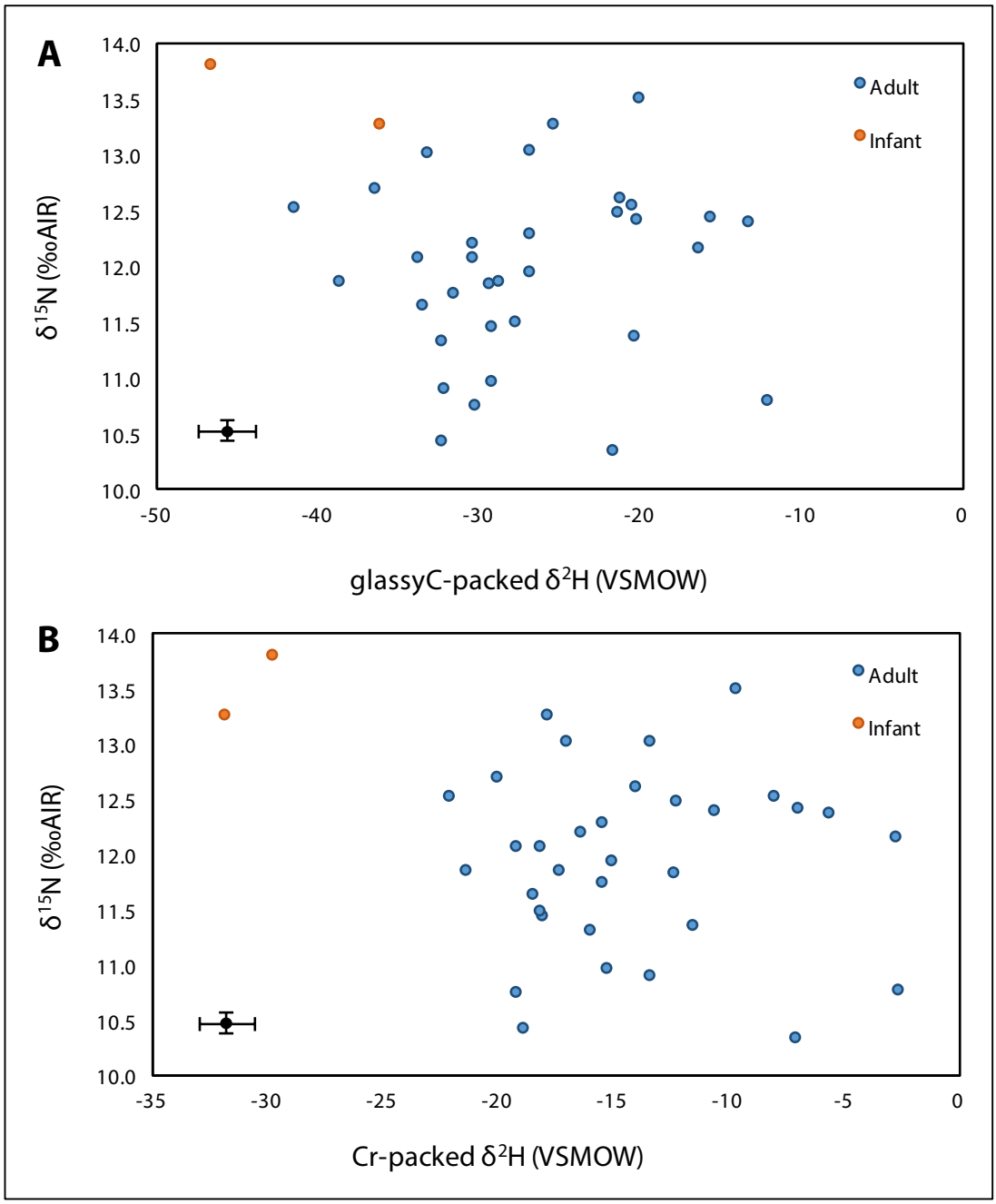


Figure 16. Glassy C δ^2H (**A**) and Cr-packed δ^2H (**B**) vs. $\delta^{15}N$ of adult and infant bone collagen.

5 Conclusion:

Multiple isotopes ($^{87}Sr/^{86}Sr$, $\delta^{18}O$, $\delta^{2}H$, $\delta^{13}C$ and $\delta^{15}N$) constrain diet and provenance of populations from three early medieval sites: Raystown, Collierstown and Johnstown. Two discrete individuals (R841 and R854) are distinguished based on their $^{87}Sr/^{86}Sr$ and $\delta^{13}C$ values and are plausible migrants when compared to the rest of the population and to existing local isotope databases of $^{87}Sr/^{86}Sr$, and $\delta^{18}O$ which provide geographical context. Further, one of these individuals was subject to extreme peri-mortal violence, indicating a potential different position in society; and the other was buried on top of this first individual. Strontium isotope composition ($^{87}Sr/^{86}Sr$) of human dental enamel from the other individuals range from 0.7085-0.7110 with a mean of 0.7091 ± 0.0002 (n=25) in good agreement with the local biosphere (plant) $^{87}Sr/^{86}Sr$ mean for this limestone-dominated area (0.7087 ± 0.0009 (n=12)).

Oxygen isotope values ($\delta^{18}O$) values of bone collagen are notably invariable for the three sites with a mean of 10.0‰ ± 0.6 (n=36). High $\delta^{15}N$ values for both animal (9.8 ‰ ± 1.7) and adult human (12.0 ‰ ± 0.8) bone collagen likely reflect ^{15}N enrichment in the biome due to manuring. A mean $\delta^{13}C$ of -21.0 ‰ ± 0.41 (n=36) for adult humans suggests a largely terrestrial source of dietary protein with insignificant marine input. A comparison between early and high medieval human $\delta^{13}C$ and $\delta^{15}N$ values from Johnstown indicates the contribution of marine food sources to diet increased over this latter period.

Hydrogen isotope values ($\delta^{2}H$) of certain organic compounds measured with a glassy carbon packed reactor are artificially skewed relative to those analysed using a Cr-packed reactor (Reynard & Tuross, 2016). Here, the first comparative results using these two reactor configurations for human samples are presented, with a mean offset of -12.2‰ ± 4.5 (n=36). The linear offset (y=1.08x-11.37) between the values measured using these two configurations could be used to correct previously published, artificially-skewed glassy-C $\delta^{2}H$ data. $\delta^{2}H$ values measured using the Cr-packed reactor are more effective at distinguishing juveniles from the population than glassy-C $\delta^{2}H$ or $\delta^{15}N$ values.

Raystown, Collierstown and Johnstown, three cemetery-settlement complexes, show evidence for multiple phases, spanning several centuries throughout the early medieval period in Ireland. The exact role and function of these sites is still a matter for debate within the archaeological sciences, however these stable and radiogenic isotope data considerably enhance the known complex nature of these societies.

Acknowledgements

This research was completed with support from the Geological Survey of Ireland through their sponsorship of a Fulbright scholarship (S.E.R). It was also supported by a Geological Survey of Ireland shortcall grant awarded to Q.G.C and a Trinity Postgraduate Scholarship awarded to S.E.R for the completion of her Ph.D. Dr. Andy Halpin and Dr. Nessa O'Connor at the National Museum of Ireland (NMI) are gratefully acknowledged for permitting the use of these human and animal remains.

References

Alcock, L., 2003, Kings and Warriors, Craftsmen and Priests in Northern Britain AD 550-850: Society of Antiquaries of Scotland.

AlQahtani, S.J., Hector, M.P., and Liversidge, H.M., 2010, Brief communication: The London atlas of human tooth development and eruption: American Journal of Physical Anthropology, v. 142, p. 481–490.

Ambrose, S.H., and Norr, L., 1993, Experimental evidence for the relationship of the carbon isotope ratios of whole diet and dietary protein to those of bone collagen and carbonate, in J. B. Lambert and G. Grupe (Eds.) Prehistoric Human Bone – Archaeology at the Molecular Level, Springer Verlag, p. 1–38.

Barrett, J.H., Locker, A.M., and Roberts, C.M., 1983, Dark Age Economics: The Origins of Towns and Trade, A.D. 600-1000: The Economic History Review, v. 36, p. 312.

Barrett, J.H., and Richards, M.P., 2004, Identity, Gender, Religion and Economy: New Isotope and Radiocarbon Evidence for Marine Resource Intensification in Early Historic Orkney, Scotland, UK: European Journal of Archaeology, v. 7, p. 249–271.

Beard, B.L., and Johnson, C.M., 2000, Strontium isotope composition of skeletal material can determine the birth place and geographic mobility of humans and animals: Journal of Forensic Sciences, v. 45, p. 1049–1061.

Beaumont, J., Geber, J., Powers, N., Wilson, A., Lee-Thorp, J.A., and Montgomery, J., 2013, Victims and survivors: Stable isotopes used to identify migrants from the Great Irish Famine to 19th century London: American Journal of Physical Anthropology, v. 150, p. 87–98.

Beaumont, J., and Montgomery, J., 2016, The great Irish famine: Identifying starvation in the tissues of victims using stable isotope analysis of bone and incremental dentine collagen: PLoS ONE, v. 11, p. 1–21.

Beaumont, J., Montgomery, J., Buckberry, J., and Jay, M., 2015, Infant mortality and isotopic complexity: New approaches to stress, maternal health, and weaning: American Journal of Physical Anthropology, v. 157, p. 441–457.

Bentley, R.A., 2006, Strontium Isotopes from the Earth to the Archaeological Skeleton: A Review: Journal of Archaeological Method and Theory, v. 13, p. 135–187.

Bentley, R.A., and Knipper, C., 2005, Geographical patterns in biologically available strontium, carbon and oxygen isotope signatures in prehistoric SW Germany: Archaeometry, v. 47, p. 629–644.

Birchall, J., O'Connell, T.C., Heaton, T.H.E., and Hedges, R.E.M., 2005, Hydrogen isotope ratios in animal body protein reflect trophic level: Journal of Animal Ecology, v. 74, p. 877–881.

Bogaard, A., Fraser, R.A., Heaton, T.H.E., Wallace, M., Vaiglova, P., Charles, M., Jones, G., Evershed, R.P., Styring, A.K., Andersen, N.H., Arbogast, R.-M., Bartosiewicz, L., Gardeisen, A., Kanstrup, M., et al., 2013, Crop manuring and intensive land management by Europe's first farmers: Proceedings of the National Academy of Sciences, v. 110, p. 12589–12594.

Bogaard, A., Heaton, T.H.E., Poulton, P., and Merbach, I., 2007, The impact of manuring on nitrogen isotope ratios in cereals: archaeological implications for reconstruction of diet and crop management practices: Journal of Archaeological Science, v. 34, p. 335–343.

Bowen, G.J., 2010, Isoscapes: spatial pattern in isotopic biogeochemistry: Annual Review of Earth and Planetary Sciences, v. 38, p. 161–187.

Bowen, G.J., Wassenaar, L.I., and Hobson, K.A., 2005, Global application of stable hydrogen and oxygen isotopes to wildlife forensics: Oecologia, v. 143, p. 337–348.

Bowen, G.J., and Wilkinson, B., 2002, Spatial distribution of $\delta^{18}O$ in meteoric precipitation: Geology, v. 30, p. 315–318.

Brady, N., 2006, Mills in medieval Ireland: looking beyond design, in S. Walton (Ed.) Wind and water, the medieval mill: Pennsylvania State University Press, p. 39–68.

Brettell, R., Montgomery, J., and Evans, J.A., 2012, Brewing and stewing: the effect of culturally mediated behaviour on the oxygen isotope composition of ingested fluids and the implications for human provenance studies: Journal of Analytical Atomic Spectrometry, v. 27, p. 778.

Bryant, D.J., and Froelich, P.N., 1995, A model of oxygen isotope fractionation in body water of large mammals: Geochimica et Cosmochimica Acta, v. 59, p. 4523–4537.

Buckberry, J., Montgomery, J., Towers, J., Müldner, G., Holst, M., Evans, J.A., Gledhill, A., Neale, N., and Lee-Thorp, J.A., 2014, Finding Vikings in the Danelaw: Oxford Journal of Archaeology, v. 33, p. 413–434.

Budd, P., Millard, A., Chenery, C.A., Lucy, S., and Roberts, C., 2004, Investigating population movement by stable isotope analysis: a report from Britain: Antiquity, v. 78, p. 127-141.

Budd, P., Montgomery, J., Barreiro, B., and Thomas, R.G., 2000, Differential diagenesis of strontium in archaeological human dental tissues: Applied Geochemistry, v. 15, p. 687–694.

Cahill Wilson, J., 2010, Becoming Irish the materiality of transcultural identities in the later Irish Iron Age: PhD thesis, University of Bristol.

Cahill Wilson, J., 2012, Lost in transcription: rethinking our approach to the archaeology of the later Iron Age in Ireland., in C. Corlett and M. Potterton (Eds.), Life and Death in the Iron Age in Ireland., Wordwell, Bray, p. 15–33.

Cahill Wilson, J., and Standish, C.D., 2016, Mobility and migration in late Iron Age and early Medieval Ireland: Journal of Archaeological Science: Reports, v. 6, p. 230–241.

Cahill Wilson, J., Standish, C.D., and O'Brien, E., 2014, Investigating mobility and migration in the later Iron Age: Late Iron Age and Roman Ireland, Discovery Programme Report No. 8. Discovery Programme, Dublin, p. 127–151.

Capo, R.C., Stewart, B.W., and Chadwick, O.A., 1998, Strontium isotopes as tracers of ecosystem processes: Theory and Methods: Geoderma, v. 82, p. 197–225.

Carlin, N., Clarke, L., and Walsh, F., 2008, The Archaeology of life and death in the Boyne Floodplain: the linear landscape of the M4, Kinnegad-Enfield-Kilcock motorway: National Roads Authority Scheme Monograhs 2.

Chenery, C.A., Evans, J.A., Mary, A., and Boyle, A., 2014, A boatload of Vikings? Journal of the North Atlantic, v. 7, p. 43–53.

Chenery, C.A., Müldner, G., Evans, J.A., Eckardt, H., and Lewis, M., 2010, Strontium and stable isotope evidence for diet and mobility in Roman Gloucester, UK: Journal of Archaeological Science, v. 37, p. 150–163.

Chesson, L.A., Podlesak, D.W., Cerling, T.E., and Ehleringer, J.R., 2009, Evaluating uncertainty in the calculation of non-exchangeable hydrogen fractions within organic materials: Rapid Communications in Mass Spectrometry, v. 23, p. 1275–1280.

Clarke, L., and Carlin, N., 2008, Living with the dead: an enclosed burial, settlement and industrial site, in N. Carlin, L. Clarke and F. Walsh, (Eds.) Life and Death in the Boyne Floodplain: Findings from the Archaeological Excavations along the route of the M4 Motorway, National Roads Authority. Wordwell., p. 55–86.

Cormie, A.B., Luz, B., and Schwarcz, H.P., 1994, Relationship between the hydrogen and oxygen isotopes of deer bone and their use in the estimation of relative humidity: Geochimica et Cosmochimica Acta, v. 58, p. 3439–3449.

Cox, G., and Sealy, J.C., 1997, Investigating identity and life histories: isotopic analysis and historical documentation of slave skeletons found on the Cape Town foreshore, South Africa: Int J Hist Archaeol, v. 1, p. 207–224.

Cramp, L.J.E., Jones, J., Sheridan, A., Smyth, J., Whelton, H., Mulville, J., Sharples, N., and Evershed, R.P., 2014, Immediate replacement of fishing with dairying by the earliest farmers of the northeast Atlantic archipelagos: Proceedings of the Royal Society B: Biological Sciences, v. 281.

Criss, R.E., 1999, Principles of Stable Isotope Distribution: New York, Oxford: Oxford University Press, 254 pp.

Crowley, B.E., 2014, Oxygen isotope values in bone carbonate and collagen are consistently offset for New World monkeys: Biology Letters, v. 10.

Curtis-Summers, S., Montgomery, J., and Carver, M., 2014, Stable Isotope Evidence for Dietary Contrast Between Pictish and Medieval Populations at Portmahomack, Scotland: Medieval Archaeology, v. 58, p. 21–43.

Dansgaard, W., 1964, Stable Isotopes in Precipitation: Tellus, v. 16, p. 436–468.

Darling, W.G., 2004, Hydrological factors in the interpretation of stable isotopic proxy data present and past: A European perspective, in Quaternary Science Reviews, v. 23, p. 743–770.

Darling, W.G., Bath, A.H., and Talbot, J.C., 2003, The O & H stable isotopic composition of fresh waters in the British Isles. 2. Surface waters and groundwater: Hydrology and Earth System Sciences, v. 7, p. 183–195.

Daux, V., Lécuyer, C., Héran, M.A., Amiot, R., Simon, L., Fourel, F., Martineau, F., Lynnerup, N., Reychler, H., and Escarguel, G., 2008, Oxygen isotope fractionation between human phosphate and water revisited: Journal of Human Evolution, v. 55, p. 1138–1147.

Deines, P., 1980, The Isotopic Composition of Reduced Organic Carbon, in P. Fritz and J.C. Fontes (Eds.), Handbook of Environmental Isotope Geochemistry, The Terrestrial Environment, v. 1. A. Elsevier, Amsterdam, p. 329–406.

DeNiro, M.J., 1985, Postmortem preservation and alteration of in vivo bone collagen isotope ratios in relation to palaeodietary reconstruction: Nature, v. 317, p. 806–809.

DeNiro, M.J., and Epstein, S., 1978, Influence of diet on the distribution of carbon isotopes in animals: Geochimica et Cosmochimica Acta, v. 42, p. 495–506.

Diefendorf, A.F., and Patterson, W.P., 2005, Survey of stable isotope values in Irish surface waters: Journal of Paleolimnology, v. 34, p. 257–269.

Eckardt, H., Chenery, C.A., Booth, P., Evans, J.A., Lamb, A.L., and Müldner, G., 2009, Oxygen and strontium isotope evidence for mobility in Roman Winchester: Journal of Archaeological Science, v. 36, p. 2816–2825.

Ehleringer, J.R., Bowen, G.J., Chesson, L. a., West, A.G., Podlesak, D.W., and Cerling, T.E., 2008, Hydrogen and oxygen isotope ratios in human hair are related to geography: Proceedings of the National Academy of Sciences of the United States of America, v. 105, p. 2788–2793.

Evans, J.A., Chenery, C.A., and Montgomery, J., 2012, A summary of strontium and oxygen isotope variation in archaeological human tooth enamel excavated from Britain: Journal of Analytical Atomic Spectrometry, v. 27, p. 754.

Evans, J.A., Montgomery, J., Wildman, G., and Boulton, N., 2010, Spatial variations in biosphere $^{87}Sr/^{86}Sr$ in Britain: Journal of the Geological Society, London, v. 167, p. 1–4.

Evans, J.A., and Tatham, S., 2004, Defining “local signature” in terms of Sr isotope composition using a tenth- to twelfth-century Anglo-Saxon population living on a Jurassic clay-carbonate terrain, Rutland, UK: Geological Society, London, Special Publications, v. 232, p. 237–248.

Fibiger, L., 2006, Report on the human skeletal remains from Raystown, Co. Meath (Excavation no. 03E1229): Unpublished report for CRDS Ltd, Dublin, Ireland.

Fogel, M.L., Tuross, N., and Owsley, D.W., 1989, Nitrogen isotope tracers of human lactation in modern and archaeological populations: in Annual Report of the Director, Geophysical Laboratory 1988-1989. Carnegie Institute of Washington.

Frei, R., and Frei, K.M., 2013, The geographic distribution of Sr isotopes from surface waters and soil extracts over the island of Bornholm (Denmark) – A base for provenance studies in archaeology and agriculture: Applied Geochemistry, v. 38, p. 147–160.

Geber, J., 2010, Diet analysis, in J Lehane and F Delaney (Eds.), Final Archaeological Excavation Report Owenbristy Co. Galway. Eachtra 8, p. 180–185.

Geological Survey of Ireland, 2009, Energy and Natural Resources: Bedrock Geology.

Hamre, S.S., and Daux, V., 2016, Stable oxygen isotope evidence for mobility in medieval and post-medieval Trondheim, Norway: Journal of Archaeological Science: Reports, v. 8, p. 416–425.

Heaton, T.H.E., 1987, The $^{15}N/^{14}N$ ratios of plants in South Africa and Namibia: relationship to climate and coastal/saline environments: Oecologia, v. 74, p. 236–246.

Hedges, R.E.M., 2004, Isotopes and red herrings: comments on Milner et al. and Lidén et al.: Antiquity, v. 78, p. 34–37.

Hedges, R.E.M., and Reynard, L.M., 2007, Nitrogen isotopes and the trophic level of humans in archaeology: Journal of Archaeological Science, v. 34, p. 1240–1251.

Hemer, K.A., Lamb, A.L., Chenery, C.A., and Evans, J.A., 2017, A multi-isotope investigation of diet and subsistence amongst island and mainland populations from early medieval western Britain: American Journal of Physical Anthropology, v. 162, p. 423–440.

Hill, P.A., and Orth, M., 1998, Bone Remodelling: British Journal of Orthodontics, v. 25, p. 101–107.

Hillson, S., 1986, Teeth: Cambridge University Press.

Hobson, K.A., 1999, Tracing origins and migration of wildlife using stable isotopes: A review: Oecologia, v. 120, p. 314–326.

Hodges, R., 1989, Dark Age Economics: The Origins of Town and Trade: London: St Martin's Press.

Horwitz, E.P., Chiarizia, R., and Dietz, M.L., 1992, A Novel Strontium-Selective Extraction Chromatographic Resin*: Solvent Extraction and Ion Exchange, v. 10, p. 313–336.

Kador, T., Fibiger, L., Cooney, G., and Fullagard, P., 2014, Movement and diet in early Irish prehistory: First evidence from multi-isotope analysis: The Journal of Irish Archaeology, v. XXIII, p. 83–96.

Kelly, A.M., 2008, A Turkish import in County Meath: Mediterranean pottery on the M3: Seanda: The NRA Archaeology Magazine, National Roads Authority, p. 16–18.

Kelly, A.M., 2010, The Discovery of Phocaean Red Slip Ware (PRSW) Form 3 and Bii ware (LR1 amphorae) on sites in Ireland - an analysis within a broader framework: Proceedings Of The Royal Irish Academy, v. 110, p. 35–88.

Kelly, J.F., Bridge, E.S., Fudickar, A.M., and Wassenaar, L.I., 2009, A test of comparative equilibration for determining non-exchangeable stable hydrogen isotope

values in complex organic materials: Rapid Communications in Mass Spectrometry, v. 23, p. 2316–2320.

Kerr, T., McCormick, F., and O'Sullivan, A., 2013, The Economy of Early Medieval Ireland: Early Medieval Archaeology Project. Irish National Strategic Archaeological Research (INSTAR) programme.

Kirsanow, K., Makarewicz, C.A., and Tuross, N., 2008, Stable oxygen ($\delta^{18}O$) and hydrogen (δD) isotopes in ovicaprid dentinal collagen record seasonal variation: Journal of Archaeological Science, v. 35, p. 3159–3167.

Kirsanow, K., and Tuross, N., 2011, Oxygen and hydrogen isotopes in rodent tissues: Impact of diet, water and ontogeny: Palaeogeography, Palaeoclimatology, Palaeoecology, v. 310, p. 9–16.

Knudson, K.J., O'Donnabhain, B., Carver, C., Cleland, R., and Price, T.D., 2012, Migration and Viking Dublin: Paleomobility and paleodiet through isotopic analyses: Journal of Archaeological Science, v. 39, p. 308–320.

Lamb, A.L., Evans, J.A., Buckley, R., and Appleby, J., 2014, Multi-isotope analysis demonstrates significant lifestyle changes in King Richard III: Journal of Archaeological Science, v. 50, p. 559–565.

Lee-Thorp, J.A., 2008, On isotopes and old bones: Archaeometry, v. 50, p. 925–950.

Lee-Thorp, J.A., and Sponheimer, M., 2006, Contributions of biogeochemistry to understanding hominin dietary ecology: Yearbook of Physical Anthropology, v. 49, p. 131–148.

Leyden, J.J., Wassenaar, L.I., Hobson, K.A., and Walker, E.G., 2006, Stable hydrogen isotopes of bison bone collagen as a proxy for Holocene climate on the Northern Great Plains: Palaeogeography, Palaeoclimatology, Palaeoecology, v. 239, p. 87–99.

Longinelli, A., 1984, Oxygen isotopes in mammal bone phosphate: A new tool for paleohydrological and paleoclimatological research? Geochimica et Cosmochimica Acta, v. 48, p. 385–390.

Luz, B., Kolodny, Y., and Horowitz, M., 1984, Fractionation of oxygen isotopes between mammalian bone-phosphate and environmental drinking water: Geochimica et Cosmochimica Acta, v. 48, p. 1689–1693.

Lynch, A., 2014, Poulnabrone: An Early Neolithic Portal Tomb in Ireland: Archaeological Monograph Series 9: Stationary Office Dublin.

Makarewicz, C.A., and Sealy, J.C., 2015, Dietary reconstruction, mobility, and the analysis of ancient skeletal tissues: Expanding the prospects of stable isotope research in archaeology: Journal of Archaeological Science, v. 56, p. 146–158.

Maurer, A.-F., Galer, S.J.G., Knipper, C., Beierlein, L., Nunn, E. V, Peters, D., Tütken, T., Alt, K.W., and Schöne, B.R., 2012, Bioavailable $^{87}Sr/^{86}Sr$ in different environmental samples - Effects of anthropogenic contamination and implications for isoscapes in past migration studies: The Science of the Total Environment, v. 433, p. 216–29.

Mays, S., and Beavan, N., 2012, An investigation of diet in early Anglo-Saxon England using carbon and nitrogen stable isotope analysis of human bone collagen: Journal of Archaeological Science, v. 39, p. 867–874.

McArthur, J.M., Howarth, R., and Bailey, T., 2001, Strontium isotope stratigraphy: LOWESS version 3: Best fit to the marine Sr-isotope curve for 0–509 Ma and accompanying look-up table for deriving: The Journal of Geology, v. 109, p. 155–170.

McCormick, F., 1992, Early faunal evidence for dairying: Oxford Journal of Archaeology, v. 11, p. 201–9.

McCormick, F., 2008, The Decline of the Cow: Agricultural and Settlement Change in Early Medieval Ireland: Peritia, v. 20, p. 210–225.

McCormick, F., Kerr, T., McClatchie, M., and O'Sullivan, A., 2011, The Archaeology of Livestock and Cereal Production in Early Medieval: Early Medieval Archaeology Project (EMAP 2) Report 5:1, Irish National Strategic Archaeological Research (INSTAR) programme.

McCormick, F., and Murray, E., 2007, Knowth and the Zooarchaeology of Early Christian Ireland. Excavations at Knowth 3: Royal Irish Academy Dublin.

Meier-Augenstein, W., Hobson, K.A., and Wassenaar, L.I., 2013, Critique: measuring hydrogen stable isotope abundance of proteins to infer origins of wildlife, food and people: Bioanalysis, v. 5, p. 751–67.

Milner, N., Craig, O.E., Bailey, G.N., and Andersen, S.H., 2006, A response to Richards and Schulting: Antiquity, v. 80, p. 456–458.

Milner, N., Craig, O.E., Bailey, G.N., Pedersen, K., and Andersen, S.H., 2004, Something fishy in the Neolithic? A re-evaluation of stable isotope analysis of Mesolithic and Neolithic coastal populations: Antiquity, v. 78, p. 9–22.

Montgomery, J., 2010, Passports from the past: Investigating human dispersals using strontium isotope analysis of tooth enamel: Annals of Human Biology, v. 37, p. 325–46.

Montgomery, J., Evans, J.A., and Chenery, C.A., 2006, Report of the lead, strontium, and oxygen isotope analysis of the Iron Age burial from Rath, Ireland: Unpublished report for CRDS Ltd, Dublin, Ireland. 13 pp.

Montgomery, J., Evans, J.A., and Neighbour, T., 2003, Sr isotope evidence for population movement within the Hebridean Norse community of NW Scotland: Journal of the Geological Society, v. 160, p. 649–653.

Montgomery, J., and Grimes, V., 2010, Appendix 21.1: Report on the isotope analysis of a burial from Ratoath, Co. Meath, in C. Corlett and M. Potterton (Eds.). Death and Burial in Early Medieval Ireland in the Light of Recent Archaeological Excavations. Wordwell, Dublin, Ireland. 316 pp, p. 309–311.

Montgomery, J., Grimes, V., Buckberry, J., Evans, J.A., Richards, M.P., and Barrett, J.H., 2014, Finding Vikings with isotope analysis: The view from wet and windy islands: Journal of the North Atlantic, v. 7, p. 54–70.

Müldner, G., Chenery, C.A., and Eckardt, H., 2011, The "Headless Romans": Multi-isotope investigations of an unusual burial ground from Roman Britain: Journal of Archaeological Science, v. 38, p. 280–290.

Müldner, G., and Richards, M.P., 2005, Fast or feast: Reconstructing diet in later medieval England by stable isotope analysis: Journal of Archaeological Science, v. 32, p. 39–48.

Müldner, G., and Richards, M.P., 2007a, Diet and diversity at Later Medieval fishergate: The isotopic evidence: American Journal of Physical Anthropology, v. 134, p. 162–174.

Müldner, G., and Richards, M.P., 2007b, Stable isotope evidence for 1500 years of human diet at the city of York, UK: American Journal of Physical Anthropology, v. 133, p. 682–697.

Mulville, J., Bond, J., and Craig, O.E., 2005, The white stuff, milking in the outer Scottish Isles, in J. Mulville and A.K. Outram (Eds.), The Zooarchaeology of Fats, Oils, Milk and Dairying, Oxford.

Novak, M., 2015, Dental health and diet in early medieval Ireland: Archives of Oral Biology, v. 60, p. 1299–1309.

Nowell, G.M., and Horstwood, M.S.A., 2009, Comments on Richards et al., Journal of Archaeological Science 35, 2008 "Strontium isotope evidence of Neanderthal

mobility at the site of Lakonis, Greece using laser-ablation PIMMS": Journal of Archaeological Science, v. 36, p. 1334–1341.

O'Hara, R., 2008, Collierstown, Co. Meath: Medieval Archaeology, v. 58, p. 367–73.

O'Hara, R., 2009, Report on the Archaeological Excavation of Collierstown 1, Co. Meath. Unpublished report prepared for Archaeological Consultancy Services Ltd.

Pietsch, S.J., Hobson, K.A., Wassenaar, L.I., and Tütken, T., 2011, Tracking cats: Problems with placing feline carnivores on $\delta^{18}O$, δD isoscapes: PLoS ONE, v. 6.

Podlesak, D.W., Torregrossa, A.M., Ehleringer, J.R., Dearing, M.D., Passey, B.H., and Cerling, T.E., 2008, Turnover of oxygen and hydrogen isotopes in the body water, CO_2, hair, and enamel of a small mammal: Geochimica et Cosmochimica Acta, v. 72, p. 19–35.

Price, T.D., Burton, J.H., and Bentley, R.A., 2002, The characterization of biologically available strontium isotope ratios for the study of prehistoric migration: Archaeometry, v. 1, p. 117–135.

Price, T.D., Frei, K.M., and Naumann, E., 2015, Isotopic Baselines in the North Atlantic Region: Journal of the North Atlantic, v. 7, p. 103–136.

Privat, K.L., O'Connell, T.C., and Richards, M.P., 2002, Stable isotope analysis of human and faunal remains from the Anglo-Saxon cemetery at Berinsfield, Oxfordshire: dietary and social implications: Journal of Archaeological Science, v. 29, p. 779–790.

Reimer, P.J., Baillie, M.G.L., Bard, E., Bayliss, A., Beck, J.W., Bertrand, C.J.H., Blackwell, P.G., Buck, C.E., Burr, G.S., Cutler, K.B., Damon, P.E., Edwards, R.L., Fairbanks, R.G., Friedrich, M., et al., 2004, IntCal04 terrestrial radiocarbon age calibration, 0–26 cal kyr BP: Radiocarbon, v. 46, p. 1029–1058.

Reynard, L.M., and Hedges, R.E.M., 2008, Stable hydrogen isotopes of bone collagen in palaeodietary and palaeoenvironmental reconstruction: Journal of Archaeological Science, v. 35, p. 1934–1942.

Reynard, L.M., Meltzer, D.J., Emslie, S.D., and Tuross, N., 2015, Stable isotopes in yellow-bellied marmot (Marmota flaviventris) fossils reveal environmental stability in the late Quaternary of the Colorado Rocky Mountains: Quaternary Research (United States), v. 83, p. 345–354.

Reynard, L.M., and Tuross, N., 2016, Hydrogen isotopic analysis with a chromium-packed reactor of organic compounds of relevance to ecological, archaeological, and forensic applications: Rapid Communications in Mass Spectrometry, p. 1857–1864.

Richards, M.P., 2000, Stable isotope analysis in archaeology: A short introduction: The archaeologist, v. 38, p. 19–20.

Richards, M.P., and Hedges, R.E.M., 1999, A Neolithic revolution? New evidence of diet in the British Neolithic: Antiquity, v. 73, p. 891–897.

Richards, M.P., Schulting, R.J., and Hedges, R., 2003, Sharp shift in diet at onset of Neolithic: Nature, v. 425, p. 366–366.

Richards, M.P., and Trinkaus, E., 2009, Isotopic evidence for the diets of European Neanderthals and early modern humans: Proceedings of the National Academy of Sciences, v. 106, p. 16034–16039.

Ritchie, A., 1977, Excavation of Pictish and Viking-age farmsteads at Buckquoy, Orkney: Proceedings of the Society of Antiquaries of Scotland, v. 108, p. 174–227.

Rowley-Conwy, P., 2004, How the West Was Lost: Current Anthropology, v. 45, p. S83–S113.

Royer, A., Daux, V., Fourel, F., and Lécuyer, C., 2017, Carbon, nitrogen and oxygen isotope fractionation during food cooking: Implications for the interpretation of the fossil human record: American Journal of Physical Anthropology, v. 163, p. 759–771.

Rozanski, K., Araguás-Araguás, L., and Gonfiantini, R., 1993, Isotopic Patterns in Modern Global Precipitation: Climate Change in Continental Isotopic Records, v. 78, p. 1–36.

Sauer, P.E., Schimmelmann, A., Sessions, A.L., and Topalov, K., 2009, Simplified batch equilibration for D/H determination of non-exchangeable hydrogen in solid organic material: Rapid Communications in Mass Spectrometry, v. 23, p. 949–956.

Schoeninger, M.J., 1985, Trophic level effects on $^{15}N/^{14}N$ and $^{13}C/^{12}C$ ratios in bone collagen and strontium levels in bone mineral: Journal of Human Evolution, v. 14, p. 515–525.

Schoeninger, M.J., and DeNiro, M.J., 1984, Nitrogen and carbon isotopic composition of bone collagen from marine and terrestrial animals: Geochimica et Cosmochimica Acta, v. 48, p. 625–639.

Schoeninger, M.J., DeNiro, M.J., and Tauber, H., 1983, Stable Nitrogen Isotope Ratios of Bone Collagen Reflect Marine and Terrestrial Components of Prehistoric Human Diet: Science, v. 220, p. 1381–1383.

Schulting, R.J., Murphy, E., Jones, C., and Warren, G., 2012, New dates from the north and a proposed chronology for Irish Court tombs.: Proceedings of the Royal Irish Academy, v. 112C, p. 1–60.

Schulting, R.J., and Richards, M.P., 2002a, Finding the coastal Mesolithic in Southwest Britain: AMS dates and stable isotope results on human remains from Caldey Island, South Wales: Antiquity, v. 76, p. 1011–1025.

Schulting, R.J., and Richards, M.P., 2002b, The Wet, the Wild and the Domesticated: the Mesolithic-Neolithic transition on the west coast of Scotland: European Journal of Archaeology, v. 5, p. 147–189.

Schweitzer, H., 2009, Iron Age toe-rings from Rath, County Meath, on the N2 Finglas-Ashbourne Road Scheme, in J. O'Sullivan and M. Stanley (Eds.), Recent Archaeological Discoveries on National Road Schemes NRA Monograph, p. 93–98.

Sealy, J.C., 2001, Body tissue chemistry and Palaeodiet, in D.R. Brothwell and A.M. Pollard (Eds.), Handbook of Archaeological Science, John Wiley & Sons, Chichester, p. 269–279.

Sealy, J.C., Armstrong, R., and Schrire, C., 1995, Beyond lifetime averages: tracing life histories through isotopic analysis of different calcified tissues from archaeological human skeletons: Antiquity, v. 69, p. 290–300.

Sealy, J.C., van der Merwe, N.J., Lee-Thorp, J.A., and Lanham, J.L., 1987, Nitrogen isotopic ecology in southern Africa: Implications for environmental and dietary tracing: Geochimica et Cosmochimica Acta, v. 51, p. 2707–2717.

Seaver, M., 2010, Against the grain: Early medieval settlement and burial on the Blackhill: excavations at Raystown, Co. Meath, in C. Corlett and M. Potterton (Eds.) Death and Burial in Early Medieval Ireland, in Light of Recent Archaeological Excavations, Dublin. Wordwell, p. 299–319.

Seaver, M., 2016, Meitheal. The Archaeology of Lives, Labours and Beliefs at Raystown, Co. Meath: Transport Infrastucture Ireland, Dublin.

Seaver, M., 2009, Report on Archaeological Excavation of Site 21, Raystown, County Meath. Unpublished CRDS report.

Seaver, M., 2005, Run of the mill? Excavation of an early medieval settlement at Raystown, Co. Meath: Archaeology Ireland, v. 19, p. 9–12.

Seaver, M., 2006, Through the mill – Excavation of an early medieval settlement at Raystown, in J. O'Sullivan & M. Stanley (Eds.) Settlement, Industry and Ritual, National Roads Authority Monograph Series 3. Dublin., National Roads Authority. Wordwell., p. 73–88.

Shaw, H., Montgomery, J., Redfern, R., Gowland, R., and Evans, J.A., 2016, Identifying migrants in Roman London using lead and strontium stable isotopes: Journal of Archaeological Science, v. 66, p. 57–68.

Shaw, B.J., Summerhayes, G.R., Buckley, H.R., and Baker, J.A., 2009, The use of strontium isotopes as an indicator of migration in human and pig Lapita populations in the Bismarck Archipelago, Papua New Guinea: Journal of Archaeological Science, v. 36, p. 1079–1091.

Sheridan, J.A., Jay, M., Montgomery, J., Pellegrini, M., and Cahill Wilson, J., 2013, "Tara Boy": local hero or international man of mystery?, in M. O' Sullivan, M. Doyle and C. Scarre (Eds.), Tara-from the past to the future, Wordwell: Dublin.

Shields, G.A., 2007, A normalised seawater strontium isotope curve: possible implications for Neoproterozoic-Cambrian weathering rates and the further oxygenation of the Earth: eEarth, v. 2, p. 35–42.

Sjögren, K.G., 2003, Megaliths, settlement, and subsistence in Bohuslan, Sweden: in G. Burenhult and S. Westergaard (Eds.), Formal disposal of the dead in Atlantic Europe during the Mesolithic-Neolithic interface 6000–3000 BC: British Archaeological Reports International Series 1201, p. 167–76.

Slovak, N.M., and Paytan, A., 2012, Applications of Sr isotopes in archaeology, in M. Baskaran (Ed.), Handbook of Environmental Isotope Geochemistry: Springer Berlin Heidelberg, p. 743-768.

Snoeck, C., Pouncett, J., Ramsey, G., Meighan, I.G., Mattielli, N., Goderis, S., Lee-Thorp, J.A., and Schulting, R.J., 2016, Mobility during the Neolithic and Bronze Age

in Northern Ireland explored using strontium isotope analysis of cremated human bone: American Journal of Physical Anthropology, v. 160, p. 397–413.

Sponheimer, M., Robinson, T., Ayliffe, L., Roeder, B., Hammer, J., Passey, B., West, A., Cerling, T.E., Dearing, D., and Ehleringer, J., 2003, Nitrogen isotopes in mammalian herbivores: hair $\delta^{15}N$ values from a controlled feeding study: International Journal of Osteoarchaeology, v. 13, p. 80–87.

Styring, A.K., Fraser, R.A., Arbogast, R.M., Halstead, P., Isaakidou, V., Pearson, J.A., Schäfer, M., Triantaphyllou, S., Valamoti, S.M., Wallace, M., Bogaard, A., and Evershed, R.P., 2015, Refining human palaeodietary reconstruction using amino acid $\delta^{15}N$ values of plants, animals and humans: Journal of Archaeological Science, v. 53, p. 504–515.

Tauber, H., 1981, ^{13}C evidence for dietary habits of prehistoric man in Denmark: Nature, v. 292.

Tauber, H., 1982, Carbon-13 evidence for the diet of prehistoric humans in Denmark: PACT, v. 7, p. 235–37.

Tieszen, L.L., and Fagre, T., 1993, Effect of diet quality and composition on the isotopic composition of respiratory CO_2, bone collagen, bioapatite, and soft tissues: in J.B. Lambert and G. Grupe (Eds.), Prehistoric Human Bone: Archaeology at the Molecular Level. Springer-Verlag, Berlin., p. 21–155.

Tobin, M., 2011, Ancestry and analyses at Holdenstown: Seanda NRA Archaeology Magazine, v. 6, p. 40–41.

Toolis, R., 2008, Excavation of Medieval Graves at St Thomas' Kirk, Hall of Rendall, Orkney with contributions by Barrett, J., Boulton, N., Chenery, C., Evans, J.A, Hall, D., MacSween, A., Melikian, M. and Richards, M.: Proceedings of the Society of Antiquaries of Scotland, v. 138, p. 239–266.

Topalov, K., Schimmelmann, A., Polly, P.D., and Sauer, P.E., 2012, Stable Isotope Applications in Bone Collagen with Emphasis on Deuterium/Hydrogen Ratios, in J. Verbeek (Ed.), Products and Applications of Biopolymers: InTech, P. 141-162

Tuross, N., 2012, Comparative decalcification methods, radiocarbon dates, and stable isotopes of the VIRI bones: Radiocarbon, v. 54, p. 837–844.

Tuross, N., Fogel, M.L., and Hare, P.E., 1988, Variability in the preservation of the isotopic composition of collagen from fossil bone: Geochimica et Cosmochimica Acta, v. 52, p. 929–935.

Tuross, N., Reynard, L.M., Harvey, E., Coppa, A., and McCormick, M., 2017, Human skeletal development and feeding behavior: the impact on oxygen isotopes: Archaeological and Anthropological Sciences.

Tuross, N., Warinner, C., Kirsanow, K., and Kester, C., 2008, Organic oxygen and hydrogen isotopes in a porcine controlled dietary study, in Rapid Communications in Mass Spectrometry, v. 22, p. 1741–1745.

Veizer, J., 1989, Strontium Isotopes in Seawater through time: Annual Review of Earth and Planetary Sciences, v. 17.

Voerkelius, S., Lorenz, G.D., Rummel, S., Quétel, C.R., Heiss, G., Baxter, M., Brach-Papa, C., Deters-Itzelsberger, P., Hoelzl, S., Hoogewerff, J., Ponzevera, E., Van Bocxstaele, M., and Ueckermann, H., 2010, Strontium isotopic signatures of natural mineral waters, the reference to a simple geological map and its potential for authentication of food: Food Chemistry, v. 118, p. 933–940.

Vogel, J.C., and van der Merwe, N.J., 1977, Isotopic evidence for early maize cultivation in New York State: American Antiquity, v. 42, p. 238–242.

Wallace, A., Montgomery, J., and Grimes, V., 2010, Excavation of an Early Medieval cemetery at Ratoath, Co. Meath., in C. Corlett & M. Potterton (Eds.) Death and burial

in Early Medieval Ireland in the light of recent archaeological excavations, Bray: Wordwell, p. 335–359.

Wassenaar, L.I., and Hobson, K.A., 2000, Improved method for determining the stable-hydrogen isotopic composition (δD) of complex organic materials of environmental interest: Environmental Science and Technology, v. 34, p. 2354–2360.

Weis, D., Kieffer, B., Maerschalk, C., Barling, J., de Jong, J., Williams, G.A., Hanano, D., Pretorius, W., Mattielli, N., Scoates, J.S., Goolaerts, A., Friedman, R.M., and Mahoney, J.B., 2006, High-precision isotopic characterization of USGS reference materials by TIMS and MC-ICP-MS: Geochemistry, Geophysics, Geosystems, v. 7, p. 1–30.

Woodman, P., 2004, The exploitation of Ireland's coastal resources – a marginal resources through time? in M. Gonzalez Morales and G.A. Clark (Eds.) The Mesolithic of the Atlantic facade: proceedings of the Santander symposium: 37-56. Anthropological research paper no. 55: Arizona State University.

6 Supplementary Tables

ID	Adult/ Juvenile	Sex	Age (year	Lab Code	Conventional Date (BP)	± 1 σ	Calibrated date (AD) 2 σ
RAYSTOWN*							
PHASE 1 (AD 500-550)							
R853	Adult	F	36-45	Wk-16823	1647	33	260-540
R854	Adult	F	36-45	Wk-17922	1598	36	390-550
R820	Adult	F	36-45	Wk-17922	1586	32	400-550
R841	Adult	M	26-35	Wk-16825	1537	34	430-600
R2398	Adult	M	> 25	Wk-16819	1574	35	410-570
R811	Adult	F	45+	Wk-16306	1528	33	430-610
PHASE 2 (AD 550-700)							
R907	Adult	M	26-35	Wk-17920	1524	31	430-610
R944	Adult	M	18-25	Wk-17919	1531	31	430-600
R417	Adult	F	45+	Wk-16822	1510	34	430-640
R984	Adult	F	45+	Wk-16827	1491	35	440-650
R848	Adult	M	18-25	Wk-16826a	1482	35	550-660
R954	Adult	U	> 25	Wk-17921	1448	35	550-660
R1053	Juvenile	U	2.2-	Wk-16821	1425	33	570-660
R928	Adult	M	45+	Wk-16308	1412	34	575-665
R988	Adult	F	45+	Wk-16828	1496	36	430-650
PHASE 3 (AD 700-800)							
R1036	Adult	F	18-25	Wk-16820b	1312	38	650-780
R831	Adult	F	36-45	Wk-16307	1334	34	640-780
PHASE 4 (AD 800-900)							
R957	Adult	M	36-45	Wk-16310	1195	34	700-950
R949	Juvenile	U	0.8-1.1	Wk-16309	1130	35	780-990
COLLIERSTOWN**							
PHASE 1							
C48		F		Beta-250161	1550	40	420-600
C58	Adult	F		Beta-247008	1550	40	420-600
C47	Adult	M	20-24	Beta-247005	1530	40	420-610
C1	Adult	F	35-44	Beta-247001	1550	40	420-600
PHASE 2							
C39	Adult	M	17-25	-	-	-	-
C54	Adoles.	U	14-17	Beta-247007	1430	40	560-660
PHASE 3							
C18	Adult	M	17-25	Beta-247003	1460	40	540-650
C13	Adult	M	17-25	Beta-247002	1210	40	690-900
JOHNSTOWN***							
PHASE 1 (AD 350-700)							
J110	Adult	F	45+	Beta-178195	1560	70	370-640
J129		U		Beta-178197	1560	70	370-640
J33	Adult	F	36-45	Beta-184610	1460	70	430-680
PHASE 2 (AD 500-700)							
J219	Adult	U		Beta-178198	1460	50	530-660

ID	Adult/ Juvenile	Sex	Age (year	Lab Code	Conventional Date (BP)	± 1 σ	Calibrated date (AD) 2 σ
J25	Adult	M	18-25	Beta-178194	1390	50	580-700
J43	Adult	M		Beta-180650	1410	60	545-700
PHASE 3 (AD 650-1000)							
J34	Adult	M	36-45	Beta-184703	1240	40	680-890
J128	Adult	M	45+	Beta-184704	1240	40	680-890
J166	Adult	F	36-45	Beta-184706	1270	70	650-900
J249	Adult	F	18-25	Beta-184613	1200	60	680-980
J21	Juvenile	U	7	-	-	-	-

Table S1. Radiocarbon dates from Raystown (*Seaver, 2016), Collierstown (**O'Hara, 2008) and Johnstown (***Clarke & Carlin, 2013), calibrated using Reimer et al., (2004). I.D. Burial number prefixes are as follows C = Collierstown, J = Johnstown, R = Raystown. Sex categories are M = Male, F = Female, U = Unsexed.

	n	$\delta^{13}C_{VPDB}$	SD	Amt%	SD	$\delta^{15}N_{AIR}$	SD	Amt%	SD	wt C/N	SD	atom C/N
R853		-20.9				12.4						
R854		-21.9				10.4						
R820		-21.1				11.9						
R841		-21.8				10.8						
R239		-20.9				12.4						
R811		-20.7				12.5						
R907		-21.1				11.4						
R944		-21.1				12.1						
R417		-20.8				12.1						
R984		-21.2				12.3						
R848		-20.3				10.7						
R954		-21.1				12.1						
R105		-20.7				13.3						
R928		-20.4				12.2						
R988		-20.8				11.3						
R103		-20.3				11.4						
R831		-20.9				11.0						
R957		-20.4				11.3						
R949		-21.0				13.8						
C58	2	-20.8	0.1	41.6	0.0	13.5	0.0	14.2	0.0	2.9	0.0	3.4
C47	2	-20.7	0.1	45.4	0.5	12.1	0.1	15.7	0.1	2.9	0.0	3.4
C1	2	-21.0	0.1	43.6	0.5	12.5	0.2	15.2	0.2	2.9	0.0	3.4
C54	2	-20.9	0.4	42.3	0.4	12.4	0.1	14.2	0.7	3.0	0.1	3.5
C18	2	-21.2	0.1	44.4	0.4	12.6	0.2	15.4	0.1	2.9	0.0	3.4
C13	2	-21.1	0.0	43.6	0.6	13.0	0.2	15.0	0.3	2.9	0.0	3.4
J110	1	-21.7		44.2		12.7		15.0		3.0		3.4
J129	1	-21.3		48.5		13.2		16.7		2.9		3.4
J33	2	-21.5	0.0	46.1	0.9	11.8	0.0	15.4	0.3	3.0	0.0	3.5
J219	2	-21.5	0.0	47.2	0.5	11.8	0.1	16.2	0.5	2.9	0.5	3.4
J25	2	-21.0	0.0	42.6	1.4	10.3	0.1	14.2	0.6	3.0	0.0	3.5
J43	2	-21.5	0.1	44.7	0.1	13.0	0.5	15.3	0.1	2.9	0.0	3.4
J34	2	-20.4	0.0	43.0	0.0	10.9	0.0	14.6	0.0	3.0	0.0	3.4
J128	1	-20.8		40.9		11.9		13.8		3.0		3.4
J166	1	-21.0		45.1		11.5		15.2		3.0		3.5
J249	2	-21.1	0.0	43.2	1.0	12.5	0.0	14.6	0.4	3.0	0.0	3.5
J21	2	-21.1	0.0	44.4	0.4	11.6	0.0	15.1	0.1	2.9	0.0	3.4
J42	1	-21.5		44.9		11.7		15.1		3.0		3.5
275 S	2	-22.3	0.2	44.5	1.5	8.1	0.2	16.5	0.5	2.7	0.0	3.1
1 O	2	-22.1	0.3	41.5	1.5	10.4	0.5	15.3	0.4	2.7	0.0	3.2
275	2	-22.1	0.1	43.6	1.8	9.1	0.1	16.2	0.8	2.7	0.0	3.1
275 2	2	-22.1	0.1	42.0	0.8	11.3	0.1	15.4	0.4	2.7	0.0	3.2
1397	2	-21.7	0.1	45.4	1.6	9.1	0.2	16.8	0.7	2.7	0.0	3.1
263 F	2	-21.1	0.1	45.1	2.7	10.9	0.2	16.8	0.8	2.7	0.0	3.1
415 F	2	-21.4	0.0	42.8	1.2	13.1	0.0	15.8	0.5	2.7	0.0	3.1
11 S	2	-21.9	0.0	46.0	1.8	11.4	0.0	17.0	0.6	2.7	0.0	3.2
1379	2	-21.3	0.0	45.4	0.7	11.3	0.0	16.9	0.3	2.7	0.0	3.1
1406	2	-22.7	0.1	44.5	0.5	7.2	0.2	16.5	0.1	2.7	0.0	3.1
1078	2	-21.8	0.0	42.5	1.2	10.2	0.2	15.8	0.4	2.7	0.0	3.1
275 2	2	-22.0	0.1	42.6	1.2	8.1	0.4	15.3	0.5	2.8	0.0	3.2
1172	2	-21.8	0.1	42.9	1.3	7.4	0.3	15.7	0.4	2.7	0.0	3.2
803 S	2	-21.9	0.1	43.9	1.2	9.8	0.2	16.0	0.4	2.7	0.0	3.2
4 C	2	-20.6	0.0	42.4	3.7	9.8	0.1	16.3	0.8	2.6	0.1	3.0

Table S2. $\delta^{13}C$ and $\delta^{15}N$ values for human and animal skeletal samples with suitably preserved collagen. Sites are represented by the following codes: C = Collierstown, J = Johnstown, R = Raystown. Values for Raystown samples are taken from Fibiger (2006).

	Cr-δ^2H_{SMOW}	± SD	n	gC-δ^2H_{SMOW}	± SD	$\delta^{18}O$	± SD	$\%O_{ace}$	$\%H_{ace}$	O/H_{ace}	$atomO/H_{ace}$	$\%O_{suc}$	$\%H_{suc}$	O/H_{suc}	$atomO/H_{suc}$	n
R853	-6.9	1.3	2	-15.6		10.2		30.9	7.3	4.2	0.27	26.9	5.7	4.7	0.30	1
R854	-18.8	0.8	2	-32.3		9.3		30.5	7.2	4.2	0.27	26.5	5.6	4.7	0.30	1
R820	-15.1	1.9	2	-26.8		10.0		25.3	5.7	4.4	0.28	25.7	5.2	4.9	0.31	1
R841	-2.5	2.2	2	-12.0		10.2		30.5	6.8	4.5	0.28	26.5	5.3	5.0	0.31	1
R2398	-5.6	0.2	2	-13.2	4.0	10.3	0.3	29.8	7.1	4.2	0.27	25.9	5.5	4.7	0.30	2
R811	-7.9	0.3	2	-20.4	0.3	10.3	0.1	27.7	6.5	4.3	0.27	25.4	5.2	4.9	0.31	2
R907	-11.5	1.4	2	-20.3		9.9		31.0	7.1	4.4	0.27	27.0	5.6	4.9	0.31	1
R944	-18.1	0.5	2	-33.8		9.3		24.6	5.7	4.3	0.27	24.9	5.2	4.8	0.30	1
R417	-19.1	4.6	4	-30.3		9.2		25.9	6.0	4.3	0.27	26.2	5.4	4.8	0.30	1
R984	-15.5	0.7	2	-26.8		10.5		25.2	5.8	4.3	0.27	25.6	5.3	4.8	0.30	1
R848	-19.1	0.1	2	-30.3		9.6		30.2	7.0	4.3	0.27	26.3	5.5	4.8	0.30	1
R954																
R1053	-31.8	0.2	2	-36.1	0.0	10.2	0.1	30.3	6.8	4.5	0.28	26.4	5.3	5.0	0.31	2
R928	-16.4	0.2	2	-30.4		11.6		24.4	5.8	4.2	0.27	24.7	5.3	4.7	0.30	1
R988	-16.0	0.0	2	-32.3		10.2		24.9	5.9	4.2	0.27	25.2	5.3	4.7	0.30	1
R1036	-18.1	2.8	2	-29.1		11.0		25.5	5.4	4.7	0.30					1
R831	-15.2	0.2	2	-29.2		10.4		25.5	5.9	4.3	0.27	25.9	5.4	4.8	0.30	1
R957																
R949	-29.8	0.4	2	-46.6	5.4	9.2	0.3	28.2	6.3	4.5	0.28	25.9	5.1	5.1	0.32	2
C48																
C58	-9.6	0.9	2	-20.0		11.8		17.3	3.7	4.6	0.29					1
C47	-2.7	1.5	2	-16.3	0.9	9.8		29.3	6.3	4.7	0.29	26.9	5.0	5.3	0.34	2
C1	-22.1	0.3	2	-41.4	0.9	10.2	0.1	28.2	6.3	4.5	0.28	25.9	5.0	5.1	0.32	2
C39	-12.0		1	-23.0	1.2	9.1	0.4	16.1	3.5	4.5	0.29					2
C54	-10.5	0.9	2	-20.1	0.3	9.4	0.1	27.7	5.9	4.7	0.30	28.8	5.5	5.23	0.33	2
C18	-14.0	0.6	2	-21.2		10.4		22.2	4.5	4.9	0.31					1
C13	-17.0	2.5	2	-26.8		9.5		22.1	5.0	4.4	0.28					1
J110	-20.0	1.3	2	-36.4		9.8		25.1	5.6	4.5	0.28					1

	Cr-δ^2H_{SMOW}	± SD	n	gC-δ^2H_{SMOW}	± SD	$\delta^{18}O$	± SD	$\%O_{ace}$	$\%H_{ace}$	O/H_{ace}	$atomO/H_{ace}$	$\%O_{suc}$	$\%H_{suc}$	O/H_{suc}	$atomO/H_{suc}$	n
J129	-17.8	0.6	2	-25.4	0.6	9.6	0.2	30.6	7.1	4.3	0.27	26.7	5.6	4.8	0.30	2
J33	-12.3	0.9	2	-29.4		9.9		26.1	6.2	4.2	0.27	26.5	5.6	4.7	0.30	1
J219	-21.3	0.3	2	-38.7		10.2		26.4	6.1	4.3	0.27					1
J25	-7.0	0.5	2	-21.7	2.5	9.9	0.1	28.3	6.3	4.5	0.28	25.9	5.1	5.1	0.32	2
J43	-13.4	4.0	6	-33.2		9.2		25.7	6.0	4.3	0.27	26.1	5.4	4.8	0.30	1
J34	-13.3	1.6	2	-32.2		9.4		24.6	5.5	4.4	0.28	24.9	5.0	4.9	0.31	1
J128	-17.3	2.4	2	-28.7		9.7		25.2	5.9	4.3	0.27					1
J166	-18.2	0.7	2	-27.6		10.3		24.7	5.7	4.3	0.27					1
J249	-12.2	1.4	2	-21.4		10.3		23.8	5.3	4.5	0.28					1
J21	-18.4	3.0	4	-33.5	1.2	10.2	0.2	26.8	6.2	4.3	0.27	24.6	5.0	4.9	0.31	2
J42	-15.4	2.1	2	-31.6		9.4		25.7	6.1	4.2	0.26	26.1	5.6	4.7	0.29	1
1 O				-61.5	3.6	9.0	0.4	26.9	6.2	4.3	0.27	28.0	5.8	4.8	0.30	2
275 O				-57.6	2.1	8.4	0.2	26.9	6.5	4.2	0.26	28.0	6.0	4.6	0.29	2
275 2				-47.1	0.7	8.6	0.1	26.9	6.5	4.2	0.26	28.0	6.0	4.6	0.29	2
1397 O				-58.1	1.8	8.7	0.1	27.0	6.5	4.2	0.26	28.1	6.1	4.6	0.29	2
1078 O				-58.0	4.0	8.8	0.8	27.1	6.4	4.2	0.27	28.2	6.0	4.7	0.30	2
1172 O				-46.2	2.5	7.9	0.3	27.2	6.4	4.2	0.27	28.3	6.0	4.7	0.30	2
263 F				-28.2	1.8	6.6	0.6	28.6	6.8	4.2	0.26	29.8	6.4	4.7	0.29	2
415 F				-31.6	0.4	6.7	0.0	27.3	6.4	4.3	0.27	28.4	6.0	4.7	0.30	2
275 S				-32.8	6.1	7.2	0.6	27.5	6.4	4.3	0.27	28.6	6.0	4.8	0.30	2
11 S				-36.4	1.7	7.1	0.0	27.5	6.6	4.2	0.26	28.6	6.1	4.7	0.29	2
1379 S				-30.1	1.3	6.3	0.1	26.9	6.3	4.3	0.27	28.0	5.9	4.8	0.30	2
1406 S				-59.1	1.9	6.7	0.0	26.0	6.0	4.3	0.27	27.1	5.6	4.8	0.30	2
275 2				-42.5	0.7	7.0	0.2	27.0	6.1	4.4	0.28	28.1	5.7	4.9	0.31	2
803 S				-33.4	0.2	6.8	0.3	27.3	6.3	4.3	0.27	28.5	5.9	4.8	0.30	2
4 C				-36.2	1.4	6.9	0.0	26.3	6.2	4.2	0.27	27.3	5.8	4.7	0.30	2

Table S3. Cr-packed and glassy C-packed δ^2H and $\delta^{18}O$ values with atomic O/H ratios.

I.D.	Element	Side	Tooth	Enamel $^{87}Sr/^{86}Sr$	±2 SE	Tooth	Dentine $^{87}Sr/^{86}Sr$	±2 SE	Additional Tooth	Enamel $^{87}Sr/^{86}Sr$	±2 SE
RAYSTOWN											
R853	Mandible	Sin	M3	0.708843	0.000005						
R854	Mandible	Sin	C	0.711006	0.000013						
R820	Mandible	Sin	M3	0.708748	0.000003						
R841	Maxilla	N/A	PM2	0.710688	0.000027						
R2398	Not present	N/A									
R811	Disarticulated	N/A	M2	0.708789	0.000016						
R907	Maxilla	Dex	M3	0.709395	0.000004						
R944	Mandible	Dex	M3	0.709330	0.000033	M3	0.708376	0.000008			
R417	Disarticulated	N/A									
R984	Maxilla	Dex									
R848	Maxilla	Sin									
R954	Disarticulated	N/A									
R1053	Mandible	Dex	M2	0.708684	0.000017						
R928	Disarticulated	N/A	M3	0.708873	0.000008						
R988	Maxilla	Dex	M2	0.708865	0.000004						
R1036	Mandible	Sin	M3	0.708632	0.000014						
R831	Mandible	Dex	M3	0.708860	0.000007						
R957	Not present	N/A									
R949	Not present	N/A	M2	0.708547	0.000019						

I.D.	Element	Side	Tooth	Enamel $^{87}Sr/^{86}Sr$	±2 SE	Tooth	Dentine $^{87}Sr/^{86}Sr$	±2 SE	Additional Tooth	Enamel $^{87}Sr/^{86}Sr$	±2 SE
COLLIERSTOWN											
C48*	Mandible	Dex	M2	0.709246	0.00001	M2	0.708623	0.000007			
C58	Disarticulated	N/A									
C47	Disarticulated	N/A									
C1	Disarticulated	N/A	M3	0.709030	0.000016						
C39	Mandible	Dex	M3	0.709015	0.000013	M1	0.708777	0.000003	M1	0.709323	0.000008
C54	Mandible	Dex	M3	0.709042	0.000013						
C18	Mandible	Dex	M3	0.709003	0.000007				M1	0.708862	0.000013
C13	Mandible	Sin	M3	0.709803	0.000005						
JOHNSTOWN											
J110	Not present	N/A									
J129	Disarticulated	N/A									
J33	Maxilla	Dex	M3	0.708755	0.000005						
J219	Mandible	Sin	M3	0.708927	0.000010	M3	0.708410	0.000005	M1	0.708763	0.000019
J25	Not present	N/A									
J43	Maxilla	Dex	M2	0.709624	0.000014						
J34	Not present	N/A									
J128	Maxilla	Sin	M2	0.708516	0.000004						
J166	Maxilla	Dex									
J249	Mandible	Sin	M3	0.708463	0.000013						
J21	Disarticulated	N/A									

I.D.	Element	Side	Tooth	Enamel $^{87}Sr/^{86}Sr$	±2 SE	Tooth	Dentine $^{87}Sr/^{86}Sr$	±2 SE	Additional Tooth	Enamel $^{87}Sr/^{86}Sr$	±2 SE
J42	Maxilla	Sin	M3	0.708698	0.000015						
RAYSTOWN FAUNA											
275 S											
1 O											
275 O				0.708837	0.000008						
275 2											
1397 O				0.709051	0.000008						
263 F				0.708572	0.000003						
415 F				0.708443	0.000004						
11 S											
1379 S											
1406 S											
1078 O											
275 2 S											
1172 O				0.709317	0.000010						
803 S				0.708553	0.000007						
4 C				0.708545	0.000006						

Table S4. $^{87}Sr/^{86}Sr$ values from human and animal dental enamel and dentine. *from Cahill-Wilson et al., (2014).

	HYDROGEN							OXYGEN						
	H	D	L	intercept	slope	R^2	predicted	H	D	L	intercept	slope	R^2	predicted
water	565	-45	-442					-5.7	-6.5	-57.5				
R841	-15	-20	-20	-18.7	0.006	0.84	-19	11.3	11.5	10.8	11.5	0.012	0.96	11.4
R848	-33	-34	-36	-34.5	0.002	0.90	-35	11.1	10.6	9.8	11.0	0.021	0.85	10.9
R853	-15	-22	-23	-20.0	0.008	0.89	-20	10.2	10.3	10.6	10.2	-0.006	1.00	10.3
R854	-32	-32	-38	-34.3	0.005	0.64	-35	10.4	9.9	10.2	10.1	-0.001	0.01	10.1
R907	-20	-26	-31	-25.9	0.011	0.98	-26	11.8	12.5	13.2	12.0	-0.020	0.76	12.1
R417	-29	-30	-34	-31.4	0.005	0.82	-32	9.2	9.2	9.2	9.2	0.000	0.77	9.2
R820	-25	-27	-34	-28.8	0.009	0.82	-29	10.8	10.0	9.6	10.5	0.015	0.63	10.4
R831	-24	-29	-31	-28.1	0.007	0.96	-28	12.2	10.4	10.6	11.4	0.014	0.18	11.3
R928	-23	-30	-27	-27.0	0.005	0.44	-27	11.0	11.6	10.5	11.4	0.016	0.71	11.3
R944	-33	-34	-37	-34.8	0.004	0.77	-35	10.3	9.3	10.4	9.7	-0.012	0.34	9.8
R984	-31	-27	-33	-30.3	0.001	0.01	-30	10.4	10.5	10.6	10.5	-0.001	0.36	10.5
R988	-30	-32	-30	-30.8	0.000	0.02	-31	10.1	10.2	10.3	10.1	-0.004	0.87	10.1
J33	-26	-29	-29	-28.4	0.003	0.81	-29	9.6	9.9	9.8	9.7	-0.001	0.02	9.7
J34	-24	-32	-32	-29.5	0.009	0.83	-30	9.7	9.4	9.3	9.5	0.003	0.31	9.5
J42	-32	-33	-34	-33.1	0.003	1.00	-33	9.2	9.2	9.3	9.2	-0.002	0.91	9.2
J43	-29	-32	-38	-33.1	0.008	0.86	-33	9.5	9.4	9.3	9.5	0.004	0.65	9.4
J110	-34	-36	-39	-36.6	0.005	0.99	-37	9.9	9.8	9.9	9.8	-0.001	0.35	9.8
J128	-27	-29	-33	-29.9	0.005	0.83	-30	10.4	9.7	10.3	10.1	-0.004	0.08	10.1
J166	-28	-28	-36	-30.9	0.007	0.57	-31	10.2	10.3	9.8	10.3	0.010	0.96	10.3
J219	-34	-39	-38	-36.8	0.004	0.66	-37	9.6	10.2	9.4	10.0	0.009	0.47	9.9

	HYDROGEN							OXYGEN						
	H	D	L	intercept	slope	R^2	predicted	H	D	L	intercept	slope	R^2	predicted
R036	-28	-29	-34	-30.6	0.005	0.75	-31	10.4	11.0	11.0	10.7	-0.006	0.25	10.7
J249	-17	-21	-25	-21.4	0.008	0.99	-22	10.3	10.3	10.2	10.3	0.002	0.97	10.3
C13	-18	-27	-29	-24.9	0.011	0.96	-25	9.1	9.5	10.5	9.2	-0.023	0.95	9.3
C18	-20	-21	-23	-21.6	0.003	0.91	-22	9.9	10.4	9.8	10.2	0.007	0.36	10.1
C54	-17	-9	-15	-13.6	-0.003	0.09	-14	11.5	10.5	10.2	11.1	0.016	0.48	11.0
C58	-20	-20	-19	-19.5	-0.001	0.73	-19	10.7	11.8	10.6	11.3	0.013	0.32	11.2
J129	-22	-25	-29	-25.7	0.007	0.98	-26	9.9	9.6	9.7	9.8	0.001	0.06	9.7
R053	-36	-36	-39	-36.9	0.002	0.68	-37	10.9	10.2	10.5	10.5	0.001	0.01	10.5
R053	-12	-13	-18	-14.3	0.006	0.86	-15	10.3	10.3	10.3	10.3	0.001	0.63	10.3
R841	-6	-12	-19	-12.5	0.012	0.98	-13	10.7	10.2	10.3	10.4	0.002	0.06	10.4
R848	-25	-30	-27	-27.6	0.002	0.19	-28	9.9	9.6	9.5	9.7	0.005	0.45	9.7
R853	-9	-16	-22	-15.6	0.013	0.99	-16	10.5	10.2	10.5	10.3	-0.002	0.25	10.3
R854	-33	-32	-32	-32.5	-0.001	0.92	-32	9.8	9.3	9.7	9.5	-0.003	0.10	9.5
R907	-16	-20	-28	-21.6	0.012	0.93	-22	10.4	9.9	10.6	10.1	-0.008	0.54	10.2
R811	-19	-20	-26	-22.0	0.007	0.80	-22	10.2	10.3	10.4	10.2	-0.002	0.97	10.3
J21	-29	-34	-38	-33.8	0.009	0.98	-34	9.9	10.2	10.0	10.0	0.001	0.04	10.0
J25	-23	-22	-27	-23.8	0.003	0.40	-24	11.8	9.9	9.8	11.0	0.021	0.30	10.8
R949	-45	-47	-49	-47.3	0.004	0.87	-47	9.2	9.2	9.2	9.2	0.001	0.46	9.2
C1	-40	-41	-45	-42.0	0.005	0.93	-42	9.6	10.2	10.1	9.9	-0.004	0.14	9.9
C47	-13	-16	-17	-15.7	0.005	0.97	-16	9.4	9.8	9.7	9.6	-0.002	0.05	9.6

Table S5. Exchange experiment results. H = heavy, D = distilled and L = light enriched.

Dependent Variable			Mean Difference (I-J)	Std. Error	Sig.
$\delta^{13}C_{VPDB}$	Raystown	Collierstown	.03441	.18260	.998
		Johnstown pre-1000 A.D.	.30305	.14880	.193
		Johnstown post-1000 A.D.	-1.15345*	.17269	.000
	Collierstown	Raystown	-.03441	.18260	.998
		Johnstown pre-1000 A.D.	.26864	.19516	.522
		Johnstown post-1000 A.D.	-1.18786*	.21393	.000
	Johnstown pre-1000 A.D.	Raystown	-.30305	.14880	.193
		Collierstown	-.26864	.19516	.522
		Johnstown post-1000 A.D.	-1.45649*	.18592	.000
	Johnstown post-1000 A.D.	Raystown	1.15345*	.17269	.000
		Collierstown	1.18786*	.21393	.000
		Johnstown pre-1000 A.D.	1.45649*	.18592	.000
$\delta^{15}N_{AIR}$	Raystown	Collierstown	-1.03294*	.33154	.018
		Johnstown pre-1000 A.D.	-.28385	.27017	.721
		Johnstown post-1000 A.D.	1.11420*	.31355	.006
	Collierstown	Raystown	1.03294*	.33154	.018
		Johnstown pre-1000 A.D.	.74909	.35434	.168
		Johnstown post-1000 A.D.	2.14714*	.38844	.000
	Johnstown pre-1000 A.D.	Raystown	.28385	.27017	.721
		Collierstown	-.74909	.35434	.168
		Johnstown post-1000 A.D.	1.39805*	.33757	.001
	Johnstown post 1000 A.D.	Raystown	-1.11420*	.31355	.006
		Collierstown	-2.14714*	.38844	.000
		Johnstown pre-1000 A.D.	-1.39805*	.33757	.001

Table S6. Results of the independent sample t-tests comparing mean $^{87}Sr/^{86}Sr$ ratios between the groups.

* = mean values are statistically different (p=<0.05).

Chapter 5: Synthesis

The key research outcomes are discussed below with respect to the aims set out in the introduction, while the significance of this thesis to the wider field of study and its implications for future directions are also considered. The aims of the thesis were to: (i) Define the influence of marine and anthropogenic Sr contribution on the Sr budget of the Irish biosphere, (ii) Characterise $^{87}Sr/^{86}Sr$ and rare earth element (REE) distribution in the biosphere of Co. Meath, accounting for both local bedrock and surficial geology, and (iii) Explore potential differences in diet and provenance between a number of individuals (human and faunal) whose archaeological remains were excavated from three early medieval cemetery-settlement sites using multiple isotope systems.

(i) A geochemical contribution from a marine reservoir was recognised in the Irish terrestrial biosphere. This marine contribution was found to obscure the local minerogenic $^{87}Sr/^{86}Sr$ signatures in coastal areas and in regions subject to high levels of precipitation by overprinting with a seawater Sr composition. This is demonstrated here by three lines of evidence: (1) diverging trends in $^{87}Sr/^{86}Sr$ plant values away from the seawater signature with increasing distance from the coast, (2) regional enrichment of marine-fingerprinting cations in topsoil along the northern coastal perimeter of Ireland and (3) clear binary mixing in surface waters between atmospheric and geogenic endmembers.

Coastal Sr enrichment and associated deviations in $^{87}Sr/^{86}Sr$ values towards a seawater signature are therefore measureable and significant. Geochemical topsoil datasets produced by the national geochemical surveying project, Tellus, further demonstrate a high marine contribution of Sr and other marine-sourced elements including Na, along the coast and in areas covered by blanket peat. Thus, peatlands effectively act as an ombrotrophic repository for time-integrated atmospheric inputs.

Surface waters draining the relatively homogenous Tertiary basalt bedrock catchment of the River Main in Co. Antrim deviate from local geological $^{87}Sr/^{86}Sr$ values. These geochemical trends are interpreted as evidence for significant

precipitation inputs into upland tributaries as in these instances, interaction with local surficial and bedrock geology has been negligible. Mature stages of the river display $^{87}Sr/^{86}Sr$ closer to that of bedrock values, unequivocally demonstrating that hydrological characteristics relating to topography and drainage are controlling factors. Therefore, rather than presuming that $^{87}Sr/^{86}Sr$ of surface waters are directly inherited from bedrock, it is possible to spatially define the relative importance of rainfall and geogenic reservoirs.

The degree to which marine/atmospheric geochemical contributions can effect terrestrial environments will depend on (i) distance from the coastline and (ii) susceptibility to high levels of precipitation. Ireland has many such environments, thus in an Irish context biosphere mapping or archaeological provenance studies should carefully consider potential marine/atmospheric contributions to study sites. This study estimates that the terrestrial Sr budget is dominated by a marine $^{87}Sr/^{86}Sr$ seawater value at the coast, declining to a lower proportion >8km inland. In a wider context, current international initiatives for creating $^{87}Sr/^{86}Sr$ isoscapes in island settings or in countries with extensive coastlines, should account for such a coastal "buffer zone" where local values are likely to deviate from geogenic reservoirs.

$^{87}Sr/^{86}Sr$ and element contents of tree cores were measured to test if the introduction and widespread use of modern agricultural practices, including the use of fertiliser, has measurably changed geochemical uptake by plants over the last century. Declining concentrations in a suite of elements (including Na, Mg, Al, K, Ca, Sr, Rb and Ba) were observed over the last century which indicates an overall net loss of these element from the bioavailable soil fraction. A small, but notable increase (+0.5‰) in $^{87}Sr/^{86}Sr$ between the first and latter half of the last century was discerned from a tree core growing on agricultural soils, coinciding with the introduction and proliferation of the use of modern fertilisers.

Ten-year increments of the sampled tree cores from Co. Antrim were analysed here, averaging a decade of environmental change and because of this, the patterns observed do not accurately demonstrate short-lived, distinct environmental changes. Therefore, there is notable capacity to refine the resolution at which the chemical variations can be deciphered in tree cores. Future work should focus on refining the sampling scale to obtain an annual time record of such variations and

in addition, take a larger sample set of cores which would provide a more extensive screening of local heterogeneities. Other site-specific details such as soil organic matter content, soil moisture, pH and rooting depth could be examined in more detail to assess the degree to which these parameters control major and trace element composition of trees.

(ii) The spatial variation in biosphere $^{87}Sr/^{86}Sr$ within a geologically diverse and archaeologically significant setting is resolved at high resolution. This new baseline dataset of bioavailable $^{87}Sr/^{86}Sr$ values for Co. Meath provides a necessary reference tool for archaeological provenance studies in Ireland by giving geographic context to human isotope values. This dataset also contributes to the production of detailed national and European Sr isoscapes and can be used to advance geochemical fingerprinting and future investigations of prehistoric mobility patterns on a wider scale.

The extent to which distinct geological units can be characterised over the study area of Co. Meath, by regionally unique $^{87}Sr/^{86}Sr$ values and REE patterns was tested using streamwater, vegetation and soil leachates. $^{87}Sr/^{86}Sr$ ranges for all major lithological units and Quaternary sediment types were established and within this region of complex bedrock and surficial geology, statistically distinct groups, or isotope 'packages' have been defined. Given the relatively wide local range in $^{87}Sr/^{86}Sr$, some units overlap in their values and are thus, not distinctive. Despite this, based on one-way ANOVA, certain packages, including Quaternary groups, could be statistically distinguished from one another on the basis of their $^{87}Sr/^{86}Sr$ values. Thus, surficial deposits should be considered as an important reservoir of Sr in the terrestrial budget.

Rare Earth Elements (REE) were used as an independent but complementary tool to examine element cycling through biosphere components. Whilst the REE concentration and normalised patterns of plants and soil leachates showed some differences as a function of underlying geology, the REE patterns of streamwaters dominantly reflected a carbonate input, irrespective of local geological setting indicating that REE are therefore less diagnostic of bedrock source input than $^{87}Sr/^{86}Sr$ values. Nonetheless, both REE and $^{87}Sr/^{86}Sr$ tracers are valuable for revealing different information about element mobility within the catchment.

Significant differences in $^{87}Sr/^{86}Sr$ were observed between plant samples and soil leachates, highlighting a procedural effect on soil leachate data. Plant material is deemed to be the most reliable proxy for bio-available Sr ranges. However, whilst it is broadly understood that shallow rooted plants tend to reflect the $^{87}Sr/^{86}Sr$ of the topsoil whilst deeper rooted plants access Sr from soil horizons at greater depth (Poszwa et al., 2002, 2004; Drouet et al., 2007; Maurer et al., 2012), the effect of rooting depth on specific plant types and species on $^{87}Sr/^{86}Sr$ values warrants further investigation, as there is no consensus on the ideal and most representative, plant type for biosphere $^{87}Sr/^{86}Sr$ mapping. For archaeological studies, it may be that target plant types should best reflect those consumed by humans and animals in their diet.

(iii) Biosphere data collected for Co. Meath has been used as a basis for comparison with animal and human skeletal remains to reconstruct paleo-mobility and subsistence of early medieval populations. $^{87}Sr/^{86}Sr$ is combined with multiple stable isotope systems ($\delta^{18}O$, $\delta^{2}H$, $\delta^{13}C$, $\delta^{15}N$) and reveal a heavy reliance by these individuals on arable and livestock farming with insignificant contribution from marine dietary sources. Assuming a local, terrestrial diet, the geographic differences in bioavailable $^{87}Sr/^{86}Sr$ of these people allow inferences to be made about those who likely lived local to the burial site throughout their lifetime and those who may have been migrants to the sites. Based on the comparison of individual tooth enamel $^{87}Sr/^{86}Sr$ values to the range of the population and local baseline values, two people were identified as statistical outliers; one of whom had extensive evidence for weapon trauma. These two individuals are conceivably of non-local origin.

To examine broad temporal variation in, two teeth were analysed from three separate individuals. Given that molars mineralise at different time periods during childhood, $^{87}Sr/^{86}Sr$ values from different molars can track an individual's mobility over part of their life-span. Using such a temporal range, two molars from three individuals demonstrated no large variation between teeth, suggesting that these individuals did not move between isotopically distinguishable environments during the life-span represented by their molar teeth.

Whilst this inter-tooth sampling can be very informative, for higher temporal resolution, intra-tooth sampling across the incremental growth lines of one or more molars is the next objective, particularly for the two statistically outlying individuals, R854 and R841, whose movements could be more tightly age constrained. Moreover, the bulk sampling of tooth enamel used here required a relatively large portion of the dental enamel and results in the averaging of time-related isotope information. Intra-tooth measurements in humans can relate this time-sensitive isotope variation in teeth to their mobility (Le Roux et al., 2014; Simonetti et al., 2008; Beaumont et al., 2013). Such analyses can be complicated by the intricate nature of enamel mineralisation and maturation (Montgomery et al., 2010; Suga, 1982), thus the sampling path across each tooth needs to be assessed and chosen carefully to establish the maturation time-lines (Montgomery et al., 2012). Two intra-tooth sampling methods could be used to minimise sample destruction whilst simultaneously addressing the timing of the inferred movement in potential migrants: (1) Incremental micro-drilling growth layers and subsequent analysis using TIMS which provides a high level of precision and (2) Laser ablation – ICP MS, which has lower precision but offers a continuous tooth enamel profile and is less destructive.

The remains of 36 individuals have tightly constrained $\delta^{13}C$ and $\delta^{15}N$ ranges, suggesting that the diet of these populations was consistently terrestrial-based and remained so throughout the early medieval period in Co. Meath, despite the sites' proximity to the Irish Sea. Sr/Ca values of tooth enamel samples is another proxy which could be used to differentiate between marine and terrestrial meat/milk consumption, which have low Sr concentrations, and cereal crops, which have a higher Sr content. This has the potential to provide additional evidence for the dietary inferences formed from the $\delta^{13}C$ and $\delta^{15}N$ ranges.

The linear offset ($y=1.08x-11.37$) between $\delta^{2}H$ values measured using two reactor configurations (glassy C and Cr-packed) can be used to correct a large body of published glassy-C $\delta^{2}H$ data, which appear to be artificially-skewed, although in a systematic manner. $\delta^{2}H$ data acquired here, demonstrate that these values are a valuable tool for reconstructing the paleo-diet of archaeological populations, since the trophic level of fauna, human juveniles and adults are well separated,

particularly so by their Cr-δ^2H values. Whilst δ^{15}N values can be controlled by site specific factors such as aridity and manuring (Bogaard et al., 2007; Styring et al., 2014), δ^2H act as an independent proxy for diet where δ^{15}N may be unreliable (Reynard and Hedges, 2008).

δ^{18}O values from bone collagen cannot be directly compared to local drinking water values in the same manner as δ^{18}O from phosphate or carbonate. Moreover, the effect of organism age (ontogeny) and body size on bone collagen δ^{18}O and δ^2H values remains unresolved. Further measurement of δ^{18}O and δ^2H values in a range of species and a larger sample set of human remains would help to discern the effect of dietary and physiological differences on these isotopic compositions. Feeding experiments would also be useful for deciphering the relative importance of different dietary components to the δ^{18}O and δ^2H of bone collagen.

Using ^{87}Sr/^{86}Sr in combination with other stable isotopes (δ^{18}O, δ^2H, δ^{13}C, δ^{15}N), soil cation concentrations and trace elements (primarily REE) expands on current knowledge of isotope and element distribution within the Irish biosphere and informs on the lives of early medieval populations in an archaeologically significant region in Europe. This applied study has illustrated both the power and constraints of using isotope values from both skeletal remains and environmental samples to address questions of past human mobility and diet. The use of multiple isotopes defines the range in 'local' populations, in a comprehensive manner, which could not have been achieved using these isotope systems individually. Such an integrated approach provides a novel and robust protocol to accurately reconstruct past human mobility and subsistence. This suite of isotope measurements (^{87}Sr/^{86}Sr, δ^{18}O, δ^2H, δ^{13}C, δ^{15}N), put in the context of the local ^{87}Sr/^{86}Sr biosphere ranges, increases the confidence at which geochemical fingerprinting can resolve movement in past populations while consolidating the value of these isotope measurements in the study of prehistoric populations.

References

Beaumont, J., Gledhill, A., Lee-Thorp, J.A., and Montgomery, J., 2013, Childhood diet: A closer examination of the evidence from dental tissues using stable isotope analysis of incremental human dentine*: Archaeometry, v. 55, p. 277–295.

Bogaard, A., Heaton, T.H.E., Poulton, P., and Merbach, I., 2007, The impact of manuring on nitrogen isotope ratios in cereals: archaeological implications for reconstruction of diet and crop management practices: Journal of Archaeological Science, v. 34, p. 335–343.

Drouet, T., Herbauts, J., Gruber, W., and Demaiffe, D., 2007, Natural strontium isotope composition as a tracer of weathering patterns and of exchangeable calcium sources in acid leached soils developed on loess of central Belgium: European Journal of Soil Science, v. 58, p. 302–319.

Maurer, A.-F., Galer, S.J.G., Knipper, C., Beierlein, L., Nunn, E. V, Peters, D., Tütken, T., Alt, K.W., and Schöne, B.R., 2012, Bioavailable $^{87}Sr/^{86}Sr$ in different environmental samples - Effects of anthropogenic contamination and implications for isoscapes in past migration studies: The Science of the Total Environment, v. 433, p. 216–29.

Montgomery, J., Evans, J.A., and Horstwood, M.S.A., 2010, Evidence for long-term averaging of strontium in bovine enamel using TIMS and LA-MC-ICP-MS strontium isotope intra-molar profiles: Environmental Archaeology, v. 15, p. 32–42.

Poszwa, A., Dambrine, E., Ferry, B., Pollier, B., and Loubet, M., 2002, Do deep tree roots provide nutrients to the tropical rainforest? Biogeochemistry, v. 60, p. 97–118.

Poszwa, A., Ferry, B., Dambrine, E., and Pollier, B., 2004, Variations of bioavailable Sr concentration and $^{87}Sr/^{86}Sr$ ratio in boreal forest ecosystems: Biogeochemistry, p. 1–20.

Reynard, L.M., and Hedges, R.E.M., 2008, Stable hydrogen isotopes of bone collagen in palaeodietary and palaeoenvironmental reconstruction: Journal of Archaeological Science, v. 35, p. 1934–1942.

Le Roux, P.J., Lee-Thorp, J.A., Copeland, S.R., Sponheimer, M., and de Ruiter, D.J., 2014, Strontium isotope analysis of curved tooth enamel surfaces by laser-ablation multi-collector ICP-MS: Palaeogeography, Palaeoclimatology, Palaeoecology, v. 416, p. 142–149.

Simonetti, A., Buzon, M.R., and Creaser, R. a., 2008, In-situ elemental and Sr isotope investigation of human enamel by laser ablation-(MC)-ICP-MS: successes and pitfalls: Archaeometry, v. 50, p. 371–385.

Styring, A.K., Fraser, R.A., Bogaard, A., and Evershed, R.P., 2014, The effect of manuring on cereal and pulse amino acid $\delta^{15}N$ values: Phytochemistry, v. 102, p. 40–45.

Suga, S., 1982, Progressive mineralization pattern of developing enamel during the maturation stage: Journal of Dental Research, v. 61, p. 1532-42.